ABSTRACT

A HIGH RESOLUTION STUDY OF PROTON INELASTIC SCATTERING FROM ^{207}Pb, ^{208}Pb, and ^{209}Bi

By

William Thomas Wagner

Angular distributions of states in ^{207}Pb, ^{208}Pb, and ^{209}Bi excited by 35 MeV protons have been measured with a resolution of 5 to 10 keV. Collective model calculations enabled the ℓ-transfers of many transitions to be identified. In ^{208}Pb, calculations for a number of the observed states were made with both phenomenologically determined and theoretically calculated wave functions. Both central and non-central two-body forces were used in the analysis and the effects of knock-on exchange were accounted for. The large number of observed unnatural parity states permitted the role of non-central forces in these inelastic transitions to be investigated. The states which are strongly populated in both the (p,p') and (e,e') reactions were analyzed in a microscopic theory using the electron scattering form factors. The possibility of excitation of giant magnetic dipole levels was also investigated.

In the nuclei ^{207}Pb and ^{209}Bi the transitions to the identified single particle levels were compared to calculations involving valence orbitals with both central and non-central interactions. The effects of core polarization

in excitation of these states were investigated with a microscopic model using an expanded shell model basis. In the framework of a weak coupling model, the transitions to many levels in these odd mass nuclei were compared to excitations in ^{208}Pb.

A HIGH RESOLUTION STUDY OF PROTON INELASTIC SCATTERING FROM ^{207}Pb, ^{208}Pb, and ^{209}Bi

By

William Thomas Wagner

A THESIS

Submitted to
Michigan State University
in partial fulfillment of the requirements
for the degree of

DOCTOR OF PHILOSOPHY

Department of Physics

1974

ACKNOWLEDGMENTS

I am indebted to Dr. G.M. Crawley for the assistance and guidance that he has given. His patience and understanding have provided sources of inspiration and aspiration. I especially thank him for suggesting this thesis topic.

I am also indebted to the entire staff and graduate student population of the Cyclotron Lab. I especially thank Julie K. Perkins for typing this thesis. The kind assistance of Mr. W.F. Steele and Mr. Joseph E. Finck in taking the data is also greatly appreciated.

To my parents I owe a large debt of gratitude for the demonstration that satisfaction can be found in performing a job.

I am also grateful for the understanding of my two daughters, Michelle and Danielle. I owe much to my wife, Barbara, for her incessant encouragement and understanding for lack of which this thesis would have suffered.

Lastly, I acknowledge my debts to Him.

TABLE OF CONTENTS

LIST OF TABLES

LIST OF FIGURES

INTRODUCTION

The lead mass region has rightly been called an ideal testing ground for nuclear models. Experimentally, the isotopes in this region exhibit a wide range of nuclear behavior. For example, levels corresponding to single nucleon excitations have been identified; states which exhibit properties associated with collective nuclear motion have also been observed. Further, the doubly-closed shell in ^{208}Pb is of such purity that low-lying levels in this nucleus are expected to have a simple theoretical description. These facts make a study of these nuclei of great interest and importance.

This mass region has been examined previously in a variety of ways. While each of the different reactions and methods used to study nuclei gives a particular kind of information, inelastic scattering probably is sensitive to the broadest range of nuclear properties. Inelastic scattering excites many different configurations including states seen in decay studies, transfer reactions and isobaric analog resonance work. Inelastic scattering can excite large nuclear collective excitations not seen in reactions involving nucleon transfer. Inelastic scattering can initiate large multipolarity transitions and hence

complements electromagnetic processes which are involved primarily in dipole and quadrupole transitions.

Experimentally, (p,p') seems an ideal mechanism to study the lead mass region. One search using 24.5 MeV protons has been done.[1,57,70] This study was performed with 25 keV resolution and at sufficiently high bombarding energy so that collective model comparisons could be made. Unfortunately, the theoretical tools for a microscopic analysis were not well developed at the time that data was taken. Theoretical analysis was limited to use of the collective model for identification of angular momentum transfer and to applications of the weak coupling model. Other (p,p') studies[2,58,60,71,72] have examined single nuclei in this region and have been limited by resolution or low bombarding energy where compound and direct nuclear effects may be present and where angular distributions involving different angular momentum transfer may not have distinct shapes.

Interest in proton inelastic scattering has been renewed by the numerous, recent experimental improvements. Primary among these is the development of ultra-high resolution techniques[19,56] in particle reactions. Energy resolution on the order of 1 part in 10000 has become possible and has opened a new chapter in experimental study. With this resolution, weakly excited states very close to other states may be cleanly separated thus permitting analysis without fear of anomalous contributions. Further, the availability of high

purity, isotopic material for targets, stable and large current accelerators, and particle detectors with high signal to background ratio strongly suggests that exceptionally high quality (p,p') data can now be collected.

While experimental techniques have improved, the solution to the nuclear problem has also progressed. The knowledge of the nucleon-nucleon forces, the proper models for structure calculations, and the theory of direct reactions has increased greatly. The success of structure[51-53] and scattering[57,60,70,72] models in the lead mass region makes testing and extension of these methods intriguing.

These facts have motivated an extensive study of inelastic proton scattering from the three nuclei: ^{207}Pb, ^{208}Pb, and ^{209}Bi. Both macroscopic and microscopic models will be used in analyzing the data. Emphasis will be placed on analysis of the unnatural parity states.

The study divides naturally into two sections: Part A, dealing with ^{208}Pb, and Part B, dealing with the other two nuclei. In the first section, the ^{208}Pb nucleus is examined in the light of collective and shell models. Part B deals with the odd mass systems and the influence of the ^{208}Pb core upon the odd particle or hole. Both weak coupling and core polarization calculations will be presented.

Five Appendices have been included. The first two deal with experimental problems and procedure. The last three contain lists of all the measured cross sections, given in the center-of-momentum coordinate system.

PART A

^{208}Pb

I. INTRODUCTION

Nuclei in the mass region about ^{208}Pb have been extensively studied both experimentally[1-17] and theoretically[51-55]. Inelastic scattering[1-9] and Coulomb excitation[10] have given information about the strongly populated states of many of these nuclei. Decay studies and transfer reactions[11-13] together with isobaric analog resonance experiments[14-17] have provided information about the microscopic structure of many of the low-lying states. The level properties and the microscopic configurations have been intensively studied in nuclear structure calculations. This mass region therefore provides an attractive place where recent developments in inelastic scattering can be applied.

The microscopic description of nucleon-nucleus scattering has progressed greatly. After the initial success of the collective model in fitting the angular distributions of the strongly excited states, inelastic scattering was used primarily to obtain ℓ-transfer information. More recently, since knock-on exchange and the central portion of the nucleon-nucleon interaction are better understood, microscopic inelastic reaction theory can more sensitively probe nuclear properties.[18] Normal parity transitions permit the testing of wave functions and transition densities of the target

nucleus since such transitions apparently depend little on the non-central two-body interactions. Non-normal parity transitions to levels with well determined wave functions allow the two-body spin-orbit and tensor forces to be studied. Recently, experiments with charged particle reactions at energies of 30 to 50 MeV and resolution better than 10 keV have become possible. This permits the extraction of cross sections and excitation energies for weakly excited states which can be reliably compared with theoretical predictions.

A (p,p') study of nuclei neighboring ^{208}Pb allows examination of the nucleon-core interaction. For these nuclei, the effects of core polarization and the applicability of the weak coupling model can be determined only after study of ^{208}Pb has provided a basis for these models.

A relatively high resolution proton inelastic scattering experiment[1] has been performed at 24.5 MeV bombarding energy with energy resolution of $\simeq$25 keV full-width-at-half-maximum (FWHM). Spin and parity assignments for the most strongly excited states below 4.7 MeV of excitation energy were made. Lately, analysis[2] of the (p,p') reaction at 54 MeV has extended ℓ-transfer assignments to states below about 7 MeV of excitation where ^{208}Pb becomes particle unstable. The resolution was about 35-40 keV FWHM. In both studies, experimental angular distributions were compared primarily with the collective model predictions. To date, these represent the most extensive and highest resolution (p,p') studies of ^{208}Pb.

This paper reports a high resolution study of $^{208}Pb(p,p')$ performed at 35 MeV with energy resolution on the order of 1 part in 5000. Angular distributions at this bombarding energy have more distinguishing features than those at lower energies yet are not so forward-angle peaked as to make identification of small ℓ-transfers difficult. About 150 states with excitation energies up to 7.5 MeV have been experimentally resolved and their angular distributions are presented. Determinations of ℓ-assignments and deformation parameters as well as comparison with previous measurements are made. Microscopic model inelastic scattering predictions are compared with the data for normal and non-normal parity excitations. The existence of magnetic dipole states is also discussed.

II. EXPERIMENTAL PROCEDURE

The experiment used the 35 MeV proton beam from the Michigan State University sector-focussed cyclotron and the scattered protons were detected using the Enge split-pole spectrometer. The high resolution data was recorded on Kodak NTB 25 μm nuclear emulsions in the spectrometer focal plane. A thin, stainless steel absorber immediately before the emulsion stopped all particles other than protons. The 10 to 15 mil absorber did not significantly broaden the line-width. However, tracks in the emulsions did show slight departures from parallel trajectories. The absorber also

decreased the particle energy thus enhancing track brightness. On-line determination of the focal plane line-width using the "speculator" technique of Blosser et al.[19] was used to optimize the resolution initially and to monitor it during data collection. Targets of about 100 $\mu g/cm^2$ thickness were used throughout the high resolution study and were prepared by vacuum evaporation on a 15-20 $\mu g/cm^2$ carbon foil with a substrate of 1 or 2 layers of formvar. The effects of target thickness on resolution are discussed in Appendix I. The plate data resolution ranged from 5 to 8 keV (FWHM) and a typical spectrum is displayed in Figure 1. Exposures on the plates were scanned in steps of 4 mils.

To complement the high resolution data, states strongly excited in inelastic scattering were first studied using a single-wire proportional counter[20] in the spectrometer focal plane. A 6.0 mg/cm^2 self-supporting foil, made by rolling, served as the target. The lead used in all target fabrication was isotopically enriched to 99.14% ^{208}Pb and was obtained from the Oak Ridge National Laboratory. Resolution of about 45 keV allowed cross sections for the first 3^-, 2^+, 4^+, 6^+, and 8^+ levels as well as the first two 5^- states to be measured. Both plate and counter data were measured relative to elastic events monitored at a scattering angle of 90° with a NaI(Tl) detector. This angle was chosen since 90° lies near a relative maximum of the elastic cross section for ^{208}Pb and also gives good separation of protons

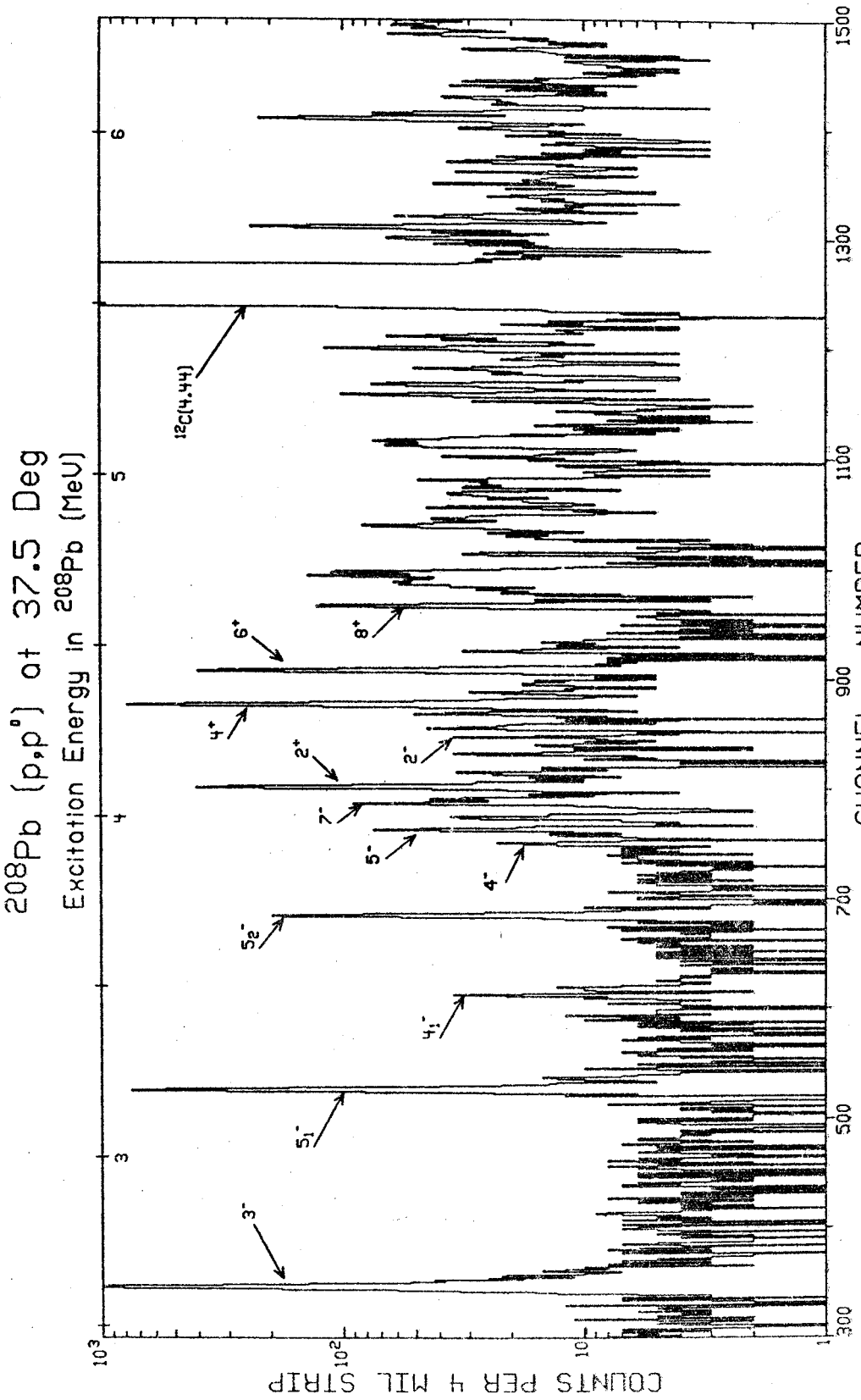

FIGURE 1.--Typical spectrum of protons scattered by ^{208}Pb. The resolution is about 6 keV.

elastically scattered from lead and light mass contaminants in the target. The beam current was monitored with a Faraday cup and microampere current integrator. There was generally good agreement between the two monitoring methods.

Absolute normalization of the counter data was done by comparison of the optical model using Becchetti-Greenlees[21] best-fit parameters with the measured elastic angular distribution. Comparing the plate data with the counter results thus determined the normalization of the plate data. Absolute normalization of the counter and plate data is believed good to about 5 and 10 percent, respectively.

Whenever possible, the more extensive counter results are displayed although both sets of data were measured in the range of 10 to 100 degrees. The counter data was taken with a 1.2 msteradian (2°x2°) solid angle while all plate data was collected with a 0.30 msteradian (1°x1°) defining aperture. Because nuclei in the lead region have large forward angle elastic cross sections, slit scattering from the entrance slit of the spectrometer can produce high particle backgrounds. For this reason, a narrow edge was machined around the opening of the defining aperture. This thinner portion sufficiently degraded 35 MeV protons to place them well out of the region of interest of the focal plane and also reduced slit scattering.

III. DATA

A. Excitation Energies

Average excitation energies were extracted for the approximately 150 resolved states. For each exposure the spectrometer focal plane momentum dispersion was determined[22] by using the positions, as determined from the plate scan, of reaction products. Clearly resolved states of ^{208}Pb, ^{16}O, and ^{12}C with well-known excitation energies were used in the energy calibration. A few iterations were performed until the input calibration energies agreed with the average predicted energies. The methods used in analyzing the data are sketched in Appendix II. The results for all observed states are tabulated in Table I and the energies used for the calibration are indicated. For comparison the excitation energies determined by previous work are also given. The energies listed are from the results of a Nuclear Data compilation,[23] the recent 54 MeV (p,p') experiment,[2] and an intensive study by Heusler et al.[24] of states below about 4.5 MeV. As may be seen the final values for the calibration reference levels are in excellent agreement with prior measurements involving (d,pγ) and (n,n'γ) high resolution work. The general agreement with previous determinations is good and appears to extend up to about 7 MeV of excitation.

Due to kinematic broadening and to the displacements of the focal planes of protons scattered from different mass

TABLE I.--Energy levels, ℓ-transfers, and deformation parameters for ^{208}Pb.

Present Work			54 MeV(p,p') Ref. 2			Compilation Ref. 23		Shell Model Study-Ref. 24	
$E_x \pm \Delta E_x$ [a]	L	β_L	E_x [a]	L	β_L [f]	E_x [a]	J^π	E_x [a]	J^π
2.6146 [b]	3	0.120	2.615	3	0.108	2.6146	3^-		
3.1978 [b]	5	0.058	3.198	5	0.055	3.1977	5^-	3.198	5^-
3.475±0.001	$J^\pi=4^-$ [c]		3.475			3.4750	4^-	3.475	4^-
3.7087 [b]	5	0.034	3.709	5	0.035	3.7085	5^-	3.709	5^-
						3.73?			
						3.76?			
3.919±0.001	$J^\pi=4^-$ [c]	3.922?				3.9202	$(6)^-$	3.919	4^-
3.946±0.003						3.946			
3.961±0.001	(5)	0.018	3.959			3.9609	$(4)^-$	3.960	5^-
3.995±0.004	$J^\pi=6^-$ [c]					3.9985		3.996	6^-
4.037±0.001	(7)	0.038	4.028	≥6		4.038	$(7)^-$	4.035	7^-
4.054±0.003	(3)	0.013				4.050	(4)	4.049	3^-
4.0855 [b]	2	0.058	4.086	2	0.058	4.086	2^+		
4.106±0.003	(3)	0.010							
4.125±0.001	$J^\pi=4^-$ [c]					4.1254	$4^-,5^-$	4.126	4^-
4.141±0.003	(2)	0.0084							
4.159±0.004	(2)	0.0067	4.150			4.155?			
4.181±0.001	(5)	0.018				4.1805	$(5)^-$	4.180	5^-
4.206±0.002	$J^\pi=6^-$ [c]					4.204	$5^-,6^-$	4.205	6^-
4.230±0.002	$J^\pi=2^-$ [c]		4.240	5	0.017	4.231	(2^-)	4.230	2^-
						4.253	$(2\text{-}4^-)$	4.255	3^-
4.256±0.002 [e]						4.258	$(4^-,5^-)$	4.256	4^-
								4.261	5^-
4.296±0.002	5	0.018				4.2961	$(5)^-$	4.296	5^-
4.3237 [b]	4	0.067	4.324	4	0.069	4.323	4^+		
4.357±0.003	$J^\pi=4^-$ [c]					4.357	(4^-)	4.360	4^-
4.385±0.003	$J^\pi=6^-$ [c]					4.382	$(6)^-$	4.388	6^-
4.403±0.002	(3)	0.0084							
	(4)	0.0077							

TABLE I.--Continued.

Present Work			54 MeV(p,p') Ref. 2			Compilation Ref. 23		Shell Model Study-Ref. 24	
$E_x \pm \Delta E_x$ [a]	L	β_L	E_x [a]	L	β_L [f]	E_x [a]	J^π	E_x [a]	J^π
4.4235 [b]	6	0.062	4.420	6	0.064	4.425	(6^+)		
4.444±0.004	(5)	0.0089							
4.463±0.004	(2)	0.0056							
4.480±0.001 [e]	$J^\pi=6^-$ [c]		4.50			4.4804	$(6)^-$	4.482	6^-
4.577±0.005									
4.610±0.001	8	0.040	4.606	(8)	0.039	4.608	$(8)^+$		
4.680±0.002	(9)	0.016							
4.698±0.001	3	0.033	4.696	3	0.037	4.6982	$(3)^-$	4.700	3^-
4.711±0.002						4.709			
4.762±0.002	7	0.015	4.749						
4.841±0.002	$J^\pi=1^-$ [d]		4.847	(1)	$\leq$0.008	4.840	(1)		
						4.859	0^+		
4.863±0.002 [e]						4.863	$(7)^+$		
4.895±0.002	$\tilde{=}10$	0.027	4.897	10	0.022	4.91	$(4\text{-}10)^+$		
4.917±0.003	≥ 6								
4.933±0.003	4	0.024	4.937	(4)	0.026	4.934	(2^+)		
4.954±0.004	3	0.017				4.953?	(4-6)		
4.973±0.003	3	0.026				4.973	$(3)^-$		
4.991±0.004	≥ 8		4.983	(6)	0.022				
5.010±0.003	9	0.017							
5.036±0.003	$J^\pi=2^-$ [c]					5.038	$(2)^-$		
5.072±0.003	(9)	0.039	5.079	10	0.030	5.077	$(5\text{-}10)^+$		
5.087±0.004	3	0.033							
5.128±0.003			5.110			5.127	$(2,3)^-$		
5.163±0.004						5.16			
5.194±0.004	3 [g]	0.016 [g]				5.20	$(8\text{-}10)^+$		
5.214±0.003			5.205	4	0.032,	5.211			
				3	0.028				
						5.236	0^+		
5.242±0.003			5.235	(3)	0.035	5.2446	$(2,3)^-$		

TABLE I.--Continued.

Present Work			54 MeV(p,p') Ref. 2			Compilation Ref. 23		Shell Model Study-Ref. 24	
$E_x \pm \Delta E_x$ [a]	L	β_L	E_x [a]	L	β_L [f]	E_x [a]	J^π	E_x [a]	J^π
5.274±0.005	3	0.013				5.281	0^-		
5.291±0.003	$J^\pi=1^-$ [d]					5.289	1^-		
5.321±0.004	3	0.017							
5.345±0.003	3	0.035	5.342	3	0.039	5.344			
5.370±0.006	5	0.016							
5.383±0.003						5.381			
5.417±0.004 [e]	(6)	0.015				5.41			
	(7)	0.016							
5.444±0.005	≥6								
5.483±0.003	5	0.045				5.482			
						5.507	-		
5.514±0.005 [e]	1&3	β_3= 0.038	5.515	(3)	0.055				
5.542±0.004	3	0.032				5.542			
						5.550	(2^+)		
5.564±0.003	2	0.017				5.563	(1,2)		
5.596±0.006						5.599	(3^-)		
5.615±0.004	≥6								
						5.629	(2^+)		
5.642±0.004 [e]									
5.658±0.003	5	0.022				5.652			
5.673±0.004	(3)	0.016							
5.689±0.003	4	0.045	5.690	4	0.051	5.685			
5.720±0.004 [e]	7	0.027				5.709			
5.743±0.004	9	0.019							
5.763±0.005	6	0.013							
5.777±0.004 [e]						5.777	(3)		
5.796±0.005						5.801	(2^+)		
5.813±0.004	3	0.028	5.808	(3)	0.026	5.810			

TABLE I.--Continued.

Present Work			54 MeV(p,p') Ref. 2			Compilation Ref. 23		Shell Model Study-Ref. 24	
$E_x \pm \Delta E_x$ [a]	L	β_L	E_x [a]	L	β_L [f]	E_x [a]	J^π	E_x [a]	J^π
5.842±0.006 [e]						5.833			
5.872±0.005 [e]	(3)	0.015				5.874	$(3)^-$		
5.898±0.004	(8)	0.016							
5.923±0.005	$J^\pi=2^-$ [c]					5.922	$(2)^-$		
5.948±0.006						5.942	1^-		
5.966±0.004	9	0.027				5.967	$(4)^-$		
5.993±0.003	6	0.049	5.988	3	0.044				
				4	0.004				
6.010±0.004	3	0.027				6.006	$(3,4^-)$		
6.035±0.005									
6.052±0.004	4	0.015				6.058			
6.082±0.005						6.083	$(2)^-$		
6.099±0.004									
6.170±0.007	2	0.0071				6.172	(2^+)		
6.191±0.005	3	0.020							
6.214±0.004 [e]									
6.233±0.005 [e]									
6.248±0.005 [e]	(7)	0.029	6.245	7	0.037	6.244			
6.261±0.006 [e]	$J^\pi=1^-$ [d]					6.258	(1)		
6.276±0.004									
6.314±0.005	(3)	0.015				6.311	1^-		
6.332±0.006	6	0.025							
6.353±0.006 [e]									
6.381±0.006 [e]	≈7	≈0.020							
6.393±0.006 [e]									
6.423±0.006 [e]									
6.443±0.006 [e]	7	0.024							
6.458±0.005									
6.483±0.006 [e]									

TABLE I.--Continued.

Present Work			54 MeV(p,p') Ref. 2			Compilation Ref. 23		Shell Model Study-Ref. 24	
$E_x \pm \Delta E_x$ [a]	L	β_L	E_x [a]	L	β_L [f]	E_x [a]	J^π	E_x [a]	J^π
6.529±0.006 [e]	(5)	0.026							
6.544±0.006									
6.572±0.005									
6.588±0.005									
6.615±0.005	3	0.023							
	4	0.026							
6.631±0.005									
6.658±0.005	4	0.023	6.525	$\simeq 7$	0.033				
6.688±0.005	5	0.041	6.675	≥ 6					
6.720±0.006 [e]									
6.737±0.005 [e]									
6.786±0.006									
6.801±0.005									
6.823±0.007									
6.843±0.006	(8)	0.021							
6.862±0.006									
6.876±0.005 [e]									
6.925±0.006 [e]	4	0.020							
6.940±0.006									
6.965±0.008	$J^\pi = 1^-$ [d]								
6.992±0.006	(3)	0.019							
7.019±0.007	(3)	0.021							
7.046±0.006									
7.061±0.005									
7.080±0.006									

TABLE I.--Continued.

Present Work			54 MeV(p,p') Ref. 2			Compilation Ref. 23		Shell Model Study-Ref. 24	
$E_x \pm \Delta E_x$ [a]	L	β_L	E_x [a]	L	β_L [f]	E_x [a]	J^π	E_x [a]	J^π
7.114±0.007	(3)	0.020							
7.174±0.005 [e]									
7.192±0.006	(4)	0.022							
7.219±0.008									
7.239±0.005	$J^\pi=1^-$ [d]								
7.268±0.008									
7.302±0.008 [e]	5	0.018							
7.325±0.007 [e]									
7.343±0.006									
7.382±0.009	(4)	0.021							
7.404±0.008 [e]									
7.549±0.008									
7.573±0.007									
7.594±0.007 [e]									
7.684±0.009									
7.723±0.008									
8.166±0.008									

[a] All energies in MeV.

[b] Level used in energy calibration.

[c] Spin and parity adopted from previous work of Ref. 23 or Ref. 24.

[d] Identified by similarity of angular distributions. Previous work (Ref. 13, 14, 23) give these as 1^- levels.

[e] Level with probable multiplet structure.

[f] Obtained from the transition rates, G_L, using $\beta_L = \sqrt{\frac{4\pi(2L+1)G_L}{Z^2(3+L)^2}}$

[g] Multiplet: β_L and L given for apparently dominant member.

nuclei the oxygen and carbon contaminant peaks appear wide in the lead spectra and these centroids are somewhat poorly determined. Also, the highest-lying ^{208}Pb state used in the calibration was the 4.423 MeV level. Thus the energies above 4.5 MeV are obtained by extrapolation. The errors in Table I reflect this since for states lying below 4.5 MeV the standard deviation in the measured energy is given as the error. Above 4.5 MeV, however, the given error includes an addition to the statistical error of 1.0 keV for each MeV of excitation to account for extrapolation as well as the uncertainties due to the increasing level density and the smaller cross sections.

Most states below 5 MeV of excitation appear to be completely resolved. Many states have been observed corresponding to levels identified previously in a variety of experiments. The 3.73 and 3.76 MeV levels reported in early $^{207}Pb(d,p)$ experiments[11] were not seen here and an upper limit of about 40 μb/sr can be set for excitation of these states by proton scattering at this energy. These states have not been observed in subsequent studies with either transfer or inelastic scattering reactions.

A peak at 4.256 MeV with a comparatively large spectral width is apparently an unresolved multiplet. A 4.251 MeV level has been seen in a (p,t) and (t,p) study at 20 MeV with 17 keV resolution performed by Igo et al.[12] A state at 4.253 has been observed in (d,pγ) studies.[13] Neither work indicated the possibility of multiplet structure. A possible doublet at about this excitation has been seen in

isobaric resonance work[14] with 9-13 keV resolution. Using the energy corrections of Reference 23 the members of the doublet lie at 4.253 and 4.259 MeV. Heusler et al.[24], using shell model systematics and a global compilation of experimental results, have concluded this multiplet to be a 4.255, 4.256, and 4.261 MeV triplet with $J^{\pi} = 3^-$, 4^-, and 5^-, respectively. The angular distribution for the 4.256 MeV multiplet, seen in Figure 2, is fairly well structured but can not be fit with a single ℓ-transfer again suggesting an unresolved multiplet at this energy.

The density of states above 5 MeV of excitation becomes increasingly large. Most of the states appear to be completely resolved but those states whose widths indicate possible multiplet structure have been indicated in Table I. In general, the poor statistics and narrow line shape prohibit reliable fitting with numerical techniques. The level at 5.194 MeV was revealed as a doublet at several angles. The previously reported[12] 5.236-5.245 MeV doublet was not resolved. The level seen here at 5.242 MeV has no apparent doublet structure suggesting that the 5.236 MeV level (reported in Reference 12 as a 0^+ 2p-2h excitation) is not populated here. A level near 5.5 MeV of excitation has been identified in many different experiments but the uncertainty in energy and spin-parity assignments suggests strongly that two states were separately observed. (See Section III-D-1).

Interestingly, eight states that had been previously reported were not found in the spectra: the 4.859, 4.968, 5.550, 5.629, 5.801, and 5.862, 5.937, and 5.973 MeV levels. These states were seen in two neutron transfer by Igo et al.[12] and have been identified as configurations with predominant 2p-2h admixtures. That these states are not excited in (p,p') is consistent with viewing inelastic proton scattering as mediated by a one body operator. A level at 5.236 MeV has been identified as a 0^+ 2p-2h level as well as a 3^- state[12,13,17]. We were unable to identify the ℓ-transfer for the observed 5.242 MeV level.

Above 6 MeV many states were also observed. At these excitation energies, states excited by inelastic scattering and levels seen with other reactions may not correspond to the same nuclear state. Due to the uncertainty in excitation energy and the increased level density comparison other than in Table I will not be made.

B. Inelastic Angular Distributions

The angular distributions for all resolved peaks resulting from inelastic scattering are shown in Figures 2 through 5. The cross sections are displayed with their corresponding excitation energies. The error bars indicate statistical errors and were drawn only when greater than the symbol size. It should be emphasized that the curves passing through the data in these figures have been drawn merely as a guide and

FIGURE 2.--Measured inelastic cross sections for ^{208}Pb. The lines drawn through the points are merely to guide the eye and do not represent fits to the data. The excitation energy of the levels is given in MeV.

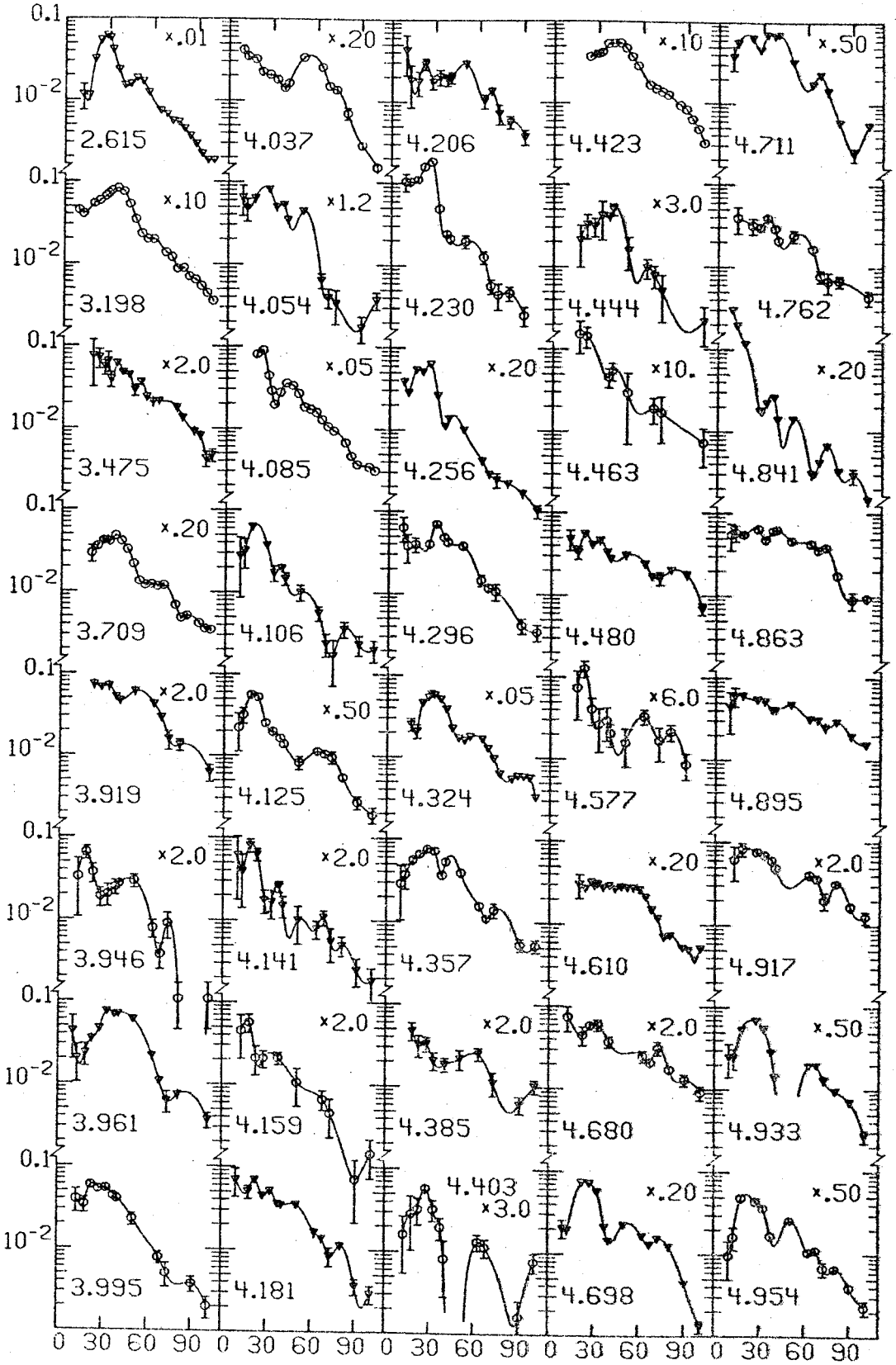
0.1
10^{-2}
×.01
2.615
×.20
4.037
4.206
×.10
4.423
×.50
4.711
×.10
3.198
×1.2
4.054
4.230
×3.0
4.444
4.762
×2.0
3.475
×.05
4.085
×.20
4.256
×10.
4.463
×.20
4.841
×.20
3.709
4.106
4.296
4.480
4.863
×2.0
3.919
×.50
4.125
×.05
4.324
×6.0
4.577
4.895
×2.0
3.946
×2.0
4.141
4.357
×.20
4.610
×2.0
4.917
×2.0
3.961
4.159
×2.0
4.385
×2.0
4.680
×.50
4.933
4.403
×3.0
3.995
4.181
×.20
4.698
×.50
4.954
0 30 60 90

FIGURE 2

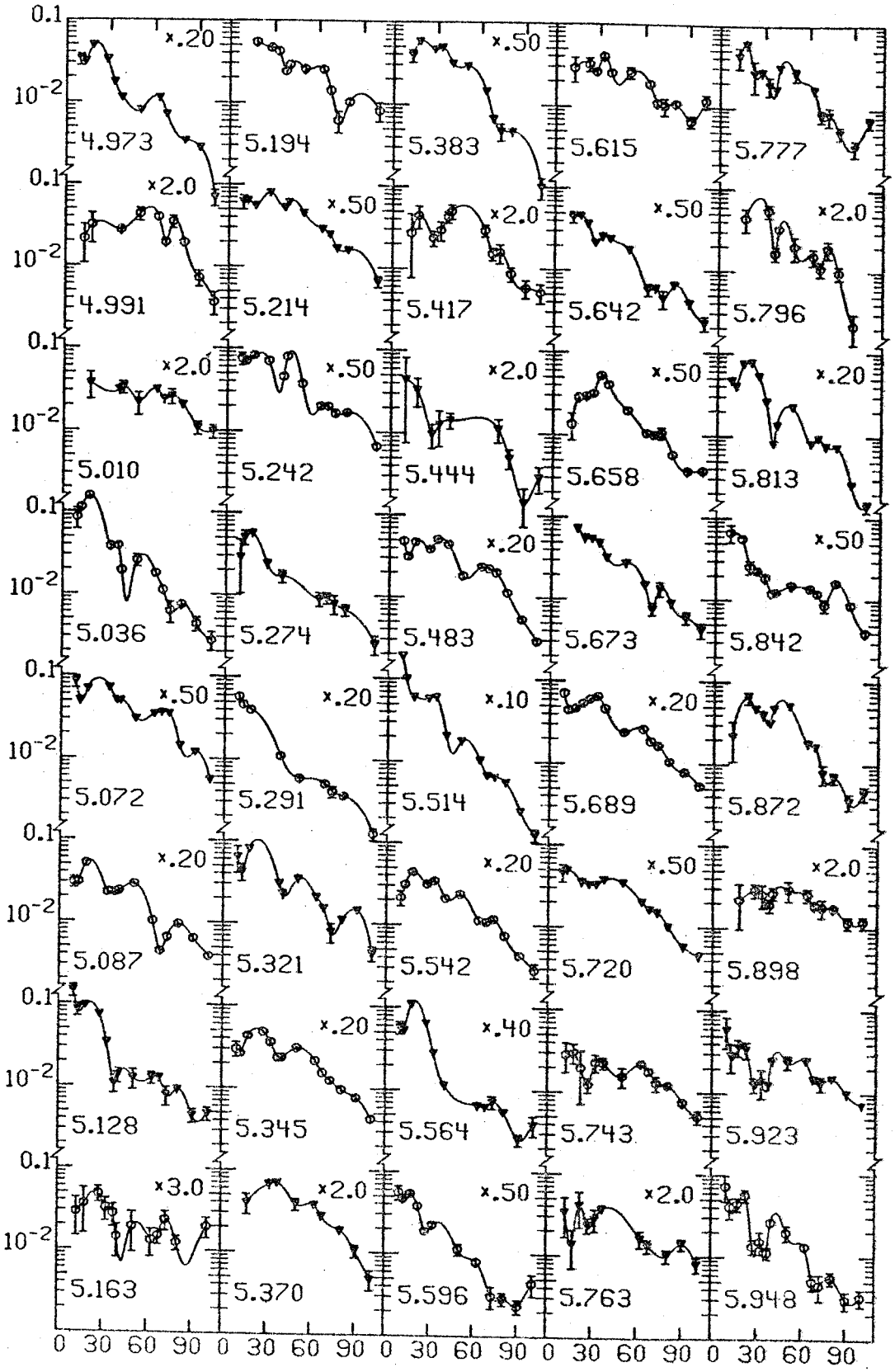

FIGURE 3.--Same as Figure 2.

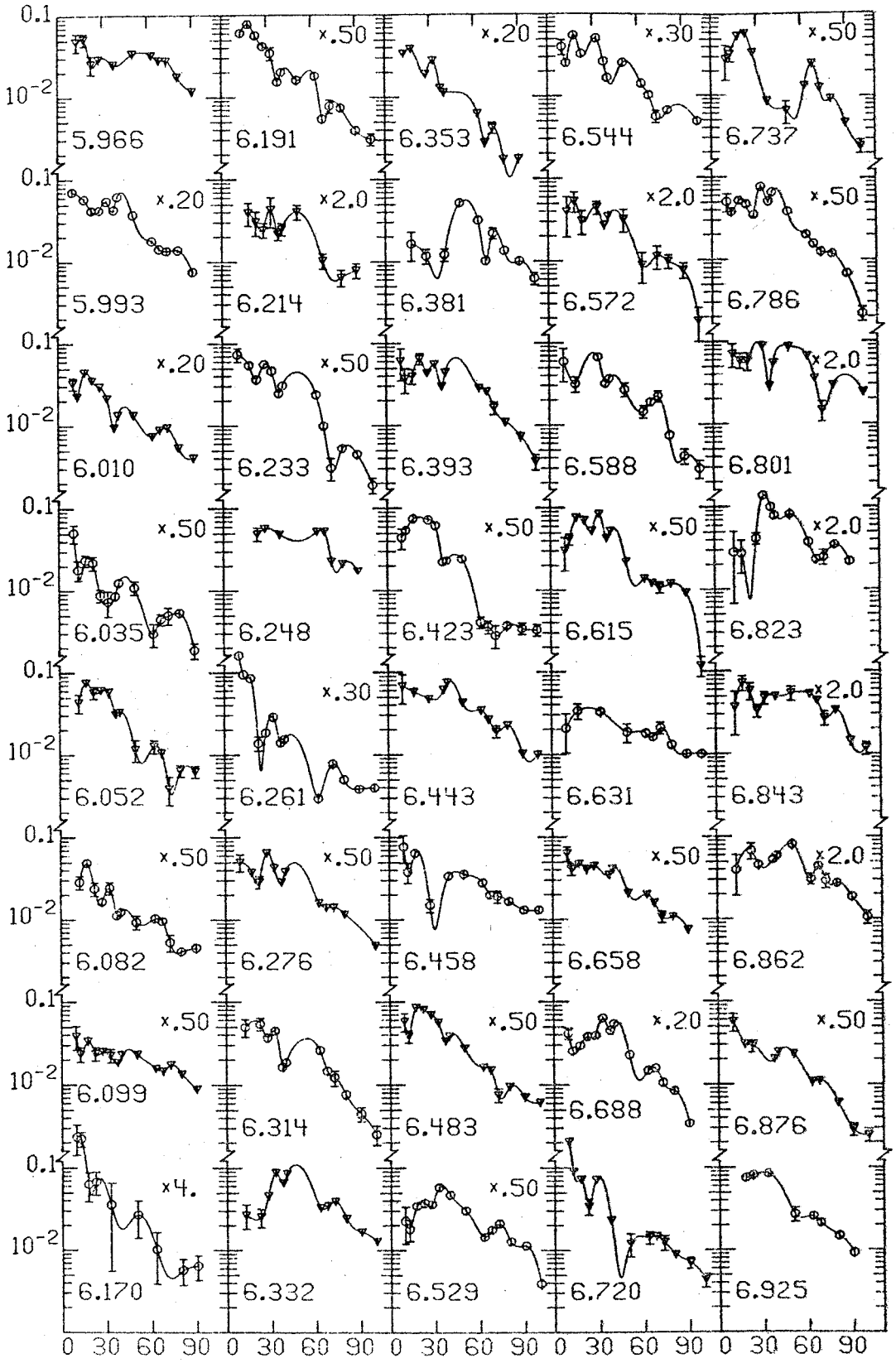

FIGURE 4.--Same as Figure 2.

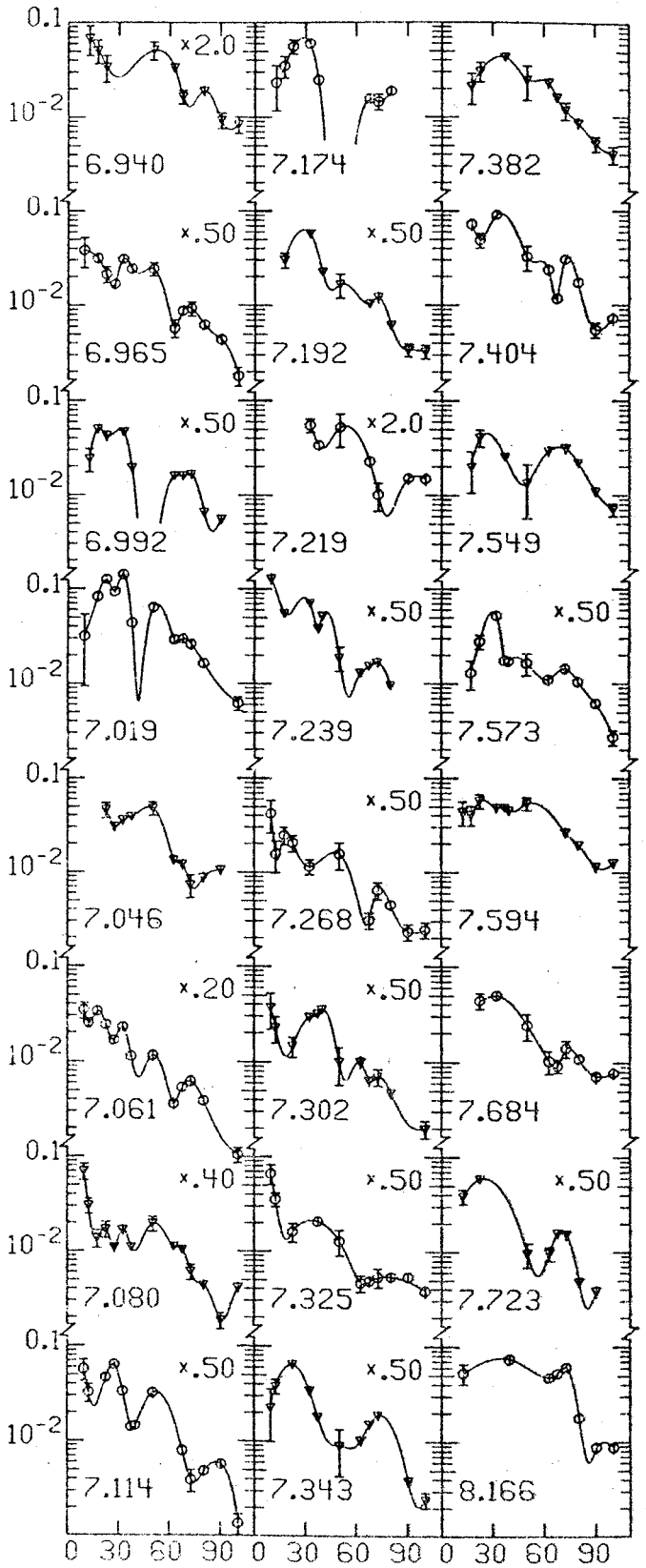

FIGURE 5.--Same as Figure 2.

do not represent theoretical fits to the curves. Gaps in the angular distributions at certain angles are due to obstruction of the peaks of interest by reaction products from the various contaminants in the target.

Since the plate results were normalized by comparison to the counter data, normalization errors due to the poorer quality counter resolution should be considered. The first 3^- and first and second 5^- levels, that is the levels emphasized in the normalization, were completely resolved in both sets of data. In the counter data, however, the 2^+, 4^+, 6^+, and 8^+ states were not completely separated from nearby levels. In the counter data, some neighboring states either were partially resolved from the stronger states, as in the case of the 7^- level being almost completely resolved from the 2^+ level, or had cross sections which were negligible compared to the more populated levels. In the latter case, the weaker peaks contributed no more than 5 per cent error to the counter data cross sections for the higher excitation energy levels.

C. Discussion of the Collective Model

A Distorted Wave Born Approximation (DWBA) angular distribution has a characteristic shape determined by the strengths of each ℓ-transfer involved in the transition. In turn, the strength of each ℓ-transfer is determined by the strengths of the nonspin-flip and spin-flip modes of

excitation. Since ^{208}Pb has a 0^+ ground state, all natural parity transitions can involve only one ℓ-transfer in the direct DWBA theory. For transitions to a natural parity state, knock-on exchange effects at 35 MeV usually preserve the shape of the direct cross section and merely increase the total cross section. For a spherical nucleus such as ^{208}Pb, the collective vibrational model can be used to obtain the characteristic ℓ-transfer shape and also to give the deformation parameter, β_L, which can be related to the rate of electromagnetic decay from the excited state to the ground state.

The DWBA collective model uses a deformed optical potential as the form factor for inelastic scattering. The optical potentials are usually obtained from fits to elastic scattering data and a number of sets of parameters for ^{208}Pb in this energy region has been determined.[4,5,9,25] Figure 6 displays the 35 MeV proton elastic scattering angular distribution measured with the wire counter. Also shown are the results of calculations for elastic scattering from ^{208}Pb using the Becchetti-Greenlees (BG) best-fit optical model parameters[21] and also parameters resulting from a search on the data with the code GIBELUMP.[26] The search was initialized with the BG values but there was no variation of the BG spin-orbit potential since 35 MeV polarization data was not available. Both the original and fitted sets yield predictions in good agreement with the

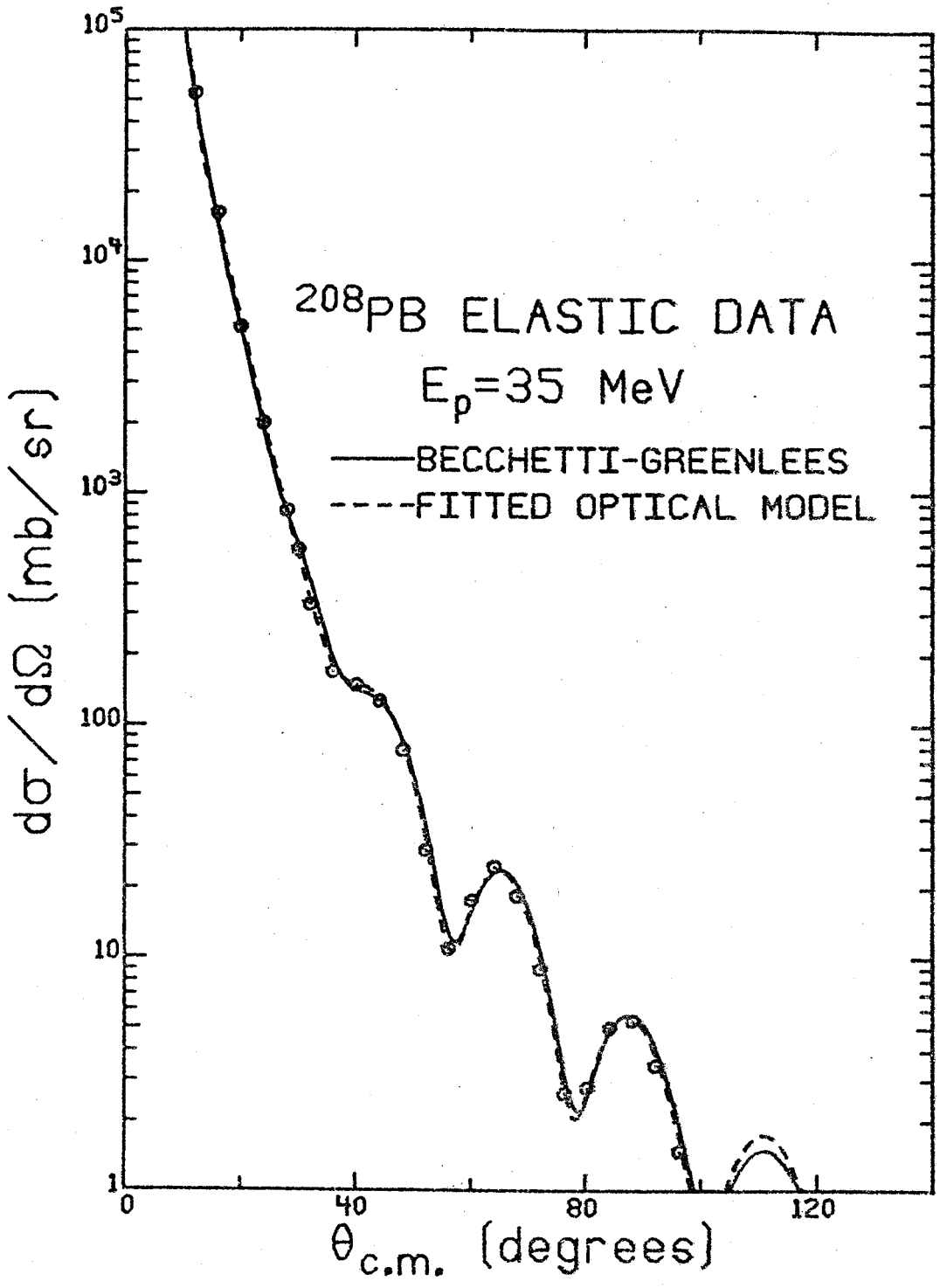

FIGURE 6.--Comparison of the measured elastic angular distribution with calculations described in the text.

data and differing only slightly from one another. Similar results were obtained in searches using real and imaginary geometries of other ^{208}Pb optical models as initial values and simply adopting their spin-orbit geometries.

Two sets of CM DWBA calculations were performed for ℓ-transfers of 2, 4, and 6 to determine the sensitivity of the β_L's to the optical potentials. In one set of calculations, the BG optical model was used for the entrance channel and form factor while the other set used the fitted optical model values. Both sets had identical exit channel parameters. Due to the much deeper surface imaginary well there was a 30 per cent larger total cross section predicted with the fitted parameters than with BG. However, the ratio of cross sections for L=2,4,6 was the same for each set. This corresponds to an overall normalization of the DWBA and has been noted before.[2]

Because the BG parameters are functions of the particle energy, the energy dependence of the incoming and outgoing distorted waves may be accounted for. Since the asymmetric optical potentials may be used, because the elastic cross section was not measured at larger angles, and because the spin-orbit geometry could not consistently be determined in the search it was decided to use the BG model in all subsequent DWBA calculations. This also made renormalization of the CM unnecessary.

D. ℓ-transfers and Deformation Parameters

CM calculations were performed with the code DWUCK[27] using the BG optical parameters. Tests involving Q-value dependence of the cross sections indicated little sensitivity and a Q=-5 MeV was assumed for each ℓ-transfer for each calculation. Coulomb excitation was included in the L=2 and 3 cases although only the smaller ℓ-transfer receives notable contribution from this mode of excitation. Integration was carried out to 20 fm and 40 partial waves were used. The fits to the states are displayed in Figure 7 and 8 and are commented on below. The ℓ-assignments were made by comparing the data with both the theoretical angular distributions and, where possible, the experimental cross sections for states with unambiguous ℓ-assignments. The β_L's, the deformation parameters, were obtained from $\beta_L^2=\sigma_{exp}/\sigma_{th}$. Both the β_L and ℓ-transfer assignments are given in Table I for comparison with the measurements of Reference 2. Where possible those states with angular distributions of unidentifiable shape have J^{π} adopted from the work of Reference 23 or Reference 24.

Table II compares measured deformation parameters of states in ^{208}Pb that have been studied in (p,p') at many different energies. The deformation parameters appear to be energy dependent. Knock-on exchange does have similar energy dependence. However, as commented above, the optical model used in the CM can also lead to marked differences.

FIGURE 7.--Collective model fits for all identified states. Displayed with the fit is the excitation energy of the state and the deformation parameter, β_L, corresponding to orbital angular momentum transfer L.

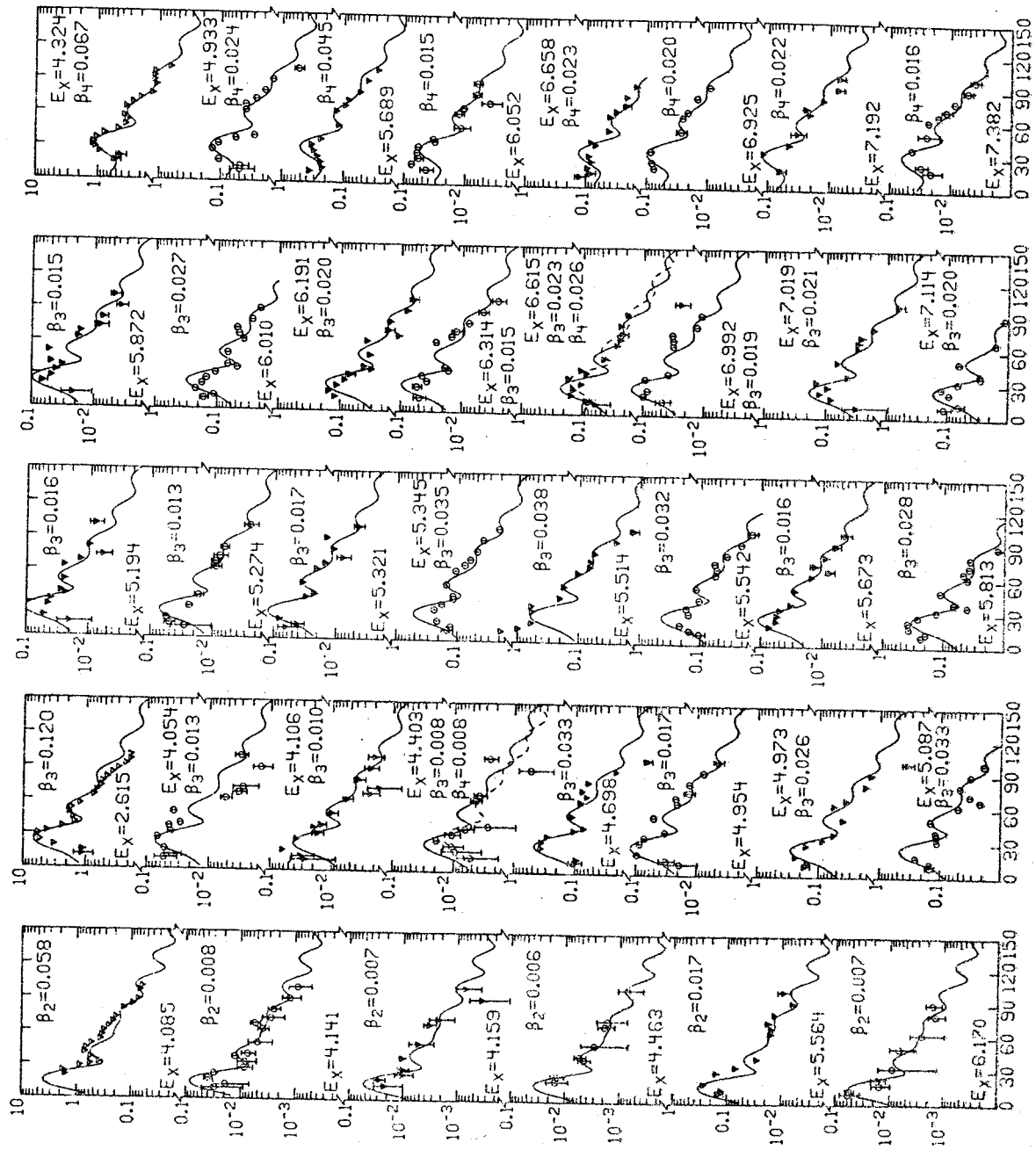
Ex=4.085
β2=0.058
Ex=4.141
β2=0.008
Ex=4.159
β2=0.007
Ex=4.463
β2=0.006
Ex=5.564
β2=0.017
Ex=6.170
β2=0.007
Ex=2.615
β3=0.120
Ex=4.054
β3=0.013
Ex=4.106
β3=0.010
Ex=4.403
β3=0.008
β4=0.008
Ex=4.698
β3=0.033
Ex=4.954
β3=0.017
Ex=4.973
β3=0.026
Ex=5.087
β3=0.033
Ex=5.194
β3=0.016
Ex=5.274
β3=0.013
Ex=5.321
β3=0.017
Ex=5.345
β3=0.035
Ex=5.514
β3=0.038
Ex=5.542
β3=0.032
Ex=5.673
β3=0.016
Ex=5.813
β3=0.028
Ex=5.872
β3=0.015
Ex=6.010
β3=0.027
Ex=6.191
β3=0.020
Ex=6.314
β3=0.015
Ex=6.615
β3=0.023
β4=0.026
Ex=6.992
β3=0.019
Ex=7.019
β3=0.021
Ex=7.114
β3=0.020
Ex=4.324
β4=0.067
Ex=4.933
β4=0.024
Ex=5.689
β4=0.045
Ex=6.052
β4=0.015
Ex=6.658
β4=0.023
Ex=6.925
β4=0.020
Ex=7.192
β4=0.022
Ex=7.382
β4=0.016
0 30 60 90 120150

FIGURE 7

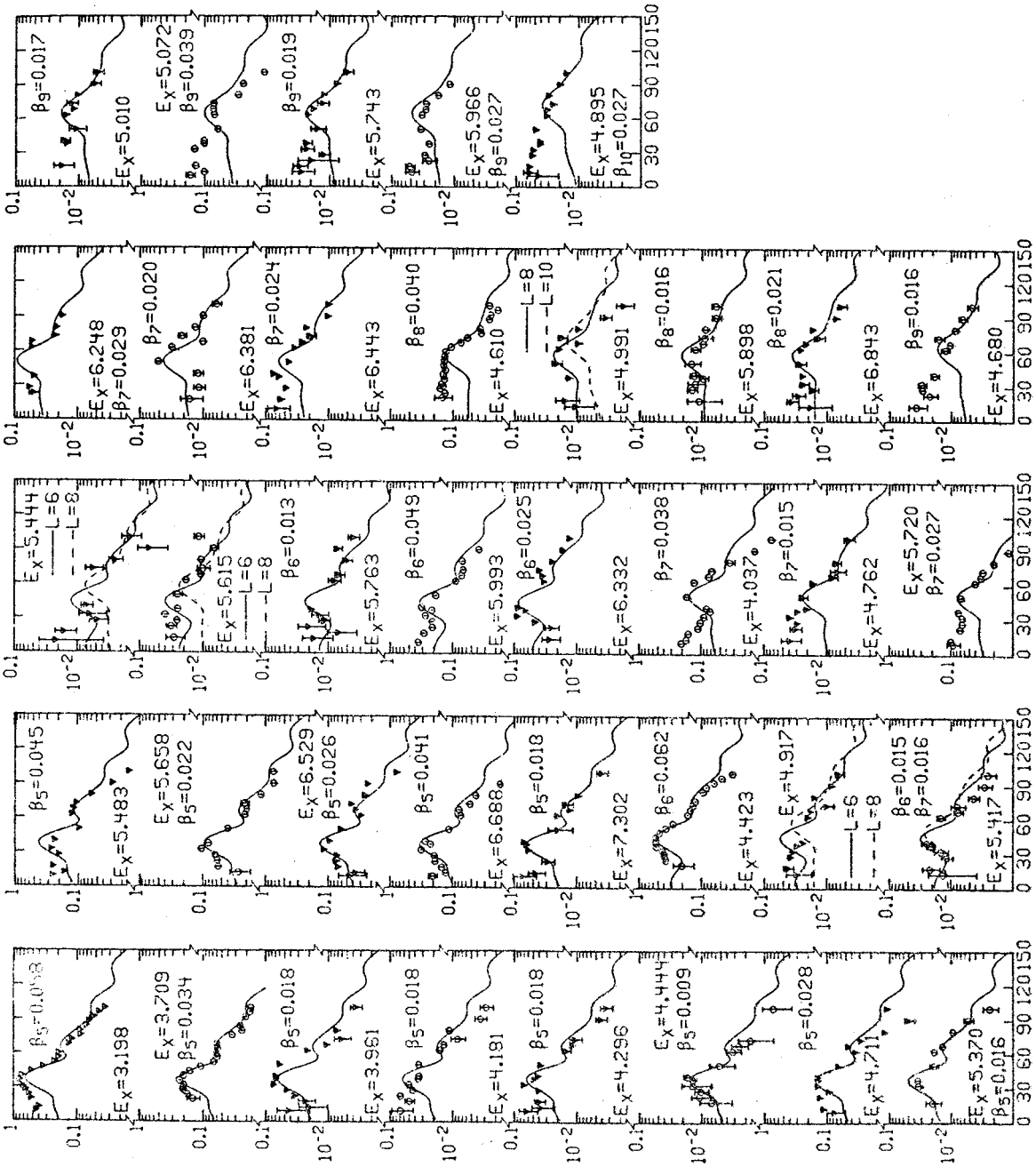

FIGURE 8.--Same as Figure 7.

TABLE II.--(p,p') collective model results.

E_x(MeV) / J^π / E_p	2.615 3^-	3.198 5^-	3.709 5^-	4.085 2^+	4.324 4^+	4.423 6^+	4.610 8^+
24.5[a]	0.12	0.072	0.034	0.058	0.066	0.057	0.045
30[b]	0.13						
30.3[c]	0.11						
31.0[d]	0.13						
35.0[e]	0.126	0.058	0.034	0.058	0.067	0.062	0.040
40.[f]	0.11						
40[g]	0.11	0.059		0.059			
54[h]	0.11	0.055	0.035	0.058	0.069	0.064	0.039
61[i]	0.098	0.043	0.027	0.053	0.062	0.055	0.039

[a] Ref. 1
[b] Ref. 7
[c] Ref. 9
[d] Ref. 4
[e] Present work
[f] Ref. 5
[g] Ref. 6
[h] Ref. 2
[i] Ref. 8

D-1. The 1^- states

The levels at 4.841, 5.291, 6.261, 6.965, and 7.239 MeV have fairly similar angular distributions, as seen in Figure 9. All are fairly strongly forward peaked and have angular distributions that oscillate together in phase. These levels have been identified[13,23] as electric dipole levels and the data appears consistent with these assignments.

At energies below 35 MeV both resonant[14,15] and non-resonant[1] (p,p') experiments reported states at about 5.505 MeV. A 5.505 MeV state seen in a resonant (p,p'γ) study[16] was assigned a spin of 1^- on the basis of its ground state gamma decay strength. ^{207}Pb(d,pγ) results[13] indicated a 1^- level at 5.506 MeV as did the two neutron transfer study of Reference 12. However, the 54 MeV inelastic proton study[2] found an unresolved doublet at 5.515 MeV and assigned a tentative 3^- spin. We observe an apparent multiplet at 5.514 MeV which has a large forward angle cross section, like the 4.841 and 6.261 MeV states, but is fit well at larger angles by an L=3 characteristic shape. These facts suggest that this excitation is a doublet with dipole and octupole members.

States near 5.94 and 6.31 MeV have been seen in (d,pγ) measurements[13] as dipole levels. A two neutron transfer experiment[12] also tentatively reported 1^- levels at 7.176, 7.319, 7.387, 7.480, and 7.523 MeV of excitation energy.

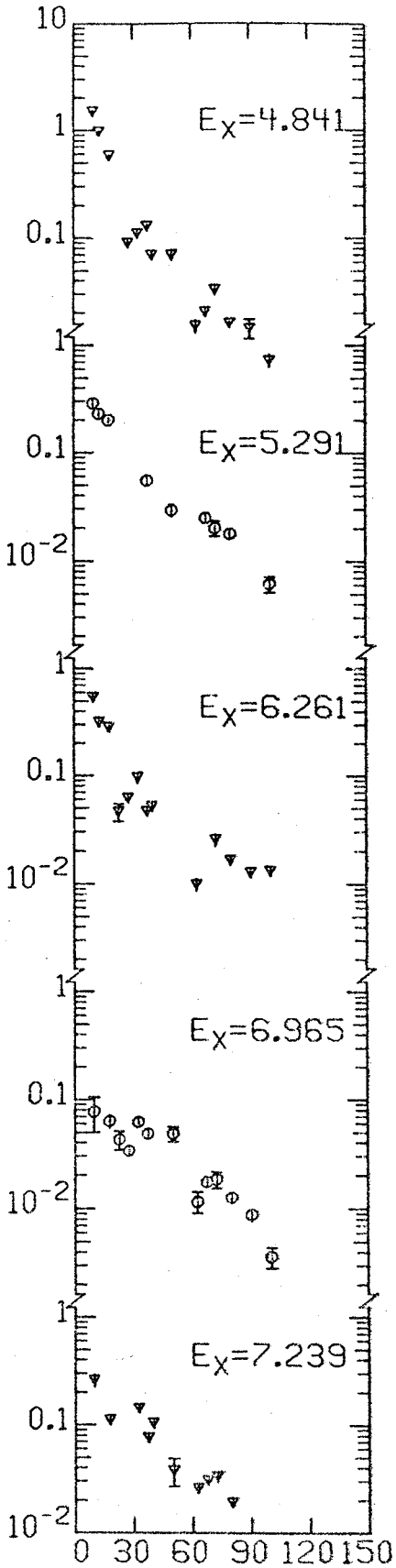

FIGURE 9.--Data for those states which have been previously identified as 1^- levels.

Here, there is no marked similarity in angular distributions of levels near these excitations with those of the levels identified above as 1^-.

D-2. Search for 1^+ states

Considerable attention has been given to the search[28,29] for magnetic dipole states in heavy mass nuclei. A recent study with 180° electron scattering[29] identified probable M1 transitions to levels at 6.2 and 7.9 MeV. Our data reveals two states which may correspond to the magnetic dipole levels identified in (e,e'). The strength of the state found at 6.233 MeV is given fairly well by a microscopic calculation using the 1^+ wave functions of Broglia et al.[30] (This calculation used the methods described in Section IV-B, below, and included central and non-central forces and exchange effects.) Not only is the magnitude well estimated but the shape is reasonably reproduced, as shown in Figure 10. A level at about 8.01 MeV has a cross section which peaks at forward angles as does the 6.233 MeV state but is unfortunately obscured by contaminants or adjacent ^{208}Pb levels at most angles. This state may correspond to the 7.9 MeV level observed in the electron scattering study and is presumably the $\Delta T\tilde{=}1$ excitation, the lower excitation being $\Delta T\tilde{=}0$. Theoretical wave functions[30,31,53] for 1^+ levels in ^{208}Pb all give ground state transition widths of about 2 eV and 80 eV for the first and second 1^+ levels,

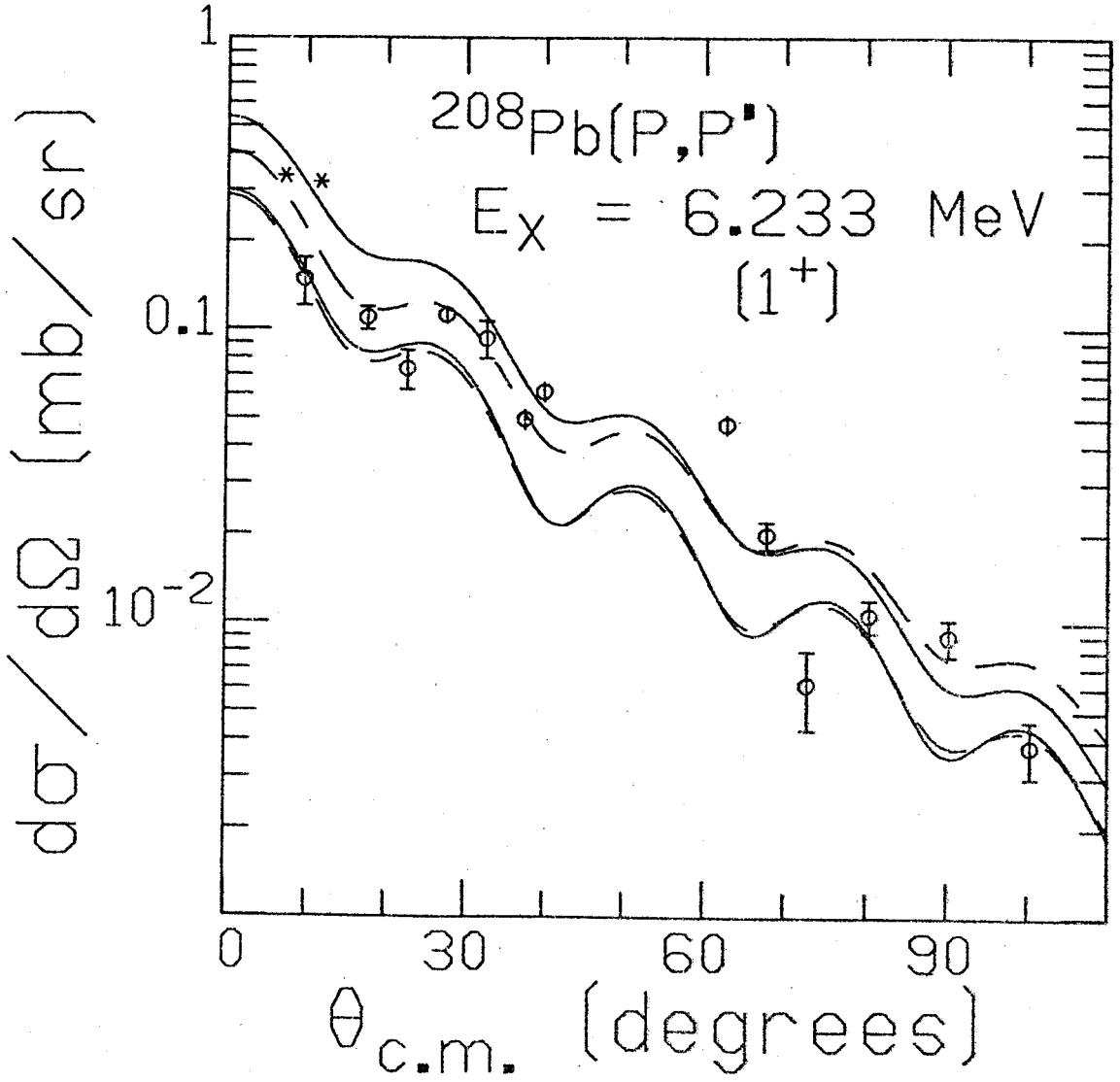

FIGURE 10.--Angular distribution for the 6.233 MeV level. The solid lines correspond to calculations done with both central and non-central forces; the dashed curves show results with only a central force. The asterisks indicate calculations including exchange effects. The curves without the asterisks show the direct contribution to the cross section only.

respectively. The (e,e') experiment reported transition widths of 11 and 44 eV for the 6.2 and 7.9 MeV transitions. The proton data is quite insensitive to mixing of the wave functions whereas the (e,e') excitation proceeds mainly through $\Delta T=1$ transitions. Calculations with the wave functions of Reference 31 suggests that a 10 per cent admixture of the $\Delta T\tilde{=}1$ state into the $\Delta T\tilde{=}0$ state will produce agreement of theory with the experimental (e,e') results. This admixture does not affect the calculated (p,p') cross sections if the nucleon-nucleon interaction has a Serber exchange mixture. Thus, the present data supports identification of the 6.23 and 8.01 MeV levels as magnetic dipole levels.

D-3. The 2^+ states

We have identified six probable quadrupole levels. The well-known 2^+ state at 4.085 MeV is a dominant feature of any inelastic proton spectrum. Two nearby states at 4.141 and 4.159 MeV are also tentatively identified as L=2 states and it seems fairly certain that the excitations at 4.463, 5.564, and 6.170 MeV are also 2^+ states. The observed 2^+ states have about 20 per cent of the total expected strength given by an energy-weighted sum rule (ESR).[32]

As mentioned previously, states excited in (p,t) and (t,p) studies[12] and identified as 2p-2h quadrupole levels were not seen here.

D-4. The 3^- levels

Many transitions involving angular momentum transfers of 3 were observed and transition strengths were extracted for them. The first excited state, with transition strength of 39.6 single particle units (SPU), exhausts about 20 per cent of an ESR,[32] revealing it as a truly collective state. Totally, the observed 3^- excitations contribute about 50 per cent to the isoscalar octupole ESR strength predicted for ^{208}Pb. Further, the observed 3^- strength is quite fractionated and many of the levels identified were previously unreported.

D-5. The 4^+ levels

A number of 4^+ states have been determined. The collective model fits to the well known 4.423 MeV level and other L=4 levels are shown in Figure 7. The angular distributions of the 4.403 and 6.615 MeV states are fit equally well by L=3 and L=4 characteristic shapes so that the ℓ-transfer is not uniquely determined for these levels. The level at 5.689 MeV is quite collective with a transition strength of about 6 SPU.

D-6. The 5^- states

Numerous states were found whose measured cross sections were similar to L=5 collective model calculations. The first two 5^- levels at 3.198 and 3.709 MeV are very collective with deformation parameters of 10.5 and 3.6 SPU,

respectively. The states at 5.483 and 6.688 MeV have inelastic transition rates of 6.3 and 5.2 SPU, respectively, revealing a rather large concentration of strength at high excitation. The 3.961 MeV level was previously suggested to be a 4^- unnatural parity excitation with possible doublet properties.[23] Our assignment of 5^- is in agreement with the conclusions of Reference 12 and 24.

D-7. 6^+ states

Besides the well-known 6^+, 4.424 MeV level other levels with shapes corresponding to L=6 were found. There is some ambiguity in assigning a spin of 6 to the 5.417 MeV level as it is probably equally well described by an L=7 shape. The 4.917, 5.444, and 5.615 MeV levels apparently involve ℓ-transfers of 6 but an exact assignment cannot be made.

D-8. States with $L \geq 7$

Transitions with large ℓ-transfer have angular distributions which fall off less rapidly and whose maxima occur at larger angles than those involving small ℓ-transfer. For $L \leq 6$ these two features generally make an assignment fairly unambiguous but for $L \geq 7$ the distinction is not so clear. The data for the 4.037 MeV level, for example, has a maximum near 60° fit by L=7 or L=8 curves but has a very rapid fall-off so that a J^π of 7^- is concluded for this level. Reference 14 has suggested a $(7^-,6^-)$ doublet at this

energy while Reference 12 identified a 7^- both supporting our identification. As exemplified by this state and as noted by Lewis et al.[2] the predicted collective model cross section for large momentum transfer usually underestimates the forward angle data, the difference between the data and the theory apparently being greater for the high spin cases. This fact and the lack of distinct shapes for states with spins larger than 6 makes ℓ-transfer identification tentative.

IV. APPLICATIONS OF THE MICROSCOPIC MODEL

A. Comparison with (e,e') for the Strongly Excited States

Inelastic electron scattering allows the portion of the proton transition density, important to low momentum transfer (p,p'), to be determined fairly unambiguously. Unfortunately (e,e') gives little information about the neutron motion in nuclear excitations. However, it appears that for collective states the ratio of the neutron to the proton transition density is the same as the ratio of the neutron number to the atomic number of the nucleus.[33-35] Bernstein[33] has shown this prescription to work well for inelastic alpha scattering.

In applying this prescription to (p,p'), we have assumed that the spin-flip and non-central forces contribute negligibly in transitions to the normal parity states. The

DWBA form factor, F^{JOJ}, for a transition to a state of spin J was obtained following Reference 36. Basically,

$$F^{JOJ} = \int (V_{pp}^{JOJ} + \frac{N}{Z} V_{pn}^{JOJ}) \rho_p r^3 dr$$

where ρ_p is the proton transition density obtained from (e,e'). V_{pp}^{JOJ} and V_{pn}^{JOJ} are the strengths of the J^{th} multipole of the proton-proton and proton-neutron interactions, respectively. Here, the interactions were effective bound state potentials (G-matrix) obtained from the separated Hamada-Johnston potential. To account for knock-on exchange the zero-range approximation of Petrovich[37] was adopted. In this approximation a zero-range pseudo potential is added to each interaction to account for the exchange process. Similar calculations[36,38,39] have been successful in other nuclei.

The charge transition densities were obtained from the work of Nagao and Torizuka[40] and of Heisenberg and Sick.[41] Since the effect of the finite proton size is small in the lead region, this correction was neglected and for each transition the proton density was taken to be the experimental charge density. The only exception was the 6^+ level. Since the experimental best fit parameters were not reported[40] the (e,e') data for this level was fit using a transferred-momentum-corrected Born approximation. The density had the radial form

$$\rho_p^J(r) = Nr^{J-1} \frac{d}{dr} \left(1+\exp\left(\frac{r-C}{A}\right)^2\right)^{-1}$$

where N is related to the B(EJ) for the transition and C and A are the usual nuclear surface parameters. Also, for the 3^- level there was some ambiguity in the transition rates. Nagao and Torizuka give a B(E3)=43.5 SPU while Heisenberg and Sick have used 39.5±2.2 SPU which was adopted from work of Ziegler and Peterson[42] involving low energy electron scattering data. A recent measurement of Friedrich[43] gives a value of 34.2±2.2 SPU. (A difference of about 5 SPU leads to about a 30 per cent difference in the (p,p') cross sections for the 3^- state.) Here, the transition density of Heisenberg and Sick was used in the calculations for the 3^-. Their B(E3) is in good agreement with the β_3=39.6 SPU extracted here using the CM (Section III-D-4). The parameters of the transition density for each state considered are given in Figure 11. The first 3^-, 2^+, 4^+, 6^+ as well as the first two 5^- levels are examined.

The results of these calculations are given in Figure 11. The dashed curves show results with (long dash) and without (short dash) the exchange approximation. The solid curve was calculated with a form factor which was the sum of the (real) approximate exchange (e,e') form factor and an imaginary CM form factor. Complex coupling has given improved fits in other studies of (p,p').[44] The strength of the imaginary form factor was obtained by comparing the cross section of a purely real CM calculation

FIGURE 11.--Results of calculations for the strongly excited states seen in both (p,p') and (e,e'). The lower and upper dashed curves correspond to calculations with and without the exchange approximation, respectively. The solid curve includes complex coupling effects as explained in the text.

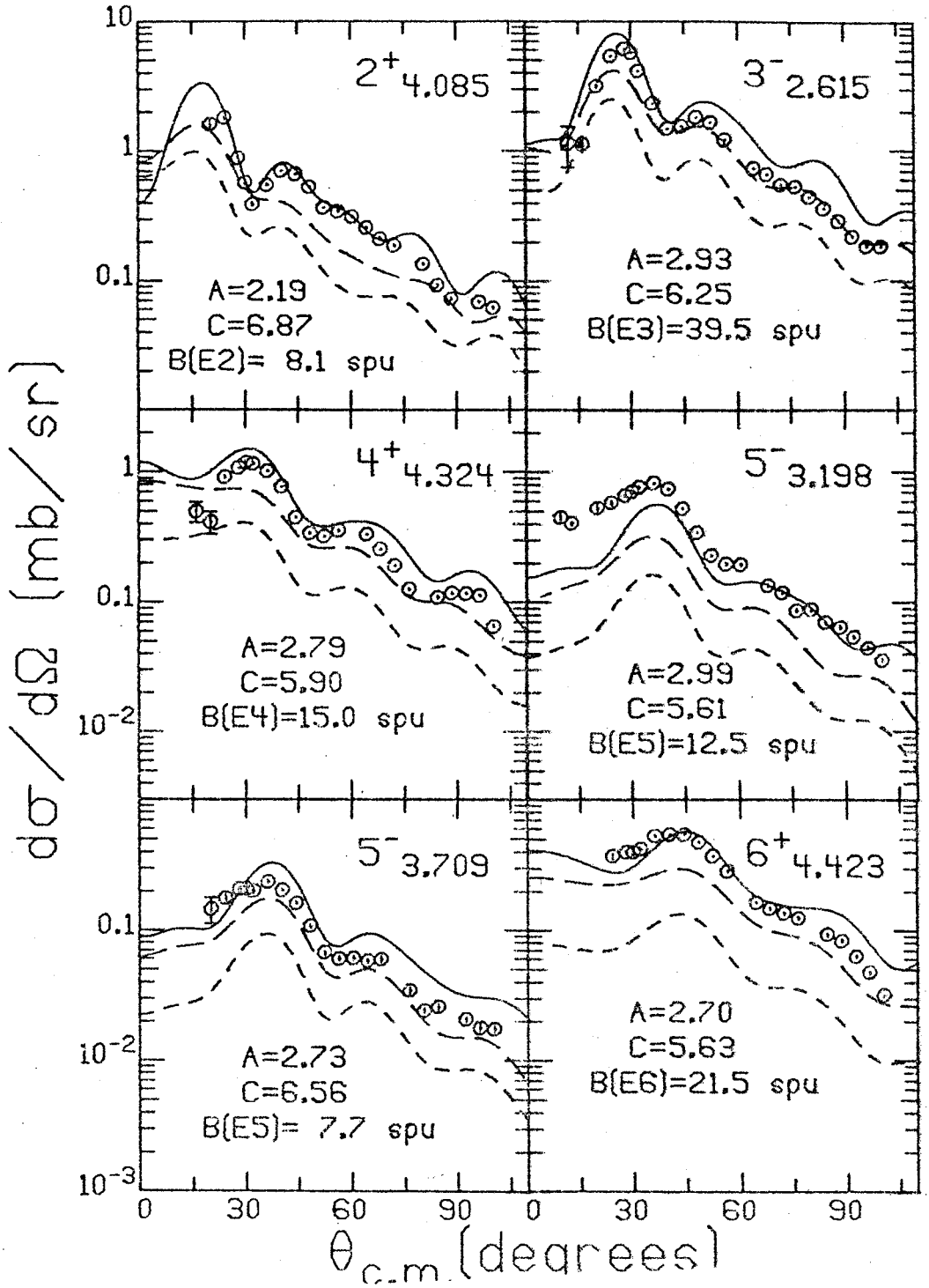
2+ 4.085
A=2.19
C=6.87
B(E2)= 8.1 spu
3- 2.615
A=2.93
C=6.25
B(E3)=39.5 spu
4+ 4.324
A=2.79
C=5.90
B(E4)=15.0 spu
5- 3.198
A=2.99
C=5.61
B(E5)=12.5 spu
5- 3.709
A=2.73
C=6.56
B(E5)= 7.7 spu
6+ 4.423
A=2.70
C=5.63
B(E6)=21.5 spu
dσ / dΩ (mb/sr)
θc.m (degrees)

FIGURE 11

with the approximate exchange (e,e') results to obtain an effective deformation parameter. Since the 2^+ state is the only one of these states significantly excited by the Coulomb interaction, the solid curve for this state includes both complex coupling and Coulomb excitation.

The first 5^- state is the only level underestimated by these calculations. Using the data of Friedrich[43] for this state, a slightly larger estimate can be made but the data is still underestimated. This indicates that the neutron and proton transition densities are not in the assumed ratio of N:Z. Indeed, the wave function used in calculations in Section IV-C has a neutron density larger than N/Z times the proton transition density and gives a better prediction of this state's inelastic strength.

For the other levels the slight overestimation is consistent with the use of the zero-range exchange approximation.[37] Further, the prescription used for the complex coupling assumes that the processes giving rise to the imaginary portion of the inelastic form factor are as constructively coherent as the processes leading to the imaginary part of the optical model potential. This need not be true so that the present prescription probably gives an upper limit for the imaginary portion of the inelastic form factor.

In conclusion, these results generally support the assumption about the ratio of the neutron and proton motions

and the dominance of the central, non-spin-flip forces in collective excitations. The transition to the first 5^- state suggests that these assumptions may not always be true. The results also support the validity of the microscopic prescriptions that were used.

B. Phenomenological Wave Functions

This section considers the results of calculations done with the phenomenological wave functions of Heusler and von Brentano.[24] These authors, using a global compilation of ^{208}Pb data involving particle transfer, gamma-ray, and (p,p') resonant data, have examined the excitation energy region in ^{208}Pb below about 4.7 MeV. This work has resolved many problems and raised interesting new questions. From shell model arguments, possible coupling schemes, and orthogonality requirements, spin and multi-component wave functions have been determined. The orthogonality conditions permit proton configurations as well as the relative signs of the proton and neutron components to be extracted. However, the orthogonality is only approximate, resulting in some ambiguity in the signs.

Microscopic model calculations using these wave functions were performed. Since many of the states examined have unnatural parity, contributions from the non-central forces may be expected to be comparable to those of the central potential. To perform calculations with non-central forces

the code DWBA70[45] was used. The numerical form of the program prevented use of externally calculated transition densities or the realistic effective interaction used in the (e,e') calculations. The Serber exchange mixture was used for the effective interaction. This effective force has been found[46,47] to be a good representation of the phenomenological force determined by fitting definitive reaction data and of the low momentum components of the separated Hamada-Johnston potential. The Serber mixture had strengths of -30:10:10:10(MeV) and the radial form was taken to be a 1 fermi range Yukawa. The tensor force was taken from the works by Crawley et al.[48] and by Fox and Austin[49] and resulted from fitting the crucial (1^+,T=0) to (0^+,T=1) transition in $^{14}N(p,p')^{14}N$(2.31 MeV) with a tensor force of OPEP form and with a r^2-Yukawa shape. The range was obtained by matching the OPEP potential and the strength adjusted to fit the nitrogen data. This study assumed that the tensor isoscalar portion was zero. The $\underline{L}\cdot\underline{S}$ force was taken from studies by Fox and Austin,[49] in which the spin-orbit potential was obtained by matching the cut-off Hamada-Johnston potential. The radial shape was given by two Yukawas with respective proton and neutron strengths (ranges) of 29.1 and 20.1 MeV (0.577 fm) and -1496 and -752 MeV (0.301 fm). In all cases considered, the spin orbit force was always dominated by the tensor force and contributed negligibly to the cross sections.

The harmonic oscillator wave functions used had an oscillator parameter, b, set to 2.47 fm, a value consistent with $^{208}Pb(e,e_0)$ results. Exchange is treated exactly in DWBA70. The BG model was used for the distorted waves, the outgoing parameters being adjusted to the proper exit channel energy. The calculations used a 0.15 fm step size and 15 fm integration limit.

The results of both direct and direct-plus-exchange calculations are shown in Figure 12 through 14. An asterisk indicates the direct-plus-exchange cross section. For these microscopic calculations, the results with only central forces are given by the dashed curves while the solid curves indicate results using the complete central+tensor+spin-orbit interaction. The 2^- level at 4.230 MeV has both magnitude and shape very well reproduced by the calculations. The central force contribution to the cross section is very weak for this 2^- state. The second and fourth 3^- states are also shown. The first octupole level at 2.615 MeV has too complex a p-h character to be established phenomenologically. The third 3^- is a member of the experimentally unresolved triplet at 4.260 MeV. The theory for the displayed 3^- levels reproduces the shape fairly well but underestimates the forward angle cross section for the 4.054 MeV state and is consistently low by a factor of 5 for the 4.698 MeV level.

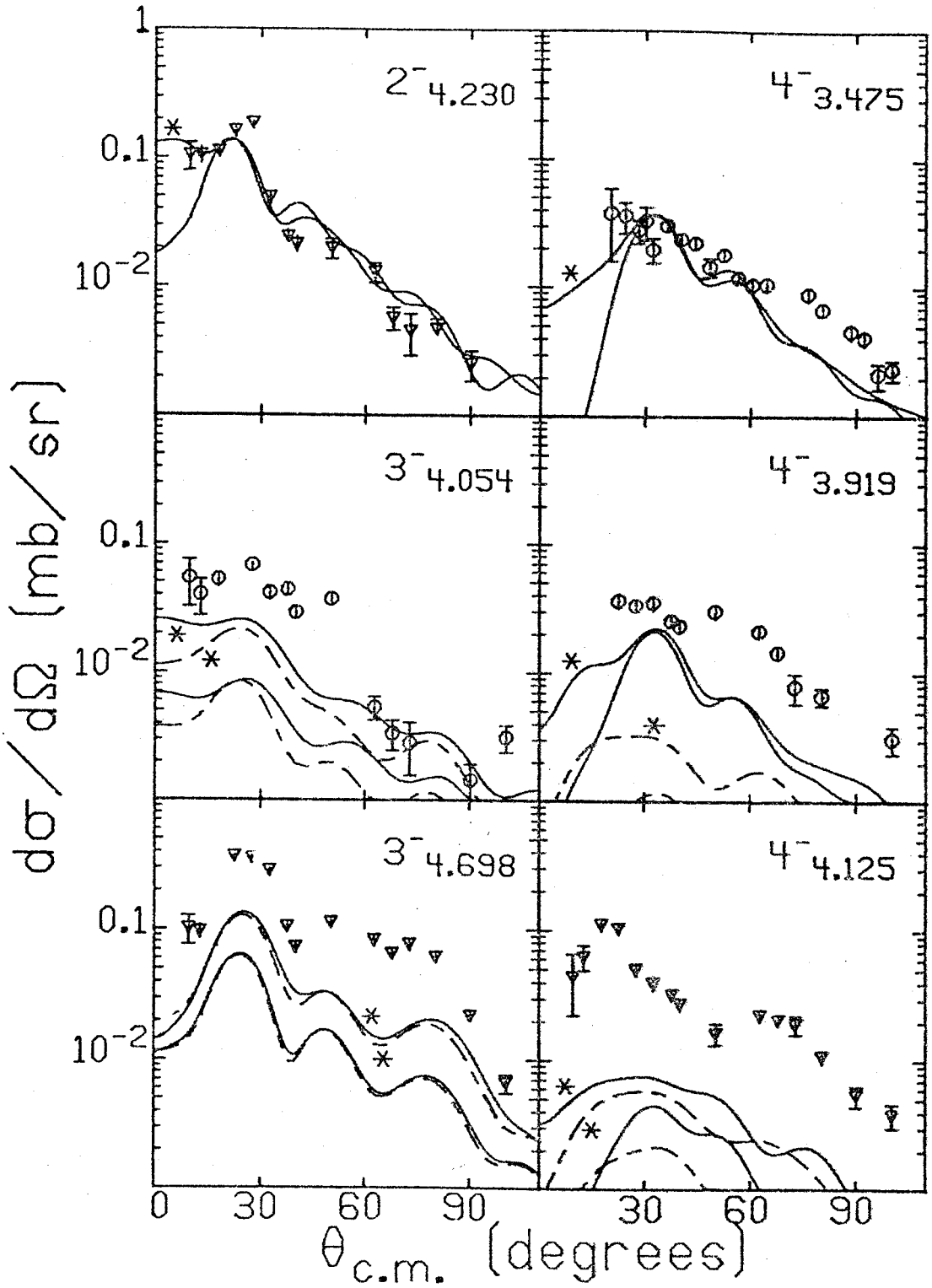

FIGURE 12.--The calculations using phenomenological wave functions for the states shown. The meaning of the asterisks is the same as in Figure 10.

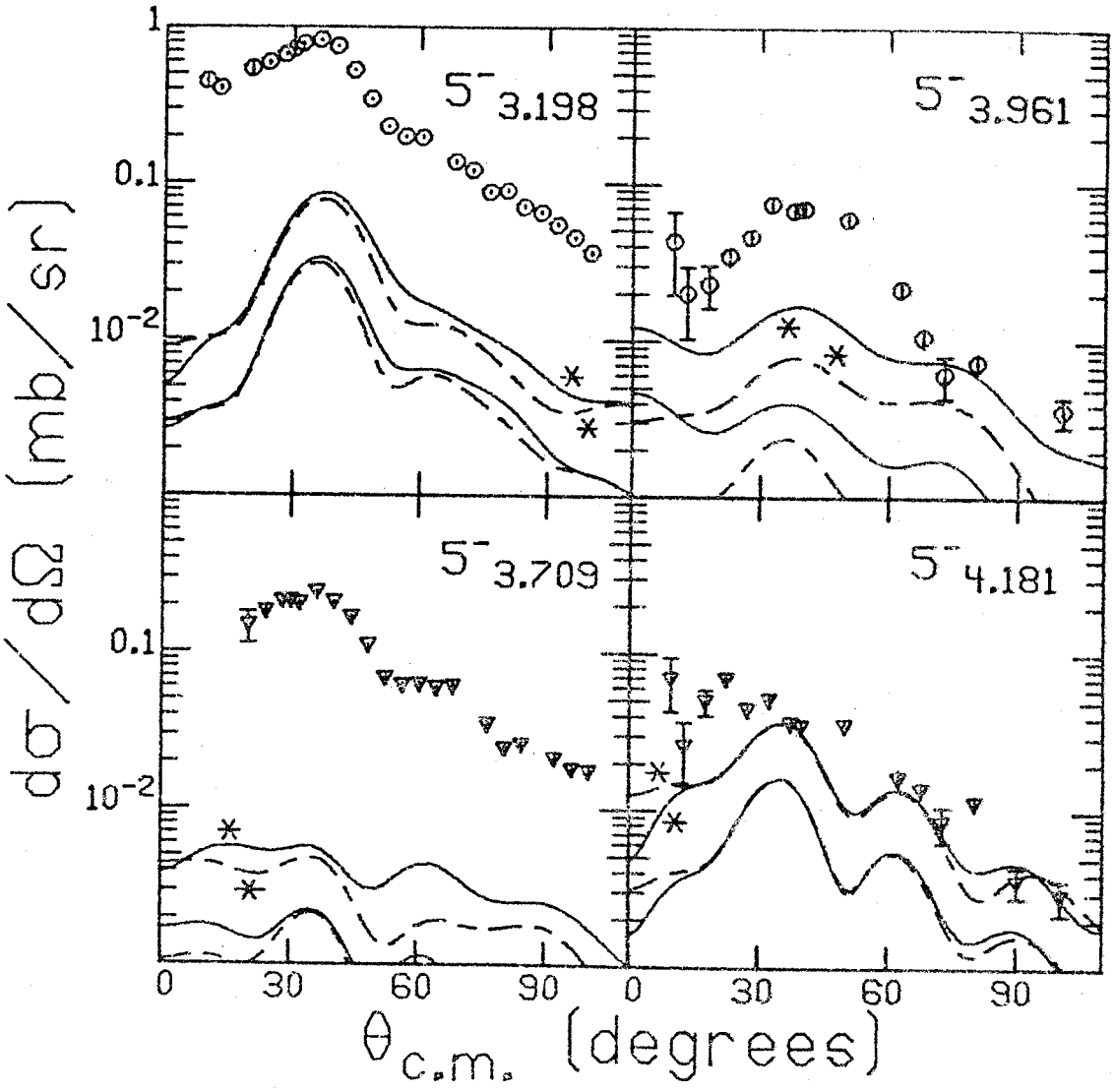

FIGURE 13.--Same as Figure 12.

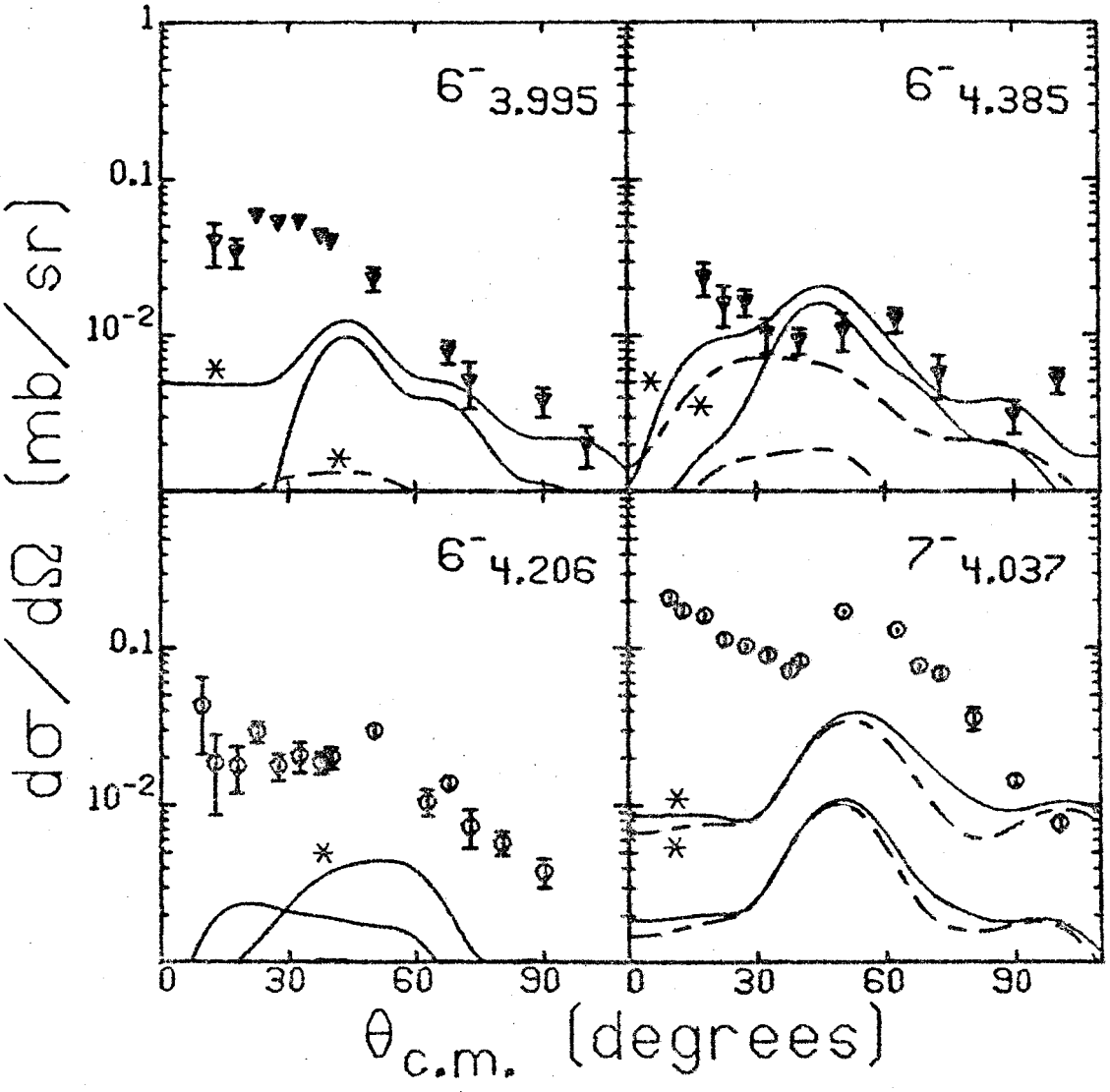

FIGURE 14.--Same as Figure 12.

The first three unnatural parity 4^- states' cross sections are also shown in Figure 12. The first 4^- level has a dominant $(2g_{9/2}\text{-}3p_{1/2}^{-1})$ neutron configuration and has been observed in analog experiments[14,15,50] and in (d,p) experiments.[11,13,17] It corresponds to the first shell model state arising from breaking the $3p_{1/2}$ neutron pair. For this state, the phenomenological wave functions allow a fair reproduction of the data. The experimental angular distribution falls off less rapidly than the theory but the phase is well predicted. The predictions for the second and third levels are both smaller than the data. Both the theoretical distributions for the first two 4^- levels are characteristic of an ℓ-transfer of 5 due to the large contribution of the tensor force which favors the higher of the allowed ℓ-transfers. The third 4^- level has a cross section underestimated by about an order of magnitude and has a shape quite different from the theoretical prediction.

The angular distributions for four 5^- levels are compared with the theory in Figure 13. The fifth 5^- state at 4.260 MeV, an unresolved component of the $3^-\text{-}4^-\text{-}5^-$ triplet, is not shown. (Calculations using the wave functions for these three states suggest that the combined strength can account for about 50 per cent of the observed transition rate.) The data for the collective 3.198 and 3.709 MeV states are stronger than predicted. The third

5^- is also underpredicted while the 4.181 MeV level is well estimated.

Predictions for the first three 6^- states and the 7^- level at 4.037 MeV all underestimate the experimental cross sections while the shapes are reproduced fairly well. This may be seen in Figure 14. The forward angle enhancement of the 7^- level can not be reproduced by the theory.

In summary, there appears to be a systematic underestimation of the cross sections using these wave functions. As might be expected, the more collective states cannot be adequately described in a few p-h basis space. Also, the non-central forces apparently enhance the non-normal parity cross section most but in general provide little enhancement for the normal parity states.

C. Theoretical Wave Functions

In the lead region many shell model calculations[51-53] have been done with both the Tamm-Dancoff and the Random Phase Approximations (RPA). The success of these calculations is based on the purity[55] of the double shell closure in ^{208}Pb. Highly collective odd parity states which have many ph components are generally better described by the RPA. For example, the electromagnetic transition rates are often given accurately with little or no need of effective charges. When comparison is possible, transition densities similar to those measured with (e,e') are often

obtained. In this section RPA wave functions for a number of states are used to describe inelastic scattering.

Excitations of normal parity were considered first. The wave functions of Gillet et al.[52] and of Kuo[53] were used to predict cross sections for the first two 1^-, 2^+, 3^-, and 7^- states, the first four 5^- levels, as well as the first 4^+ and 6^+ excitations. The Gillet vectors were used for the 2^+ and 4^+ calculations. As an estimate of the single particle strength, the neutron configuration $(g_{9/2}\text{-}i^{-1}_{13/2})$--which is prominent in the 2^+ and completely dominant in the 4^+ first excited states wave functions--was taken to be the single configuration of the 6^+ level. Scattering to the negative parity states was calculated with the vectors of Kuo. In the calculations the same central and non-central forces were used as in the phenomenological wave function study. DWBA70 was also used and the RPA wave functions were converted to G-vectors (X'=X+Y, Y'=0) for all these calculations.

The RPA model space involves only 1 $\hbar\omega$ ph excitations. This should allow a reasonable estimate for the lower-lying, negative parity states. However, the number of possible configurations leading to even parity states is quite restricted and thus the strong even parity states are not expected to be given well in this basis.

Figure 15 shows calculations with the Gillet G-vectors for the lowest lying 2^+ states, lying at 4.085 and 4.141 MeV, and for the 4^+ state at 4.323 MeV. The calculations

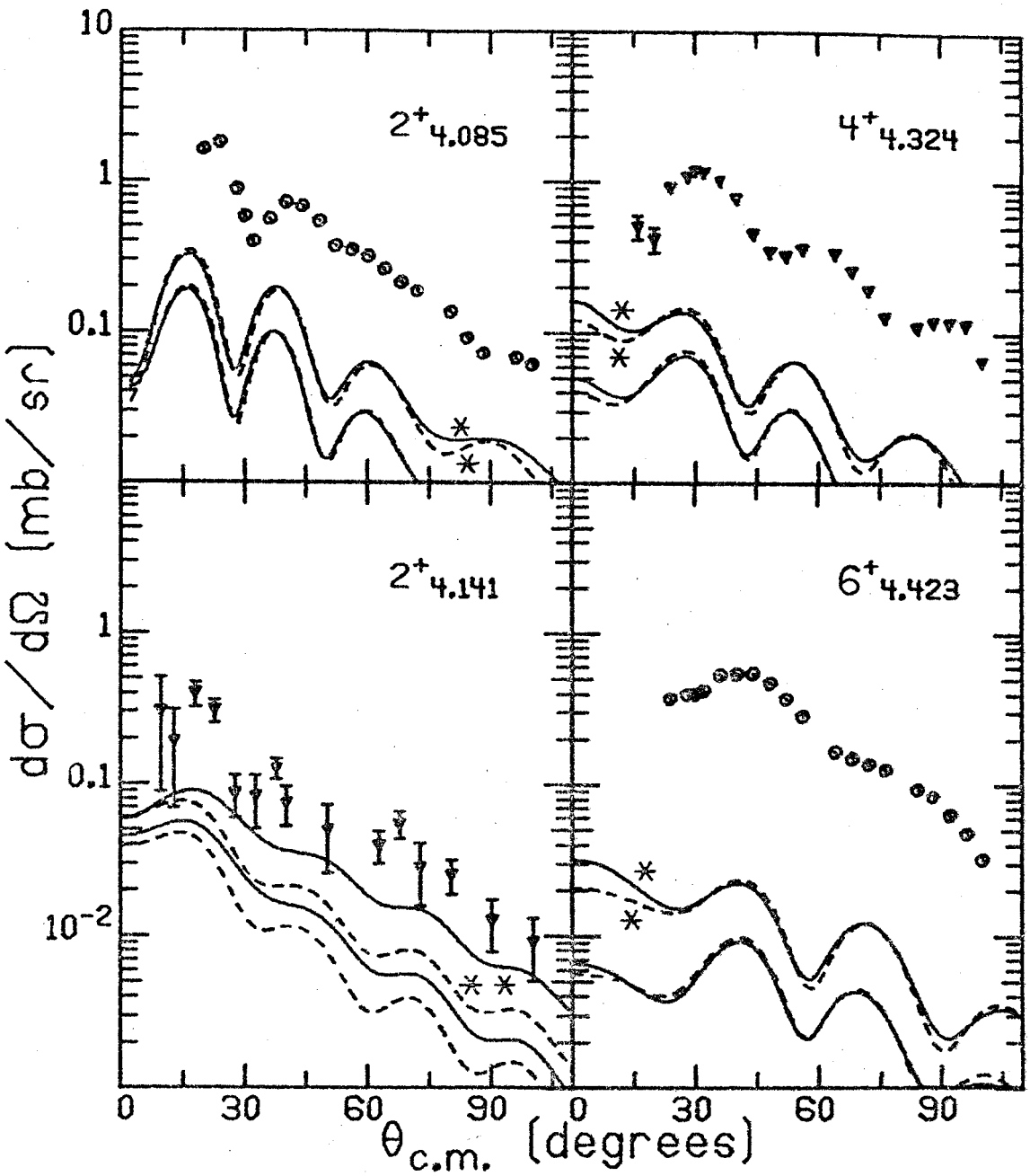

FIGURE 15.--Calculations for the indicated states using theoretical wave functions as cited in the text. The curves are labeled with asterisks as described in Figure 10.

for the 6^+ state at 4.423 MeV were done with the single configuration mentioned above. The second 2^+ state cross section is under-estimated by about a factor of two but does have its shape well reproduced. The non-central forces contribute substantially to this cross section even though the excitation is one of natural parity. This is due to the large spin-flip amplitude of the proton $(h_{9/2}\text{-}h^{-1}_{11/2})$ configuration which is the largest component (0.88) of the wave function.

The first 4^+ and 2^+ levels are underestimated by almost an order of magnitude. Correspondingly, the calculated B(EJ)'s for those states are much weaker than the observed transition rates, as noted previously.[52] However, comparison with recent (e,e') results[40] indicate that for the lower 2^+ state an effective charge less than 1 is necessary to produce agreement with the magnitude of the electron form factor. For the 4^+ level an effective charge of about 1.8 is required. These results suggest that for the 2^+ and probably the 4^+ states, inclusion of core polarization effects could bring the theoretical estimate into reasonable agreement with the experimental (p,p') cross sections without introducing deformed components into the wave functions.

The 6^+ level is badly described, the data being about thirty times larger than the prediction. This state is apparently seen in both the (p,t) and the (t,p) reactions at 20 MeV[12] and also in studies of the $g_{9/2}$ analog resonance.[14,15] No definite knowledge of its exact structure

seems available but it appears complex. These results thus seem consistent. The cross section does display the forward angle enhancement which can be given by the non-central forces, especially in the exchange calculation.

Figure 16 displays the results of calculations using the Kuo wave vectors. Both of the 1^- angular distributions have well estimated strengths but badly reproduced phases. The unusual shape of the calculations for the first 1^- is due to the radial extension of the neutron spin-flip transition density beyond the non-spin-flip density. At forward angles, the cross section is then dominated by the spin flip amplitude. Excitation via the Coulomb interaction is not included but should result in approximately a 10 per cent increase in the total cross section for the first state and about a 5 per cent decrease for the second. For the 3^- levels, the fits to the angular distributions for both states appear satisfactory. The wave function for the second 3^- is dominated by just a few components but seems to give proper estimation of the inelastic transition strength.

As shown in Figure 17, the results for the first two 5^- levels are quite dissimilar. The wave function calculated for the 3.198 MeV level gives good predictions for both (p,p') and gamma decay transition rates. On the other hand, the second 5^- has a B(E5) roughly one-half the measured value whereas the (p,p') prediction is 10 times weaker than

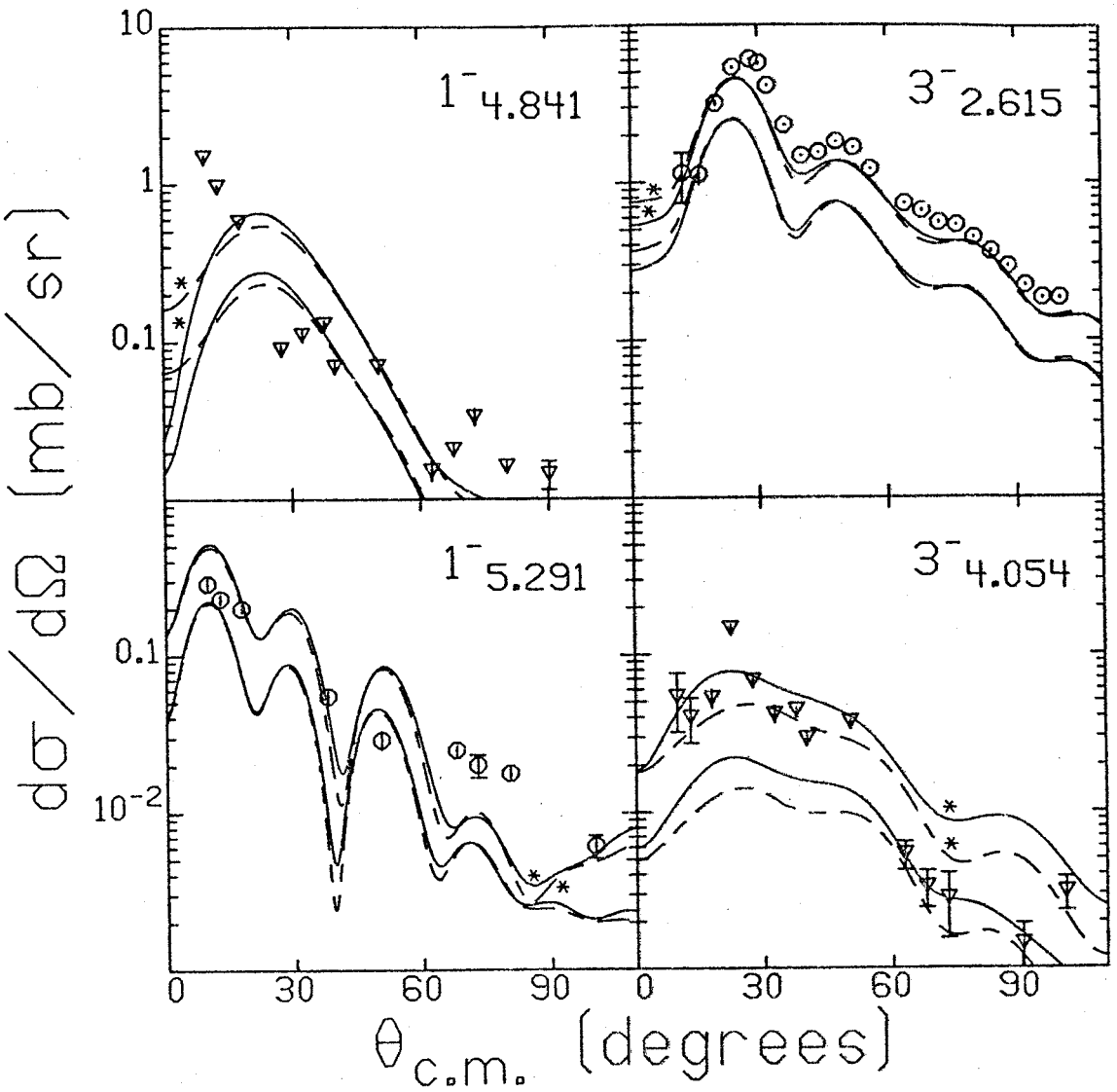

FIGURE 16.--Same as Figure 15.

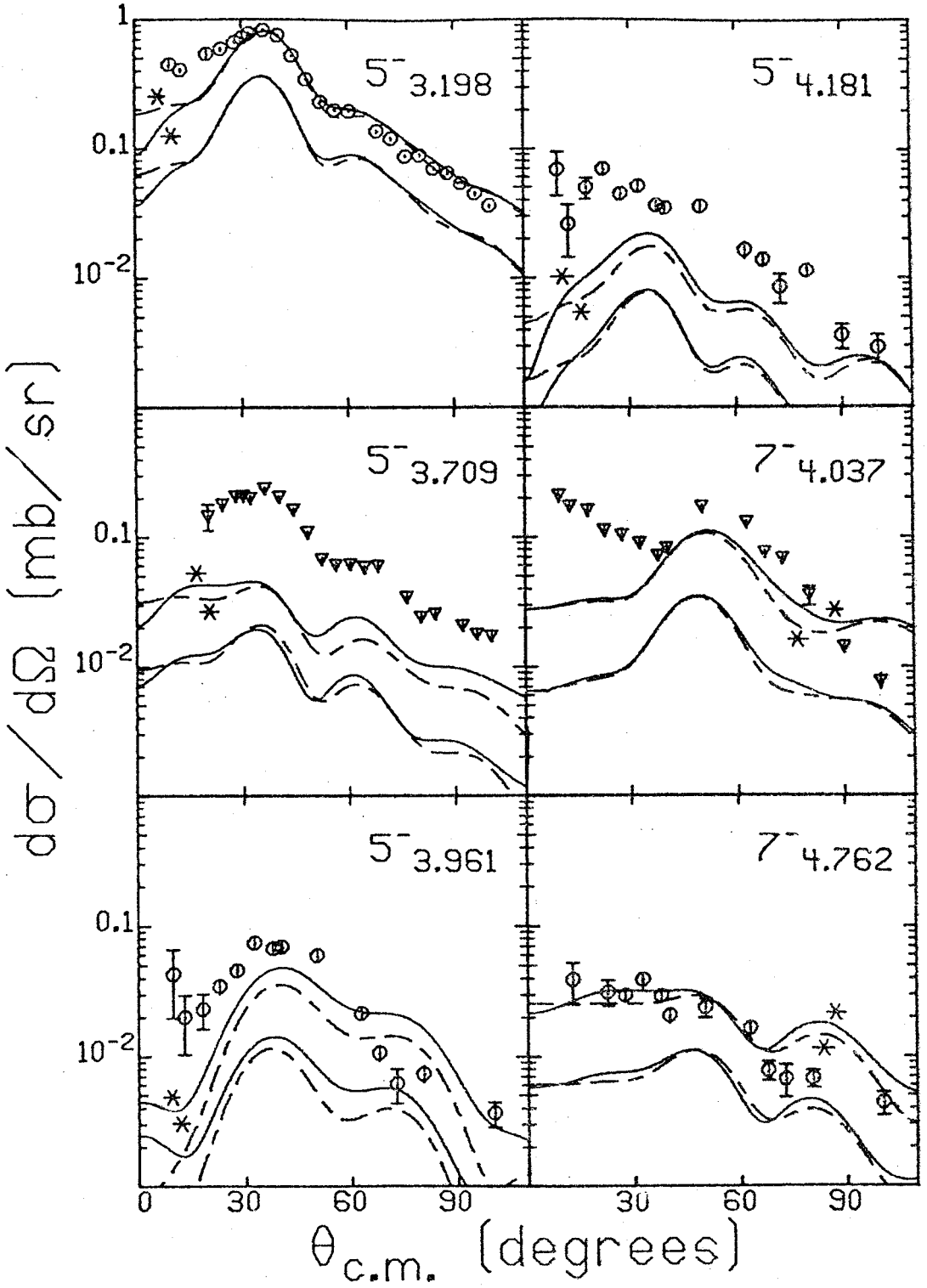

FIGURE 17.--Same as Figure 15.

the scattering data. The third 5^- at 3.961 MeV has a poor estimate of the shape but the strength of the angular distribution is well given. The fourth 5^- is underpredicted by a factor of 5 and has a somewhat poor agreement in shape. The Gillet wave functions for the first 3^- and 5^- states gave results smaller than the Kuo calculations and are not shown here.

The first and second 7^- excitations are also shown. The first of these very high spin states is underestimated by the calculation, especially at the larger angles. The forward angle plateau of the data is lacking in the predicted cross section for the first 7^-. The second 7^- is given well at forward angles but overestimated at back angles.

Transitions to the unnatural parity states were studied using the vectors of Kuo and Figure 18 displays these results for the first three 2^- and 6^- states and the first, second, and fourth 4^- levels. As in the case of the phenomenological wave functions, it is most interesting that the transitions to these states proceed only weakly through the spin-flip portion of the central effective interaction. It appears that almost the entire transition to these states comes about through the tensor portion of the non-central forces, the spin-orbit force being negligible for the configurations considered here. There is very good agreement in the cases of the first 4^- and the third 6^- states. The

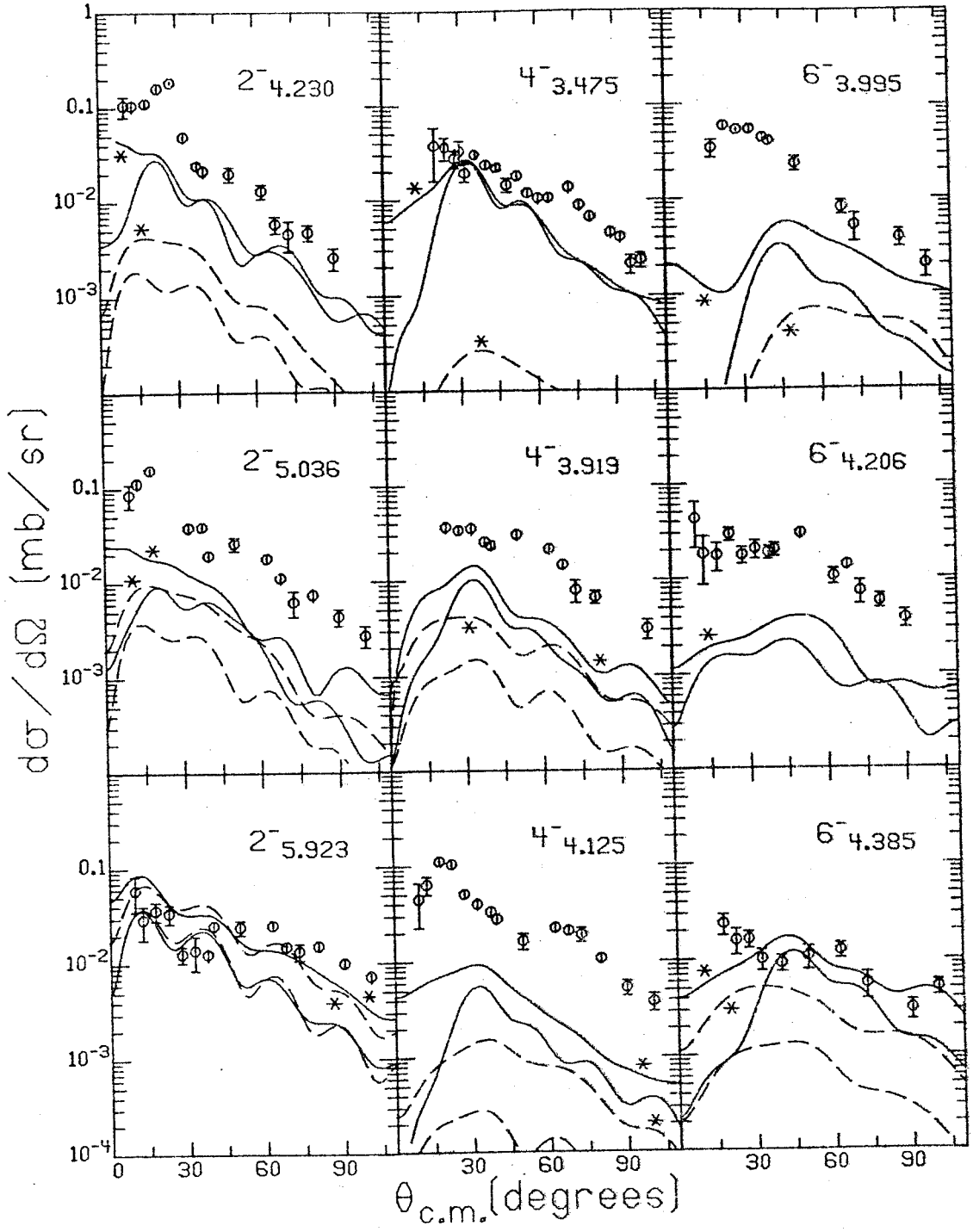

FIGURE 18.--Same as Figure 15.

4^- at 3.919 MeV excitation appears very difficult to describe with either the phenomenological or theoretical wave functions.

Comparison of the results of the theoretical with the phenomenological wave functions indicate that the theoretical vectors give better predictions of the (p,p') transitions to the natural parity states, especially in the cases of collective motion. For the unnatural parity states, the phenomenological vectors give perhaps a slightly better prediction of strengths as compared to the theoretical estimates.

In summary, the calculations with the phenomenological and RPA state vectors give results that are consistent with the adopted models. Due to the small ph basis, the former set of wave functions can not describe the highly collective states. On the average, however, both sets do well in estimating the cross sections for those states with little collectivity and with only a few dominant ph components. For the RPA results, the good agreement between the <u>average</u> of the experimental and the theoretical transition strengths for the weakly excited states is to be expected. The large difference between the predicted and measured cross sections for the positive parity states is a consequence of the 1 $\hbar\omega$ space and the one particle-one hole basis used in the RPA structure calculations.[52] The requirement for large effective charges to reproduce the measured B(EJ)'s for these

positive parity states is consistent with the lack of calculated (p,p') strength. As expected, the RPA vectors[53] for the lowest-lying, negative parity collective levels give a good estimate of the (p,p') strength and require little or no effective charge.

V. CONCLUSION

^{208}Pb has been investigated using high resolution proton inelastic scattering. Angular distributions for all resolved states have been presented and excitation energies have been extracted. Spins, parities, and deformation parameters have been obtained using a collective model fit to the data. These results were generally found to be in good agreement with previous measurements.

Microscopic model calculations using theoretical wave functions and phenomenological transition densities and wave functions were compared with the data. The highly collective states were studied with form factors based on (e,e') measurements and a simple model for neutron motion in these collective excitations. With a G-matrix interaction for the nucleon-nucleon potential, the results were fairly consistent with the data but required complex-coupling to match the observed strengths. Non-central forces were not used for these calculations and are not expected to contribute significantly to the cross sections.

The phenomenological wave functions of Heusler and von Brentano[24] were used with an effective interaction including both central and non-central parts to give reasonable descriptions for many of the states observed. Although, in general, the calculations underestimate the data slightly the results are encouraging.

Angular distributions were also predicted for inelastic scattering using RPA wave functions. The strongly populated odd, normal parity states had cross sections comparable to the theoretical estimates. The cross sections of the unnatural parity states were also described fairly well using these wave functions but were typically underestimated by the calculations. The use of an effective tensor interaction based on the OPEP form, which saw reasonable success in describing transitions in the case of ^{14}N, appears to work well in the lead region. Continued study of the unnatural parity states promises that more knowledge of the tensor portion of the effective interaction can be obtained.

PART B

^{207}Pb and ^{209}Bi

I. INTRODUCTION

Nuclei that are only one or two particles away from a shell closure permit the valence nucleon-core interaction to be investigated. The lead mass region is well suited for such investigation due to the purity of the double shell closure and the knowledge of many states in ^{208}Pb. This paper reports the (p,p') study of ^{207}Pb and ^{209}Bi each of which can be considered as a ^{208}Pb core with a valence neutron hole or proton particle. Inelastic proton scattering was used to excite a variety of states in these nuclei. Collective, single particle, and apparently complex excitations have all been observed and angular distributions recorded.

Experimentally, ^{207}Pb and ^{209}Bi are difficult to study because of the high level density and fractionation of inelastic transition strength. In ^{208}Pb many levels are well separated. In ^{207}Pb or ^{209}Bi, however, weak coupling to core excitations produces a spread of inelastic transition strength among many levels. Often, members of the multiplet are separated from one another or other states by only a few keV of excitation energy. For example, the 3.1 MeV multiplet in ^{209}Bi, apparently arising from the $h_{9/2}$ valence proton weak coupled[57] to the 3.2 MeV 5^- vibration in ^{208}Pb, has doublet members separated by less than 5 keV, spans an excitation energy region of only 225 keV, and lies within 15 keV of other states. Such problems necessitate

the use of ultra-high resolution techniques for separation and identification of multiplet members from other levels. With data of high quality, spin-parity assignments for multiplet constituents and searches for weak coupled states built on high excitation energy collective core states are possible.

Aside from the weak coupling excitations, inelastic proton scattering from these nuclei allows study of the single particle and single hole states and of the extent of core polarization in their excitation. Core polarization effects in transitions to the most well known single hole states in $^{207}Pb^{58,59}$ and to the $i_{13/2}$ proton state in $^{209}Bi^{60}$ have been examined. Here it was hoped to determine the importance of both the ^{208}Pb core and the non-central forces in the excitation of some of these states.

Section II discusses the experimental set-up and procedure. The reduction of the data, angular momentum transfer identification, and comparison with previous work are discussed in Section III. Calculations involving the weak coupling theory and the microscopic Distorted Wave Born Approximation (DWBA) are shown in Sections IV and V.

II. EXPERIMENTAL PROCEDURE

The experiment used 35 MeV protons extracted from the Michigan State University cyclotron with beams on target ranging between 1/2 and 1 microampere, the smaller current being used on the lower melting point bismuth. Protons scattered from targets of ^{209}Bi and ^{207}Pb were observed using

both a wire proportional counter and photographic emulsions in the focal plane of the Enge split-pole spectrometer. The high resolution cyclotron-spectrograph system was used to obtain typical plate data resolution of 5-10 keV full-width-at-half-maximum (FWHM). The plate data spanned the region of excitation energy between about 0.5 and 8.0 MeV. The counter data had a resolution which was detector limited to about 50 keV FWHM and examined the lowest 5 MeV of excitation.

Initially, angular distributions were measured using thick lead and bismuth targets and the wire counter-scintillator set-up.[20] Protons exciting the low-lying states were generally well resolved with good statistics. Measurement of the elastic angular distribution was also made. Comparing the elastic cross sections with the optical model calculations using Becchetti-Greenlees best-fit parameters[21] determined the absolute normalization to about 5%. Comparing the completely resolved inelastic states in both plate and counter data gave the absolute normalization of the plate data to about 10%. Whenever possible the better statistics counter data is displayed.

The high resolution data was recorded on Kodak 25 μm NTB emulsion with a piece of 0.015" stainless steel shim stock before the plate to enhance track brightness and to absorb heavier mass particles. Spectra were recorded from 10° to 100°. Fifteen angles were recorded for the plate data. Most plate data was taken with a 1° x 1° spectrometer entrance slit but some ^{209}Bi spectra were taken with a 2° x 2°

slit as a reasonable compromise of resolution and count rate. Before beginning a run, the resolution was optimized using the on-line focal plane line width determination system and dispersion matching.[19]

Typical spectra of ^{207}Pb and ^{209}Bi are shown in Figure 19. Also shown is a spectrum of ^{208}Pb to allow comparison. The fragmentation of ^{208}Pb collective states into multiplets is apparent. Many single particle states were resolved and are also indicated. The increase in level density from ^{208}Pb to ^{207}Pb to ^{209}Bi is striking. Discrete structure can be seen up to 6 MeV in the two lead spectra but the bismuth spectrum is essentially a continuum above 5.5 MeV of excitation.

Since Bi is monoisotopic, few contaminants were found in the bismuth data, the major ones being oxygen and carbon from the thin carbon foil-formvar backing. The ^{207}Pb targets were made from an isotopically enriched lead sample obtained from the Oak Ridge National Laboratory and was 99.81% ^{207}Pb, 0.13% ^{208}Pb, and had small amounts of other lead isotopes. The lead targets also had backings. Target thickness was about 100 $\mu g/cm^2$ and 3 mg/cm^2 for the plate and counter studies, respectively. The effects of target thickness on resolution are discussed in Appendix I.

III. DATA

A. Excitation Energies

The excitation energies of the 170 levels observed in ^{207}Pb and the 80 levels seen in ^{209}Bi are listed in

FIGURE 19.--Typical spectrum of ^{207}Pb, ^{208}Pb, and ^{209}Bi. Multiplets built on strong levels in ^{208}Pb are apparent in the other spectra.

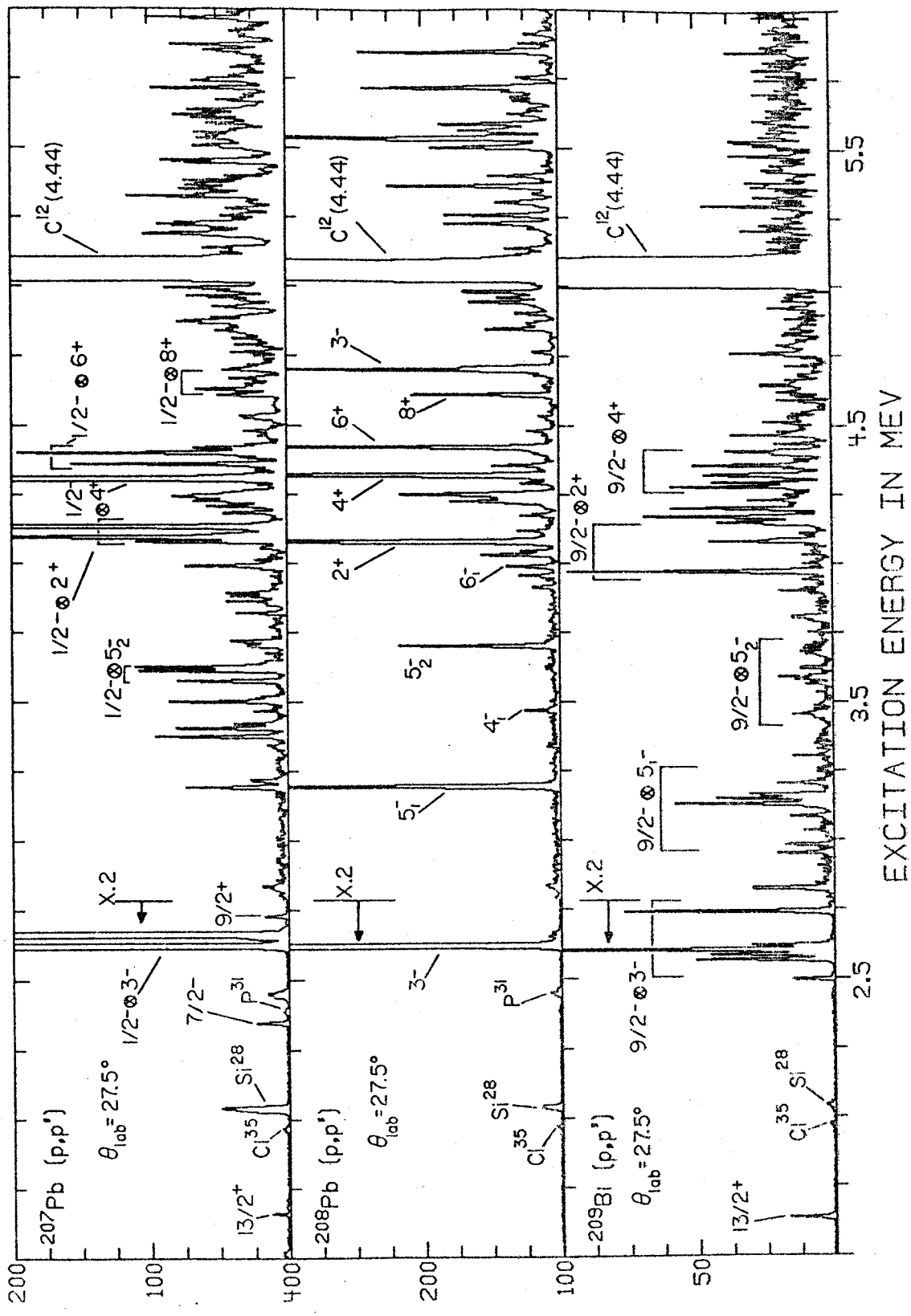
COUNTS PER ΔΩ
EXCITATION ENERGY IN MEV
^{207}Pb (p,p')
θ_{lab} = 27.5°
^{208}Pb (p,p')
θ_{lab} = 27.5°
^{209}Bi (p,p')
θ_{lab} = 27.5°
X.2
13/2+
9/2+
7/2−
1/2−⊗3−
1/2−⊗2+
1/2−⊗5$_2^-$
1/2−⊗4+
1/2−⊗6+
1/2−⊗8+
3−
5$_1^-$
4$_1^-$
5$_2^-$
2+
4+
6+
8+
6$_1^-$
9/2−⊗3−
9/2−⊗5$_1^-$
9/2−⊗5$_2^-$
9/2−⊗2+
9/2−⊗4+
P^{31}
Si^{28}
Cl^{35}
C^{12}(4.44)
200
100
400
200
100
50
2.5
3.5
4.5
5.5

FIGURE 19

Tables III and IV along with the results of recent Nuclear Data Sheets.[61,62] The energy calibration for each plate exposure was made using lead or bismuth levels whose focal plane positions were unambiguously known and whose excitation energies were well determined in previous high resolution studies. Levels used for calibration are noted in the tables. The calibration involved using the best experimentally determined excitation energies initially, predicting average energies with all plate spectrum, and iterating until the average energies were consistently obtained. The well-known levels of ^{12}C, ^{13}C, and ^{16}O were also used in the calibration whenever possible.

The large level population at even low excitation energies prevented the use of many levels in the calibration. In ^{207}Pb and ^{209}Bi the excitation energies above 2.730 and 3.155 MeV, respectively, were determined by extrapolation. Therefore, below these energies the error is simply the standard deviation. Above these energies the error is the standard deviation plus an additional 1 keV/MeV of extrapolated energy. This systematic error is an estimate of both the interpolation error and the uncertainties caused by the high level density.

B. Inelastic Angular Distributions

Angular distributions for which no definite ℓ-transfer assignment could be made are shown in Figures 20 through 22, for ^{207}Pb, and in Figure 23, for ^{209}Bi. Figures 25 through 27 display angular distributions which are reasonably well fit by collective model calculations for these isotopes.

TABLE III.--Energy levels, ℓ-transfers, and deformation parameters for ^{207}Pb.

Present Work			Compilation[e]		
E_x[a] $\pm\Delta E_x$	L	β_L	E_x[a]	J^π	L
0.5709[b]	2	0.026	0.56967	$5/2^-$	
0.8985[b]	2	0.025	0.8976	$3/2^-$	
1.6337[b]	6,7	0.019,0.019	1.63329	$13/2^+$	
2.3398[b]	4	0.024	2.33989	$7/2^-$	4
			2.368?		
			2.563?		
2.6230[b]	3	0.076	2.6241	$5/2^+$	3
2.6626[b]	3	0.087	2.6619	$7/2^+$	3
2.702±0.005			2.705?		
2.7276[b]	5	0.024	2.726	$9/2^+$	6
			2.840?		
			2.902?		
			2.909?		
			3.004?		
			3.057?		
			3.180?		
3.200±0.003			3.202		5
3.223±0.002	5	0.013	3.222		5
			3.267?		
			3.298	$1/2^-$	
			3.319?		
			3.335?		
			3.344?		
3.384±0.002	(5)	0.027	3.382	$(9/2^+,11/2^+)$	5
3.413±0.002	4	0.021	3.409	$9/2^-$	4
3.429±0.002	(5)	0.016	3.426		6
3.476±0.003	(5)	0.013			
3.509±0.002	(5)	0.025	3.499		
3.583±0.002	5	0.023	3.580		5
3.620±0.002	5	0.028	3.620		5
3.634±0.002	3	0.019	3.632		
3.650±0.003	9	0.020			
3.672±0.003					
3.709±0.004					
3.726±0.003					

TABLE III.--Continued.

Present Work			Compilation[e]		
E_x[a]$\pm\Delta E_x$	L	β_L	E_x[a]	J^π	L
3.829±0.003	5	0.014			
3.857±0.004	7,8	0.014,0.015			
3.869±0.002	(5)	0.016			
3.887±0.003					
3.901±0.002	7,8	0.023,0.023			
3.925±0.005[d]					
3.986±0.002					
3.999±0.003					
4.017±0.003					
4.034±0.005	(3)	0.007			
4.062±0.004					
4.088±0.004			4.089		2
4.103±0.003	2	0.036	4.113		
4.140±0.003	2	0.045	4.127		2
4.190±0.003	7,6	0.026,0.024			
4.213±0.003	5	0.022			
4.232±0.005					
4.250±0.004					
4.270±0.004	(6)	0.010			
4.287±0.006	4	0.0080	4.288		4
4.313±0.004	4	0.067	4.318		
4.342±0.006	(3)	0.009	4.339		6
4.364±0.003	6	0.042	4.380		6
4.387±0.004			4.387		
4.404±0.003	6	0.047			
4.422±0.003	(2)	0.017			
4.465±0.005[d]					
4.479±0.004					
4.494±0.005	(8)	0.009			
4.514±0.004			4.513		
4.527±0.004	(2)	0.010			
4.538±0.004			4.541		
			4.546		

TABLE III.--Continued.

Present Work			Compilation[e]		
E_x[a] $\pm\Delta E_x$	L	β_L	E_x[a]	J^π	L
4.558±0.003					
4.592±0.006					
4.612±0.003					
4.630±0.003	(8)	0.028	4.629		
4.656±0.005	2	0.013			
4.671±0.003	(8)	0.025			
4.700-4.730[c]					
4.733±0.003					
4.745±0.003	(8)	0.016			
4.761±0.004					
4.785±0.004	7				
4.806±0.005					
4.835±0.006[d]					
4.870±0.004					
4.884±0.003					
4.921±0.004					
4.943±0.004					
4.957±0.004					
4.975±0.006					
4.987±0.005[d]	3	0.022			
5.018±0.005	9	0.021			
5.039±0.005	9	0.021			
5.053±0.005					
5.081±0.004	3	0.029			
5.117±0.006[d]					
5.129±0.005[d]			5.129		
5.156±0.006	(3)	0.010			
5.177±0.006[d]	3	0.029	5.178		
5.193±0.005					
5.217±0.005			5.219		
5.245±0.008	3	0.017	5.252		
5.267±0.005	3	0.016			

TABLE III.--Continued.

Present Work			Compilation[e]		
E_x[a] $\pm\Delta E_x$	L	β_L	E_x[a]	J^π	L
5.290±0.005					
5.310±0.005					
5.321±0.005	3	0.020			
5.336±0.005	3	0.023			
5.352±0.005	3	0.026			
5.369±0.005	(6)	0.027			
5.383±0.005					
5.402±0.006					
5.428±0.005	3	0.018	5.417		
5.440±0.005	3	0.022			
5.454±0.005					
5.474±0.004					
5.487±0.006					
5.501±0.005	4	0.017			
5.526±0.004[d]	(7)	0.027			
5.537±0.005					
5.548±0.006					
5.569±0.005	3	0.020			
5.584±0.004					
5.598±0.005					
5.614±0.006	(3)	0.019			
5.648±0.006					
5.668±0.005					
5.689±0.005					
5.720±0.006					
5.735±0.006					
5.765±0.007					
5.803±0.006					
5.822±0.006					
5.840±0.006					
5.868±0.006					
5.897±0.007					
5.915±0.008					

TABLE III.--Continued.

Present Work			Compilation[e]		
E_x[a]$\pm\Delta E_x$	L	β_L	E_x[a]	J^π	L
5.934±0.007					
5.952±0.005					
5.969±0.006					
5.998±0.006					
6.010±0.005					
6.031±0.006					
6.041±0.007					
6.064±0.007					
6.073±0.006					
6.090±0.007					
6.105±0.006	(3)	0.015			
6.146±0.005[d]					
6.170±0.008	(7)	0.017			
6.188±0.007[d]	(7)	0.024			
6.228±0.007					
6.251±0.006					
6.262±0.006					
6.276±0.006	(3)	0.016			
6.310±0.007					
6.332±0.007					
6.360±0.005					
6.381±0.007					
6.402±0.006					
6.449±0.007					
6.483±0.008	(3)	0.013			
6.547±0.008					
6.627±0.008[d]					
6.654±0.008					
6.670±0.008					
6.716±0.007[d]					

TABLE III.--Continued.

Present Work			Compilation[e]		
E_x[a] $\pm \Delta E_x$	L	β_L	E_x[a]	J^π	L
6.762±0.007[d]					
6.788±0.009					
6.864±0.008					
6.912±0.008[d]					
6.939±0.009					
6.955±0.009					
7.048±0.009					

[a]All energies in MeV.
[b]State used in energy calibration.
[c]Spectral region with unresolved multiplet structure.
[d]Level with probable multiplet structure.
[e]Reference 61.

TABLE IV.--Energy levels, ℓ-transfers, and deformation parameters for ^{209}Bi.

Present Work			Compilation[e]		
E_x[a] $\pm \Delta E_x$	L	β_L	E_x[a]	J^π	L
0.8959[b]	(2)	0.013	0.8966	$7/2^-$	2
1.6081[b]	3	0.027	1.6085	$13/2^+$	3
2.492±0.001	3	0.026	2.492	$3/2^+$	3
2.564±0.001	3	0.047	2.563	$9/2^+$	3
2.581±0.002	3	0.041	2.582	$7/2^+$	3
2.599±0.001	3	0.074	2.599	$11/2^+$	3
			2.601	$13/2^+$	3
2.617±0.002	3	0.035	2.616	$5/2^+$	3
2.7404[b]	3	0.057	2.741	$15/2^+$	3
2.766±0.002	4	0.013	2.762		
2.8251[b]			2.822	$5/2^-$	
			2.827		
			2.91		
2.956±0.003	(4)	0.014	2.957		
2.986±0.001	5	0.021	2.987	$13/2^+$	5
3.038±0.002	5	0.013	3.038	$3/2^+$	5
3.091±0.003	5	0.014	3.091	$5/2^+$	5
3.118±0.002			3.116	$3/2^-$	
3.1339[b]	5	0.036	3.135	$11/2^+, 19/2^+$	5
3.1534[b]	5	0.032	3.154	$17/2^+, 7/2^+$ or $17/2^+, 9/2^+$	5
3.168±0.002	5	0.026	3.170	$15/2^+$	5
			3.197		
3.211±0.001	5	0.020	3.212	$9/2^+$ or $1/2^+, 7/2^+$	5
			3.222		
3.309±0.003	(3)	0.009	3.311		
3.358±0.002			3.363		
			3.379		
			3.393		
			3.406		
			3.433?		

TABLE IV.--Continued.

Present Work			Compilation[e]		
E_x[a] $\pm\Delta E_x$	L	β_L	E_x[a]	J^π	L
			3.450		
3.466±0.002[d]	5	0.019	3.465		
			3.476		
			3.489		
3.501±0.005			3.503		
3.579±0.003	5	0.012	3.579		L=5 Group
3.597±0.002[d]	5	0.020	3.597		
3.633±0.004			3.640	$1/2^-$	
			3.670		
3.685±0.003	5	0.015	3.683		
3.703±0.004	5	0.015	3.692		
3.710-3.750[c]			3.719		
			3.735		
			3.753		
3.765±0.003[d]			3.763		
3.803±0.004	(3)	0.013	3.802		
3.815±0.002	(7,8)	0.031,0.026	3.818		
3.839±0.004[d]			3.839		
3.855±0.003			3.855		
			3.880		
3.892±0.003			3.893		L=2 Group
			3.909		
3.924±0.005[d]	(3)	0.013	3.919		
			3.937		
3.950±0.005	(3)	0.012	3.950		
			3.962		
3.981±0.003	2	0.033	3.981		
			3.994		
4.013±0.005			4.015		
			4.038		

TABLE IV.--Continued.

Present Work			Compilation[e]		
E_x[a]$\pm\Delta E_x$	L	β_L	E_x[a]	J^π	L
4.047±0.005			4.050		
			4.079		
4.092±0.004	2	0.027	4.096		
4.116±0.004	(7)	0.022	4.121		
			4.133		
4.157±0.004	2	0.027			
4.177±0.004	3	0.033	4.178		
4.210±0.004	3	0.029			L=4 Group
4.235±0.004					
4.257±0.004					
4.286±0.003	4	0.034	4.276		
4.301±0.003	≃7	≃0.033			
4.326±0.003			4.32?		
4.362±0.003	4	0.032			
4.397±0.003			4.397		
4.411±0.003	≃8	≃0.035	4.421	$1/2^-$	
4.441±0.004[d]	4	0.017	4.447	$7/2^-$	
4.469±0.003[d]					
4.485±0.004					
4.512±0.005			4.519		
4.532±0.004[d]	≃8	0.021			
4.592±0.006			4.601		
4.613±0.005[d]					
4.630-4.745[c]			4.650		
			4.745		
4.760 0.004[d]					
4.791 0.006[d]					
4.828 0.005					
4.853 0.005					
4.949 0.004[d]					
4.965 0.005					

TABLE IV.--Continued.

Present Work			Compilation[e]		
E_x[a]$\pm\Delta E_x$	L	β_L	E_x[a]	J^π	L
4.998±0.006					
5.056±0.005[d]					
5.131±0.006[d]	≃7	≃0.022			
5.241±0.007			5.20		
5.282±0.005					
5.312±0.005[d]			5.304		
5.333±0.005					
5.360±0.006[d]					
5.423±0.006[d]			5.43		
5.463±0.005					
5.509±0.006[d]					
5.569±0.010[d]			5.57		
5.769±0.005			5.77		
5.795±0.007[d]					
5.835±0.008[d]					
			6.394		
			7.169		
			7.176		
			7.416		
			7.637		

[a]All energies in MeV.
[b]State used in energy calibration.
[c]Spectral region with unresolved multiplet structure.
[d]Level with probable multiplet structure.
[e]Reference 62.

FIGURE 20.--Measured inelastic cross sections in ^{207}Pb for which collective model assignments could not be made. The lines drawn through the points are merely to guide the eye and do not represent fits to the data. The excitation energy of the levels is given in MeV.

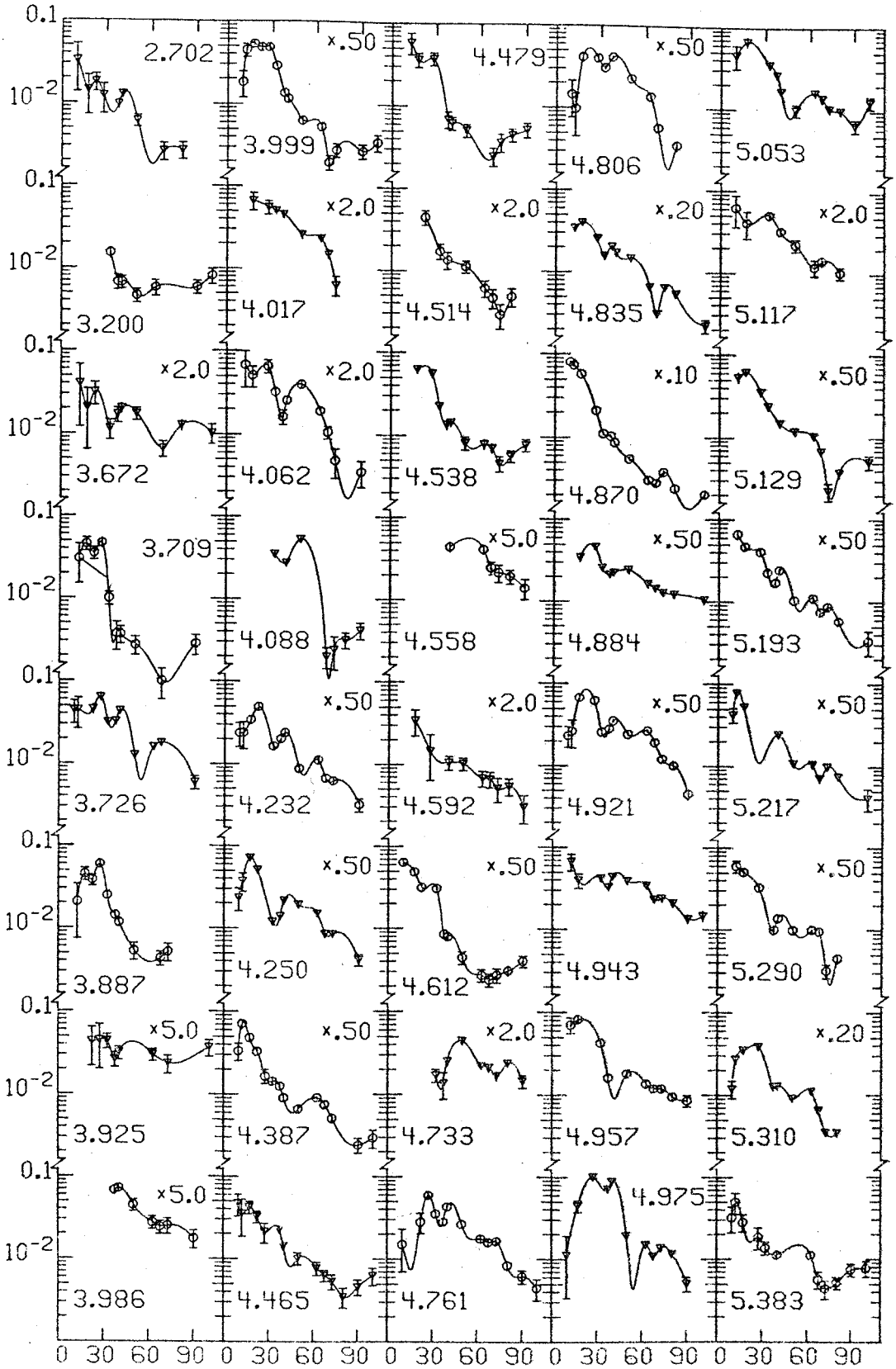
0.1
10^{-2}
2.702
3.200
3.672
3.709
3.726
3.887
3.925
3.986
3.999
4.017
4.062
4.088
4.232
4.250
4.387
4.465
4.479
4.514
4.538
4.558
4.592
4.612
4.733
4.761
4.806
4.835
4.870
4.884
4.921
4.943
4.957
4.975
5.053
5.117
5.129
5.193
5.217
5.290
5.310
5.383
x.50
x2.0
x5.0
x.20
x.10
0 30 60 90

FIGURE 20

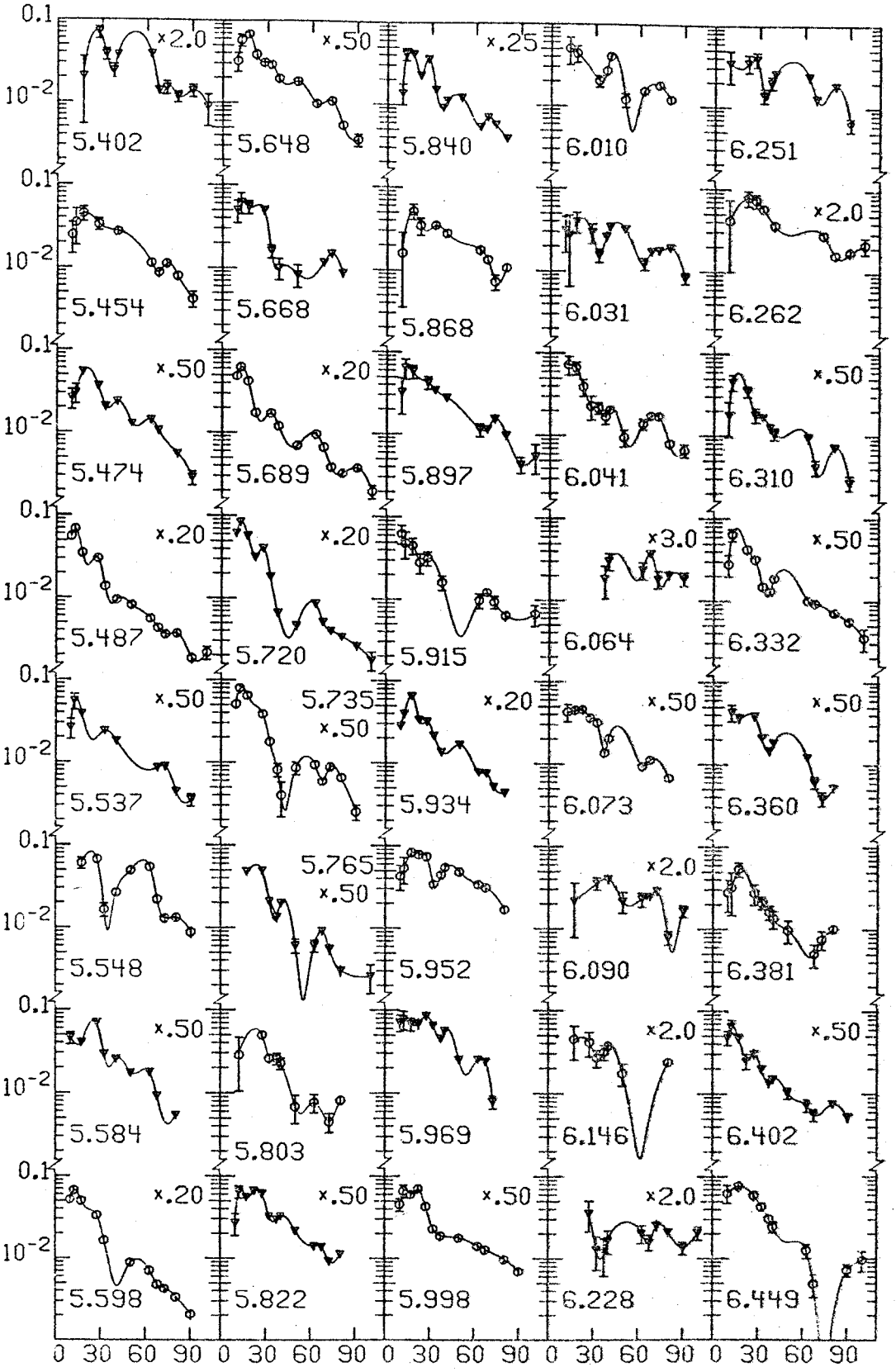

FIGURE 21.--Same as Figure 20.

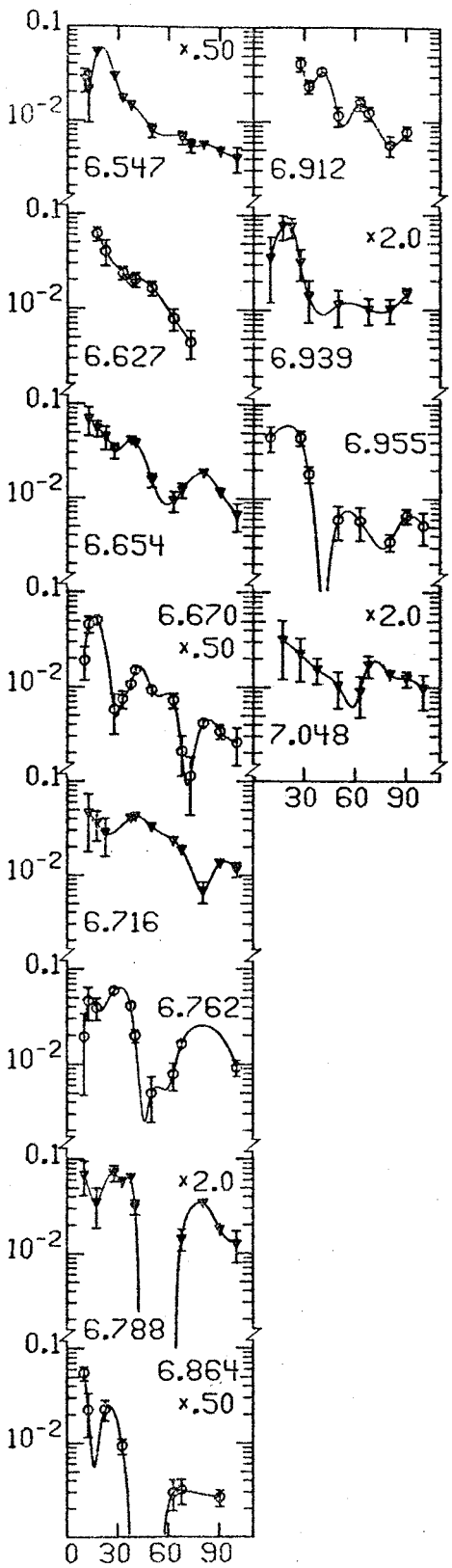

FIGURE 22.--Same as Figure 20.

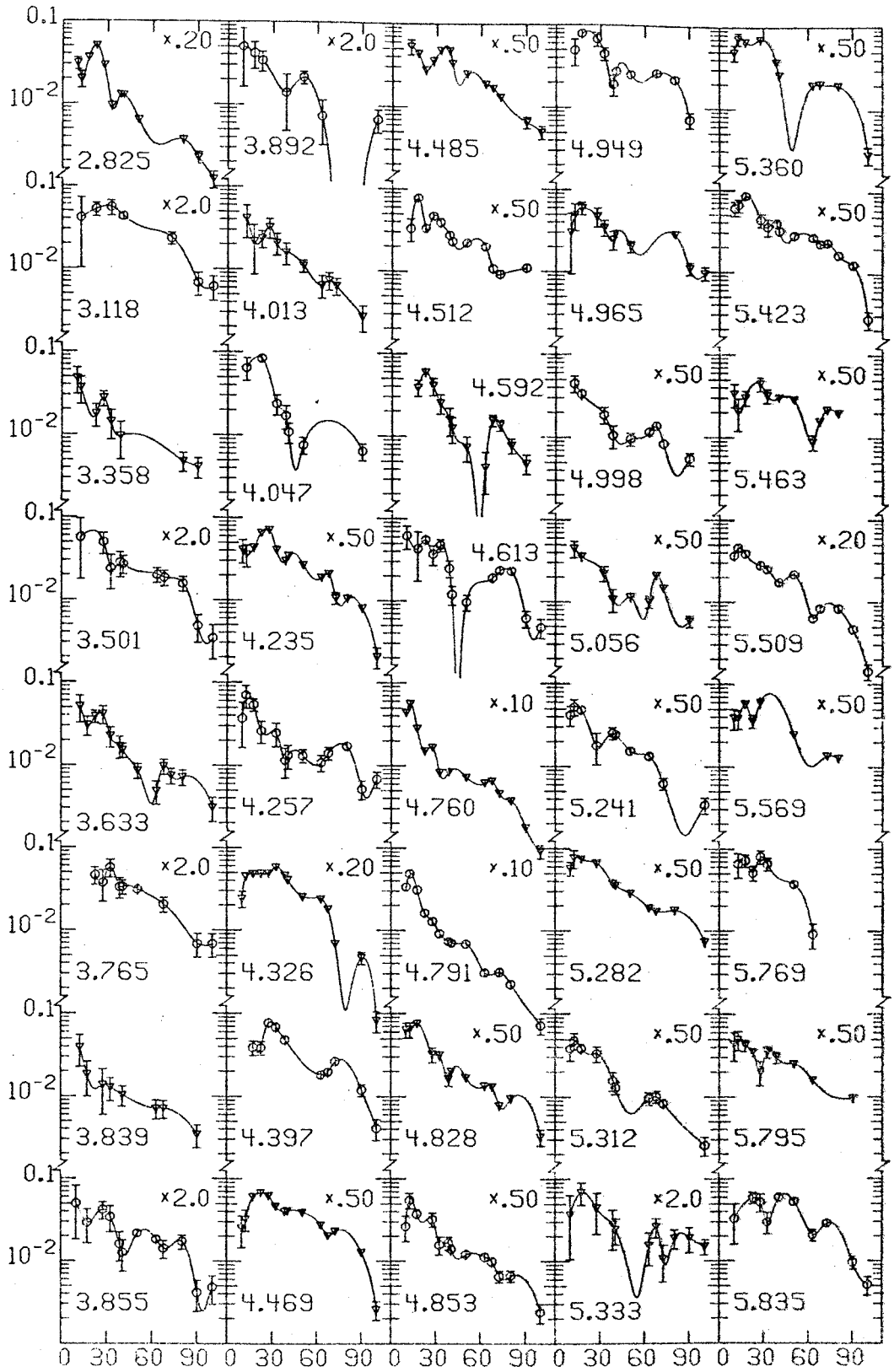

FIGURE 23.--Same as Figure 20 but for ^{209}Bi.

The latter are discussed in Section III-D and E and the former are discussed here. In all cases only the levels apparent in six or more plate exposures are displayed in the figures. The error bars drawn indicate only statistical errors and are shown only when larger than the size of the symbol. Gaps in the angular distributions occur when the peak of interest was obscured by a contaminant.

In some cases multiplet structure is suggested in the data by a larger-than-average peak width or by resolution of a peak into a doublet at a few angles. States having such features have been noted in the tables as possible multiplets. For both isotopes, as indicated in Tables III and IV, some regions of the spectra have level densities too great for states to be resolved.

In ^{207}Pb many of states observed have been previously reported. There are some states reported in (d,d') and (d,t)[3] or other[61] studies which were not observed here. An upper limit of about 40 μb/sr can be set for the peak differential cross section for excitation of these states by (p,p'). A large number of previously unidentified levels have been observed, especially in the excitation energy region above 4.5 MeV. Because of the large level density, identification of levels at high excitation which correspond to those seen in other reactions is quite uncertain.

In both ^{207}Pb and ^{209}Bi, (p,p') excites states which have been populated in a variety of single nucleon transfer

reactions.[3,11,63-67] In ^{207}Pb the $p_{1/2}$, $f_{5/2}$, $p_{3/2}$, $i_{13/2}$, and $f_{7/2}$ neutron hole configurations were seen and in ^{209}Bi the $h_{9/2}$, $f_{7/2}$, $i_{13/2}$, $f_{5/2}$, $p_{3/2}$, and $p_{1/2}$ proton particle levels were excited. Thus these nuclei permit the study of hole and particle states in the same major oscillator shell. The angular distributions for these levels have fairly characteristic shapes and many of them are discussed in Section V.

In ^{209}Bi, inelastic proton scattering apparently excites most states seen in direct reactions but is most sensitive to collective nuclear motion. Some of the states populated in the (p,p') study of Cleary[62,72] were not seen here. That study with 14.95 and 16.1 MeV protons examined ^{209}Bi both on and off the $g_{9/2}$ isobaric resonance. At those energies many of the configurations formed are sensitive to the compound nucleus energy and are not expected to be strongly populated at 35 MeV.

Another study of ^{209}Bi using the ^{207}Pb(α,d)[69] reaction excited levels not observed here. This particular transfer reaction is expected to excite configurations involving $(\pi\nu\nu^{-1})$ as the final state, where the neutron hole is in the $p_{1/2}$ orbital. Because (p,p') can be described by a one body operator in the quantum space of the nucleus it is expected that states excited in both (p,p') and (α,d) should involve $(\pi_{h_{9/2}} \nu\nu^{-1}_{p_{1/2}})$. The states not excited in both reactions are the 2.91, 2.979, and 4.133 MeV levels

suggesting that these are 2p-1h states not involving the $h_{9/2}$ proton orbital.

Many levels in the region above 4.6 MeV of excitation were resolved in this study of ^{209}Bi that were not reported before. In this excitation region the extremely high population of levels and the fractionation of strength makes resolving states very difficult.

C. Discussion of the Collective Model

The primary information required for a conventional collective model (CM) calculation is the nucleon-nucleus elastic scattering optical model potential. This potential is usually obtained with search codes that vary the model parameters until the best chi-square fit to elastic scattering data and, often, to polarization data is achieved. Figure 24 compares the ^{207}Pb and ^{209}Bi elastic data with optical model calculations using the best-fit Becchetti-Greenlees[21] (BG) parameters and those obtained with the optical model search program GIBELUMP.[26] Since there is no polarization data for 35 MeV protons the search was performed with fixed BG spin-orbit geometry. Spin-orbit sets adopted from other studies at other bombarding energies gave similar good agreement between the measured and calculated elastic cross sections.

However, collective model calculations with the BG and fitted sets yield different cross section predictions. With the BG and fitted optical models for either nucleus, the CM gives about a 40 per cent difference between results for the same ℓ-transfer. However, the ratio of ℓ-transfers within

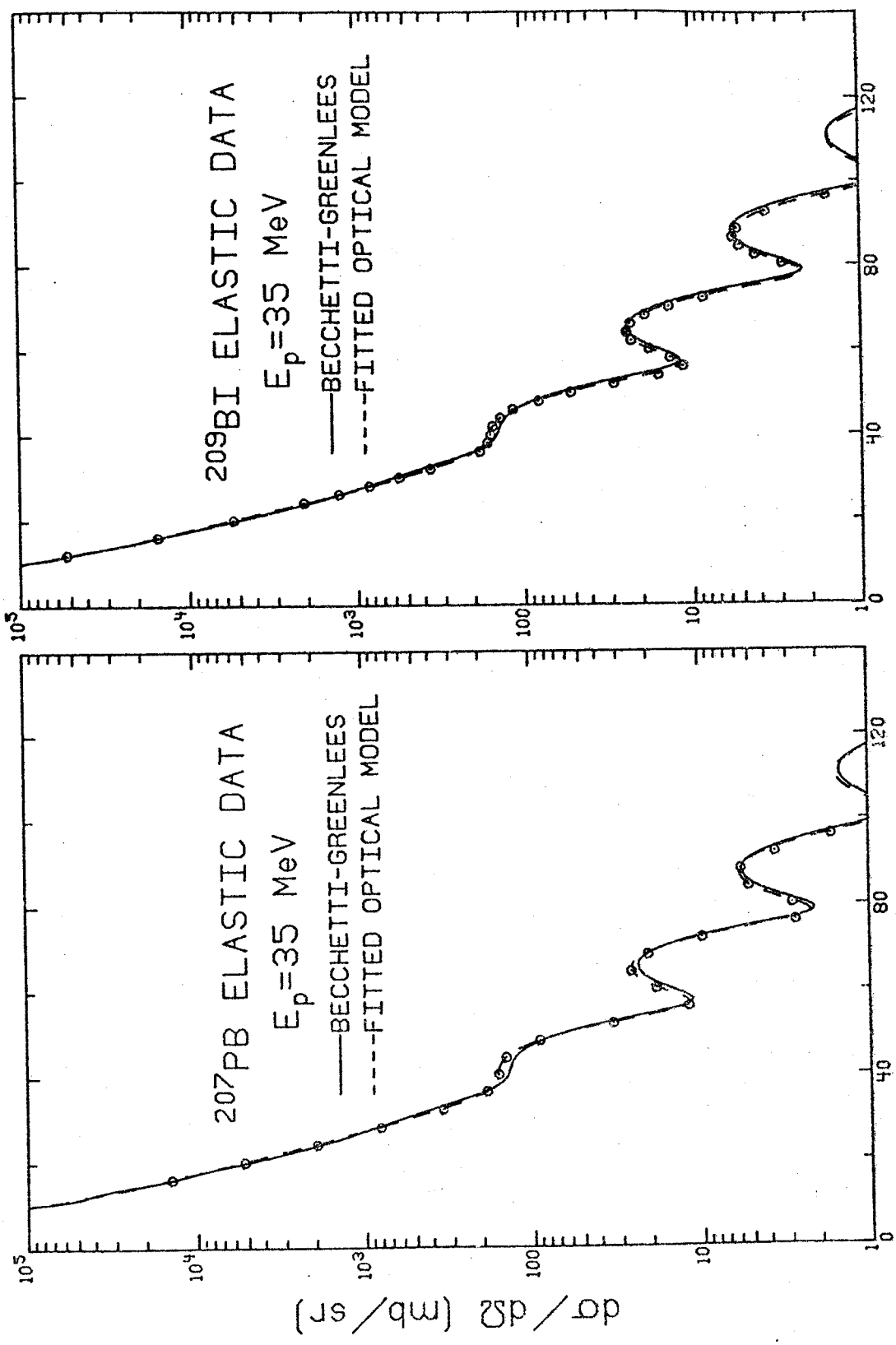

FIGURE 24.--Comparison of the measured elastic angular distribution with calculations described in the text.

a set is identical. This ambiguity in normalization of the DWBA cross section has been noticed previously.[2] For this reason and because of the lack of polarization and large angle data the BG optical model parameters have been used in all macroscopic and microscopic model calculations in this study. Use of these parameters gives excellent agreement with previous CM analysis of these nuclei using the (p,p') reaction.

In the collective model calculations, the code DWUCK[27] was used with 40 partial waves, integration limit of 20 fm, and integration step of 0.1 fm. Both the real and imaginary parts of the optical model were deformed and, since there is little sensitivity to the reaction Q-value, all calculations were for transitions to states lying at 5 MeV of excitation energy. Coulomb excitation was included in the L=2 and 3 cases but only in the former excitation is the contribution significant. The deformation parameter, β_L, was calculated as the square root of the ratio of the experimental and predicted CM cross sections. There was no accounting for the initial and final state spins involved.

For L greater than about 5 the forward angle CM fits to the data are not good. The data consistently shows forward angle strength not predicted by the CM. This fact and the rather similar angular distributions for $L \geq 6$ makes large L assignments quite tentative.

The results for the CM fits are discussed below. The actual fits are shown in Figures 25 through 27 and the

FIGURE 25.--Collective model fits for all identified states in ^{207}Pb. Displayed with the fit is the excitation energy of the state and the deformation parameter, β_L, corresponding to orbital angular momentum transfer L.

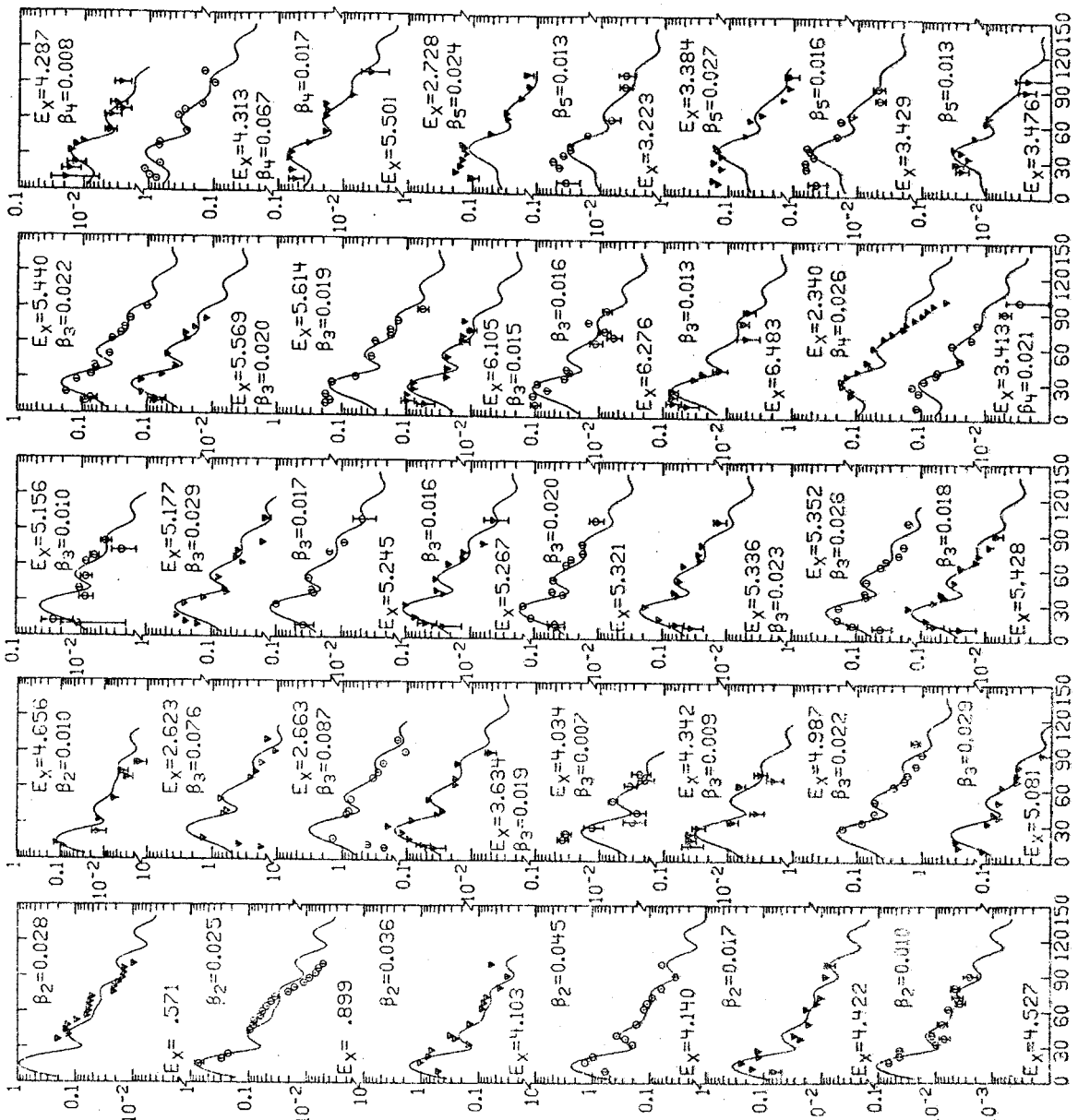
Ex=.571
β2=0.028
Ex=4.103
β2=0.045
Ex=4.140
β2=0.017
Ex=4.422
β2=0.010
Ex=4.527
Ex= .899
β2=0.025
Ex=4.656
β2=0.010
Ex=2.623
β3=0.076
Ex=2.663
β3=0.087
Ex=3.634
β3=0.019
Ex=4.034
β3=0.007
Ex=4.342
β3=0.009
Ex=4.987
β3=0.022
Ex=5.081
β3=0.029
Ex=5.156
β3=0.010
Ex=5.177
β3=0.029
Ex=5.245
β3=0.017
Ex=5.267
β3=0.016
Ex=5.321
β3=0.020
Ex=5.336
β3=0.023
Ex=5.352
β3=0.026
Ex=5.428
β3=0.018
Ex=5.440
β3=0.022
Ex=5.569
β3=0.020
Ex=5.614
β3=0.019
Ex=6.105
β3=0.015
Ex=6.276
β3=0.016
Ex=6.483
β3=0.013
Ex=3.413
β4=0.021
Ex=2.340
β4=0.026
Ex=4.313
β4=0.067
Ex=5.501
β4=0.017
Ex=3.223
β5=0.024
Ex=3.429
β5=0.013
Ex=3.476
β5=0.013
Ex=4.287
β4=0.008
Ex=2.728
β5=0.013
Ex=3.384
β5=0.027
0 30 60 90 120 150

FIGURE 25

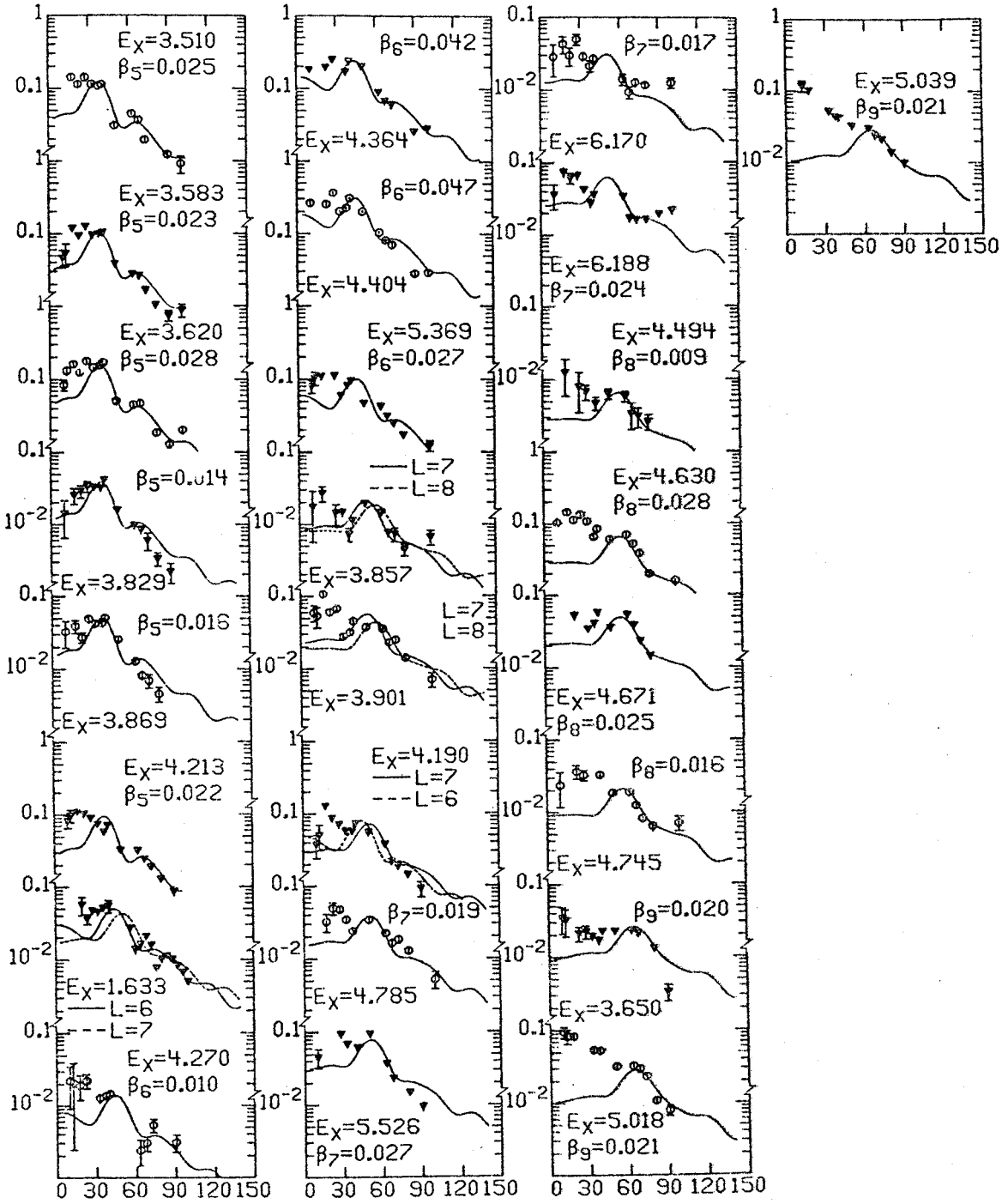

FIGURE 26.--Same as Figure 25.

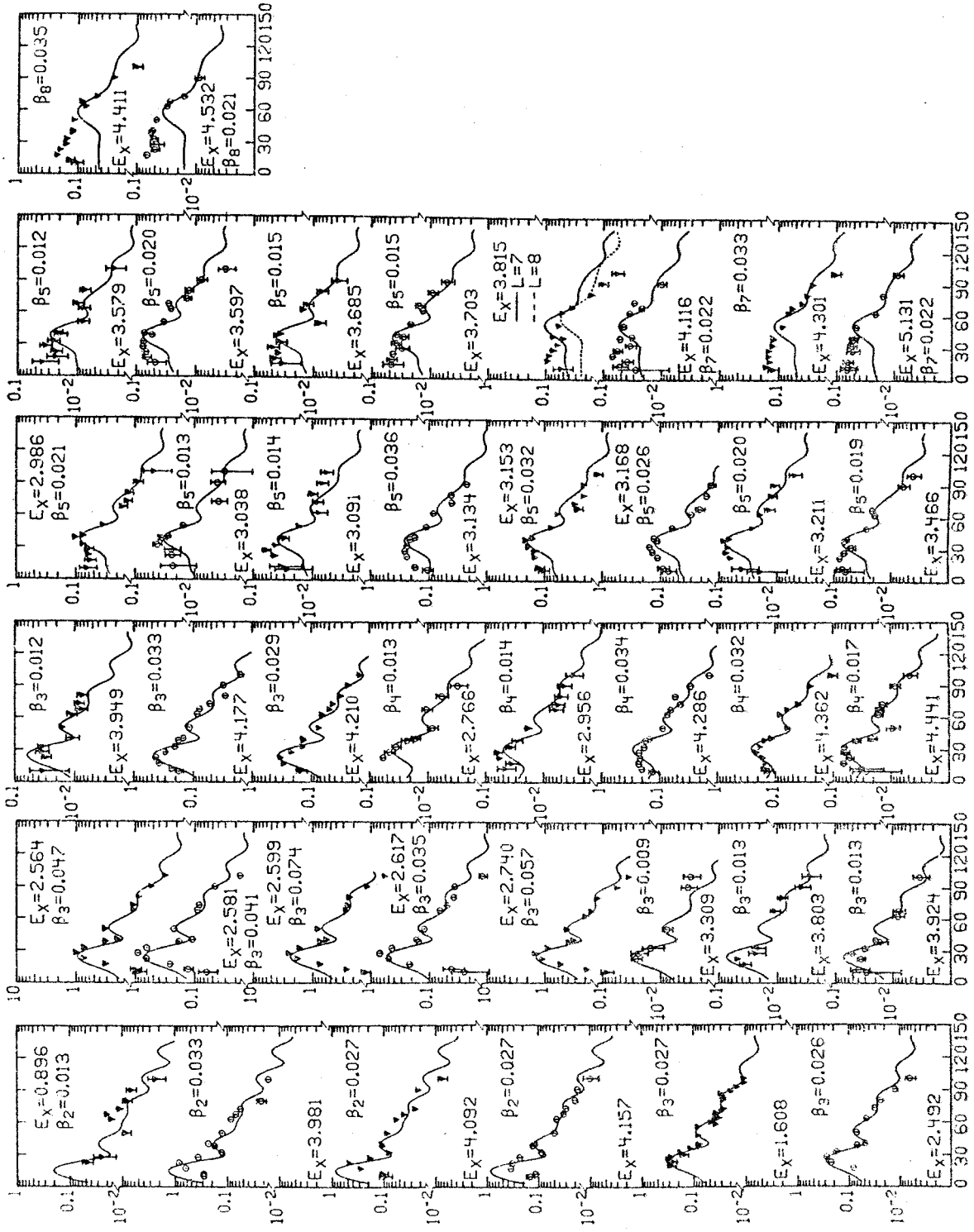

FIGURE 27.--Same as Figure 25 but for ^{209}Bi.

deformation parameters and L assignments are listed in Tables III and IV.

D. ℓ-transfers and Deformation Parameters for ^{207}Pb

The results of CM fits to the ^{207}Pb data are displayed in Figures 25 and 26. Whenever possible, comparison of the data with angular distributions for levels of known ℓ-transfer was made. In ^{207}Pb, considerable fractionation of the strength seen in ^{208}Pb generally occurs. States are discussed in the following sections according to L.

D-1. Quadrupole excitations.

The states at 0.571 and 0.899 MeV of excitation, previously identified[11,63-65,68] as single particle states, are excited predominantly with L=2. The rate of fall of the angular distributions are well reproduced and the phase of the data is also reasonably well given. These $f_{5/2}$ and $p_{3/2}$ neutron hole states have been shown[58-59] to have significant contributions from quadrupole core polarization excitations.

The ^{208}Pb 2^+ state at 4.086 MeV is apparently split into a doublet with members at 4.103 and 4.140 MeV. Vallois et al.[1,70] have identified strong quadrupole excitations at 4.090 and 4.125 MeV. Within experimental error, the excitation energies and deformation parameters from that study agree with our values. However, a 4.115 MeV

state seen[3,61] in (d,p) suggests that a doublet may lie near this excitation energy. Our data does reveal a weakly excited state at about 4.112 MeV which is unfortunately seen at only a few angles. When resolved its cross section is less than 5 per cent of that of the 4.103 MeV state.

Tentative identifications of states involving L=2 transitions have been made for the states at 4.422 and 4.527 MeV. Identification of the 4.656 MeV level as L=2 is fairly certain.

D-2. Octupole excitations

There were many transitions involving L=3 angular momentum transfer. This is to be expected since there are many 1p-2h configurations that can arise from the large number of 1p-1h octupole configurations in the ^{208}Pb core. The well known doublet with members at 2.623 and 2.663 MeV dominates any inelastic spectrum and was so intense at some angles as to be unscannable. Both members of the doublet have characteristic L=3 shapes.

The 4.342 MeV level is believed to be an octupole excitation. Vallois et al.[1,70] identified a state at 4.340±0.015 MeV as being an L=6 level. As there is no state observed in our data within 15 keV of the 4.342 MeV state we conclude that either a doublet is present at that energy or the initial L assignment is incorrect.

The level at 5.177 MeV appears to be a multiplet. An L=3 assignment has been made for the strongest member.

D-3. States involving L=4.

Collective model calculations for states involving L=4 transitions were similar to only a few experimental angular distributions. The L=4 strength appears concentrated in only a few levels. The 2.340 MeV state, which has been identified as the $f_{7/2}$ neutron hole state, has an angular distribution with characteristic L=4 shape. According to direct DWBA theory this state can be reached only by L=2 or 4.

The state at 4.313 MeV has been assumed to be the unresolved weak coupling doublet built on the 4.323 MeV 4^+ vibration in ^{208}Pb. This ^{207}Pb state has a small satellite at 4.287 MeV which is weakly excited but has an identifiable L=4 shape.

D-4. States with L=5.

As in ^{208}Pb there are many states that involve L=5 transitions. In particular, the region from 3.20 to 3.62 MeV of excitation has many weakly excited levels that have ℓ-transfers of 5. The states at 3.583 and 3.620 MeV both have L=5 shapes. The 2.728 and 3.429 MeV levels were previously assigned[70] L=6. We have assigned L=5 for both states. The 2.728 MeV level is seen[3,61] in (d,p) with ℓ_n=4.

The neutron configuration of $g_{9/2}$ coupled to ^{206}Pb(0.00 MeV) which has been suggested[3,11,65,68] for this state is consistent with both identifications.

A significant fraction of the L=5 strength seen in ^{208}Pb is not seen in ^{207}Pb. Probably most interesting is the lack of L=5 strength in the excitation region of ^{207}Pb corresponding to the first excited 5^- state in ^{208}Pb. This missing strength is discussed in section IV-B, below.

Higher excitation L=5 strength seen in ^{208}Pb has not been observed in ^{207}Pb. This may be due to configuration mixing or masking of the strength by other ^{207}Pb levels. We also noted a similar lack of octupole strength corresponding to that seen in high-lying levels in ^{208}Pb. This probably has the same explanation.

D-5. States with L≥6.

A few states apparently involve L=6 transfers. The weak coupling doublet with parentage in the 6^+ state in ^{208}Pb apparently lies at 4.364 and 4.404 MeV. The 1.634 MeV state which is highly excited in single particle transfers[11,63-65,68] is excited in (p,p') by L=6 or 7. Direct DWBA theory allows the transition to proceed through only L=5 or 7.

All angular momentum transfer assignments for L=7 or larger are quite tentative. As noted above, this is due to the generally similar shapes of these high ℓ-transfers. States which possibly involve high spin transfer are found

at 3.650, 3.857, 3.901, 4.494, 4.630, 4.671, 4.745, 4.785, 5.018, 5.039, 5.526, 6.170, and 6.188 MeV. Most of these levels have tentative assignments and many appear to have multiplet structure.

E. ℓ-transfers and Deformation Parameters for ^{209}Bi.

The ^{209}Bi(p,p') data displayed in Figure 27 has been compared with CM characteristic shapes. The large level density and the apparent extreme splitting of the strength of ^{208}Pb core excitations made L assignment difficult. In general, the bismuth angular distributions were similar to those of ^{207}Pb.

E-1. Quadrupole excitations.

The single particle state at 0.896 MeV ($J^{\pi}=7/2^{-}$) seen in the (^{3}He,d)[66] and (α,t)[67] reactions is populated primarily by an L=2 transition although L=0,2,4,6,8 are allowed for transitions to this state.

Three distinct quadrupole excitations at 3.981, 4.092, and 4.157 MeV have been resolved. The total deformation parameter for this triplet is about 0.050. Bertrand and Lewis,[71] in an inelastic proton study of ^{209}Bi, reported an L=2 group centered at about 3.96 MeV of excitation and with a β_2=0.049. These two measurements are in good agreement. The 3.981 MeV level has been suggested[62] to be an unresolved doublet.

E-2. Octupole excitations.

There were a number of states seen with characteristic L=3 angular distributions. Most interesting is the dominant six-member group centered at about 2.6 MeV. This is the well-known multiplet resulting from the $h_{9/2}$ proton coupling to the octupole vibration at 2.615 MeV in ^{208}Pb.

The $i_{13/2}$ single particle level at 1.608 MeV also has an angular distribution well fit by an L=3 CM calculation. This state has been shown[60] to have a large admixture of the $13/2^+$ member of the 2.6 MeV multiplet.

Other states with L=3 were found at 3.309, 3.803, 3.924, 3.950, 4.177, and 4.210 MeV. The last two levels show a fairly large concentration of octupole strength in an excitation region where no comparable strength is found in ^{208}Pb.

E-3. Levels with L=4.

Two low-lying states at 2.766 and 2.956 MeV were observed that previously were seen[72] in (p,p') work near 15 MeV bombarding energy. There, the lower state was concluded to be a member of the multiplet built on the lowest 5^- level in ^{208}Pb. The upper state was assigned a spin of $3/2^+$. Our data indicates that the cross sections for these states are fit only by the L=4 shape. This is in disagreement with the previous conclusions.

A strongly populated group near 4.3 MeV was also observed to have two members with L=4 shapes. The members lie at 4.286 and 4.362 MeV. The 4.441 MeV excitation, which is probably a multiplet, has been assigned L=4. The level at 5.509 MeV may correspond to the L=4 level at 5.20±0.5 MeV observed[71] at 62 MeV, but we could not make an assignment of L.

E-4. Transitions with L=5.

The bismuth spectra have two dominant groups at about 3.13 and 3.56 MeV and with characteristic L=5 shapes. These groups have been identified in other (p,p') studies as L=5 excitations. The 62 MeV work[71] extracted deformation parameters of 0.050 and 0.029 for the lower and higher states, respectively. We have obtained total deformations of 0.065 and 0.037 for these transitions. The disagreement may arise from problems in background subtraction in the higher energy data. We are in good agreement with the results given in Reference 72.

No other L=5 identifications could be made.

E-5. States with $L \geq 6$.

A few states were identified as having angular momentum transfer greater than 5. As in the case of the ^{207}Pb data, the experimental angular distributions for high ℓ-transfers are difficult to distinguish because of the similar shapes. States at 4.116, 4.301, and 5.131 MeV showed possible L=7 strength. States at 4.411 and 4.532 MeV revealed possible

L=8 strength. No L=6, 9, or 10 transitions were found in the data. This might result from the fractionation of core strength by weak coupling.

F. Summary of the Collective Model Results.

The results of the CM fits are presented in Figure 28. There, the strength for each ℓ-transfer ranging from 2 to 9 has been displayed according to excitation energy for each of the three nuclei, ^{207}Pb, ^{208}Pb, and ^{209}Bi. It is clear that the distribution of inelastic strength is quite similar in each nucleus. This similarity will be discussed in the next section.

IV. THE WEAK COUPLING MODEL

A. Discussion

It is evident from the spectral plots of Figure 19 and from the deformation parameter verses excitation energy display of Figure 28 that the strong excitations in ^{208}Pb split into multiplets in ^{207}Pb and ^{209}Bi. The characteristics of these multiplets are that they are centered about the energy of the core excitation, their total strength is about equal to that of the core level, and the ratio of members' cross sections is roughly constant. The cross sections for ^{208}Pb states, which apparently are the bases on which these multiplets are built, are compared with the angular distributions for corresponding multiplet members in Figures 29 and 30. The similarity between angular distributions of the core state and states in the odd A nuclei is quite striking.

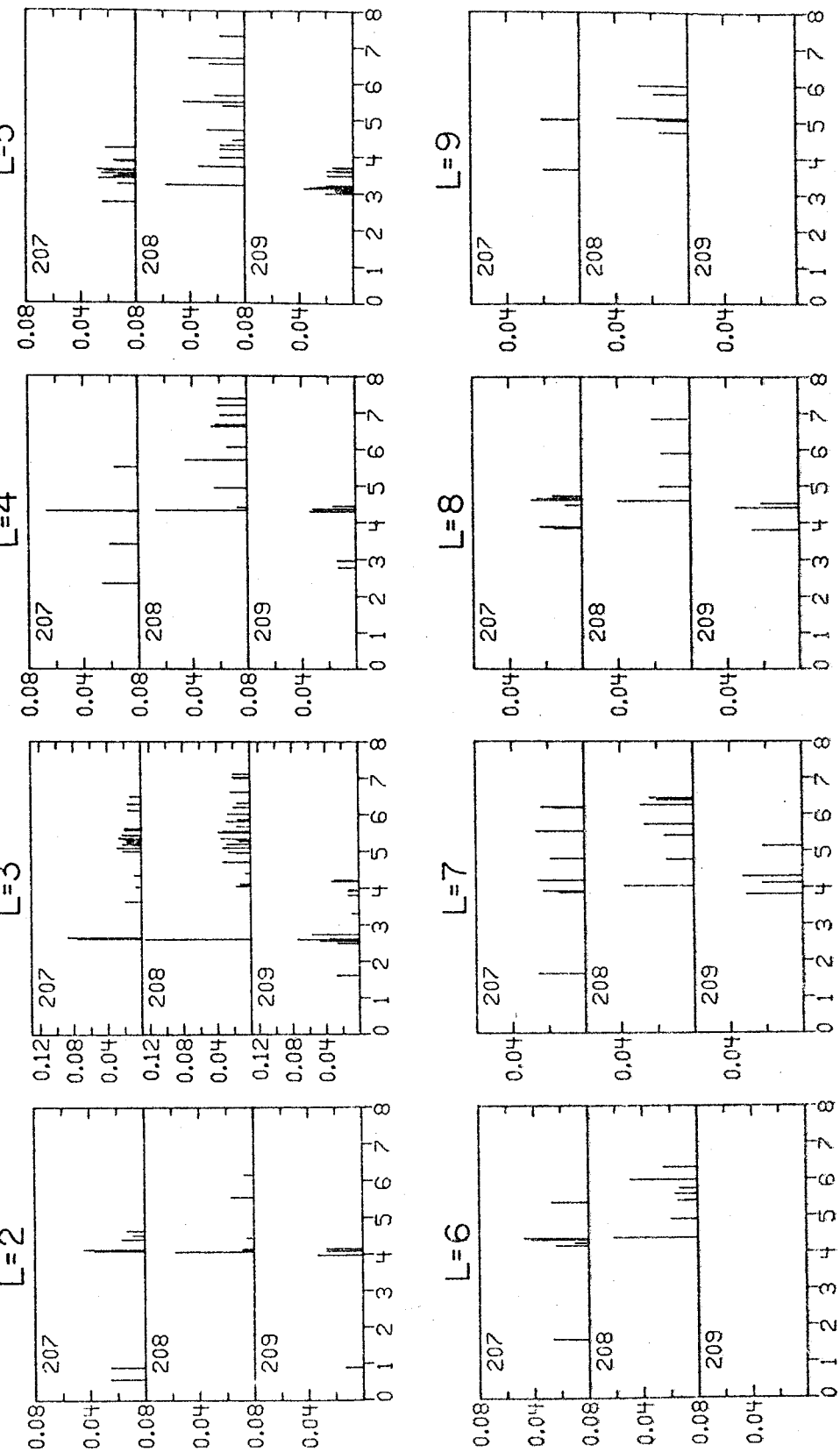

FIGURE 28.--Summary of the collective model results for the three nuclei. The deformation parameter, β_L, is plotted against excitation energy for a number of ℓ-transitions.

FIGURE 29.--Comparison of ^{208}Pb angular distributions with cross sections for weak coupling multiplets in ^{207}Pb built on the indicated ^{208}Pb excitation. The curves result from smooth interpolation through the ^{208}Pb data for the indicated level.

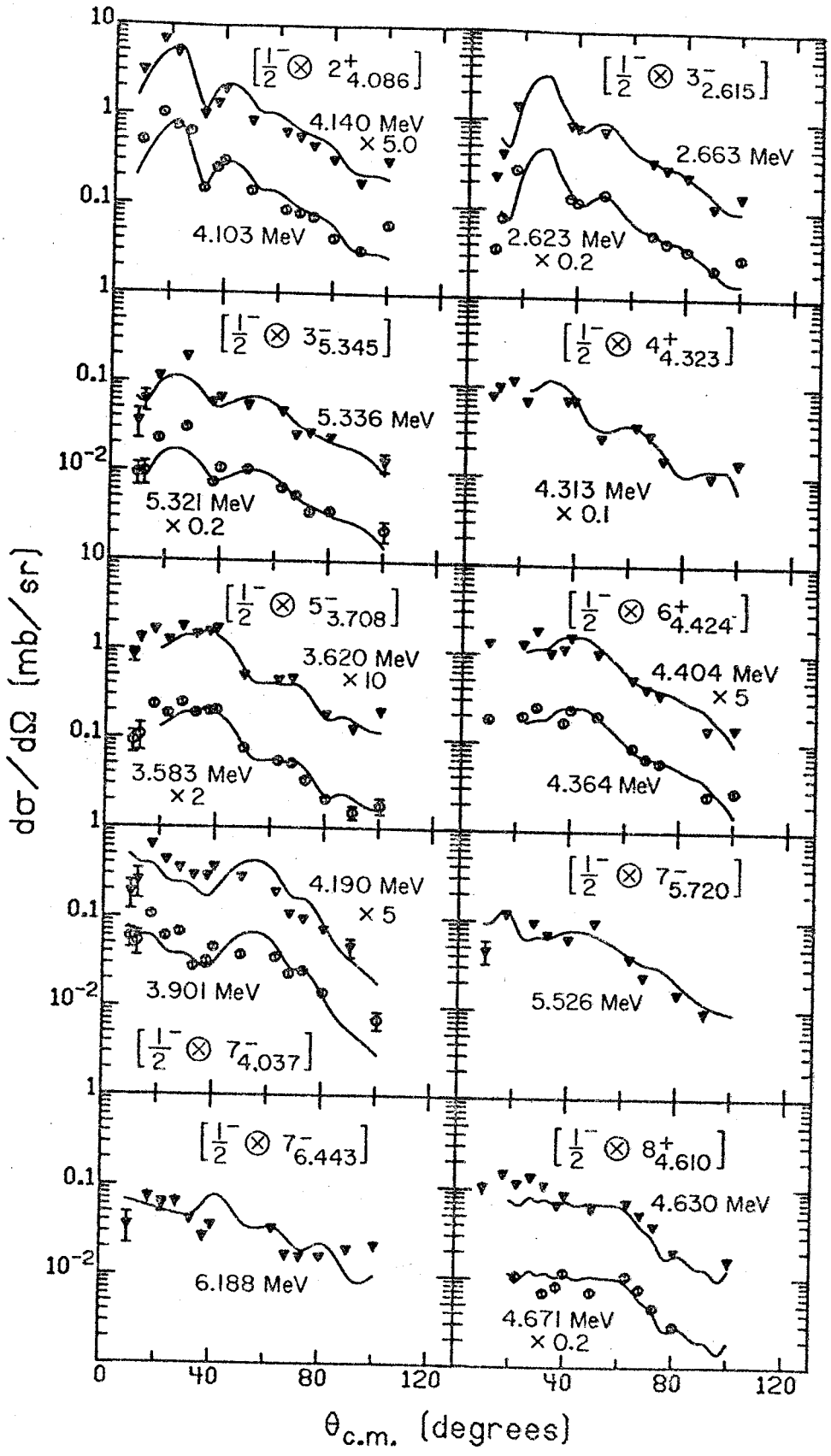
$[\frac{1}{2}^- \otimes 2^+_{4.086}]$
4.140 MeV
× 5.0
4.103 MeV
$[\frac{1}{2}^- \otimes 3^-_{2.615}]$
2.663 MeV
2.623 MeV
× 0.2
$[\frac{1}{2}^- \otimes 3^-_{5.345}]$
5.336 MeV
5.321 MeV
× 0.2
$[\frac{1}{2}^- \otimes 4^+_{4.323}]$
4.313 MeV
× 0.1
$[\frac{1}{2}^- \otimes 5^-_{3.708}]$
3.620 MeV
× 10
3.583 MeV
× 2
$[\frac{1}{2}^- \otimes 6^+_{4.424}]$
4.404 MeV
× 5
4.364 MeV
4.190 MeV
× 5
3.901 MeV
$[\frac{1}{2}^- \otimes 7^-_{4.037}]$
$[\frac{1}{2}^- \otimes 7^-_{5.720}]$
5.526 MeV
$[\frac{1}{2}^- \otimes 7^-_{6.443}]$
6.188 MeV
$[\frac{1}{2}^- \otimes 8^+_{4.610}]$
4.630 MeV
4.671 MeV
× 0.2
dσ / dΩ (mb/sr)
θc.m. (degrees)

FIGURE 29

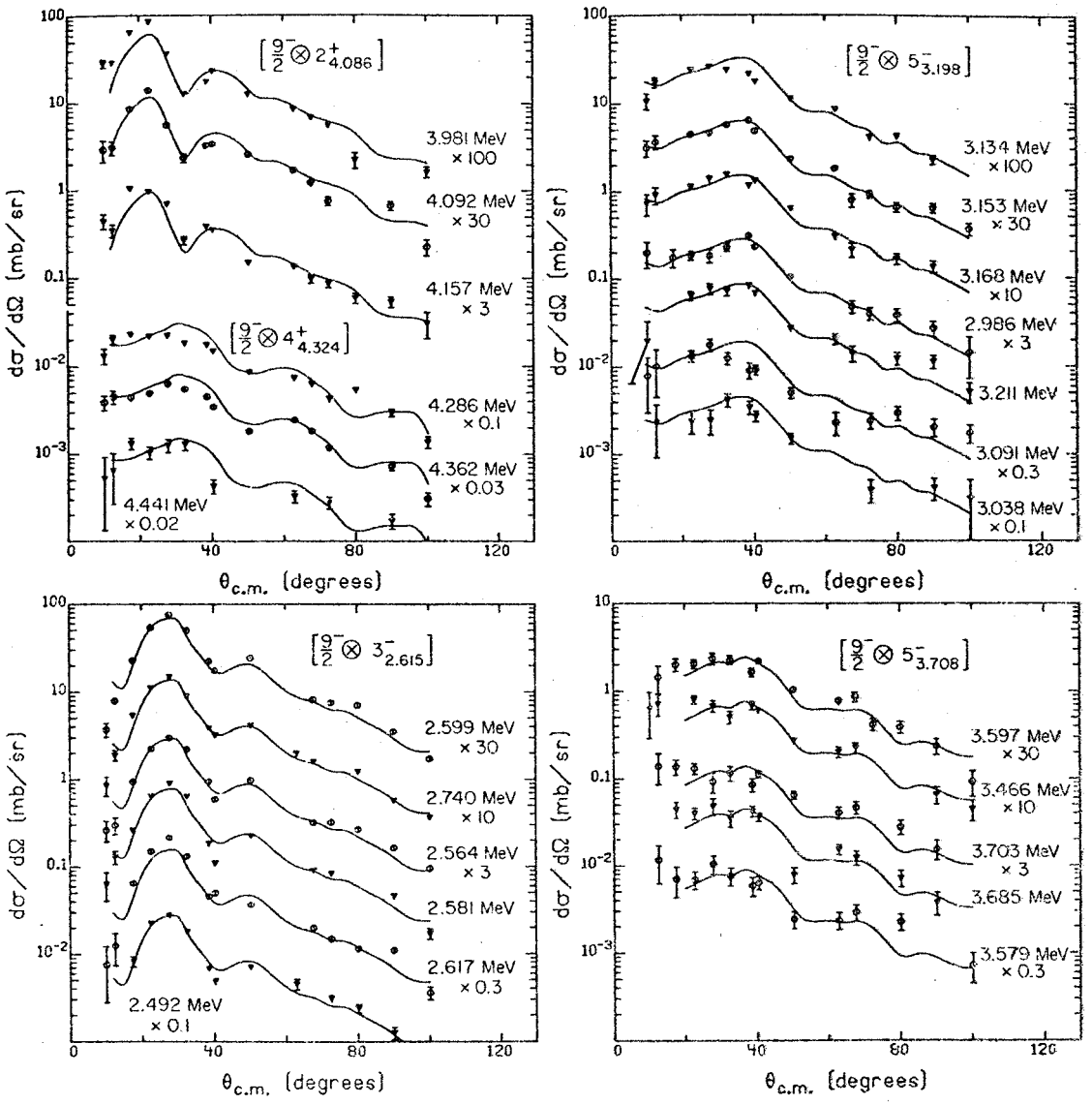

FIGURE 30.--Same as Figure 29 but for multiplets in ^{209}Bi.

These properties are given by the weak coupling model[74] which assumes that a valence particle or hole nucleon interacts only weakly with a collective core excitation. This assumption leads to a number of predictions which have been applied to the data assuming a ^{208}Pb core and which are summarized in Tables V and VI. These predictions are also discussed below. It should be noted that Cleary et al.[75] have found that weak coupling to excitations in a ^{210}Bi core can equally well describe levels in ^{209}Bi in the excitation energy region between 2.98 and 3.65 MeV. There is, however, no evidence to decide the more proper alternative.

According to the weak coupling model, members of a multiplet have cross sections, σ_m, which are related to the core cross section, σ_c, by a simple spin-statistics factor. If J_c, J_w, and j_m are the spins of the core excitation, the weak coupled particle, and a particular multiplet member, respectively, then

$$\sigma_m = \frac{(2j_m+1)}{(2J_c+1)(2J_w+1)} \sigma_c.$$

Summing this expression over possible multiplet spins predicts that the total multiplet strength should equal that of the core. Due to experimental difficulties, the data for these nuclei were taken at slightly different scattering angles. Since the cross sections vary fairly rapidly with angle, a direct comparison of the total strength

TABLE V.--Weak coupling results for ^{207}Pb.

L	E_{core} (MeV)	SWES[a] (MeV)	β_L(core)	$\sqrt{\Sigma\beta_L^2(E_i)}$	E_i (MeV)	J_i^π	Ratio[b]
3	2.615	2.646	0.12	0.12	2.623	$5/2^+$	1.06 0.02
					2.663	$7/2^+$	0.94 0.02
5	3.708	3.603	0.034	0.036	3.583	$9/2^+$	0.85 0.03
					3.620	$11/2^+$	1.12 0.04
7	4.037	4.055	0.038	0.035	3.901	$13/2^+$	0.89 0.05
					4.190	$15/2^+$	1.04 0.05
2	4.086	4.125	0.058	0.058	4.103	$3/2^-$	1.10 0.02
					4.140	$5/2^-$	0.93 0.02
4	4.323	4.313	0.067	0.067	4.313	$7/2^-,9/2^-$	1.00 0.02
6	4.424	4.386	0.062	0.063	4.364	$1/2^-$	0.97 0.02
					4.404	$13/2^-$	1.01 0.02
8	4.610	4.649	0.040	0.037	4.630	$17/2^-$	1.16 0.05
					4.671	$15/2^-$	0.76 0.04
3	5.345	5.330	0.035	0.030	5.321	$5/2^+$	1.03 0.05
					5.336	$7/2^+$	0.96 0.04
7	5.720	5.526	0.027	0.027	5.526	$13/2^+,15/2^+$	1.00 0.05
7	6.443	6.188	0.024	0.024	6.188	$13/2^+,15/2^+$	1.00 0.06

[a]Spin weighted energy sum: $\frac{\Sigma E_i(2J_i+1)}{\Sigma(2J_i+1)}$

[b]For unresolved doublets the ratio is identically equal to one.

TABLE VI.--Weak coupling results for ^{209}Bi.

L	E_{core} (MeV)	SWES[a] (MeV)	β_L(core)	$\sqrt{\Sigma\beta_L^2(E_i)}$	E_i (MeV)	J_i^π	Ratio
3	2.615	2.620	0.126	0.120	2.492	$3/2^+$	0.68±0.02
					2.563	$9/2^+$	1.08±0.03
					2.581	$7/2^+$	0.98±0.03
					2.599	$11/2^+$,$13/2^+$	1.02±0.02
					2.617	$5/2^+$	0.97±0.03
					2.740	$15/2^+$	0.93±0.02
5	3.198	3.072	0.058	0.065	2.986	$11/2^+$	0.92±0.07
					3.038	$3/2^+$	1.14±0.12
					3.091	$5/2^+$	.92±0.09
					3.134	$13/2^+$,$19/2^+$	.93±0.05
					3.153	$7/2^+$,$15/2^+$	1.06±0.06
					3.169	$17/2^+$	1.05±0.06
					3.211	$9/2^+$	1.04±0.07
5	3.708	3.591	0.034	0.037	3.466	$13/2^+$,$15/2^+$	0.98±0.09
					3.579	$11/2^+$	0.87±0.11
					3.597	$1/2^+$,$3/2^+$, $5/2^+$,$19/2^+$	1.04±0.09
					3.685	$7/2^+$,$9/2^+$	0.83±0.09
					3.703	$17/2^+$	1.00±0.10

TABLE VI.--Continued.

L	E_{core} (MeV)	SWES[a] (MeV)	β_L(core)	$\sqrt{\Sigma\beta_L^2(E_i)}$	E_i (MeV)	J_i^π	Ratio
2[b]	4.086	4.061	0.058	0.050	3.981	$9/2^-,11/2^-$	1.11±0.04
					4.092	$13/2^-$	0.93±0.04
					4.157	$5/2^-,7/2^-$	0.82±0.03
4[b]	4.324	4.335	0.067	0.050	4.286	$7/2^-,15/2^-$ $17/2^-$	1.02±0.04
					4.362	$1/2^-,9/2^-$, $11/2^-,13/2^-$	0.96±0.04
					4.441	$5/2^-$	0.91±0.07

[a]Spin weighted energy sum: $\dfrac{\Sigma E_i(2J_i+1)}{\Sigma(2J_i+1)}$

[b]For these ℓ-transfers the total strength in ^{209}Bi probably has not been found. Spin assignments are very tentative.

with that of the core could not be done reliably. However, by using the CM deformation parameters the angle averaged strengths of the data can be compared. For this reason the total effective deformation parameters for the multiplet is compared with the corresponding core deformation in the tables.

In the case of a single multiplet member the above equation predicts that the expression

$$\frac{(2J_c+1)(2J_w+1)}{(2j+1)} \frac{\sigma_m}{\sigma_c} = 1$$

only for the choice of $j=j_m$. If members of the group are degenerate then a similar expression, involving a sum of (2j+1) factors in the denominator, will be one only for the proper choice of spins. This method of checking spin assignments has been used and the results for each multiplet level is displayed in the ratio column of Tables V and VI. Again, since the core and multiplet data were not measured at exactly the same angles, the core cross section was taken to be the sum of multiplet member cross sections. If the complete strength of the multiplet has been identified this is a safe procedure. For most cases it appears, from comparison with the core strength, that the total strength has been found. The ratio listed is the weighted average of the values determined at each possible angle. The given error corresponds to the mean deviation in the

ratio. The tables also give the spin weighted energy average for each multiplet. Of course, in the limit of no particle-core interaction, this energy is expected to be identical to that of the core excitation.

B. ^{207}Pb Results

B-1. Coupling to the 3^- core state

The doublet arising from the coupling of the $p_{1/2}$ neutron hole to the lowest octupole level in ^{208}Pb has members at 2.623 and 2.663 MeV. Calculations for these states have been performed by Hamamoto[76] and indicate that the intensity ratio should conform to the expected weak coupling prescription. However, those results[76] also suggest that the states should absorb only 94 per cent of the observed core strength. We have found that the total strength of this doublet is about 95 per cent that of the ^{208}Pb 3^- vibration and that the intensity of each member is fairly consistent with the assigned spins of $5/2^+$ and $7/2^+$. A study,[77] involving inelastic proton excitation functions of the 5^- and 4^- analog resonances in ^{208}Bi, supports these spin assignments and is independent of assumptions about the weak coupling model.

The 2.623 and 2.663 MeV states have been examined in a variety of inelastic scattering experiments.[1,42,70,73,78,79] Two of these studies[42,79] were unable to resolve the doublet

but did detect strength about equal to the strength of the core state. The remaining studies[1,70,73,78] found the relative strengths generally consistent with the predictions of a weak coupling model. References 1 and 70 observed about 91 per cent of the total strength, however. A (d,d') experiment[73] reported only 87 per cent of the core strength. The deuteron experiment was performed at 13 MeV so that compound nucleus processes may be important. Therefore, it seems that inelastic experiments generally support the weak coupling model for this doublet.

Since the ^{208}Pb 2.615 MeV octupole vibration is very collective it might be expected that neutron holes other than the $p_{1/2}$ could couple to this vibration as well. The work of Grosse et al.[80] has suggested that levels observed at about 3.210 and 3.580 MeV could correspond to configurations with the $f_{5/2}$ and $p_{3/2}$ holes coupling to the octupole, respectively. We were unable to assign an ℓ-transfer value to the 3.200 MeV level observed in our data. The 3.223 MeV excitation has an L=5 assignment. The state seen at 3.583 MeV of excitation energy has a definite L=5 assignment and seems to be a member of the weak coupling doublet built on the second 5^- core state. The only state in this excitation region having an L=3 identification is the 3.634 MeV level which has a transition rate only 2 per cent of the core octupole. Thus, there appear to be no multiplets in ^{207}Pb arising from coupling of the ^{208}Pb 3^- level to other neutron holes.

B-2. Coupling to the ^{208}Pb first 5^- state

The level at 3.198 MeV excitation in ^{208}Pb is a strong collective state with about 10 single particle units strength. However, there are apparently no L=5 states in ^{207}Pb in the region about 3.2 MeV that exhaust more than 5 per cent of the inelastic transition strength of the core state. A strong level at 2.728 MeV does involve an angular momentum transfer of 5 but this level has been shown[11,65,68] to have the configuration of the $g_{9/2}$ neutron coupled to the ground state and first excited 2^+ state of ^{206}Pb. Thus it seems that the weak coupling model breaks down here. This has been noted[1,70,73] before. The missing strength probably can be explained by the fact that the ^{208}Pb 5^- wave function[24,51-53] has a large (>0.6) amplitude neutron ($g_{9/2}$-$p^{-1}_{1/2}$) component. Thus, the inelastic strength for excitation of the core 5^- level is severely hindered by the missing $p_{1/2}$ strength.

B-3. Coupling to the ^{208}Pb second 5^- state

We observe states at 3.583 and 3.620 MeV which are definitely L=5 excitations and whose summed strength agrees fairly well with the core-particle model. However, the relative intensities are not in good agreement with the predictions. Since a number of other L=5 states lie nearby, this disagreement may have a possible explanation in the configuration mixing of these levels.

Reference 70 reported states at 3.575 and 3.615 MeV excitation for which ℓ-transfer assignments could not be made. Alster[79] reported L=5 excitations in ^{207}Pb near 3.4 and 3.7 MeV that have combined strength equal to that of the ^{208}Pb 5^-_2. Thus, inelastic scattering results tend to support a weak coupling configuration for these two levels.

B-4. Coupling to the ^{208}Pb quadrupole excitation.

The levels at 4.103 and 4.140 MeV are excellent candidates for weak coupling members of a multiplet with parentage in the 4.085 MeV 2^+ excitation in ^{208}Pb. The inelastic transition rates are in good agreement and the intensities agree fairly well with the weak coupling model prescription. Alster[79] detected 100 per cent of the core cross section in his (α,α') study and Vallois et al.[70] reported an intensity identical to that of the core but observed relative population of the levels not in agreement with the theory.

B-5. The unresolved multiplet at 4.313 MeV

Although there were no experimental indications of multiplet structure for this level we conclude that the 4.313 MeV state corresponds to a weak coupling doublet built on the 4^+ level in ^{208}Pb. Other studies[1,70,79] reported a single level at this energy and observed a cross section equal to that of the core state. We also observe the same strength as that of the core vibration so that a doublet assignment for this level seems fairly certain.

B-6. Other possible weak coupling levels

The 6^+(4.424 MeV) and the 8^+(4.610 MeV) in ^{208}Pb are both fairly strongly excited in (p,p') and could be expected to lead to multiplets in ^{207}Pb. The ^{207}Pb levels at 4.364 and 4.404 MeV, with L=6, and the levels at 4.630 and 4.671 MeV, with L=8, have relative intensities and summed cross sections in agreement with the weak coupling model predictions.

Although L=7 levels observed in ^{207}Pb and ^{208}Pb have tentative spin identification it seems that multiplets with parent 7^- core states have been found. The total strength and location near the core excitation energies suggests identification of these levels as weak coupling states. The lowest 7^- state in ^{208}Pb, at 4.037 MeV, leads to two levels at 3.901 and 4.190 MeV in ^{207}Pb. The summed strength is slightly less than that observed in

the core and the relative intensities are in fair agreement with the model.

The 7^- levels in ^{208}Pb at 5.720 and 6.443 MeV may correspond to degenerate doublets in ^{207}Pb at 5.526 and 6.188 MeV. However, the ^{207}Pb states are separated from the excitation energies of the corresponding core states by a much larger energy gap than the other levels discussed above. The strength of these levels is essentially equal to that of the core states. The large energy separation and the uncertain L assignments, however, makes identification of these levels as weak coupling multiplets quite tentative.

Lastly, the doublet with constituents at 5.321 and 5.336 MeV, apparently $5/2^+$ and $7/2^+$ states, respectively, may have parentage in the 5.345 MeV octupole excitation in ^{208}Pb. The total core strength is nearly reproduced and the relative intensities are about in the ratio given by the model. Again, a possible explanation of the missing strength lies in mixing with nearby octupole levels.

C. ^{209}Bi Results

C-1. Coupling to the 3^- core state

In the particle-core coupling model, coupling of the $h_{9/2}$ proton to the ^{208}Pb octupole vibration can lead to a septuplet of states. Our study and a number of other charged particle studies[72,73,78] of this multiplet have only resolved six members. However, assuming a (2J+1) cross

section dependence, the strength of the 2.599 MeV state suggests that this level is a degenerate $11/2^+$, $13/2^+$ doublet. Coulomb excitation[81] has shown that his level is a doublet with members separated by only about 2 keV, the larger spin state lying higher. We have found the total strength of this multiplet nearly equal to that of the core excitation. The assigned spins are in agreement with those given in References 72,73,78, and 81 and the relative intensities agree quite well with the weak coupling model predictions.

C-2. Coupling to the ^{208}Pb first 5^- state

Spin assignments for this multiplet have been made and compared with the weak coupling theory in Table VI. A total strength greater than that of the core excitation was observed. The intensities follow a (2J+1) rule quite well and, as shown in Table VII, the agreement with previous spin assignments is good. In all assignments but that of Francillon et al.[57] the $1/2^+$ level of the multiplet has not been located. Since this $1/2^+$ state is expected to have a very small cross section, identification of this level is expected to be difficult. The 3.309 MeV level, identified by Francillon et al. as the $1/2^+$ state, has a distinct L=3 shape in our data. Unless a doublet lies at this energy it appears that the 3.309 MeV state can not be a member of the multiplet. Cleary[72] suggested that a very weak state seen at 2.847 MeV may be the $1/2^+$ level but the cross section was

TABLE VII.--Spin and parity assignments for the $9/2^-$ x 5^-_1 multiplet in ^{209}Bi.

E_x(MeV)	Present Work	Ref. 57	Ref. 72	Ref. 73
2.766	-	-	$3/2^+$	-
2.986	$11/2^+$	$13/2^+$	$19/2^+$	$13/2^+$
3.038	$3/2^+$	$3/2^+$	$5/2^+$	$3/2^+$
3.091	$5/2^+$	$7/2^+$	$7/2^+$	$5/2^+$
3.134	$13/2^+$,$19/2^+$	$11/2^+$,$19/2^+$	$11/2^+$,$15/2^+$	$11/2^+$,$19/2^+$
3.153	$7/2^+$,$15/2^+$	$5/2^+$,$17/2^+$	$9/2^+$,$17/2^+$	$7/2^+$,$17/2^+$
3.169	$17/2^+$	$15/2^+$	$13/2^+$	$15/2^+$
3.211	$9/2^+$	$9/2^+$	-	$9/2^+$
3.315	-	$1/2^+$	-	-

so small that an angular distribution could not be measured. Our spectra show no states near 2.847 MeV.

Using techniques independent of any weak coupling assumptions, Cleary also identified the 2.986 MeV level as having spin $19/2^+$. However, the strength he measured for this level was much less than that predicted by the weak coupling model assuming $J^\pi=19/2^+$. The strength that was measured is consistent with our spin assignment and the weak coupling picture. Being very sure of the spin assignment, however, Cleary attributed the difference between the weak coupling model and experiment to mixing of this level with the higher lying $19/2^+$ state associated with the decuplet built on the ^{208}Pb second excited 5^-. Our analysis of the two L=5 multiplets, however, indicates that mixing of these two states is not required if one assumes that the 2.986 MeV level has spin 11/2. It should also be noted that Cleary concluded that the 3.211 MeV level had a microscopic configuration based on coupling of the $h_{9/2}$ particle to the unnatural parity 4^- level in ^{208}Pb. Our bismuth data indicates that the 3.211 MeV level is the $9/2^+$ weak coupling member of the 5^-_1 multiplet.

Our assignment of doublet spins to the 3.153 MeV level is consistent with the results of Reference 73 which found two members at about this energy and with separation of about 4 keV. That work also suggested possible doublet structure and spin assignment for the 3.134 MeV level and concluded that its members are separated by at most 3 keV.

C-3. Coupling to the ^{208}Pb second 5^- state

Five members of a multiplet near 3.6 MeV have angular distributions similar to those of the second 5^- level in ^{208}Pb. The total cross section is slightly greater than that seen in the core. It also seems that many of the levels are degenerate since coupling of the valence proton to the core excitation is expected to result in 10 states. This apparent degeneracy makes the spin assignments quite uncertain.

C-4. Other possible weak coupling levels

Excitations involving angular momentum transfers of 2 and 4 were identified in ^{209}Bi that lie near the excitation energies of the first 2^+ and 4^+ levels in ^{208}Pb. In both cases the total strength of the core was not observed and it seems that some fragmented strength has not been resolved. However, spins have been assigned assuming that all possible strength was observed and that the relative intensities are given by the (2J+1) rule. Therefore, the spins given in Table VI for the L=2 and L=4 multiplets are quite tentative.

About 75 per cent of the core quadrupole strength was found. Cleary[72] reported an additional L=2 excitation at 4.213 MeV and observed about 72 per cent of the expected strength. Reference 62 has suggested that the 3.981 MeV level is really a doublet. A gamma-ray resonance

experiment[82] on ^{209}Bi identified L=2 transitions to levels at 3.977, 4.083, 4.156, 4.176, and 4.206 MeV, the lower three levels corresponding to our identified L=2 states. The levels seen here at 4.177 and 4.210 MeV have definite assignments of L=3, although doublet structure is possible. It seems that complete identification of the 2^+ and 4^+ weak coupling multiplets in ^{209}Bi requires higher resolution than currently possible.

V. THE SINGLE PARTICLE STATES AND A MICROSCOPIC MODEL

Both ^{207}Pb and ^{209}Bi have states strongly populated in single particle transfer reactions and thus identified as single particle levels. Most of these states have been observed in the present (p,p') study. It is expected from electromagnetic measurements[83] and other inelastic scattering experiments[58,60] that the inelastic transitions to these states involve strength greater than that given by a model involving a single valence nucleon.

A. The States in ^{207}Pb

To explain the measured angular distributions for the inelastic scattering from the first $5/2^-$, $3/2^-$, $13/2^+$, and $7/2^-$ excited states in ^{207}Pb, DWBA calculations were made which included only the valence orbits. Figure 31 compares these theoretical results with the data. The curves give both direct and direct-plus-exchange predictions.

The valence calculations shown in Figure 31a used a central nucleon-nucleon force and an approximate treatment of knock-on exchange.[37] This exchange approximation has been shown to predict cross sections slightly larger than those for exact calculations, the overestimation being larger for small ℓ-transfers. For the direct amplitude, the projectile-target interaction was taken to be the two-body effective bound state interaction (G-matrix) derived from the Hamada-Johnston (HJ) potential. In these calculations, harmonic oscillator wave functions were used with the size parameter set to 0.405 fm^{-1} which reproduces the results of elastic electron scattering on ^{208}Pb. The optical model parameters for the results shown in Figure 31 were those of Becchetti and Greenlees,[21] although use of other sets gave similar results. In Figure 31a, only the dominant, non-spin-flip (S=0) transitions are displayed. The calculations underestimate the data, the data being 3 to 10 times stronger. The shapes of the angular distributions predicted by the theory are generally not in good agreement with the data.

A previous study,[84] using central and tensor forces for the 20 MeV data[58] for these states, suggested important tensor contributions in the transition to the $3/2^-$ state. It is interesting to determine if non-central forces could significantly improve the fits to the data. Calculations were therefore carried out still assuming a simple valence description of ^{207}Pb and using the code DWBA70[45] which allows the use of spin-orbit and tensor

FIGURE 31.--Measured differential cross sections and valence orbital model predictions for single particle states in ^{207}Pb. (a) Predictions using a purely central force. The broken and solid curves give the direct (D) and direct-plus-exchange (DE) results, respectively. (b) DE results using the code DWBA70. The broken curve gives the predictions using a central force only. The solid line displays calculations including non-central interactions.

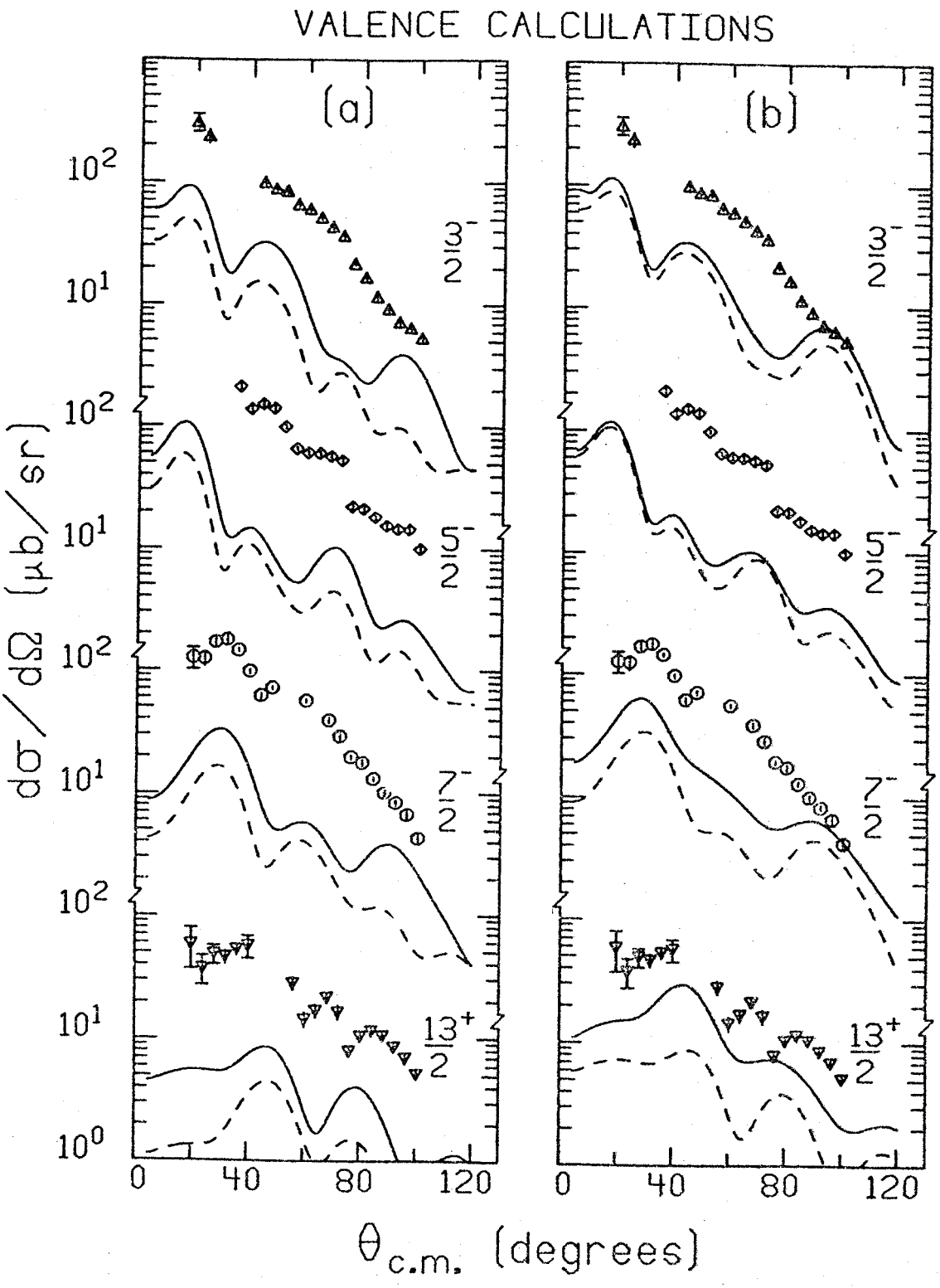
VALENCE CALCULATIONS
(a)
(b)
10^2
10^1
10^0
$d\sigma/d\Omega$ (μb/sr)
3^-_2
5^-_2
7^-_2
13^+_2
0
40
80
120
$\theta_{c.m.}$ (degrees)

FIGURE 31

two-body forces and treats exchange exactly. The central portion of the nucleon-nucleon effective force was taken to be a Serber exchange mixture; the Yukawa radial shape had a 1 fermi range and strength of -30 MeV for V_o. (With this even-state, central interaction, results compare well with the HJ and the approximate exchange calculations as can be seen in Figure 31b.) For the non-central analysis the tensor and $\underset{\sim}{L}\cdot\underset{\sim}{S}$ potentials were identical to those used in the ^{208}Pb microscopic calculations, above.

Figure 31b displays the results using the central-plus-non-central forces. In the DWBA70 calculations, contributions from both S=0 and S=1 transitions were included. For each state, the tensor dominates the spin-orbit contribution, even in the case of the $13/2^+$ state where the allowed orbital angular momentum transfers are 5 and 7. The angular distributions are somewhat improved in shape but are still lower than the data by factors of 3 to 6. The predictions for the $13/2^+$ state show the most dramatic increase. Calculations with DWBA70 using Woods-Saxon wave functions give enhanced forward angle cross sections but renormalization by factors of 2 to 6 is still needed.

The renormalization of the two-body force needed to match the data is related to the effective charge in electromagnetic transitions, both being corrections for core polarization effects. Bernstein[33] and Astner et al.[35] have given a semi-quantitative relation between these two parameters. Using the results of the calculations with

harmonic oscillator wave functions and assuming the proton-proton force is half as strong as the proton-neutron force, effective charges of 0.75, 1.1, 0.62, and 0.42 were obtained for the $3/2^-$, $5/2^-$, $7/2^-$, and $13/2^+$ states, respectively. For the first two levels these are in fairly good agreement with values measured using electromagnetic techniques.[83]

It is clear from these results that a model involving only pure, single hole states cannot reproduce the data even though both central and non-central forces are used. More complicated excitations of the core particles are apparently significant. Such core polarization effects were calculated using two different models. First, the phenomenological model of Love and Satchler[85] was used. The core polarization (CP) form factor (FF) was summed coherently with the direct-plus-exchange valence FF for the S=0, L=J transition of each state. The strength of the CP was chosen to give the fits shown in Figure 32a; the CP contribution was always larger than the valence term. Becchetti and Greenlees optical model parameters were used in the collective model for the core. In this macroscopic model,[85] a radial matrix element of r^L relates the CP strength to the effective charge; these matrix elements were calculated using Woods-Saxon wave functions in a well of radius 1.2 $A^{1/3}$F, diffuseness 0.70 F, spin-orbit strength of 25 MeV, and depth adjusted

FIGURE 32.--Measured differential cross sections and core polarization model predictions for single particle states in ^{207}Pb. (a) The macroscopic core polarization prediction is given by the solid line; for comparison, the broken curve shows the DE valence model. (b) the DE microscopic core polarization results are given by the broken curve. The solid curve shows results using complex coupling.

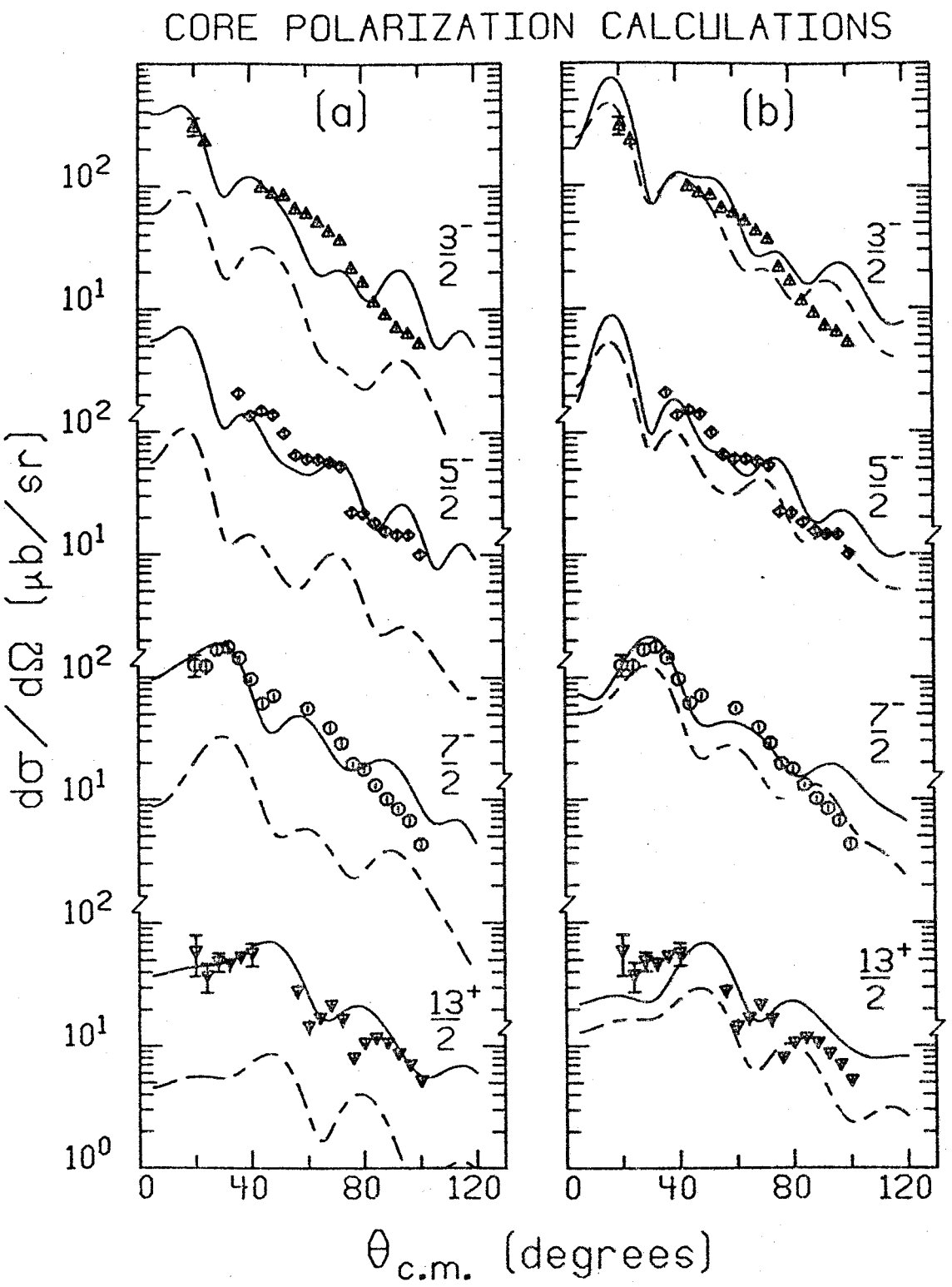
CORE POLARIZATION CALCULATIONS
(a)
(b)
3⁻/2
5⁻/2
7⁻/2
13⁺/2
dσ/dΩ (μb/sr)
θc.m. (degrees)
0
40
80
120

FIGURE 32

to give the correct binding energy. Expressed as $\langle r^L \rangle / (1.2\ A^{1/3})^L$, these matrix elements have values of 0.625, 0.722, 0.778, and 0.716, in order of excitation energy. Effective charges of 0.74, 0.95, 0.61, and 0.43 were extracted for the $3/2^-$, $5/2^-$, $7/2^-$ and $13/2^+$ levels, respectively. These values are consistently smaller than the effective charges obtained at 20 MeV[58] using the same model. This apparent discrepancy is probably due to contributions to the cross section from exchange effects which are more important at 20 MeV and which were not included in the lower energy calculations. However, the effective charges extracted here compare very well with those extracted from the renormalization of the valence calculations given above. For the $13/2^+$ level, this CP model cannot give the forward angle enhancement shown in both the data and exchange calculations.

Second, CP effects were calculated with a completely microscopic model. Admixtures of 1 particle-2 hole core excitations in each state were determined using first order perturbation theory. The CP wave function, $|J\rangle_{CP}$, for a state of spin j was given by

$$|j\rangle_{CP} = |j\rangle + \Sigma\ A(j'Jj)|(j'J)j\rangle,$$

the sum running over j' and J. The ket $|j\rangle$ denotes a valence state of spin j corresponding to the appropriate neutron hole. $|(j'J)j\rangle$ refers to a component of total

spin j resulting from the coupling of a neutron hole of spin j' to a particle-hole state of the core with angular momentum J. The amplitude of a particular component is given by

$$A(j'Jj) = -\langle (j'J)j|V|j\rangle/\Delta E$$

where the energy denominator $E=E_j-E_{j'}-E_J$. The energies for the orbitals were taken either from the zero deformation Nilsson scheme or from experiment. The orbitals included are listed in Table VIII. Harmonic oscillator wave functions with length parameter $\alpha=0.405$ fm^{-1} were used. The coupling potential, V, was the Kallio-Kolltveit force.[86] Similar treatments[59,60] in this mass region have given encouraging results. For the transitions from the ground state to the $3/2^-$ and $5/2^-$ levels, respective B(E2) values of 189 and 231 e^2fm^4 were calculated using these wave functions and using no effective charge; these values are in fairly good agreement with experimental measurements.[83]

Distorted wave calculations using these CP wave functions are displayed in Figure 32b. The broken curve gives the results for the direct-plus-approximate exchange calculations. Only central forces were used. In each case the experimental strength is underestimated. Unfortunately, numerical limitations prevented calculations using DWBA70 and including non-central forces.

Table VIII. Proton and neutron orbits used in the core polarization calculations. Lack of J subscript indicates both $j=\ell\pm 1/2$ were used.

PROTONS		NEUTRONS	
Particles	Holes	Particles	Holes
$0h_{9/2}$	$0h_{11/2}$	$0i_{11/2}$	$2s_{1/2}$
1f	$2s_{1/2}$	1g	0g
0i	1d	0j	1d
2p	0g	2d	0h
1g	1p	1h	1f
0j	0f	$3s_{1/2}$	2p
2d		$0k_{17/2}$	$0i_{13/2}$
1h		$2f_{7/2}$	
$3s_{1/2}$		$0l_{19/2}$	
$0k_{17/2}$			
$2f_{7/2}$			
$0l_{19/2}$			

The solid curve in the figure shows results using a complex FF. The imaginary portion of the collective vibrational model FF was added to the approximate exchange microscopic CPFF. The strength of the complex FF was obtained from a CM fit to the data. As seen in other instances,[44,59] introduction of complex coupling improves the agreement; the strength seems well estimated although the large angle data is still overestimated.

To summarize, the strengths of the inelastic transitions to the first four excited states in ^{207}Pb are fairly well predicted by a microscopic model. However, using realistic interactions with non-central components and accounting for exchange effects, calculations reproduce only 20%-50% of the observed cross sections when simple neutron hole wave functions are used. A macroscopic core polarization description of these states is consistent with lower energy results. Microscopic core polarization wave functions give reasonable estimates of electromagnetic strengths using no effective charge but, with central forces, predict inelastic cross sections slightly lower than those observed. Addition of an imaginary portion to the real, microscopic CPFF gives the best fits. The importance of the tensor and spin-orbit forces in this CP description remains to be investigated.

B. The States in ^{209}Bi

The single particle orbits seen in ^{209}Bi lie at 0.896, 1.608, 2.825, 3.118, and 3.633 MeV of excitation energy

and have spins and parities of $7/2^-$, $13/2^+$, $5/2^-$, $3/2^-$, and $1/2^-$, respectively. Following the above procedure, inelastic scattering to these states was first calculated using a simple valence proton model. The calculations used an effective bound state interaction, used the BG optical model for the distorted waves, included the results of knock-on exchange using the approximation of Petrovich[37], and were done with the code DWUCK.[27] All possible LSJ triads were included. For the $13/2^+$ level twenty such triads are possible. For each state, the cross sections for each LSJ transition were summed to give the total cross section. For the $13/2^+$ level, the L1J transitions were comparable in strength to the usually dominant L0L transitions. The results of these central force and valence particle calculations are given in Figure 33 by the short dashed curves. In all instances the calculations fall at least a factor of 10 below the data.

The effects of the non-central nucleon-nucleon forces were investigated using the code DWBA70.[45] Because of numerical limitations only the cross sections for the $1/2^-$ and $3/2^-$ states could be calculated. The Serber exchange mixture was used for the central interaction and the spin-orbit and tensor forces were identical to those used above. The long dashed curves for these two states shown in Figure 33 show the results of these non-central and central forces with valence particle calculations. Apparently,

FIGURE 33.--Calculations for the single particle states in ^{209}Bi. The meaning of the curves is given in the text.

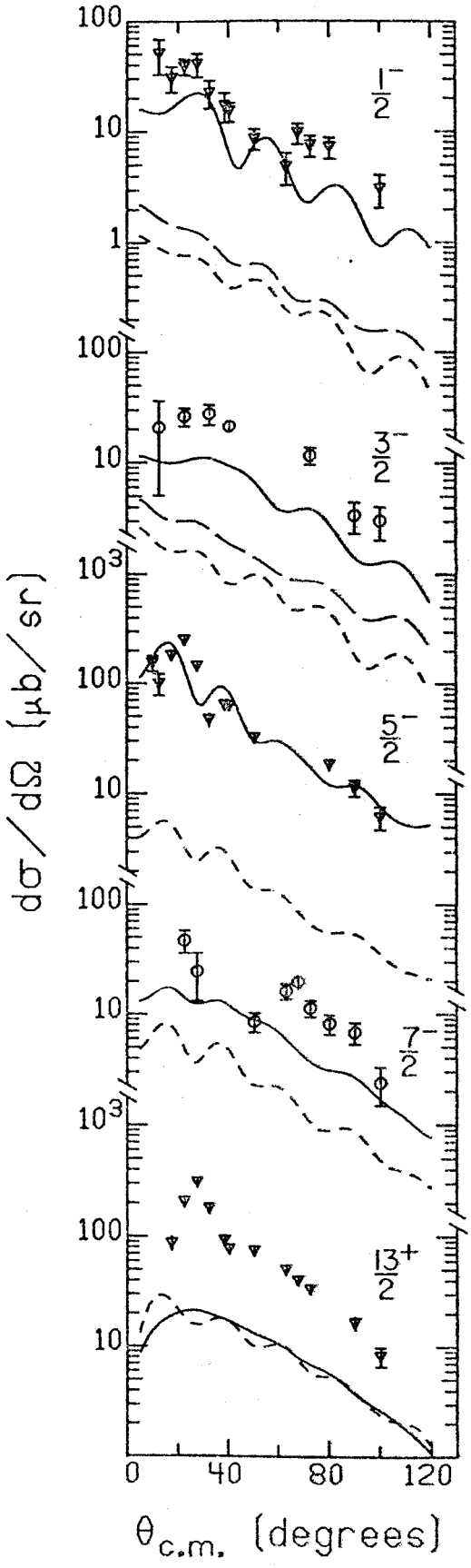
100
10
1
100
10
10³
100
10
100
10
10³
100
10
1/2⁻
3/2⁻
5/2⁻
7/2⁻
13/2⁺
dσ/dΩ (μb/sr)
0
40
80
120
θc.m. (degrees)

FIGURE 33

non-central forces cannot sufficiently enhance the theoretical cross sections to match the strength of the data.

Finally, microscopic core polarization calculations were done. The 2p-1h admixtures in the wave functions for these levels were calculated using first order perturbation theory as above. For those states whose quadrupole transition rates have been measured,[83] the core polarization wave functions give B(E2) values in fair agreement with experiment. Values of 22 and 572 e^2fm^4 were calculated without effective charge for the $7/2^-$ and $5/2^-$ transitions, respectively. The measured values[83] are 24 and 288 e^2fm^4. Transition densities obtained with the resulting wave functions were folded with the effective bound state interaction used above. The zero range approximation was again used to account for knock-on exchange and the code DWUCK[27] was again utilized. The results of these calculations are given by the solid lines in Figure 33. In all cases but the $13/2^+$ transition the agreement with the data has greatly improved. In the case of the $3/2^-$ level the calculated strength falls only about a factor of two below the data. For the $5/2^-$ cross section the calculation gives a good fit to the data.

The worst case is the $13/2^+$ calculation where the core polarization results essentially reproduce the valence calculations. In the core polarization results the L0L transitions have become more dominent while the L1J transitions

have lost much of the strength possessed in the valence model. The net result is that the cross section remains about the same as it was in the valence calculation. This state has been shown[60,66] to have a large admixture of the weak coupled $13/2^+$ state. The effect of this admixture has been studied[60] in a (p,p') experiment at 39.5 MeV where good agreement with the experimental cross section was obtained only when the weak coupled admixture was included. Since the perturbation prescription used here cannot produce the coherent 2p-1h components found in the admixture, the present results for the $i_{13/2}$ single particle state are to be expected.

To summarize, it seems that the single particle states can only be explained when core polarization effects are treated. The microscopic calculation involving simple 2p-1h and 2h-1p models for these single particle states in ^{209}Bi and ^{207}Pb apparently can account for much of the observed core polarization strength in transitions not involving contributions from coherent excitations of the core.

VI. CONCLUSION

The (p,p') reaction has allowed an intensive study of the macroscopic behavior to be made. In both ^{207}Pb and ^{209}Bi collective model fits to states enabled the transfered angular momentum to be identified. A large number of states

in both nuclei had features corresponding to the weak coupling of the valence hole or particle to core excitations. In ^{209}Bi the extremely high level density and fractionation of strength permitted only a few multiplets to be studied. Of these, the weak coupling groups corresponding to the first 3^- and the first and second 5^- levels in ^{208}Pb had most of their strength identified and were found to conform to a weak coupling prescription. Spins and parities were assigned using this fact and were found in good agreement with previous studies. The less dense level structure in ^{207}Pb apparently permitted more weak coupled states to be identified. Most of the states expected to be built on the very strong ^{208}Pb core excitations were observed and a few high-lying ^{207}Pb states were found corresponding to high lying core states. Most interesting was the absence of a weak coupling multiplet with parentage in the lowest 5^- level in ^{208}Pb. This missing strength may possibly be explained by examining the ph structure of the core state.

The single particle states in ^{207}Pb and ^{209}Bi were excited in this (p,p') study and examined using microscopic models. As expected from electromagnetic measurements, transitions to these states were found to be greatly enhanced by the core polarization effects. Calculations with the single valence nucleon, exchange effects, and non-central forces apparently cannot reproduce the observed cross sections. A first order perturbation theory calculation using a large number of neutron and proton shell model orbitals

gave a core transition density comparable to that of the valence particle. The DWBA calculations with the core polarization density and purely central forces gave reasonable reproductions of the data in all cases but that of the ^{209}Bi $13/2^+$ state which has been shown to have significant mixing with the weak coupling $13/2^+$ lying at higher excitation. It is concluded that these single particle states are properly described only in models which properly account for core polarization.

APPENDICES

APPENDIX I

Optimum Target Thickness

In most nuclear experiments the best resolution consistent with the highest count rate is desired. The target thickness, $\rho\delta x$, can affect both the resolution and the count rate in particle experiments. With other factors fixed, target thickness is related linearly to the count rate but there is no clear relation of thickness to resolution. For this reason the optimum target thickness for high resolution (p,p') was determined experimentally.

A number of bismuth targets were made with similar backings but of varying thicknesses. Care was taken to insure thickness uniformity and the foils ranged from about 50 to 1300 $\mu g/cm^2$. The relative target thickness was measured using a 90° monitor and the Elcor charge integrator. The thickest target was measured with the alpha guage, and all other thicknesses were calculated relative to it using the monitor-charge results.

It was assumed that the target effect was a function of the density of electrons in the target material and not of the atomic electron structure. Of course, with this assumption, the results found for ^{209}Bi would hold for the entire lead mass region.

Using 40 MeV protons, the cyclotron-transport-spectrograph system was tuned for best resolution using a thin

target and the "speculator" technique of Blosser et al.[19] The 1° x 2° solid angle aperture was used. All parameters were held fixed except the spectrograph magnetic field and the target thickness. The data obtained is displayed in Figure I-1. There the resolution of the elastic peak in keV is plotted against the target thickness. It has been assumed that the focal plane line shape is Gaussian. The errors in the resolution correspond to the statistical uncertainties in the speculator measurements. The target thicknesses are probably accurate to about 10%.

For sufficiently thick targets the straggling contribution to the line width is expected to dominate the intrinsic thin target line width. The dashed curve in the figure gives the results of adding an assumed intrinsic line width of 6.5 keV in quadrature to the straggling effect which was calculated assuming a Vavilov distribution. The solid curve displays the results from linearly combining the assumed width and the straggling contributions. It appears that the linear folding of the effects compares best with the data. Since the actual energy distributions determine the proper method for combination, the proper combinatorial technique is not clear. Also, target non-uniformities could possibly contribute anomalously to the measured resolution.

From this data it appears that targets of 100 to about 250 $\mu g/cm^2$ areal density affect the resolution very little. The targets finally used in the high resolution runs were

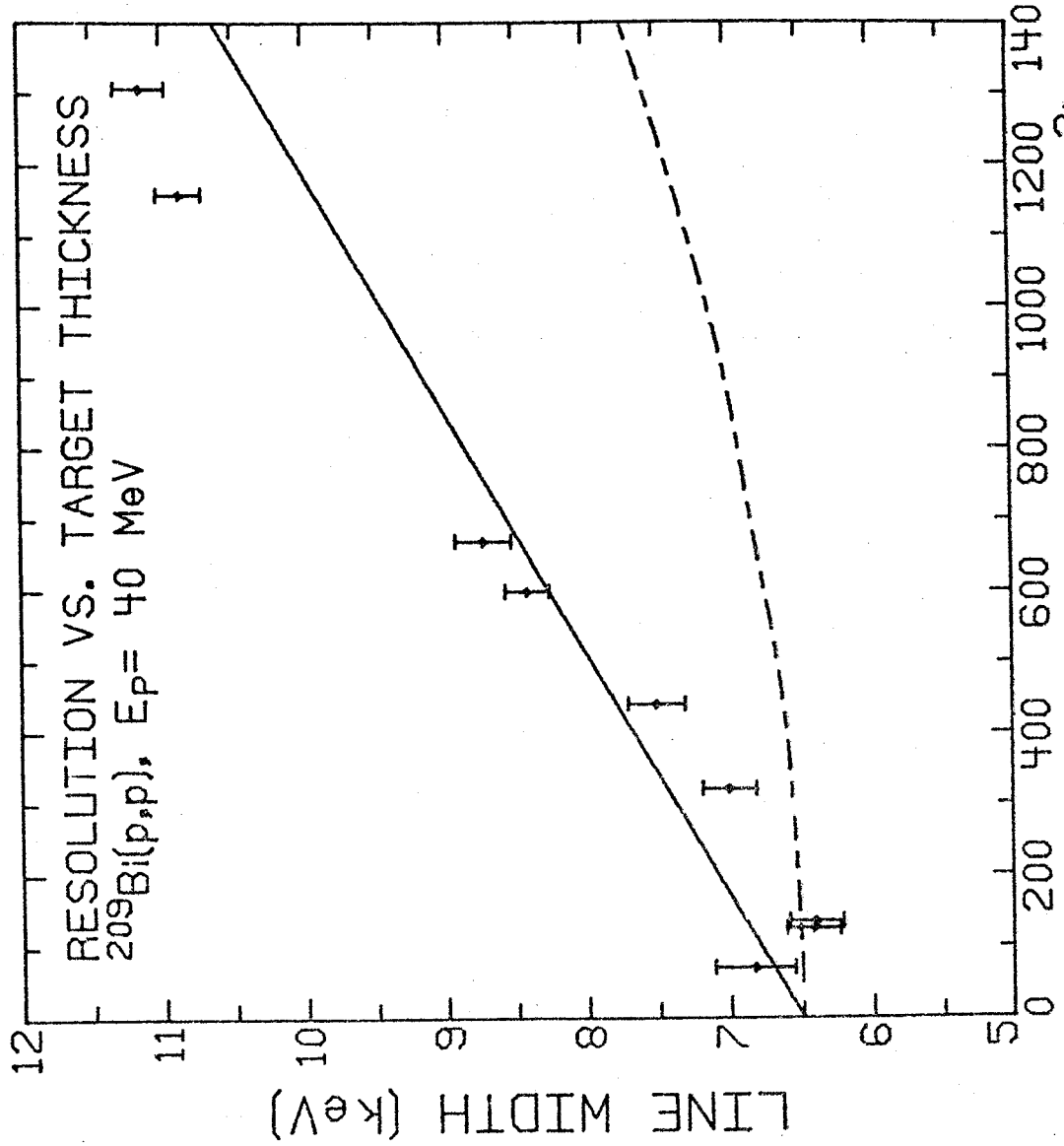

FIGURE I-1.--The effects of target thickness on resolution.

made about 100 $\mu g/cm^2$ to allow for the uncertainties in these measurements and for the bombarding energy being 35 rather than 40 MeV.

APPENDIX II

Analysis of the Data

The plate data was scanned in vertical strips whose height was dictated by the optical systems of the scanning microscopes. Each band was scanned so that extraneous background was excluded. For each exposure, the separate passes were combined using the program JABBERWOCKY[87] written by S. Ewald. This program allowed combination of the separate vertical passes in two ways: straight addition or addition after shifting of the passes so that the centroids of specified peaks were alligned as closely as possible. The latter option permits compensation for skewness in the focal plane images or zeroing errors in scanning. The program used a least-squares, Gaussian fitting routine to indicate which of the two methods yielded the tallest, thinnest peaks. In almost all cases, the straight addition mode gave the better line width. The counter data was taken using the data acquisition program TOOTSIE.[88]

With the data in counts-verses-channel number form, the program MOD7[89] was used for the data reduction. This program permits background approximation with polynomials and allows peak areas and centroids to be extracted. Although a number of numerical peak-fitting routines were available for reduction of the data, they were tested and found less desirable to use than MOD7. The very narrow line shape

(the peaks were only two to four channels wide at half maximum) and the small number of counts in most peaks prevented these routines from giving results that were believed to be more consistent or more reliable than those given by MOD7. For a few cases, comparison indicated that equivalent peak areas and centroids were obtained using either method of analysis. Further, use of MOD7 is probably faster than use of the numerical codes.

With the reduced data, the programs[22] CALIB and MONSTER were used for further analysis. The correspondence between excitation energy and focal plane position was found with the code CALIB which can perform a search on beam energy, scattering angle and focal plane parameters to determine the best fit to the positions of peaks of known energy. For our data, the searches were limited to the angle and to the focal plane variables because, since particles other than protons were excluded from the emulsions, the beam energy could not be uniquely determined. Instead, the bombarding energy was determined using the bending magnets' N.M.R. readings and a correction empirically established using the momentum cross-over technique.[90] Beam energies can be calculated better than 1 part in 1000 with the correction. Much of the data was taken at a single bombarding energy and, since the spectrometer is run in the energy loss mode, there is little sensitivity to the actual beam energy.

The focal plane parameters from CALIB were entered into

the program MONSTER which was used to calculate the excitation energies of peaks and the laboratory to center-of-momentum conversion. Output from that program was used in the program DMBEX[91] which was used to catalogue and normalize the data. With the large volume of data collected use of such a program was indispensable. DMBEX served to identify all peaks whose corresponding excitation energies were within a given energy interval of a specified energy. With this criteria, the program referenced cross sections for plotting, statistical analysis and other usage.

APPENDIX III

^{208}Pb Angular Distributions

APPENDIX III ^{208}Pb Angular Distributions

EX= .000 MEV,J=3		
THETA	SIGMA	ERROR
12.1	53060.	3843.
16.1	16200.	574.
20.1	5165.	120.
24.1	1035.	23.
28.1	335.5	6.6
30.1	565.7	7.2
32.1	328.0	2.3
36.2	65.40	.96
40.2	48.10	.54
44.2	26.30	.53
48.2	77.89	.30
52.2	28.75	.13
56.2	0.800	.060
60.2	7.550	.095
64.3	24.49	.11
68.3	8.320	.090
72.3	8.936	.058
76.3	8.620	.020
80.3	2.752	.016
84.3	4.900	.029
88.3	5.372	.028
92.3	3.461	.018
96.3	1.481	.010
100.3	.691	.006

EX= 2.615 MEV,J=2		
THETA	SIGMA	ERROR
16.1	11.2	1.8
20.1	31.6	1.4
24.1	53.57	.93
28.1	60.69	.70
30.1	57.1	1.1
32.2	41.15	.48
36.2	23.19	.26
40.2	14.83	.13
44.2	15.55	.15
48.2	18.15	.19
52.2	16.67	.16
56.3	12.16	.14
64.3	7.324	.093
68.3	6.60	.11
72.3	5.52	.11
76.3	5.312	.078
80.3	4.407	.056
84.3	3.606	.062
88.3	2.899	.050
92.3	2.197	.038
96.3	1.837	.035
100.3	1.834	.032

EX= 3.198 MEV,J=1		
THETA	SIGMA	ERROR
16.1	298.	92.
20.1	535.	52.
24.1	586.	25.
28.1	461.	18.
30.1	713.	31.
32.2	772.	18.
36.2	824.	15.
40.2	748.7	8.9
44.2	526.3	5.6
48.2	343.0	8.0
52.2	230.0	5.4
56.3	197.4	5.2
60.3	195.9	5.6
68.3	135.9	4.8
72.3	119.9	4.7
76.3	86.9	3.2
80.3	88.7	2.7
84.3	70.1	2.7
88.3	64.4	2.4
92.3	54.0	1.9
96.3	44.5	1.7
100.3	35.8	1.4

EX= 3.475 MEV,J=1		
THETA	SIGMA	ERROR
20.1	37.	22.
24.1	35.9	9.8
28.1	27.4	5.6
30.1	32.5	9.5
32.2	19.6	4.3
36.2	20.3	3.5
40.2	23.4	2.1
44.2	21.8	2.3
48.2	14.3	2.4
52.2	17.8	1.5
56.3	11.8	1.5
60.3	10.3	1.6
64.3	10.5	1.3
72.3	13.7	2.1
76.3	8.8	1.2
80.3	6.67	.88
88.3	4.57	.70
92.3	4.06	.61
96.3	2.13	.48
100.3	2.34	.43

EX= 3.709 MEV,J=1		
THETA	SIGMA	ERROR
20.1	146.	34.
24.1	177.	15.
28.1	208.	11.
30.1	209.	17.
32.2	201.4	9.7
36.2	238.4	8.0
40.2	206.0	4.8
44.2	162.8	5.0
48.2	108.2	4.6
52.2	67.2	3.1
56.3	60.4	3.1
60.3	61.2	3.3
64.3	58.3	2.6
68.3	39.5	3.2
76.3	34.2	2.1
80.3	24.0	1.4
84.3	25.6	1.7
92.3	20.7	1.2
96.3	17.9	1.1
100.3	17.3	1.0

EX= 4.085 MEV,J=2		
THETA	SIGMA	ERROR
20.1	16.1	1.1
24.1	17.90	.46
28.1	8.78	.22
30.1	5.72	.28
32.2	3.90	.13
36.2	5.51	.12
40.2	7.599	.086
44.2	6.698	.097
48.2	5.328	.098
52.2	3.654	.070
56.3	3.438	.070
60.3	3.143	.072
64.3	2.574	.054
68.3	2.123	.059
72.3	1.977	.061
80.3	1.353	.031
84.3	.921	.032
88.3	.727	.026
96.3	.680	.021
100.3	.614	.019

EX= 4.324 MEV,J=2		
THETA	SIGMA	ERROR
16.1	5.00	.92
20.1	4.15	.82
24.1	9.19	.32
28.1	10.78	.24
30.1	11.85	.41
32.2	11.54	.22
36.2	10.19	.16
40.2	7.698	.090
44.2	4.497	.070
48.2	3.420	.079
52.2	3.204	.056
56.3	3.570	.072
64.3	3.332	.061
68.3	2.561	.064
72.3	1.925	.060
76.3	1.259	.039
84.3	1.090	.038
88.3	1.182	.032
92.3	1.168	.026
96.3	1.129	.027
100.3	.652	.020

EX= 4.424 MEV,J=1		
THETA	SIGMA	ERROR
20.1	206.	77.
24.1	370.	20.
28.1	397.	14.
30.1	398.	24.
32.2	421.	13.
36.2	531.	12.
40.2	540.6	7.6
44.2	545.0	8.7
48.2	472.3	9.5
52.2	362.8	7.1
56.3	284.1	6.4
64.3	164.3	4.4
68.3	147.9	5.0
72.3	135.9	5.0
76.3	124.9	4.0
84.3	93.1	3.5
88.3	83.3	2.8
92.3	62.9	2.1
96.3	47.7	1.8
100.3	31.9	1.5

EX= 4.610 MEV,J=1		
THETA	SIGMA	ERROR
20.1	150.	48.
24.1	135.	15.
28.1	161.	10.
30.1	145.	15.
32.2	153.1	9.1
36.2	138.2	7.0
40.2	145.0	4.4
44.2	132.4	5.0
48.2	141.4	5.8
52.2	137.9	4.8
56.3	135.7	4.9
60.3	130.5	4.8
64.3	106.6	3.7
68.3	75.7	4.0
72.3	59.1	3.7
76.3	35.5	2.3
80.3	36.9	1.8
88.3	26.3	1.7
92.3	24.7	1.4
96.3	19.1	1.2
100.3	25.9	1.4

KEY: FOR J=1,2,OR 3, CROSS SECTION UNITS ARE MICRO-, 100 MICRO-, OR MILLI-BARNS/STERADIAN, RESPECTIVELY.

EX= 3.919 MEV/U=1		
THETA	SIGMA	ERROR
22.7	36.4	5.2
27.7	33.6	3.8
32.6	34.9	5.4
37.7	25.4	2.9
40.1	23.1	2.3
50.3	30.1	4.2
62.8	21.0	2.7
67.8	14.4	1.8
72.8	7.8	2.1
80.3	6.6	1.1
100.4	3.08	.75

EX= 3.946 MEV/U=1		
THETA	SIGMA	ERROR
12.8	16.	11.
18.0	32.2	6.2
22.7	18.4	4.8
27.7	9.5	2.5
32.6	10.2	3.1
37.7	12.4	2.6
40.1	13.6	2.1
50.3	14.6	2.6
62.8	3.93	.95
67.8	1.89	.67
72.8	4.5	1.6
80.3	.54	.31
100.4	.54	.31

EX= 3.961 MEV/U=1		
THETA	SIGMA	ERROR
9.7	43.	23.
12.8	19.9	9.7
18.0	23.0	7.1
22.7	34.6	4.9
27.7	45.8	4.3
32.6	74.3	7.3
37.7	67.9	5.1
40.1	69.3	5.3
50.3	59.3	4.6
62.8	21.5	2.7
67.8	10.6	1.6
72.8	6.2	1.9
80.3	7.3	1.1
100.4	3.62	.81

EX= 3.995 MEV/U=1		
THETA	SIGMA	ERROR
12.8	39.	13.
18.0	34.0	7.4
22.7	58.4	5.9
27.7	52.5	4.7
32.6	53.4	5.4
37.7	43.1	4.3
40.1	39.7	4.2
50.3	22.8	4.0
67.8	7.8	1.4
72.8	5.0	1.7
80.3	3.76	.82
100.4	1.99	.60

EX= 4.037 MEV/U=1		
THETA	SIGMA	ERROR
9.7	209.	28.
12.8	172.	17.
18.0	160.0	9.6
22.7	112.	10.
27.7	102.9	6.0
32.6	89.6	7.9
37.7	71.1	5.2
40.1	81.5	5.6
50.3	159.8	7.4
62.8	128.7	5.5
67.8	75.4	4.2
72.8	67.7	6.2
80.3	35.2	6.2
90.3	14.1	1.6
100.4	7.6	1.2

EX= 4.051 MEV/U=1		
THETA	SIGMA	ERROR
9.7	54.	22.
12.8	40.	13.
18.0	52.3	7.3
27.7	67.4	4.7
32.6	41.3	5.6
37.7	43.7	4.2
40.1	28.9	3.5
50.3	36.8	3.7
62.8	5.3	1.1
67.8	3.31	.88
72.8	2.8	1.3
90.3	1.43	.51
100.4	3.08	.75

EX= 4.106 MEV/U=1		
THETA	SIGMA	ERROR
9.7	27.	19.
12.8	32.	12.
18.0	62.1	7.0
27.7	37.1	3.6
32.6	17.2	3.0
37.7	19.6	2.5
40.1	14.6	2.6
50.3	9.9	2.2
62.8	5.5	1.1
67.8	2.36	.75
72.8	1.68	.37
80.3	3.68	.80
90.3	2.32	.66
100.4	1.99	.60

EX= 4.123 MEV/U=1		
THETA	SIGMA	ERROR
9.7	44.	22.
12.8	63.	14.
18.0	110.7	8.5
22.7	103.8	7.8
27.7	50.1	4.1
32.6	39.4	5.5
37.7	32.6	3.6
40.1	27.5	3.5
50.3	16.4	3.1
62.8	22.4	2.7
67.8	20.8	2.2
72.8	19.0	3.3
80.3	10.7	1.4
90.3	5.36	.98
100.4	3.80	.83

EX= 4.141 MEV/U=1		
THETA	SIGMA	ERROR
9.7	30.	21.
12.8	19.	12.
18.0	39.9	7.6
22.7	31.0	5.5
27.7	8.7	2.7
32.6	8.3	3.2
37.7	12.7	2.0
40.1	7.5	2.2
50.3	5.0	2.4
62.8	3.93	.95
67.8	5.4	1.1
72.8	2.8	1.3
80.3	2.50	.67
90.3	1.25	.47
100.4	.91	.41

EX= 4.159 MEV/U=1		
THETA	SIGMA	ERROR
12.8	22.	12.
18.0	28.1	7.2
22.7	10.4	4.1
27.7	10.3	2.5
37.7	10.4	1.8
50.3	5.3	2.6
67.8	3.31	.88
72.8	2.2	1.1
90.3	.35	.25
100.4	.72	.36

EX= 4.181 MEV/U=1		
THETA	SIGMA	ERROR
9.7	69.	26.
18.0	49.7	9.3
22.7	68.8	7.2
27.7	44.1	3.9
32.6	50.8	6.2
37.7	35.9	3.4
40.1	34.3	3.4
50.3	35.1	4.2
62.8	16.2	2.5
67.8	13.7	1.8
72.8	8.4	2.2
80.3	11.3	1.4
90.3	3.58	.80
100.4	2.90	.72

EX= 4.206 MEV/U=1		
THETA	SIGMA	ERROR
9.7	43.	22.
12.8	18.1	9.6
18.0	17.5	5.8
22.7	23.2	4.7
27.7	17.6	3.5
32.6	20.3	4.4
37.7	18.6	3.0
40.1	20.0	3.2
50.3	23.5	4.0
62.8	10.4	2.0
67.8	13.7	1.8
72.8	7.3	2.0
80.3	5.7	1.0
90.3	3.76	.82

EX= 4.230 MEV/U=1		
THETA	SIGMA	ERROR
9.7	190.	25.
12.8	104.	17.
18.0	111.1	9.4
22.7	160.3	9.1
27.7	184.9	7.6
32.6	48.9	6.1
37.7	24.1	3.4
40.1	21.1	3.2
50.3	19.6	3.5
62.8	12.7	2.3
67.8	5.7	1.2
72.8	4.5	1.6
80.3	4.65	.91
90.3	2.50	.67

EX= 4.256 MEV/U=1		
THETA	SIGMA	ERROR
9.7	192.	26.
12.8	141.	17.
18.0	270.	13.
22.7	255.	11.
27.7	315.8	9.9
32.6	130.9	9.6
37.7	55.4	4.3
40.1	69.3	5.1
50.3	50.3	4.9
62.8	21.0	2.8
67.8	14.4	1.8
72.8	12.3	2.6
80.3	11.1	1.4
90.3	8.4	1.2
100.4	5.07	.96

EX= 4.296 MEV/U=1		
THETA	SIGMA	ERROR
9.7	63.	22.
12.8	38.	15.
18.0	39.5	7.9
27.7	40.1	4.2
32.6	69.9	7.0
37.7	48.6	4.3
40.1	41.8	4.1
50.3	38.0	4.5
62.8	14.6	2.4
67.8	11.8	1.7
72.8	10.6	2.4
90.3	4.11	.86
100.4	3.44	.79

EX= 4.357 MEV/U=1		
THETA	SIGMA	ERROR
9.7	29.	18.
12.8	37.	12.
18.0	55.6	8.2
22.7	64.9	6.8
27.7	74.7	5.3
32.6	71.2	7.2
37.7	36.5	3.5
40.1	53.0	4.5
50.3	38.9	4.7
62.8	15.7	2.3
67.8	11.1	1.6
72.8	14.0	2.8
90.3	5.36	.98
100.4	5.25	.98

EX= 4.385 MEV/U=1		
THETA	SIGMA	ERROR
18.0	23.4	5.9
22.7	15.9	4.8
27.7	16.2	3.3
32.6	10.2	2.5
40.1	9.2	1.8
50.3	10.8	3.0
62.8	12.5	2.2
72.8	5.6	1.8
90.3	3.04	.74
100.4	5.07	.96

EX= 4.403 MEV/U=1		
THETA	SIGMA	ERROR
9.7	33.	19.
12.8	5.3	3.6
18.0	9.5	5.1
22.7	10.8	3.9
27.7	13.2	2.9
32.6	10.8	3.2
37.7	6.5	2.0
40.1	2.7	1.8
62.8	4.4	1.0
67.8	2.78	.95
90.3	.54	.31
100.4	2.53	.68

KEY: FOR U=1,2,OR 3, CROSS SECTION UNITS ARE MICRO-, 100 MICRO-, OR MILLI-BARNS/STERADIAN, RESPECTIVELY.

EX= 4.444 MEV,J=1

THETA	SIGMA	ERROR
18.0	6.9	3.7
22.7	10.8	3.6
27.7	10.3	2.7
32.6	14.0	7.0
37.7	13.7	2.1
40.1	16.6	2.8
50.3	5.3	2.3
62.8	3.23	.86
67.8	2.60	.78
72.8	1.68	.97
100.4	.72	.36

EX= 4.463 MEV,J=1

THETA	SIGMA	ERROR
18.0	15.3	6.6
22.7	14.4	4.1
27.7	4.6	1.2
40.1	5.4	1.4
50.3	2.9	2.2
67.8	1.89	.67
72.8	1.68	.97
100.4	.72	.36

EX= 4.480 MEV,J=1

THETA	SIGMA	ERROR
12.8	48.	13.
18.0	33.3	6.3
22.7	55.5	5.5
27.7	41.4	4.4
32.6	46.4	5.9
37.7	33.3	3.3
40.1	27.9	3.1
50.3	30.7	4.0
62.8	24.0	2.7
67.8	17.0	2.0
72.8	16.2	3.0
80.3	20.2	1.9
90.3	17.9	2.7
100.4	6.9	1.1

EX= 4.577 MEV,J=1

THETA	SIGMA	ERROR
18.0	12.4	7.5
22.7	21.3	4.9
27.7	5.8	2.5
32.6	4.4	2.5
37.7	4.9	2.1
40.1	3.4	1.1
50.3	2.6	1.3
62.8	5.5	1.1
72.8	2.8	1.3
80.3	3.58	.80
90.3	1.43	.51

EX= 4.680 MEV,J=1

THETA	SIGMA	ERROR
12.8	37.	13.
22.7	22.3	5.8
27.7	29.2	3.3
32.6	29.9	4.8
40.1	18.7	3.0
62.8	12.5	2.1
67.8	10.4	1.6
72.8	15.7	3.0
80.3	8.6	1.2
90.3	6.4	1.1
100.4	4.53	.91

EX= 4.698 MEV,J=1

THETA	SIGMA	ERROR
9.7	102.	26.
12.8	86.	13.
22.7	365.	12.
27.7	357.	10.
32.6	284.	14.
37.7	104.4	5.0
40.1	72.3	5.2
50.3	113.1	5.3
62.8	82.3	4.4
67.8	64.8	3.9
72.8	76.7	5.5
80.3	61.3	3.3
90.3	21.8	2.0
100.4	6.5	1.1

EX= 4.711 MEV,J=1

THETA	SIGMA	ERROR
9.7	76.	25.
12.8	112.	15.
22.7	127.9	8.3
27.7	92.9	5.4
32.6	139.8	9.8
37.7	136.3	6.7
40.1	140.9	7.1
50.3	65.5	5.1
62.8	34.9	2.8
67.8	45.6	3.3
72.8	29.1	4.0
80.3	12.0	1.5
90.3	4.83	.93
100.4	11.0	1.4

EX= 4.762 MEV,J=1

THETA	SIGMA	ERROR
12.8	39.	14.
22.7	31.3	7.0
27.7	28.5	3.8
32.6	38.7	5.6
37.7	29.0	3.5
40.1	30.7	3.2
50.3	23.7	4.1
62.8	16.4	2.4
67.8	7.8	1.4
72.8	6.7	1.9
80.3	6.8	1.1
100.4	4.34	.89

EX= 4.841 MEV,J=2

THETA	SIGMA	ERROR
9.7	14.94	.54
12.8	9.67	.26
18.0	5.78	.17
27.7	.893	.055
32.6	1.105	.088
37.7	1.295	.068
40.1	.696	.050
50.3	.699	.057
62.8	.152	.023
67.8	.208	.022
72.8	.336	.043
80.3	.163	.017
90.3	.145	.030
100.4	.072	.011

EX= 4.863 MEV,J=1

THETA	SIGMA	ERROR
9.7	55.	20.
12.8	58.	13.
18.0	54.8	6.9
27.7	54.7	4.9
32.6	47.6	5.1
37.7	51.3	4.8
40.1	53.2	4.8
50.3	46.2	4.9
62.8	42.7	3.5
67.8	35.7	2.9
72.8	38.6	4.7
80.3	17.7	1.8
90.3	8.9	2.1
100.4	9.4	1.3

EX= 4.895 MEV,J=1

THETA	SIGMA	ERROR
9.7	44.	23.
12.8	60.	16.
18.0	60.7	7.5
27.7	54.2	4.4
32.6	52.1	6.2
37.7	40.8	3.6
40.1	40.4	4.1
50.3	47.6	5.0
62.8	31.6	3.0
67.8	30.7	2.7
72.8	25.2	3.8
80.3	29.3	2.3
90.3	19.5	1.9
100.4	15.4	1.7

EX= 4.917 MEV,J=1

THETA	SIGMA	ERROR
12.8	31.	14.
18.0	41.3	7.6
27.7	37.9	4.0
32.6	34.9	5.3
37.7	30.0	3.7
40.1	24.1	3.3
62.8	20.1	2.5
67.8	18.2	2.1
72.8	10.1	2.4
80.3	15.7	1.7
90.3	8.4	1.2
100.4	6.3	1.1

EX= 4.933 MEV,J=1

THETA	SIGMA	ERROR
9.7	49.	22.
12.8	48.	14.
18.0	106.7	9.5
27.7	137.0	6.6
32.6	108.6	8.7
37.7	86.4	4.9
40.1	28.2	3.4
62.8	38.3	3.3
67.8	39.3	3.0
72.8	26.3	3.8
80.3	19.0	1.8
90.3	14.1	1.6
100.4	5.43	.99

EX= 4.954 MEV,J=1

THETA	SIGMA	ERROR
9.7	19.2	9.6
12.8	32.	10.
18.0	97.2	8.4
27.7	87.7	5.4
32.6	73.1	7.2
37.7	38.3	3.3
50.3	51.1	4.8
62.8	21.0	2.5
67.8	22.0	2.3
72.8	13.4	2.7
80.3	13.2	1.5
90.3	7.9	1.2
100.4	4.53	.91

EX= 4.973 MEV,J=1

THETA	SIGMA	ERROR
9.7	164.	26.
12.8	154.	18.
18.0	240.	12.
27.7	161.9	7.2
32.6	85.8	7.8
37.7	56.1	4.3
50.3	39.5	4.3
62.8	56.2	3.9
67.8	35.5	2.9
80.3	17.0	1.7
90.3	13.9	1.6
100.4	3.44	.79

EX= 4.991 MEV,J=1

THETA	SIGMA	ERROR
12.8	10.7	5.3
18.0	15.7	6.5
37.7	13.7	2.1
50.3	21.3	4.0
62.8	19.6	2.1
67.8	9.7	1.5
72.8	17.4	3.1
80.3	9.7	1.3
90.3	3.58	.80
100.4	1.81	.57

EX= 5.010 MEV,J=1

THETA	SIGMA	ERROR
18.0	18.3	6.6
37.7	15.3	2.2
40.1	16.3	2.8
50.3	10.8	3.4
62.8	15.5	1.9
67.8	11.8	1.7
72.8	12.9	2.7
80.3	10.2	1.3
90.3	5.36	.98
100.4	4.89	.94

EX= 5.036 MEV,J=1

THETA	SIGMA	ERROR
9.7	95.	24.
12.8	113.	17.
18.0	155.	10.
32.6	38.1	5.4
37.7	38.5	4.2
40.1	19.4	2.6
50.3	25.7	4.3
62.8	17.8	2.0
67.8	11.1	1.6
72.8	6.2	1.9
80.3	7.3	1.1
90.3	4.29	.88
100.4	2.72	.70

KEY: FOR J=1,2,OR 3, CROSS SECTION UNITS ARE MICRO-, 100 MICRO-, OR MILLI-BARNS/STERADIAN, RESPECTIVELY.

EX= 5.072 MEV;J=1

THETA	SIGMA	ERROR
9.7	168.	28.
12.8	100.	14.
18.0	137.0	9.8
32.6	142.0	9.9
37.7	100.5	5.7
40.1	100.2	6.1
50.3	59.9	5.2
62.8	68.8	4.2
67.8	72.1	4.1
72.8	70.5	6.3
80.3	28.2	2.2
90.3	23.8	2.1
100.4	11.0	1.4

EX= 5.087 MEV;J=1

THETA	SIGMA	ERROR
9.7	150.	25.
12.8	150.	17.
18.0	255.	12.
32.6	113.7	8.9
37.7	113.8	6.6
40.1	118.5	6.6
50.3	143.8	7.5
62.8	50.8	3.7
67.8	22.0	2.3
72.8	32.5	4.3
80.3	47.2	2.9
90.3	31.6	2.4
100.4	19.4	1.9

EX= 5.128 MEV;J=1

THETA	SIGMA	ERROR
9.7	143.	24.
12.8	84.	15.
18.0	93.9	9.4
27.7	73.6	5.4
32.6	38.7	5.3
37.7	10.8	2.6
40.1	13.6	2.8
50.3	12.6	3.5
62.8	12.7	2.2
67.8	12.8	1.7
72.8	7.8	2.1
90.3	9.3	1.3
100.4	4.47	.89
	4.71	.92

EX= 5.153 MEV;J=1

THETA	SIGMA	ERROR
12.8	9.6	4.8
18.0	12.1	6.9
27.7	16.0	3.5
32.6	10.8	3.4
37.7	9.1	2.8
40.1	4.8	2.1
50.3	6.4	3.3
62.8	4.4	1.6
67.8	5.0	1.1
72.8	7.8	2.1
80.3	4.11	.86
100.4	6.5	1.9

EX= 5.194 MEV;J=1

THETA	SIGMA	ERROR
18.0	34.1	7.8
27.7	46.3	4.8
32.6	41.9	5.7
37.7	24.1	2.8
40.1	28.9	3.1
50.3	25.7	4.1
62.8	25.4	2.4
67.8	14.2	1.8
72.8	6.2	1.9
80.3	10.4	1.4
100.4	8.1	2.1

EX= 5.214 MEV;J=1

THETA	SIGMA	ERROR
9.7	122.	25.
12.8	126.	17.
18.0	110.	11.
27.7	162.0	7.3
37.7	105.0	5.9
40.1	121.9	6.7
50.3	95.3	5.0
62.8	58.2	3.9
67.8	50.1	3.4
72.8	34.1	4.4
80.3	32.5	2.4
100.4	13.4	2.2

EX= 5.242 MEV;J=1

THETA	SIGMA	ERROR
9.7	148.	26.
12.8	141.	17.
18.0	165.	13.
27.7	140.8	7.0
37.7	90.7	6.0
40.1	159.	16.
50.3	75.1	5.9
62.8	40.4	3.4
67.8	40.2	3.1
72.8	33.0	4.3
80.3	34.2	2.5
100.4	13.4	1.9

EX= 5.274 MEV;J=1

THETA	SIGMA	ERROR
9.7	29.	18.
12.6	50.	10.
17.6	56.8	7.6
27.7	24.1	3.6
37.7	17.0	3.0
62.8	9.0	1.8
67.8	9.2	1.5
72.8	7.8	2.1
80.3	6.6	1.1
100.4	2.53	.68

EX= 5.291 MEV;J=1

THETA	SIGMA	ERROR
9.7	289.	32.
12.6	230.	17.
17.6	200.	13.
37.7	54.8	4.8
50.3	29.2	4.1
67.8	25.1	2.4
72.8	20.1	3.4
80.3	17.9	1.8
100.4	6.2	1.1

EX= 5.321 MEV;J=1

THETA	SIGMA	ERROR
9.7	63.	23.
12.6	42.	10.
17.6	80.1	9.1
37.7	30.3	3.9
40.1	22.8	3.5
50.3	34.8	4.7
62.8	20.8	2.6
67.8	15.1	1.9
72.8	7.8	2.1
80.3	11.1	1.4
90.3	14.5	1.5
100.4	4.34	.89

EX= 5.345 MEV;U=1

THETA	SIGMA	ERROR
9.7	148.	31.
12.6	130.	15.
17.6	214.	14.
27.7	239.4	8.6
32.6	180.	13.
37.7	117.8	6.6
40.1	118.5	7.0
50.3	153.7	7.7
62.8	108.4	5.3
67.8	77.3	4.3
72.8	62.7	5.9
80.3	48.4	2.9
90.3	38.6	2.6
100.4	21.2	2.0

EX= 5.370 MEV;J=1

THETA	SIGMA	ERROR
17.6	19.9	3.7
32.6	33.7	5.0
37.7	34.9	3.9
50.3	19.0	3.2
62.8	19.7	2.1
67.8	13.7	1.8
80.3	9.3	1.3
90.3	5.18	.96
100.4	2.35	.65

EX= 5.383 MEV;U=1

THETA	SIGMA	ERROR
12.6	77.	13.
17.6	115.	11.
27.7	92.1	5.5
32.6	97.2	8.2
40.1	62.8	5.6
50.3	58.5	5.0
62.8	29.1	2.6
67.8	13.5	1.8
72.8	9.3	2.3
80.3	9.5	1.3
100.4	1.99	.60

EX= 5.417 MEV;U=1

THETA	SIGMA	ERROR
12.6	13.5	9.7
17.6	21.9	6.9
27.6	11.7	2.5
32.6	14.6	3.9
37.7	21.2	3.5
40.1	24.8	5.0
62.8	14.6	2.4
67.8	7.6	1.3
72.8	7.8	2.1
80.3	4.29	.88
90.3	2.86	.72
100.4	2.53	.68

EX= 5.444 MEV;U=1

THETA	SIGMA	ERROR
9.7	22.	18.
17.6	16.4	6.3
27.6	4.8	1.6
32.6	6.4	3.0
40.1	7.1	1.5
72.8	5.6	1.8
80.3	2.50	.67
90.3	.72	.26
100.4	1.45	.51

EX= 5.483 MEV;U=1

THETA	SIGMA	ERROR
9.7	241.	32.
12.6	156.	16.
17.6	235.	14.
27.6	193.	10.
32.6	253.	13.
40.1	221.8	9.4
50.3	90.9	6.6
62.8	117.8	5.5
67.8	112.0	5.1
72.8	99.6	7.5
80.3	56.7	3.8
90.3	26.6	2.2
100.4	14.5	1.6

EX= 5.514 MEV;U=2

THETA	SIGMA	ERROR
9.7	18.88	.58
12.6	9.96	.30
17.6	5.03	.22
27.6	3.78	.18
32.6	6.03	.20
40.1	2.027	.090
50.3	1.753	.081
62.8	1.040	.051
67.8	.676	.040
72.8	.644	.060
80.3	.554	.031
90.3	.247	.021
100.4	.127	.022

EX= 5.542 MEV;J=1

THETA	SIGMA	ERROR
9.7	106.	23.
12.6	134.	16.
17.6	217.	14.
27.6	156.6	9.1
32.6	171.	11.
40.1	104.6	5.8
50.3	117.5	7.0
62.8	56.6	3.9
67.8	53.9	3.6
72.8	58.8	5.7
80.3	36.8	2.6
90.3	21.3	2.0
100.4	14.1	2.8

KEY: FOR U=1,2,OR 3, CROSS SECTION UNITS ARE MICRO-, 100 MICRO-, OR MILLI-BARNS/STERADIAN, RESPECTIVELY.

Ex= 5.564 MEV,J=1

THETA	SIGMA	ERROR
9.7	142.	25.
12.6	130.	15.
17.6	273.	15.
27.6	160.4	9.2
32.6	69.9	7.3
40.1	28.5	4.2
62.8	16.2	2.3
67.8	15.6	1.9
72.8	17.9	3.2
80.3	13.4	1.5
90.3	6.3	1.1
100.4	9.4	2.6

Ex= 5.596 MEV,J=1

THETA	SIGMA	ERROR
9.7	111.	23.
12.6	93.	14.
17.6	107.	11.
22.7	75.2	8.3
27.6	37.3	4.6
32.6	44.5	6.2
50.3	22.5	3.3
62.8	15.9	2.4
72.8	6.2	1.9
80.3	5.7	1.0
90.3	4.65	.91
100.4	8.7	2.6

Ex= 5.613 MEV,J=1

THETA	SIGMA	ERROR
12.6	89.0	9.8
22.7	32.1	6.1
27.6	26.1	3.7
32.6	40.0	6.1
37.7	25.1	2.9
50.3	25.4	4.3
62.8	18.7	2.5
67.8	10.9	1.6
72.8	10.1	2.4
80.3	10.7	1.4
90.3	6.6	1.1
100.4	11.8	2.3

Ex= 5.642 MEV,J=1

THETA	SIGMA	ERROR
12.6	89.	15.
17.6	92.	10.
22.7	73.9	9.2
27.6	43.7	4.8
32.6	52.1	6.7
37.7	48.6	4.7
50.3	35.9	4.6
62.8	11.6	2.0
67.8	12.1	1.7
72.8	9.0	2.2
80.3	13.2	1.5
90.3	7.9	1.2
100.4	4.53	.91

Ex= 5.658 MEV,J=1

THETA	SIGMA	ERROR
12.6	26.9	9.7
17.6	56.8	8.2
22.7	58.3	8.4
27.6	63.4	5.8
32.6	104.2	8.7
37.7	80.2	5.5
50.3	39.5	4.4
62.8	21.0	2.2
67.8	20.1	2.2
72.8	21.3	3.4
80.3	11.6	1.4
90.3	7.3	1.1
100.4	7.4	1.2

Ex= 5.673 MEV,J=1

THETA	SIGMA	ERROR
17.6	73.3	9.8
22.7	56.2	8.2
27.6	54.9	5.4
32.6	48.9	6.3
37.7	32.6	3.6
50.3	27.8	3.0
62.8	15.0	1.9
67.8	7.6	1.3
72.8	13.4	2.7
80.3	8.9	1.2
90.3	5.9	1.0
100.4	4.16	.87

Ex= 5.683 MEV,J=1

THETA	SIGMA	ERROR
9.7	353.	33.
12.6	224.	18.
17.6	235.	15.
22.7	269.	14.
27.6	80.4	13.
32.6	328.	15.
37.7	233.2	8.7
50.3	119.2	6.8
62.8	131.4	5.8
67.8	93.6	4.7
72.8	82.3	6.8
80.3	52.6	3.1
90.3	39.2	2.6
100.4	26.6	2.2

Ex= 5.720 MEV,J=1

THETA	SIGMA	ERROR
9.7	92.	23.
12.6	98.	14.
22.7	70.	10.
27.6	65.0	5.9
32.6	64.8	7.4
37.7	74.7	5.5
50.3	68.4	5.8
62.8	40.2	3.4
67.8	32.6	2.8
72.8	30.2	4.1
80.3	20.2	1.9
90.3	11.6	1.4
100.4	9.1	1.3

Ex= 5.743 MEV,J=1

THETA	SIGMA	ERROR
12.6	28.	11.
17.6	30.1	3.2
22.7	19.	12.
27.6	12.3	2.6
32.6	22.9	5.4
37.7	22.5	3.6
50.3	15.5	4.3
62.8	21.9	2.6
67.8	18.0	2.1
72.8	12.9	2.7
80.3	12.2	1.5
90.3	7.5	1.2
100.4	5.07	.95

Ex= 5.763 MEV,J=1

THETA	SIGMA	ERROR
12.6	17.0	8.7
17.6	6.8	3.4
22.7	20.5	9.6
27.6	11.7	2.5
32.6	14.0	4.3
37.7	18.6	2.5
62.8	8.1	1.9
67.8	6.6	1.3
80.3	5.00	.95
90.3	7.0	1.1
100.4	3.98	.85

Ex= 5.777 MEV,J=1

THETA	SIGMA	ERROR
12.6	42.	12.
17.6	59.5	9.3
22.7	26.	11.
27.6	27.2	3.8
32.6	19.1	4.8
37.5	17.2	2.3
40.0	31.4	3.5
50.3	26.3	4.8
62.8	17.1	2.4
67.8	8.3	1.4
72.8	8.4	2.2
80.3	5.18	.96
90.3	3.40	.78
100.4	7.1	1.1

Ex= 5.796 MEV,J=1

THETA	SIGMA	ERROR
17.6	21.9	6.9
32.6	27.3	5.0
37.5	8.3	1.6
40.0	16.5	2.3
50.3	9.9	3.3
62.8	7.6	1.7
67.8	5.4	1.1
72.8	9.5	2.3
80.3	4.83	.93
90.3	1.07	.44

Ex= 5.813 MEV,J=1

THETA	SIGMA	ERROR
9.7	234.	31.
12.6	190.	12.
17.6	374.	18.
22.7	388.	26.
27.6	265.	12.
32.6	130.9	9.7
37.5	40.7	3.6
40.0	67.9	5.2
50.3	112.8	6.8
62.8	40.6	3.4
67.8	47.3	3.3
72.8	38.1	4.6
80.3	37.0	2.4
90.3	13.1	1.5
100.4	7.1	1.1

Ex= 5.842 MEV,J=1

THETA	SIGMA	ERROR
9.7	132.	32.
17.6	112.	11.
22.7	51.0	9.3
27.6	45.3	4.9
32.6	37.5	5.9
37.5	24.2	2.8
40.0	24.7	3.1
50.3	30.4	4.6
62.8	27.7	2.9
67.8	24.1	2.4
72.8	17.4	3.1
80.3	32.5	2.4
90.3	17.3	1.8
100.4	8.0	1.2

Ex= 5.872 MEV,J=1

THETA	SIGMA	ERROR
12.6	22.	11.
22.7	65.	10.
27.6	47.9	5.1
32.6	40.6	6.4
37.5	32.1	3.2
40.0	48.2	4.3
50.3	52.3	5.1
62.8	18.3	2.5
67.8	16.5	2.0
72.8	7.8	2.1
80.3	7.0	1.1
90.3	3.58	.80
100.4	4.53	.91

Ex= 5.898 MEV,J=1

THETA	SIGMA	ERROR
17.6	11.0	5.1
27.6	14.4	2.8
32.6	12.7	4.0
37.5	9.5	1.7
40.0	13.3	2.3
50.3	14.6	4.1
62.8	12.7	2.3
67.8	9.5	1.5
72.8	9.0	2.2
80.3	8.8	1.3
90.3	5.9	1.0
100.4	6.0	1.0

Ex= 5.923 MEV,J=1

THETA	SIGMA	ERROR
9.7	59.	24.
12.6	29.	11.
17.6	36.3	8.4
22.7	34.0	7.6
27.6	12.8	2.6
32.6	14.0	5.5
37.5	12.7	2.0
40.0	25.1	3.1
50.3	24.3	4.4
62.8	23.2	2.4
67.8	15.1	1.9
72.8	13.4	2.7
80.3	15.4	1.7
90.3	10.0	1.3
100.4	7.2	1.1

Ex= 5.948 MEV,J=1

THETA	SIGMA	ERROR
9.7	73.	26.
12.6	40.	12.
17.6	43.8	8.2
22.7	56.1	9.8
27.6	13.3	2.7
32.6	15.2	4.7
37.5	11.1	1.9
40.0	26.3	3.2
50.3	19.6	4.2
62.8	13.2	1.7
67.8	5.0	1.1
72.8	4.5	1.6
80.3	5.5	1.0
90.3	3.04	.74
100.4	3.26	.77

KEY: FOR J=1,2,OR 3, CROSS SECTION UNITS ARE MICRO-, 100 MICRO-, OR MILLI-BARNS/STERADIAN, RESPECTIVELY.

EX= 5.966 MEV/U=1		
THETA	SIGMA	ERROR
12.6	43.	12.
17.6	51.3	9.0
22.7	25.5	6.6
27.6	29.3	4.0
37.5	25.1	2.8
50.3	34.2	4.7
62.8	32.8	2.8
67.8	28.4	2.6
72.8	28.0	4.0
80.3	17.9	1.8
90.3	11.8	1.5

EX= 5.993 MEV/U=1		
THETA	SIGMA	ERROR
9.7	355.	35.
17.6	287.	16.
22.7	211.	19.
27.6	211.	11.
32.6	273.	14.
37.5	214.9	8.3
40.0	311.	11.
50.3	185.6	6.3
62.8	89.2	4.8
67.8	72.1	4.1
72.8	67.7	6.2
80.3	69.6	3.5
90.3	37.7	2.6

EX= 6.010 MEV/U=1		
THETA	SIGMA	ERROR
9.7	164.	27.
12.6	113.	14.
17.6	224.	14.
22.7	177.	17.
27.6	148.6	8.9
32.6	107.3	9.6
37.5	47.4	3.9
40.0	67.5	5.1
50.3	67.5	5.5
62.8	37.4	3.4
67.8	44.5	3.2
72.8	47.6	5.2
80.3	27.0	2.2
90.3	20.2	1.9

EX= 6.035 MEV/U=1		
THETA	SIGMA	ERROR
9.7	102.	25.
12.6	36.	10.
17.6	47.2	7.7
22.7	44.2	8.7
27.6	17.6	3.1
32.6	14.6	5.0
37.5	17.2	8.3
40.0	25.1	3.1
50.3	21.9	4.1
62.8	6.0	1.9
67.8	9.0	1.5
72.8	10.1	2.4
80.3	10.7	1.4
90.3	3.76	.82

EX= 6.052 MEV/U=1		
THETA	SIGMA	ERROR
12.6	43.	11.
17.6	76.0	9.6
22.7	57.8	9.9
27.6	61.3	5.7
32.6	58.4	8.9
37.5	31.1	3.1
40.0	32.9	3.6
50.3	11.7	3.6
62.8	12.7	2.3
67.8	10.6	1.6
72.8	3.9	1.5
80.3	6.4	1.1
90.3	6.3	1.1

EX= 6.082 MEV/U=1		
THETA	SIGMA	ERROR
12.6	57.	11.
17.6	98.	10.
22.7	47.6	9.0
27.6	33.0	4.2
32.6	48.9	8.3
37.5	22.6	2.7
40.0	24.7	3.1
50.3	18.7	3.6
62.8	20.8	2.5
67.8	19.1	2.1
72.8	10.6	2.4
80.3	8.2	1.2
90.3	9.1	1.3

EX= 6.099 MEV/U=1		
THETA	SIGMA	ERROR
9.7	77.	25.
12.6	46.7	9.7
17.6	67.8	9.3
22.7	47.6	9.0
27.6	50.6	5.2
32.6	45.1	8.5
37.5	37.2	3.4
40.0	46.3	4.3
50.3	46.5	5.2
62.8	31.2	3.2
67.8	29.1	2.6
72.8	34.7	4.4
80.3	26.8	2.2
90.3	17.7	1.8

EX= 6.170 MEV/U=1		
THETA	SIGMA	ERROR
9.7	59.	24.
12.6	36.	11.
17.6	15.7	6.1
22.7	17.0	5.4
32.6	8.9	7.5
50.3	6.7	3.2
62.8	2.5	1.6
80.3	1.43	.51
90.3	1.61	.54

EX= 6.191 MEV/U=1		
THETA	SIGMA	ERROR
12.6	122.	15.
17.6	156.	13.
22.7	114.	14.
27.6	84.2	6.7
32.6	69.	13.
37.5	30.8	3.1
40.0	40.4	4.0
50.3	32.4	4.8
62.8	36.3	2.9
67.8	10.9	1.6
72.8	15.7	3.0
80.3	14.8	1.6
90.3	7.9	1.2
100.4	6.2	1.1

EX= 6.214 MEV/U=1		
THETA	SIGMA	ERROR
17.6	19.9	6.3
22.7	15.3	5.1
27.6	12.3	2.6
32.6	21.6	8.7
37.5	10.8	1.9
40.0	12.6	2.2
50.3	20.3	4.3
67.8	5.2	1.1
80.3	3.22	.76
90.3	3.93	.84

EX= 6.233 MEV/U=1		
THETA	SIGMA	ERROR
9.7	147.	28.
17.6	109.	10.
22.7	73.	11.
27.6	111.3	7.7
32.6	93.	13.
37.5	49.3	4.0
40.0	61.2	4.9
62.8	47.4	3.7
67.8	19.9	2.2
72.8	6.2	1.9
80.3	10.5	1.4
90.3	8.9	1.3
100.4	3.80	.83

EX= 6.248 MEV/U=1		
THETA	SIGMA	ERROR
22.7	49.3	9.2
27.6	57.5	5.5
37.5	48.6	3.9
62.8	52.7	3.5
67.8	52.7	3.5
72.8	22.9	3.6
80.3	21.5	2.0
90.3	17.3	1.8

EX= 6.261 MEV/U=1		
THETA	SIGMA	ERROR
9.7	340.	38.
12.6	317.	19.
17.6	283.	15.
22.7	45.9	8.8
27.6	61.8	5.7
32.6	96.	13.
37.5	46.7	3.9
40.0	51.8	4.5
62.8	9.9	1.5
72.8	25.7	3.8
80.3	16.6	1.7
90.3	12.9	1.5
100.4	13.2	1.5

EX= 6.276 MEV/U=1		
THETA	SIGMA	ERROR
9.7	100.	24.
17.6	75.3	9.4
22.7	57.8	9.9
27.6	130.5	8.3
32.6	86.	13.
37.5	57.8	4.3
40.0	77.3	5.5
62.8	32.1	3.3
67.8	28.1	2.6
72.8	28.5	4.0
80.3	23.4	2.0
100.4	9.8	1.3

EX= 6.314 MEV/U=1		
THETA	SIGMA	ERROR
12.6	50.	12.
22.7	54.4	9.6
27.6	37.3	4.5
32.5	44.9	5.8
37.5	16.5	2.3
40.0	18.8	2.7
62.8	26.6	2.9
67.8	14.9	1.9
72.8	12.3	2.6
80.3	7.7	1.2
90.3	4.47	.89
100.4	2.53	.68

EX= 6.332 MEV/U=1		
THETA	SIGMA	ERROR
12.6	26.9	8.9
22.7	25.5	4.6
27.6	46.3	5.0
32.5	89.0	8.2
37.7	67.2	6.7
40.0	86.7	5.8
62.8	33.3	3.2
67.8	35.0	2.9
72.8	39.7	4.7
80.3	24.3	2.1
90.3	16.6	1.7
100.4	12.9	1.5

EX= 6.353 MEV/U=1		
THETA	SIGMA	ERROR
12.6	170.	17.
17.6	194.	14.
27.6	95.3	7.1
32.5	140.	10.
37.7	64.2	7.9
40.0	56.5	4.7
62.8	31.2	3.3
67.8	13.7	1.8
72.8	20.7	3.4
80.3	8.6	1.2
90.3	8.8	1.3

EX= 6.381 MEV/U=1		
THETA	SIGMA	ERROR
17.6	16.4	6.4
27.6	11.7	2.5
40.0	12.2	2.2
50.3	51.4	5.7
62.8	31.4	3.1
67.8	10.2	1.6
72.8	21.8	3.5
80.3	13.4	1.5
90.3	10.0	1.3

KEY: FOR U=1,2,OR 3, CROSS SECTION UNITS ARE MICRO-, 100 MICRO-, OR MILLI-BARNS/STERADIAN, RESPECTIVELY.

EX= 6.392 MEV,J=1		
THETA	SIGMA	ERROR
9.7	65.	26.
12.6	37.	13.
17.6	39.7	8.5
22.7	55.	10.
27.6	43.7	4.8
32.5	55.5	5.5
37.5	29.9	3.1
40.0	44.3	4.2
62.8	28.2	3.1
67.8	25.5	2.5
72.8	16.2	3.0
80.3	10.9	1.4
90.3	7.3	1.1
100.4	6.2	1.1

EX= 6.423 MEV,J=1		
THETA	SIGMA	ERROR
9.7	88.	25.
12.6	109.	16.
17.6	150.	12.
27.6	145.4	8.6
32.5	124.0	9.7
37.5	44.8	3.8
40.0	46.3	4.3
50.3	48.5	5.3
62.8	8.1	1.4
67.8	7.1	1.3
72.8	5.6	1.3
80.3	7.3	1.1
90.3	6.8	1.1
100.4	6.5	1.1

EX= 6.443 MEV,J=1		
THETA	SIGMA	ERROR
9.7	67.	27.
17.6	57.5	8.5
27.6	47.4	5.0
37.5	61.6	4.4
40.0	75.3	5.4
50.3	42.7	5.0
62.8	34.2	2.8
67.8	26.5	2.5
72.8	19.0	3.3
80.3	22.5	2.0
90.3	10.2	1.3
100.4	10.0	1.3

EX= 6.458 MEV,J=1		
THETA	SIGMA	ERROR
9.7	77.	29.
12.6	38.	11.
17.6	64.4	9.1
27.6	14.9	2.8
40.0	33.7	3.6
50.3	35.7	5.2
62.8	28.0	2.5
67.8	19.9	2.2
72.8	19.0	3.3
80.3	16.6	1.7
90.3	13.1	1.5
100.4	13.0	1.5

EX= 6.483 MEV,J=1		
THETA	SIGMA	ERROR
9.7	115.	30.
12.6	76.	13.
17.6	171.	13.
22.7	160.	16.
27.6	139.0	8.6
32.5	111.8	9.2
37.5	67.1	4.6
40.0	76.5	5.5
50.3	54.9	5.5
62.8	32.1	3.2
67.8	29.8	2.7
72.8	15.1	2.9
80.3	19.1	1.8
90.3	14.1	1.6
100.4	12.3	1.5

EX= 6.529 MEV,J=1		
THETA	SIGMA	ERROR
9.7	45.	22.
12.6	35.	11.
17.6	69.1	8.6
22.7	75.	11.
27.6	71.9	6.2
32.5	115.7	9.4
40.0	93.4	5.1
50.3	60.8	5.8
62.8	29.1	3.0
67.8	35.5	2.9
72.8	42.0	4.8
80.3	25.4	2.1
90.3	22.6	2.0
100.4	7.2	1.2

EX= 6.544 MEV,J=1		
THETA	SIGMA	ERROR
9.7	133.	28.
12.6	85.	12.
17.6	183.	13.
22.7	100.	14.
32.5	167.	11.
37.5	87.4	5.3
40.0	54.5	4.6
50.3	83.9	6.7
62.8	46.2	3.8
67.8	33.3	2.8
72.8	18.6	3.2
80.3	22.0	2.0
100.4	16.1	1.7

EX= 6.572 MEV,J=1		
THETA	SIGMA	ERROR
12.6	20.	10.
17.6	26.7	7.4
22.7	15.3	5.1
32.5	22.1	4.1
37.5	13.7	2.1
40.0	17.3	2.6
50.3	15.8	5.0
62.8	4.4	1.8
72.8	5.6	1.8
80.3	4.83	.93
90.3	3.76	.82
100.4	.91	.41

EX= 6.588 MEV,J=1		
THETA	SIGMA	ERROR
9.7	59.	26.
17.6	31.5	6.9
32.5	66.9	7.1
37.5	31.8	3.2
40.0	36.5	3.8
50.3	26.6	5.2
62.8	14.3	2.5
67.8	18.7	2.1
72.8	21.8	3.5
80.3	7.3	1.1
90.3	4.11	.86
100.4	2.90	.72

EX= 6.615 MEV,J=1		
THETA	SIGMA	ERROR
9.7	60.	26.
12.6	84.	13.
17.6	153.	13.
22.7	141.	15.
27.6	105.	10.
32.5	168.	11.
37.5	85.8	5.2
40.0	105.1	6.4
50.3	44.4	5.9
62.8	27.3	3.2
67.8	24.3	2.4
72.8	21.3	3.4
80.3	23.6	2.1
90.3	18.2	1.8
100.4	2.35	.65

EX= 6.631 MEV,J=1		
THETA	SIGMA	ERROR
9.7	21.	10.
17.6	33.5	7.5
32.5	32.7	5.0
50.3	18.4	4.2
62.8	17.8	2.7
67.8	16.1	2.0
72.8	20.7	3.4
80.3	12.9	1.5
90.3	10.0	1.3
100.4	10.0	1.3

EX= 6.658 MEV,J=1		
THETA	SIGMA	ERROR
9.7	196.	26.
12.6	82.	14.
17.6	94.5	9.9
22.7	82.	12.
27.6	89.0	6.9
32.5	69.6	4.7
40.0	81.6	5.7
50.3	41.5	5.6
62.8	40.2	3.7
67.8	31.7	2.7
72.8	21.3	3.4
80.3	21.5	2.0
90.3	14.8	1.6

EX= 6.688 MEV,J=1		
THETA	SIGMA	ERROR
9.7	206.	33.
12.6	127.	16.
17.6	149.	12.
22.7	189.	18.
27.6	196.	10.
32.5	314.	15.
37.5	223.4	8.4
40.0	269.	10.
50.3	113.1	7.8
62.8	73.0	4.7
67.8	77.8	4.3
72.8	52.1	5.4
80.3	41.8	2.7
90.3	17.0	1.7

EX= 6.720 MEV,J=1		
THETA	SIGMA	ERROR
9.7	206.	30.
12.6	90.	14.
17.6	72.5	9.1
22.7	34.0	7.6
27.6	71.9	6.2
37.5	22.9	2.7
50.3	12.0	3.8
62.8	14.1	2.5
67.8	14.7	1.9
72.8	12.3	2.6
80.3	8.8	1.3
90.3	7.0	1.1
100.4	4.34	.89

EX= 6.737 MEV,J=1		
THETA	SIGMA	ERROR
9.7	56.	26.
12.6	66.	14.
17.6	100.	11.
22.7	117.	14.
27.6	68.2	6.0
37.5	17.5	2.4
50.3	13.2	4.2
62.8	26.8	3.1
67.8	49.9	3.4
72.8	25.2	3.8
80.3	18.6	1.8
90.3	9.5	1.3
100.4	4.89	.94

EX= 6.786 MEV,J=1		
THETA	SIGMA	ERROR
9.7	100.	25.
12.6	76.	12.
17.6	103.	10.
22.7	94.	13.
27.6	69.8	6.1
32.5	152.	11.
37.5	101.7	5.7
40.0	130.6	7.2
50.3	76.3	7.2
62.8	39.7	3.7
67.8	30.5	2.7
72.8	24.6	3.7
80.3	23.2	2.0
90.3	13.4	1.5
100.4	4.34	.89

EX= 6.801 MEV,J=1		
THETA	SIGMA	ERROR
12.6	35.	12.
17.6	29.4	6.3
22.7	28.9	7.0
32.5	44.1	5.8
37.5	14.3	2.1
40.0	27.5	3.3
50.3	43.0	6.2
62.8	33.0	3.4
67.8	17.7	2.0
72.8	7.3	2.0
80.3	14.7	1.6
100.4	12.1	1.5

EX= 6.823 MEV,J=1		
THETA	SIGMA	ERROR
12.6	14.	11.
17.6	13.7	5.0
27.6	20.8	3.9
32.5	58.5	7.2
37.5	48.9	4.0
40.0	33.2	3.9
50.3	40.6	6.2
62.8	18.7	2.9
67.8	11.6	1.7
72.8	12.3	2.6
80.3	17.3	1.8
90.3	10.9	1.4

KEY: FOR J=1,2,OR 3, CROSS SECTION UNITS ARE MICRO-, 100 MICRO-, OR MILLI-BARNS/STERADIAN, RESPECTIVELY,

EX= 6.843 MEV,J=1

THETA	SIGMA	ERROR
12.6	18.	10.
17.6	36.3	7.9
22.7	28.9	7.0
27.6	16.5	3.0
32.5	23.6	4.2
40.0	24.7	3.1
50.3	26.9	5.4
62.8	20.3	2.5
67.8	21.7	2.3
72.8	13.4	2.7
80.3	16.6	1.7
90.3	7.2	1.1
100.4	5.8	1.0

EX= 6.862 MEV,J=1

THETA	SIGMA	ERROR
12.6	20.	10.
22.7	34.0	7.6
27.6	22.9	3.5
37.5	26.4	2.9
40.0	29.4	3.4
50.3	40.3	6.1
62.8	15.2	2.5
67.8	21.7	2.3
72.8	14.6	2.9
80.3	13.6	1.6
90.3	9.3	1.3
100.4	5.35	.98

EX= 6.876 MEV,J=1

THETA	SIGMA	ERROR
9.7	113.	28.
17.6	60.9	8.4
22.7	57.8	9.9
37.5	40.7	3.6
40.0	49.0	4.4
50.3	46.5	6.3
62.8	21.5	2.9
67.8	22.0	2.3
80.3	12.0	1.5
90.3	5.7	1.0
100.4	4.89	.94

EX= 6.925 MEV,J=1

THETA	SIGMA	ERROR
17.6	75.3	9.9
22.7	82.	12.
32.5	85.2	8.1
50.3	26.9	5.4
62.8	25.4	2.4
67.8	21.0	2.2
80.3	14.7	1.6
90.3	9.1	1.3

EX= 6.940 MEV,J=1

THETA	SIGMA	ERROR
12.6	34.	12.
17.6	25.3	7.2
22.7	17.0	5.4
50.3	25.4	5.5
62.8	16.6	2.0
67.8	8.3	1.4
80.3	9.5	1.3
90.3	4.65	.91
100.4	4.16	.87

EX= 6.963 MEV,J=1

THETA	SIGMA	ERROR
9.7	77.	28.
17.6	63.0	9.4
22.7	42.5	8.5
27.6	33.6	4.2
32.5	61.6	6.8
37.5	48.6	3.9
50.3	48.2	7.9
62.8	11.6	2.6
67.8	17.5	2.0
72.8	13.5	3.2
80.3	12.5	1.5
90.3	8.8	1.3
100.4	3.62	.81

EX= 6.992 MEV,J=1

THETA	SIGMA	ERROR
12.6	48.	14.
17.6	100.	11.
22.7	85.	12.
32.5	92.8	8.4
37.5	38.5	3.5
62.8	31.9	3.5
67.8	31.9	2.7
72.8	33.0	4.3
80.3	13.0	1.5
90.3	11.1	1.4

EX= 7.019 MEV,J=1

THETA	SIGMA	ERROR
9.7	32.	22.
17.6	83.	10.
22.7	126.	15.
27.6	93.7	7.1
32.5	142.	10.
37.5	43.6	3.7
50.3	64.0	8.5
62.8	29.3	3.5
67.8	29.8	2.7
72.8	26.3	3.8
80.3	16.4	1.7
100.4	6.2	1.1

EX= 7.046 MEV,J=1

THETA	SIGMA	ERROR
22.7	45.9	8.8
27.6	30.4	4.0
32.5	35.8	5.2
37.5	38.8	3.5
50.3	47.6	9.1
62.8	13.4	1.8
67.8	12.1	1.7
72.8	7.3	2.0
80.3	8.8	1.3
90.3	10.5	1.4

EX= 7.061 MEV,J=1

THETA	SIGMA	ERROR
9.7	172.	34.
12.6	126.	17.
17.6	167.	14.
22.7	121.	14.
27.6	82.5	6.6
32.5	113.4	9.3
37.5	56.2	4.2
50.3	57.9	8.1
62.8	18.2	2.7
67.8	26.9	2.5
72.8	31.3	4.2
80.3	19.5	1.9
100.4	5.25	.98

EX= 7.080 MEV,J=1

THETA	SIGMA	ERROR
9.7	173.	34.
12.6	75.	14.
17.6	34.2	7.6
22.7	42.5	8.5
27.6	27.2	3.8
32.5	41.8	5.6
37.5	27.3	2.9
50.3	49.1	9.1
62.8	27.7	2.5
67.8	26.0	2.5
72.8	15.1	2.9
80.3	10.9	1.4
90.3	4.65	.91
100.4	10.3	1.4

EX= 7.114 MEV,J=1

THETA	SIGMA	ERROR
9.7	114.	29.
12.6	65.	14.
22.7	94.	13.
27.6	126.2	8.2
32.5	66.9	7.1
37.5	22.3	3.0
40.0	29.0	3.4
50.3	65.	10.
67.8	15.8	1.9
72.8	7.9	2.1
80.3	9.7	1.3
90.3	11.4	1.4
100.4	2.72	.70

EX= 7.174 MEV,J=1

THETA	SIGMA	ERROR
12.6	23.	12.
17.6	34.9	9.0
22.7	56.1	9.8
32.5	60.1	6.8
37.5	24.8	2.8
67.8	15.6	1.9
72.8	14.6	2.9
80.3	18.8	1.8

EX= 7.192 MEV,J=1

THETA	SIGMA	ERROR
17.6	90.	11.
32.5	115.6	9.4
40.0	44.7	4.2
50.3	33.0	9.6
67.8	20.8	2.2
72.8	24.1	3.7
80.3	12.3	1.5
90.3	6.8	1.1
100.4	6.5	1.1

EX= 7.219 MEV,J=1

THETA	SIGMA	ERROR
32.5	27.4	4.6
37.5	16.8	2.3
50.3	26.	10.
67.8	11.3	1.6
72.8	8.0	1.7
90.3	7.5	1.2
100.4	7.4	1.2

EX= 7.239 MEV,J=1

THETA	SIGMA	ERROR
9.7	260.	38.
17.6	111.	13.
32.5	143.	10.
37.5	76.2	4.9
40.0	104.3	6.4
50.3	38.	11.
62.8	26.1	3.2
67.8	30.7	2.7
72.8	33.6	4.3
80.3	19.1	1.8

EX= 7.268 MEV,J=1

THETA	SIGMA	ERROR
9.7	84.	33.
12.6	31.	12.
17.6	49.	11.
22.7	40.8	8.3
32.5	22.8	4.2
50.3	31.0	9.9
67.8	6.1	1.2
72.8	12.9	2.7
80.3	8.9	1.3
90.3	4.65	.91
100.4	4.89	.94

EX= 7.302 MEV,J=1

THETA	SIGMA	ERROR
9.7	74.	31.
12.6	45.	14.
22.7	23.9	7.0
32.5	58.6	6.7
37.5	63.6	4.5
40.0	70.2	5.2
50.3	19.9	2.5
62.8	20.1	3.1
67.8	12.8	1.7
72.8	14.0	2.8
80.3	9.5	1.3
100.4	3.98	.85

KEY: FOR J=1,2,OR 3, CROSS SECTION UNITS ARE MICRO-, 100 MICRO-, OR MILLI-BARNS/STERADIAN, RESPECTIVELY.

EX= 7.325 MEV,J=1		
THETA	SIGMA	ERROR
9.7	132.	32.
12.6	71.	12.
22.7	32.3	7.4
37.5	41.6	3.6
50.3	25.7	8.0
62.8	9.2	1.9
67.8	9.7	1.5
72.8	10.6	2.4
80.3	10.7	1.4
90.3	10.7	1.4
100.4	7.6	1.2

EX= 7.343 MEV,J=1		
THETA	SIGMA	ERROR
9.7	45.	26.
12.6	76.	14.
22.7	129.	15.
32.5	68.5	7.2
37.5	36.2	3.4
50.3	17.8	9.2
62.8	20.8	3.0
67.8	30.5	2.7
72.8	38.1	4.6
90.3	7.7	1.2
100.4	4.89	.94

EX= 7.382 MEV,J=1		
THETA	SIGMA	ERROR
17.6	21.2	7.7
22.7	30.6	7.2
37.5	43.2	3.7
50.3	24.8	9.9
62.8	23.3	3.1
67.8	16.1	1.9
72.8	11.8	2.6
80.3	8.6	1.2
90.3	5.18	.96
100.4	3.98	.85

EX= 7.404 MEV,J=1		
THETA	SIGMA	ERROR
17.6	73.	11.
22.7	49.3	9.2
32.5	91.3	8.3
50.3	32.7	9.9
62.8	23.8	3.4
67.8	11.8	1.7
72.8	30.8	4.2
80.3	17.5	1.8
90.3	5.5	1.0
100.4	7.2	1.1

EX= 7.549 MEV,J=1		
THETA	SIGMA	ERROR
17.6	19.8	9.3
22.7	40.8	8.3
37.5	25.7	2.9
50.3	13.4	7.8
62.8	29.8	4.0
72.8	31.3	4.2
80.3	22.0	2.0
90.3	10.9	1.4
100.4	7.1	1.1

EX= 7.573 MEV,J=1		
THETA	SIGMA	ERROR
17.6	26.0	8.9
22.7	56.1	9.8
32.5	105.0	8.9
37.5	35.3	3.3
40.0	34.5	2.7
50.3	33.0	3.8
62.8	22.2	3.2
72.8	29.1	4.0
80.3	20.9	1.9
90.3	12.3	1.5
100.4	5.43	.99

EX= 7.594 MEV,J=1		
THETA	SIGMA	ERROR
12.6	44.	13.
17.6	41.	10.
22.7	57.8	9.9
32.5	48.7	6.1
37.5	49.2	4.0
40.0	45.5	4.2
50.3	54.3	8.8
72.8	26.3	3.8
80.3	19.3	1.9
90.3	11.4	1.4
100.4	12.5	1.5

EX= 7.684 MEV,J=1		
THETA	SIGMA	ERROR
22.7	44.2	8.7
30.5	50.2	6.2
50.3	24.2	7.5
62.8	10.4	2.9
67.8	9.2	1.5
72.8	14.0	2.8
80.3	10.9	1.4
90.3	7.2	1.1
100.4	7.8	1.2

EX= 7.723 MEV,J=1		
THETA	SIGMA	ERROR
12.6	77.	14.
22.7	119.	14.
50.3	19.3	5.8
62.8	19.4	3.4
67.8	31.7	2.7
72.8	30.8	4.2
80.3	9.7	1.3
90.3	7.7	1.2

EX= 8.166 MEV,J=1		
THETA	SIGMA	ERROR
12.6	53.	13.
40.0	74.5	5.4
62.8	47.6	4.4
67.8	53.0	3.5
72.8	61.0	5.8
80.3	17.9	1.8
90.3	8.8	1.3
100.4	8.7	1.3

KEY: FOR J=1,2,OR 3, CROSS SECTION UNITS ARE MICRO-, 100 MICRO-, OR MILLI-BARNS/STERADIAN, RESPECTIVELY.

APPENDIX IV

^{207}Pb Angular Distributions

APPENDIX IV ^{207}Pb Angular Distributions

EX= .899 MEV/NUCL		
THETA	SIGMA	ERROR
16.1	14090.	151.
20.1	5284.	30.
24.1	949.0	6.2
28.1	307.1	2.4
32.1	43.00	.79
36.2	66.40	.71
40.2	58.80	.57
44.2	43.10	.47
48.2	89.35	.38
52.2	32.93	.12
56.2	1.830	.050
60.2	8.330	.070
64.3	5.720	.093
68.3	9.380	.068
72.3	9.720	.056
76.3	2.781	.013
80.3	2.857	.015
84.3	5.128	.014
88.3	5.683	.017
92.3	3.589	.010
96.3	1.668	.010
100.3	.713	.006

EX= .971 MEV/NUCL		
THETA	SIGMA	ERROR
32.1	13.7	1.4
36.2	2.01	.13
40.2	1.814	.097
44.2	1.444	.078
48.2	1.330	.065
52.2	.943	.034
56.2	.625	.026
60.2	.580	.026
64.3	.574	.024
68.3	.544	.025
72.3	.505	.036
76.3	.213	.010
80.3	.209	.012
84.3	.176	.008
88.3	.149	.008
92.3	.140	.006
96.3	.140	.008
100.3	.096	.007

EX= .999 MEV/NUCL		
THETA	SIGMA	ERROR
16.1	726.	144.
20.1	295.	25.
24.1	287.5	8.6
44.2	95.2	9.5
48.2	94.5	3.9
52.2	80.9	3.3
56.2	62.8	2.9
60.2	57.7	2.7
64.3	49.3	2.5
68.3	41.2	2.3
72.3	35.0	3.1
76.3	20.67	1.00
80.3	16.00	.93
84.3	11.10	.43
88.3	8.80	.60
92.3	6.91	.35
96.3	6.19	.56
100.3	5.13	.52

EX= 1.034 MEV/NUCL		
THETA	SIGMA	ERROR
20.1	56.	16.
24.1	35.3	5.8
28.1	46.9	4.9
32.2	44.6	2.0
36.2	31.0	5.8
40.2	54.	11.
56.3	27.0	3.6
60.3	13.9	2.0
64.3	16.2	2.0
68.3	20.6	2.0
72.3	15.9	2.2
76.3	7.66	.68
80.3	10.12	.83
84.3	11.18	.55
88.3	10.14	.56
92.3	8.25	.43
96.3	6.69	.58
100.3	4.98	.44

EX= 2.333 MEV/NUCL		
THETA	SIGMA	ERROR
16.1	427.	68.
20.1	122.	14.
24.1	130.1	5.0
28.1	142.9	4.7
32.2	170.5	3.1
36.2	139.4	5.1
40.2	93.5	4.3
44.2	55.3	3.3
48.2	68.7	3.4
60.3	53.8	2.5
68.3	37.6	2.3
72.3	27.9	2.6
76.3	15.9	1.0
80.3	17.0	1.1
84.3	12.62	.57
88.3	9.72	.59
92.3	8.06	.42
96.3	6.44	.57
100.3	4.12	.40

KEY: FOR U=1,2,OR 3, CROSS SECTION UNITS ARE MICRO-, 100 MICRO-, OR MILLI-BARNS/STERADIAN, RESPECTIVELY.

EX= 2.623 MEV,J=2

THETA	SIGMA	ERROR
10.1	1.78	.19
12.6	3.91	.29
17.5	13.64	.32
37.6	6.70	.12
40.2	6.00	.11
50.1	7.42	.11
67.7	2.614	.066
72.8	2.163	.060
80.3	1.759	.052
90.2	1.080	.049
100.2	1.439	.073

EX= 2.663 MEV,J=2

THETA	SIGMA	ERROR
10.1	2.25	.19
12.6	4.06	.28
17.5	14.01	.33
37.6	8.66	.14
40.2	8.06	.13
50.1	7.43	.11
67.7	3.407	.075
72.8	2.835	.069
80.3	2.346	.060
90.2	1.963	.048
100.2	1.414	.072

EX= 2.702 MEV,J=1

THETA	SIGMA	ERROR
10.1	33.	19.
17.5	14.4	7.2
22.6	18.0	4.4
27.7	12.1	4.8
37.6	9.6	1.5
40.2	12.8	1.6
50.1	6.2	1.0
67.7	2.66	.67
80.3	2.73	.64

EX= 2.728 MEV,J=1

THETA	SIGMA	ERROR
12.6	99.	19.
17.5	182.	14.
22.6	154.	11.
27.7	143.	10.
32.6	123.9	5.6
37.6	132.7	5.6
40.2	144.8	5.4
50.1	52.2	3.0
62.7	27.8	2.8
67.7	29.5	2.2
80.3	17.1	1.6
90.2	12.9	1.7
100.2	13.6	2.2

EX= 3.200 MEV,J=1

THETA	SIGMA	ERROR
32.6	15.2	2.4
37.6	6.8	1.4
40.2	6.7	1.2
50.1	4.61	.89
62.7	5.8	1.3
90.2	5.9	1.1
100.2	8.1	1.7

EX= 3.223 MEV,J=1

THETA	SIGMA	ERROR
10.1	35.	14.
22.6	44.6	6.2
27.7	55.3	7.2
32.6	38.4	3.3
37.6	23.8	2.9
40.2	30.3	2.5
50.1	15.9	1.6
62.7	6.8	1.9
90.2	4.16	.95
100.2	4.0	1.2

EX= 3.334 MEV,J=1

THETA	SIGMA	ERROR
10.1	143.	16.
12.6	172.	22.
22.6	127.	10.
27.7	169.	10.
32.6	125.7	5.5
37.6	141.8	5.7
40.2	156.0	5.6
50.1	53.8	3.2
62.7	46.1	2.8
67.7	30.3	3.9
80.3	14.1	1.5
90.2	11.4	1.6
100.2	11.0	2.8

EX= 3.413 MEV,J=1

THETA	SIGMA	ERROR
10.1	119.	17.
22.6	110.9	9.8
27.7	140.7	9.7
32.6	92.0	4.7
37.6	60.4	3.8
40.2	57.3	3.4
50.1	25.5	2.3
62.7	34.1	2.4
67.7	16.8	2.5
80.3	13.6	1.4
90.2	5.0	1.1
100.2	2.9	1.9

EX= 3.429 MEV,J=1

THETA	SIGMA	ERROR
10.1	44.	15.
22.6	64.1	7.5
27.7	65.3	7.2
32.6	48.7	3.5
37.6	55.8	3.7
40.2	61.9	3.5
50.1	21.0	2.1
62.7	18.3	1.9
67.7	12.5	1.9
80.3	4.54	.83
90.2	4.8	1.0

EX= 3.476 MEV,J=1

THETA	SIGMA	ERROR
22.6	24.5	5.7
27.7	28.4	3.5
32.6	19.4	2.4
37.6	24.9	2.7
40.2	31.7	2.5
50.1	14.9	1.8
62.7	9.9	1.3
67.7	9.2	1.2
90.2	2.41	.73
100.2	2.2	1.3

EX= 3.510 MEV,J=1

THETA	SIGMA	ERROR
17.5	142.	17.
22.6	113.7	9.8
27.7	142.8	9.6
32.6	115.4	5.3
37.6	108.1	5.0
40.2	113.7	4.8
50.1	31.1	2.5
62.7	45.0	2.8
67.7	37.0	2.5
72.8	19.6	2.0
90.2	12.5	1.7
100.2	9.2	2.6

EX= 3.583 MEV,J=1

THETA	SIGMA	ERROR
10.1	46.	13.
12.6	54.	19.
17.5	118.	12.
22.6	93.6	9.0
27.7	124.8	9.1
32.6	95.5	4.4
37.6	99.6	4.8
40.2	103.2	4.6
50.1	38.4	2.7
62.7	27.8	2.2
67.7	26.3	2.1
72.8	16.9	2.2
80.3	10.5	1.3
90.2	7.4	1.3
100.2	8.8	1.2

EX= 3.620 MEV,J=1

THETA	SIGMA	ERROR
10.1	84.	15.
12.6	132.	19.
17.5	162.	13.
22.6	125.	10.
27.7	178.	10.
32.6	146.0	5.9
37.6	156.5	6.0
40.2	171.2	5.9
50.1	50.8	3.1
62.7	45.4	2.8
67.7	47.2	2.8
80.3	18.5	1.7
90.2	12.9	1.7
100.2	20.2	2.7

EX= 3.634 MEV,J=1

THETA	SIGMA	ERROR
10.1	39.	14.
12.6	57.	15.
17.5	91.	10.
22.6	117.3	9.8
27.7	196.	11.
32.6	83.0	4.4
37.6	33.5	2.9
40.2	28.0	2.4
50.1	45.8	2.9
62.7	17.7	1.7
67.7	17.6	1.7
80.3	15.4	1.6
90.2	5.3	1.1

EX= 3.650 MEV,J=1

THETA	SIGMA	ERROR
10.1	34.	14.
12.6	32.	13.
22.6	20.9	4.8
27.7	22.1	4.3
32.6	19.2	2.3
37.6	16.8	2.2
40.2	22.3	2.1
50.1	22.6	2.1
62.7	22.9	2.0
67.7	20.6	1.9
80.3	13.0	1.4
90.2	3.28	.85

EX= 3.672 MEV,J=1

THETA	SIGMA	ERROR
12.6	20.	14.
17.5	10.3	7.1
22.6	15.8	4.9
32.6	5.8	1.6
37.6	8.5	1.8
40.2	10.2	1.4
50.1	8.7	1.5
67.7	3.33	.74
80.3	6.36	.98
100.2	5.2	1.4

EX= 3.709 MEV,J=1

THETA	SIGMA	ERROR
12.6	30.	15.
17.5	45.8	8.4
22.6	35.3	6.0
27.7	46.9	6.9
32.6	10.0	1.9
37.6	3.7	1.4
40.2	3.66	.86
50.1	2.73	.68
67.7	1.00	.41
90.2	2.84	.79

EX= 3.725 MEV,J=1

THETA	SIGMA	ERROR
10.1	44.	14.
12.6	44.	18.
22.6	45.3	6.7
27.7	53.2	7.5
32.6	31.7	3.0
37.6	32.6	2.9
40.2	43.5	3.0
50.1	12.6	1.7
62.7	16.0	1.7
67.7	18.0	1.7
90.2	5.9	1.1

KEY: FOR J=1,2,OR 3, CROSS SECTION UNITS ARE MICRO-, 100 MICRO-, OR MILLI-BARNS/STERADIAN, RESPECTIVELY.

Ex= 3.829 MEV/J=1

THETA	SIGMA	ERROR
10.1	13.9	7.5
17.5	25.3	6.4
22.6	28.8	5.8
27.7	33.7	6.1
32.6	33.0	3.0
37.6	32.0	3.0
40.2	41.8	2.9
50.1	15.7	1.8
62.7	9.7	1.3
67.7	8.5	1.2
72.8	6.0	1.6
80.3	3.33	.71
90.2	2.19	.69

Ex= 3.857 MEV/J=1

THETA	SIGMA	ERROR
10.1	17.	12.
17.5	26.7	6.4
27.7	14.2	4.6
32.6	14.5	2.2
37.6	7.2	1.6
40.2	11.2	1.5
50.1	19.3	2.0
62.7	14.7	1.6
67.7	7.7	1.1
72.8	7.2	1.6
80.3	4.39	.82
100.2	6.6	1.6

Ex= 3.869 MEV/J=1

THETA	SIGMA	ERROR
10.1	33.	13.
17.5	39.0	8.1
22.6	27.3	4.4
27.7	49.5	7.0
32.6	42.6	3.3
37.6	42.7	3.3
40.2	51.4	3.2
50.1	25.8	2.3
62.7	12.8	1.5
67.7	8.2	1.2
72.8	6.9	1.5
80.3	4.5	1.1

Ex= 3.887 MEV/J=1

THETA	SIGMA	ERROR
12.6	21.	13.
17.5	45.1	8.0
22.6	38.1	6.1
27.7	59.5	7.2
32.6	24.8	2.6
37.6	14.2	2.1
40.2	11.6	1.5
50.1	5.3	1.3
67.7	4.33	.85
72.8	5.2	1.3

Ex= 3.901 MEV/J=1

THETA	SIGMA	ERROR
10.1	59.	15.
12.6	53.	17.
17.5	105.	10.
22.6	60.5	7.5
27.7	67.4	7.7
32.6	27.7	2.8
37.6	31.7	2.9
40.2	45.3	3.0
50.1	37.3	2.7
62.7	35.1	2.4
67.7	22.8	1.9
72.8	24.8	2.3
80.3	14.1	1.5
100.2	7.0	1.6

Ex= 3.925 MEV/J=1

THETA	SIGMA	ERROR
22.6	8.6	4.3
27.7	9.0	5.0
32.6	3.7	1.8
37.6	5.3	1.1
40.2	6.3	1.1
62.7	5.0	1.0
72.8	4.7	1.2
100.2	7.4	1.6

Ex= 3.986 MEV/J=1

THETA	SIGMA	ERROR
37.6	13.6	2.0
40.2	14.2	1.7
50.1	8.9	1.5
62.7	5.46	.97
67.7	4.83	.90
72.8	5.0	1.1
90.2	3.50	.88

Ex= 3.999 MEV/J=1

THETA	SIGMA	ERROR
10.1	36.	13.
12.6	39.	16.
17.5	106.	11.
22.6	95.7	9.2
27.7	96.	10.
32.6	57.4	3.8
37.6	26.9	2.7
40.2	22.9	2.2
50.1	12.6	1.7
62.7	10.7	1.4
67.7	3.99	.82
72.8	5.6	1.1
90.2	5.5	1.1
100.2	7.0	1.6

Ex= 4.017 MEV/J=1

THETA	SIGMA	ERROR
17.5	33.5	8.2
27.7	27.9	5.3
32.6	25.4	2.7
37.6	23.0	2.5
50.1	13.2	1.7
62.7	11.9	1.4
67.7	7.7	1.1
72.8	3.22	.88

Ex= 4.034 MEV/J=1

THETA	SIGMA	ERROR
17.5	38.3	7.7
22.6	33.8	5.9
27.7	13.2	4.6
32.6	3.1	1.2
40.2	2.64	.73
50.1	6.3	1.0
62.7	3.41	.76
67.7	2.00	.58
72.8	2.42	.80

Ex= 4.062 MEV/J=1

THETA	SIGMA	ERROR
12.6	34.	15.
17.5	25.3	7.1
27.7	32.7	6.1
32.6	16.1	2.3
37.6	8.1	1.7
40.2	12.8	1.6
50.1	20.0	2.0
62.7	9.6	1.3
67.7	5.33	.94
72.8	2.42	.95
90.2	1.75	.62

Ex= 4.088 MEV/J=1

THETA	SIGMA	ERROR
32.6	35.0	3.0
40.2	27.6	2.4
50.1	53.5	3.2
67.7	2.00	.58
72.8	2.4	1.1
80.3	3.13	.69
90.2	4.16	.95

Ex= 4.103 MEV/J=2

THETA	SIGMA	ERROR
10.1	4.24	.24
17.5	10.24	.27
22.6	7.44	.24
27.7	6.49	.19
32.6	1.473	.059
37.6	2.532	.076
40.2	3.068	.079
50.1	1.425	.051
62.7	.875	.040
67.7	.805	.037
72.8	.728	.036
80.3	.419	.025
90.2	.311	.026
100.2	.600	.047

Ex= 4.140 MEV/J=2

THETA	SIGMA	ERROR
10.1	6.04	.26
17.5	13.59	.31
22.6	9.80	.27
32.6	1.997	.068
37.6	2.667	.078
40.2	3.820	.088
50.1	1.712	.055
62.7	1.261	.046
67.7	1.120	.043
72.8	.899	.039
80.3	.629	.031
90.2	.350	.028
100.2	.615	.048

Ex= 4.190 MEV/J=1

THETA	SIGMA	ERROR
10.1	37.	13.
12.6	50.	19.
17.5	127.	11.
22.6	85.7	9.0
27.7	70.6	8.5
32.6	58.0	3.5
37.6	57.1	3.7
40.2	72.3	3.8
50.1	55.2	3.2
62.7	37.9	2.5
67.7	21.6	1.9
72.8	18.8	1.9
80.3	14.4	1.5
90.2	9.2	2.2

Ex= 4.213 MEV/J=1

THETA	SIGMA	ERROR
10.1	81.	16.
12.6	97.	20.
17.5	109.	11.
22.6	101.5	9.4
27.7	89.0	8.8
32.6	73.2	4.2
37.6	58.0	3.8
40.2	70.5	3.8
50.1	32.5	2.5
62.7	31.9	2.3
67.7	24.3	2.0
72.8	19.0	1.9
80.3	12.9	1.4
90.2	8.8	1.4

Ex= 4.232 MEV/J=1

THETA	SIGMA	ERROR
10.1	48.	16.
12.6	48.	18.
17.5	68.4	8.7
22.6	97.9	9.2
32.6	32.8	3.0
37.6	40.5	3.2
40.2	47.7	3.1
50.1	17.4	2.0
62.7	22.3	2.0
67.7	13.3	1.5
72.8	12.4	1.5
90.2	6.3	1.2

Ex= 4.250 MEV/J=1

THETA	SIGMA	ERROR
10.1	47.	15.
12.6	74.	19.
17.5	143.	12.
22.6	102.2	9.4
32.6	23.9	2.6
37.6	27.8	2.8
40.2	43.0	3.0
50.1	38.4	2.8
62.7	30.2	2.3
67.7	17.1	1.7
72.8	17.1	1.8
90.2	8.3	1.3

KEY: FOR J=1,2,OR 3, CROSS SECTION UNITS ARE MICRO-, 100 MICRO-, OR MILLI-BARNS/STERADIAN, RESPECTIVELY.

EX= 4.270 MEV/U=1		
THETA	SIGMA	ERROR
10.1	22.	13.
12.6	21.	15.
17.5	19.1	7.2
22.6	22.3	5.1
32.6	12.7	2.0
37.6	13.8	2.1
40.2	14.6	1.7
62.7	2.39	.93
67.7	3.00	.71
72.8	5.3	1.1
90.2	3.06	.82

EX= 4.287 MEV/U=1		
THETA	SIGMA	ERROR
10.1	19.	13.
17.5	16.4	5.5
22.6	13.7	4.5
32.6	15.6	2.2
37.6	12.9	2.0
40.2	10.0	1.4
50.1	3.93	.82
62.7	3.8	1.1
67.7	2.50	.64
72.8	3.06	.90
90.2	2.63	.76

EX= 4.313 MEV/U=2		
THETA	SIGMA	ERROR
10.1	7.74	.28
12.6	9.78	.32
17.5	11.59	.29
22.6	6.76	.23
37.6	6.97	.12
40.2	6.85	.12
50.1	2.615	.069
62.7	3.567	.078
67.7	2.819	.068
72.8	1.502	.050
90.2	.972	.046
100.2	1.389	.072

EX= 4.342 MEV/U=1		
THETA	SIGMA	ERROR
12.6	38.	14.
17.5	37.6	7.0
22.6	38.9	6.4
27.7	29.0	6.8
32.6	8.5	1.7
40.2	3.66	.86
62.7	6.5	1.1
67.7	2.00	.58
72.8	3.22	.72

EX= 4.364 MEV/U=1		
THETA	SIGMA	ERROR
10.1	183.	18.
22.6	195.	13.
27.7	248.	13.
37.6	168.3	6.2
40.2	235.7	6.9
50.1	200.1	6.1
62.7	88.2	3.9
67.7	66.7	3.3
72.8	39.4	3.2
90.2	25.6	2.4
100.2	28.3	3.2

EX= 4.387 MEV/U=1		
THETA	SIGMA	ERROR
10.1	67.	16.
12.6	141.	20.
17.5	96.4	9.5
22.6	66.5	7.7
27.7	33.2	5.6
32.6	23.8	2.7
37.6	24.9	2.6
40.2	18.1	1.9
50.1	13.3	1.5
62.7	13.1	1.8
67.7	15.0	1.6
72.8	10.1	1.4
90.2	4.8	1.0
100.2	5.9	1.5

EX= 4.404 MEV/U=1		
THETA	SIGMA	ERROR
10.1	262.	19.
22.6	253.	14.
27.7	352.	15.
32.6	201.3	5.8
37.6	224.5	7.1
40.2	206.2	7.9
50.1	200.8	6.0
62.7	103.4	4.2
67.7	80.9	3.7
72.8	69.9	3.4
90.2	28.0	2.5
100.2	28.7	3.3

EX= 4.422 MEV/U=1		
THETA	SIGMA	ERROR
10.1	64.	15.
12.6	155.	19.
17.5	241.	14.
22.6	121.	10.
27.7	124.3	9.6
37.6	23.6	2.5
40.2	29.6	2.5
50.1	16.9	1.7
62.7	18.8	1.8
67.7	12.3	1.4
72.8	10.6	1.4
90.2	8.5	1.4
100.2	7.4	1.6

EX= 4.465 MEV/U=1		
THETA	SIGMA	ERROR
10.1	47.	14.
12.6	35.	17.
17.5	41.7	7.2
22.6	32.4	5.3
27.7	21.1	5.8
37.6	22.5	2.5
40.2	14.2	1.7
50.1	10.1	1.8
62.7	7.7	1.4
67.7	6.3	1.0
72.8	5.3	1.1
80.3	3.48	.97
90.2	4.6	1.0
100.2	6.3	1.5

EX= 4.479 MEV/U=1		
THETA	SIGMA	ERROR
12.6	59.	17.
17.5	36.2	7.3
27.7	37.4	6.6
37.6	7.0	1.6
40.2	6.3	1.1
50.1	5.13	.94
67.7	2.50	.64
72.8	3.70	.95
80.3	4.54	.83
90.2	5.3	1.1

EX= 4.494 MEV/U=1		
THETA	SIGMA	ERROR
17.5	12.3	6.4
27.7	7.9	4.4
32.6	6.7	1.6
40.2	4.67	.97
50.1	6.3	1.0
62.7	5.80	.99
67.7	3.3	1.3
72.8	3.06	.95
80.3	2.57	.62

EX= 4.514 MEV/U=1		
THETA	SIGMA	ERROR
22.6	22.3	4.6
32.6	8.7	1.8
37.6	6.8	1.6
50.1	5.64	.98
62.7	3.07	.72
67.7	2.33	.62
72.8	1.45	.48
80.3	2.42	.61

EX= 4.527 MEV/U=1		
THETA	SIGMA	ERROR
17.5	65.7	8.8
22.6	43.2	6.4
27.7	42.7	6.3
32.6	10.0	1.8
37.6	7.2	1.6
40.2	11.8	1.5
50.1	7.9	1.5
62.7	6.1	1.0
67.7	3.83	.80
72.8	4.3	1.0
80.3	4.70	.84
90.2	2.63	.76

EX= 4.538 MEV/U=1		
THETA	SIGMA	ERROR
17.5	62.9	8.1
27.7	56.4	7.0
32.6	22.8	2.5
37.6	13.6	2.0
40.2	14.4	1.7
50.1	8.2	1.5
62.7	8.0	1.2
67.7	7.2	1.1
72.8	4.7	1.0
80.3	5.76	.93
90.2	7.9	1.3

EX= 4.558 MEV/U=1		
THETA	SIGMA	ERROR
40.2	8.9	1.3
62.7	8.4	1.2
67.7	4.99	.91
72.8	4.3	1.1
80.3	3.94	.77
90.2	2.84	.79

EX= 4.592 MEV/U=1		
THETA	SIGMA	ERROR
17.3	17.1	6.0
27.7	7.4	4.2
40.2	5.3	1.0
50.1	5.13	.94
62.7	3.41	.76
67.7	3.33	.74
72.8	2.58	.85
80.3	2.73	.64
90.2	1.53	.58

EX= 4.612 MEV/U=1		
THETA	SIGMA	ERROR
10.1	128.	16.
17.5	98.	10.
22.6	63.3	8.2
32.6	31.6	3.9
37.6	17.1	2.2
40.2	15.8	1.8
50.1	8.9	1.6
62.7	5.46	.97
67.7	4.83	.90
72.8	5.5	1.1
80.3	6.21	.97
90.2	8.1	1.3

EX= 4.630 MEV/U=1		
THETA	SIGMA	ERROR
10.1	103.	16.
17.5	145.	12.
22.6	113.	10.
27.7	134.3	9.5
32.6	108.0	5.1
37.6	65.9	4.0
40.2	85.3	4.2
50.1	60.7	3.5
62.7	70.6	3.5
67.7	52.3	2.9
72.8	38.8	2.6
80.3	19.8	1.7
100.2	15.8	2.4

KEY: FOR J=1,2,OR 3, CROSS SECTION UNITS ARE MICRO-, 100 MICRO-, OR MILLI-BARNS/STERADIAN, RESPECTIVELY.

EX= 4.656 MEV/J=1

THETA	SIGMA	ERROR
10.1	84.	14.
12.6	122.	20.
17.5	13.7	5.0
32.6	12.9	1.7
50.1	5.8	1.4
67.7	2.83	.69
72.8	3.70	.95
80.3	1.51	.48

EX= 4.671 MEV/J=1

THETA	SIGMA	ERROR
22.6	52.5	8.2
32.6	34.1	3.0
37.6	40.7	5.7
40.2	57.7	3.4
50.1	35.5	2.7
62.7	53.6	3.0
67.7	38.3	2.5
72.8	23.3	2.0
80.3	14.4	1.5

EX= 4.733 MEV/J=1

THETA	SIGMA	ERROR
32.6	8.5	1.6
37.6	6.8	2.4
40.2	12.6	1.6
50.1	22.2	1.9
62.7	11.1	1.4
67.7	10.5	1.3
72.8	8.4	1.2
80.3	12.0	1.3
90.2	7.2	1.3

EX= 4.745 MEV/J=1

THETA	SIGMA	ERROR
10.1	24.	12.
22.6	36.7	7.9
27.7	32.7	5.5
40.2	23.1	2.6
50.1	18.5	1.8
62.7	18.8	1.8
67.7	12.5	1.4
72.3	8.2	1.1
80.3	6.36	.98
100.2	7.0	1.6

EX= 4.761 MEV/J=1

THETA	SIGMA	ERROR
10.1	15.0	8.0
22.6	28.1	8.0
27.7	59.5	6.8
32.6	35.0	3.1
37.6	25.0	3.2
40.2	42.6	2.9
50.1	26.1	2.5
62.7	17.6	1.7
67.7	15.8	1.6
72.8	16.3	1.8
80.3	8.3	1.1
90.2	6.1	1.2
100.2	4.4	1.3

EX= 4.785 MEV/J=1

THETA	SIGMA	ERROR
17.5	32.1	9.0
22.6	49.7	9.6
27.7	47.9	6.2
32.6	34.6	3.1
37.6	24.1	2.5
50.1	34.3	2.8
62.7	22.3	2.0
67.7	16.5	1.7
72.8	18.4	1.9
80.3	12.9	1.4
100.2	5.2	1.4

EX= 4.806 MEV/J=1

THETA	SIGMA	ERROR
10.1	29.	14.
12.6	19.	10.
17.5	82.	11.
27.7	79.5	7.6
32.6	61.4	4.0
37.6	32.1	4.6
50.1	45.3	3.1
62.7	27.3	2.2
67.7	11.5	1.4
80.3	7.0	1.0

EX= 4.835 MEV/J=1

THETA	SIGMA	ERROR
12.6	172.	22.
17.5	200.	15.
27.7	127.4	8.2
32.6	79.0	4.5
37.6	101.3	4.7
40.2	85.7	4.2
50.1	74.2	3.0
62.7	33.3	2.7
67.7	15.5	1.6
72.8	32.7	2.3
80.3	27.1	2.0
100.2	11.0	2.0

EX= 4.870 MEV/J=1

THETA	SIGMA	ERROR
10.1	807.	28.
12.6	733.	33.
17.5	578.	22.
27.7	211.	11.
32.6	111.8	5.3
37.6	104.2	5.1
40.2	86.7	4.2
50.1	55.0	3.4
62.7	30.2	2.5
67.7	28.0	2.2
72.8	37.7	2.6
80.3	23.8	1.9
100.2	20.2	2.7

EX= 4.884 MEV/J=1

THETA	SIGMA	ERROR
17.5	69.0	9.5
27.7	93.2	7.9
32.6	51.8	3.7
37.6	43.1	3.4
40.2	45.3	3.0
50.1	48.7	3.2
62.7	32.8	2.4
67.7	29.0	2.2
72.8	25.6	2.1
80.3	24.4	1.9
100.2	21.0	2.8

EX= 4.921 MEV/J=1

THETA	SIGMA	ERROR
10.1	47.	13.
12.6	52.	20.
17.5	135.	13.
27.7	124.8	9.3
32.6	51.5	3.8
37.6	56.2	4.0
40.2	71.1	3.8
50.1	48.9	3.2
62.7	53.7	3.0
67.7	38.8	2.5
72.8	24.3	2.1
80.3	20.1	1.7
90.2	9.0	1.4

EX= 4.943 MEV/J=1

THETA	SIGMA	ERROR
12.6	67.	15.
17.5	39.7	8.3
32.6	42.2	3.4
37.6	33.0	3.1
40.2	44.3	3.0
50.1	30.3	2.3
62.7	34.8	2.4
67.7	23.3	2.0
72.8	24.0	2.1
80.3	20.9	1.8
90.2	13.6	1.7
100.2	14.7	2.3

EX= 4.957 MEV/J=1

THETA	SIGMA	ERROR
12.6	70.	15.
17.5	82.	10.
32.6	42.8	3.4
37.6	16.2	2.3
50.1	18.3	2.1
62.7	13.6	1.5
67.7	12.0	1.4
72.8	11.9	1.5
80.3	9.5	1.2
90.2	8.5	1.4

EX= 4.975 MEV/J=1

THETA	SIGMA	ERROR
10.1	11.2	7.9
17.5	44.4	7.3
27.7	101.1	8.2
37.6	72.4	4.6
40.2	89.1	4.3
50.1	19.5	2.1
62.7	15.2	1.6
67.7	11.0	1.4
72.8	13.8	1.6
80.3	11.7	1.3
90.2	5.0	1.1

EX= 4.987 MEV/J=1

THETA	SIGMA	ERROR
27.7	169.	10.
32.6	84.8	4.7
40.2	54.4	3.3
50.1	54.4	3.4
62.7	28.0	2.2
67.7	19.3	1.8
72.8	17.1	1.8
80.3	12.7	1.4
90.2	10.3	1.5
100.2	12.9	2.2

EX= 5.013 MEV/J=1

THETA	SIGMA	ERROR
10.1	94.	17.
12.6	83.	19.
17.3	83.	11.
32.6	54.2	4.0
37.6	52.7	3.9
50.1	32.0	2.7
62.7	32.6	2.4
67.7	29.6	2.2
72.8	23.3	2.1
80.3	10.8	1.3
90.2	7.9	1.3

EX= 5.039 MEV/J=1

THETA	SIGMA	ERROR
12.6	118.	21.
17.5	101.	11.
32.6	82.2	3.8
37.6	43.5	3.5
40.2	42.0	2.9
50.1	32.5	2.8
62.7	30.0	2.3
67.7	23.5	2.0
72.8	20.9	1.9
80.3	13.8	1.4
90.2	9.8	1.5

EX= 5.053 MEV/J=1

THETA	SIGMA	ERROR
10.1	46.	14.
17.5	67.7	9.8
32.6	35.7	3.2
37.6	27.4	2.8
40.2	17.3	1.9
50.1	15.3	1.7
62.7	15.7	1.7
67.7	14.3	1.5
72.8	13.8	1.4
80.3	10.1	1.2
90.2	6.8	1.2
100.2	12.9	2.2

KEY; FOR J=1,2,OR 3, CROSS SECTION UNITS ARE MICRO-, 100 MICRO-, OR MILLI-BARNS/STERADIAN, RESPECTIVELY.

EX= 5.081 MEV/J=1		
THETA	SIGMA	ERROR
10.1	113.	13.
12.6	273.	25.
17.5	299.	17.
32.6	96.2	5.1
37.6	64.3	4.1
40.2	76.5	3.9
50.1	58.9	3.7
62.7	56.3	3.1
67.7	33.4	2.4
72.8	33.5	2.4
80.3	31.4	2.2
90.2	13.8	1.7

EX= 5.117 MEV/J=1		
THETA	SIGMA	ERROR
10.1	31.	13.
17.5	20.5	7.4
32.6	25.4	2.8
40.2	15.2	1.8
50.1	11.1	2.0
62.7	6.0	1.4
67.7	7.2	1.1
80.3	5.15	.88

EX= 5.120 MEV/J=1		
THETA	SIGMA	ERROR
12.6	108.	17.
17.5	124.	13.
27.7	71.1	8.7
32.6	47.7	5.7
40.2	29.8	2.5
50.1	23.9	2.4
62.7	21.0	1.9
67.7	13.6	1.5
72.8	4.5	1.1
80.3	7.6	1.1
100.2	10.3	1.9

EX= 5.156 MEV/J=1		
THETA	SIGMA	ERROR
10.1	11.2	9.2
12.6	27.	14.
32.6	8.7	2.2
40.2	10.8	1.5
50.1	8.5	1.8
62.7	8.5	1.2
67.7	6.3	1.0
72.8	2.4	1.0
80.3	4.24	.80

EX= 5.177 MEV/J=1		
THETA	SIGMA	ERROR
10.1	163.	18.
12.6	245.	24.
17.5	340.	17.
27.7	256.	12.
32.6	130.3	5.7
37.6	87.8	3.9
40.2	61.9	3.5
50.1	76.9	4.0
62.7	33.1	2.7
67.7	41.9	2.9
72.8	38.8	2.7
80.3	16.1	1.6
100.2	14.4	2.3

EX= 5.193 MEV/J=1		
THETA	SIGMA	ERROR
12.6	133.	19.
17.5	94.3	9.8
27.7	81.1	7.2
32.6	45.3	3.5
37.6	34.1	3.2
40.2	48.3	3.1
50.1	20.7	2.6
62.7	22.2	1.9
67.7	15.0	1.9
72.8	17.4	1.9
80.3	11.5	1.3
100.2	6.6	2.2

EX= 5.217 MEV/J=1		
THETA	SIGMA	ERROR
10.1	85.	17.
12.6	156.	20.
17.5	105.	11.
40.2	48.9	3.2
50.1	21.7	2.3
62.7	21.2	2.4
67.7	14.3	1.8
72.8	19.8	2.0
80.3	15.0	1.5
100.2	8.1	2.4

EX= 5.245 MEV/J=1		
THETA	SIGMA	ERROR
10.1	39.	12.
12.6	105.	20.
27.7	99.5	8.2
37.6	26.7	3.0
40.2	28.8	2.4
50.1	31.8	2.9
72.8	15.3	1.8
80.3	9.1	1.2
100.2	4.8	1.9

EX= 5.267 MEV/J=1		
THETA	SIGMA	ERROR
10.1	26.	13.
12.6	49.	16.
17.5	71.8	9.4
27.7	99.0	8.4
37.6	25.8	3.1
40.2	32.9	2.6
50.1	34.0	3.1
62.7	21.3	1.9
67.7	13.0	1.5
72.8	12.6	1.7
80.3	6.36	.98
100.2	4.4	1.8

EX= 5.290 MEV/J=1		
THETA	SIGMA	ERROR
12.6	119.	21.
17.5	101.	10.
27.7	65.3	7.4
37.6	19.9	2.7
40.2	27.6	2.4
50.1	19.8	2.5
62.7	20.1	1.9
67.7	19.1	1.8
72.8	6.4	1.2
80.3	9.1	1.2

EX= 5.310 MEV/J=1		
THETA	SIGMA	ERROR
10.1	59.	15.
12.6	136.	19.
17.5	175.	13.
27.7	196.	11.
37.6	63.7	4.1
40.2	64.8	3.6
50.1	46.0	3.2
62.7	56.1	3.1
67.7	32.6	2.3
72.8	17.6	1.7
80.3	17.4	1.6

EX= 5.321 MEV/J=1		
THETA	SIGMA	ERROR
10.1	47.	13.
12.6	48.	15.
17.5	113.	10.
27.7	151.1	9.8
37.6	36.5	3.1
40.2	53.2	3.3
50.1	51.3	3.3
62.7	32.2	2.3
67.7	27.0	2.1
72.8	17.6	1.7
80.3	17.9	1.6
100.2	11.0	2.9

EX= 5.336 MEV/J=1		
THETA	SIGMA	ERROR
10.1	33.	13.
12.6	61.	16.
17.5	113.	10.
27.7	198.	11.
37.6	57.5	3.9
40.2	65.1	3.6
50.1	53.6	3.4
62.7	46.2	2.8
67.7	25.3	2.1
72.8	26.7	2.2
80.3	23.6	1.9
100.2	12.9	3.0

EX= 5.352 MEV/J=1		
THETA	SIGMA	ERROR
10.1	43.	14.
12.6	115.	20.
17.5	195.	13.
27.7	186.	11.
37.6	70.2	4.3
40.2	73.1	3.9
50.1	69.6	3.8
62.7	41.8	2.7
67.7	34.3	2.7
72.8	21.9	2.0
80.3	18.3	1.7
100.2	15.5	2.4

EX= 5.369 MEV/J=1		
THETA	SIGMA	ERROR
10.1	79.	16.
12.6	103.	21.
17.5	109.	11.
27.7	110.6	9.1
32.6	59.6	6.2
37.6	82.5	4.6
40.2	95.0	4.4
50.1	46.6	3.2
62.7	42.5	2.7
67.7	31.1	2.3
72.8	24.8	2.2
80.3	17.1	1.6
100.2	12.1	2.1

EX= 5.383 MEV/J=1		
THETA	SIGMA	ERROR
10.1	32.	11.
12.6	50.	15.
17.5	88.5	6.7
27.7	18.4	5.6
32.6	13.6	2.6
40.2	11.2	1.5
62.7	11.1	1.4
67.7	5.7	1.3
72.8	4.3	1.1
80.3	5.15	.88
90.2	7.4	1.3
100.2	7.7	1.7

EX= 5.402 MEV/J=1		
THETA	SIGMA	ERROR
17.5	10.3	7.5
27.7	35.3	6.2
32.6	19.0	3.0
37.6	12.0	2.3
40.2	18.7	1.9
62.7	19.1	1.8
67.7	7.0	1.1
72.8	7.6	1.4
80.3	5.91	.95
90.2	7.0	1.2
100.2	4.4	1.9

EX= 5.428 MEV/J=1		
THETA	SIGMA	ERROR
10.1	25.	11.
12.6	63.	18.
17.5	84.1	9.2
27.7	155.	10.
32.6	63.8	4.4
37.6	44.4	3.5
40.2	48.9	3.2
50.1	30.2	2.9
62.7	24.2	2.0
67.7	13.8	1.5
72.8	12.6	1.4
80.3	8.3	1.1
90.2	6.3	1.2

KEY: FOR J=1,2,OR 3, CROSS SECTION UNITS ARE MICRO-, 100 MICRO-, OR MILLI-BARNS/STERADIAN, RESPECTIVELY.

EX= 5.440 MEV/U=1		
THETA	SIGMA	ERROR
10.1	80.	15.
12.6	74.	16.
17.5	175.	13.
27.7	121.2	8.8
32.6	73.4	4.7
37.6	60.8	4.0
40.2	64.2	3.6
50.1	37.6	3.1
62.7	34.3	2.4
67.7	25.5	2.1
72.8	22.2	1.9
80.3	17.9	1.6
90.2	10.1	1.5

EX= 5.454 MEV/U=1		
THETA	SIGMA	ERROR
10.1	25.	10.
12.6	34.	16.
17.5	44.4	9.0
27.7	33.2	5.6
40.2	27.2	2.4
62.7	11.3	1.4
67.7	8.7	1.2
72.8	11.1	1.6
80.3	7.9	1.1
90.2	4.16	.95

EX= 5.474 MEV/U=1		
THETA	SIGMA	ERROR
10.1	52.	14.
12.6	60.	16.
17.5	108.	12.
27.7	72.7	7.8
32.6	40.8	3.9
40.2	47.1	3.1
50.1	25.3	2.7
62.7	28.1	2.2
67.7	21.0	1.9
80.3	11.1	1.3
90.2	5.7	1.1

EX= 5.487 MEV/U=1		
THETA	SIGMA	ERROR
10.1	277.	18.
12.6	339.	25.
17.5	174.	13.
27.7	150.6	9.8
32.6	68.1	4.5
40.2	46.9	3.1
50.1	40.5	3.1
62.7	27.6	2.2
67.7	21.3	1.9
72.8	17.7	1.9
80.3	18.3	1.7
90.2	9.2	1.4
100.2	10.7	2.0

EX= 5.501 MEV/U=1		
THETA	SIGMA	ERROR
10.1	55.	14.
17.5	61.5	8.7
27.7	66.9	6.8
32.6	60.9	4.5
40.2	33.7	2.6
50.1	18.8	2.2
62.7	18.4	2.3
67.7	17.3	1.7
72.8	18.5	1.9
80.3	7.1	1.0
100.2	3.7	1.7

EX= 5.524 MEV/U=1		
THETA	SIGMA	ERROR
10.1	43.	13.
17.5	119.	11.
27.7	93.8	7.9
32.6	68.7	4.7
40.2	61.5	3.5
50.1	94.3	4.6
62.7	37.2	2.5
67.7	23.3	2.0
80.3	14.8	1.5
90.2	9.4	1.4

EX= 5.537 MEV/U=1		
THETA	SIGMA	ERROR
10.1	52.	14.
12.6	110.	24.
17.5	76.6	9.7
32.6	47.3	3.9
40.2	35.0	2.7
67.7	17.1	1.7
72.8	17.7	1.9
80.3	8.8	1.2
90.2	7.0	1.2

EX= 5.548 MEV/U=1		
THETA	SIGMA	ERROR
17.5	60.2	9.7
27.7	66.9	7.2
32.6	16.3	3.1
40.2	26.2	2.3
50.1	49.2	3.4
62.7	54.3	3.0
67.7	21.8	1.9
72.8	12.9	1.6
80.3	13.2	1.4
90.2	8.8	1.4

EX= 5.569 MEV/U=1		
THETA	SIGMA	ERROR
10.1	73.	15.
12.6	74.	23.
17.5	119.	12.
27.7	122.2	9.5
32.6	58.7	4.5
40.2	37.0	4.1
50.1	48.2	3.5
62.7	24.2	2.0
67.7	25.5	2.1
72.8	18.2	1.9
80.3	12.1	1.4

EX= 5.584 MEV/U=1		
THETA	SIGMA	ERROR
10.1	91.	16.
17.5	80.0	9.6
27.7	139.1	9.8
32.6	57.6	4.2
40.2	50.3	5.1
50.1	34.3	2.9
62.7	35.0	2.4
67.7	18.1	1.7
80.3	10.8	1.3

EX= 5.598 MEV/U=1		
THETA	SIGMA	ERROR
10.1	258.	18.
12.6	334.	24.
17.5	248.	15.
27.7	166.	10.
32.6	81.9	4.9
50.1	43.9	3.2
62.7	35.1	2.4
67.7	23.8	2.0
72.8	21.1	2.0
80.3	16.7	1.6
90.2	10.3	1.5

EX= 5.614 MEV/U=1		
THETA	SIGMA	ERROR
10.1	182.	12.
12.6	155.	23.
17.5	180.	14.
27.7	143.3	9.8
32.6	61.8	4.6
50.1	35.4	3.1
62.7	30.5	2.9
67.7	17.8	1.7
72.8	17.9	1.9
80.3	13.5	1.4
90.2	5.7	1.1

EX= 5.648 MEV/U=1		
THETA	SIGMA	ERROR
10.1	64.	16.
12.6	118.	20.
17.5	137.	14.
22.6	77.	12.
27.7	61.6	8.6
32.6	57.6	4.6
37.6	39.2	4.3
50.1	36.6	3.4
62.7	19.6	2.4
72.8	21.3	2.1
80.3	10.8	1.3
90.2	7.2	1.3

EX= 5.668 MEV/U=1		
THETA	SIGMA	ERROR
10.1	50.	15.
12.6	62.	18.
17.5	55.	10.
27.7	50.0	6.9
32.6	16.1	3.0
37.6	10.1	3.0
50.1	8.4	2.6
57.7	12.0	1.4
72.8	15.3	1.8
80.3	8.9	1.2

EX= 5.689 MEV/U=1		
THETA	SIGMA	ERROR
10.1	242.	20.
12.6	310.	26.
17.5	209.	15.
22.6	86.	11.
32.6	85.7	5.1
37.6	59.7	5.0
50.1	35.0	3.0
62.7	47.9	2.9
67.7	33.6	2.4
72.8	19.3	2.0
80.3	15.4	1.5
90.2	19.0	2.0
100.2	9.9	1.9

EX= 5.720 MEV/U=1		
THETA	SIGMA	ERROR
10.1	307.	21.
12.6	417.	28.
17.5	286.	16.
22.6	159.	14.
27.7	202.	10.
32.6	91.7	5.3
37.6	33.0	3.7
50.1	23.2	2.9
62.7	43.3	2.7
67.7	25.8	2.1
72.8	20.1	2.1
80.3	17.0	1.6
90.2	13.1	1.7
100.2	8.8	2.3

EX= 5.735 MEV/U=1		
THETA	SIGMA	ERROR
10.1	102.	15.
12.6	158.	22.
17.5	129.	11.
27.7	76.9	8.0
32.6	35.3	3.6
37.6	16.2	3.1
40.2	7.9	3.6
50.1	17.1	3.1
62.7	18.8	1.8
67.7	11.8	1.4
72.8	17.5	2.0
80.3	13.0	1.4
90.2	5.0	1.1

EX= 5.765 MEV/U=1		
THETA	SIGMA	ERROR
17.5	96.	10.
27.7	98.5	7.2
32.6	41.7	5.1
37.6	26.7	3.8
40.2	39.6	3.8
50.1	12.1	2.4
62.7	12.1	2.1
67.7	18.3	2.2
72.8	11.1	1.8
80.3	6.06	.96
100.2	5.2	2.0

KEY: FOR U=1,2,OR 3, CROSS SECTION UNITS ARE MICRO-, 100 MICRO-, OR MILLI-BARNS/STERADIAN, RESPECTIVELY.

EX= 5.803 MEV;J=1

THETA	SIGMA	ERROR
13.6	28.	18.
27.7	49.5	6.9
32.6	25.9	3.3
37.6	25.6	4.1
40.2	22.5	3.7
50.1	6.8	2.6
62.7	7.7	1.9
72.3	4.5	1.2
80.3	8.2	1.1

EX= 5.822 MEV;J=1

THETA	SIGMA	ERROR
10.1	54.	16.
12.6	129.	22.
17.5	111.	12.
22.6	132.	13.
27.7	122.2	9.8
32.6	64.7	4.6
37.6	50.3	4.6
40.2	65.4	4.6
50.1	43.6	3.3
62.7	26.3	2.9
67.7	27.6	2.1
72.8	18.5	2.3
80.3	22.6	1.8

EX= 5.840 MEV;J=1

THETA	SIGMA	ERROR
10.1	55.	16.
12.6	164.	27.
17.5	165.	14.
22.6	91.	11.
27.7	144.	10.
32.6	61.8	4.5
37.6	37.2	4.0
40.2	44.9	4.1
50.1	49.1	3.5
62.7	21.7	2.5
67.7	28.3	2.2
72.8	23.0	2.2
80.3	15.6	1.5

EX= 5.858 MEV;J=1

THETA	SIGMA	ERROR
10.1	16.	13.
17.5	51.	11.
22.6	34.5	8.1
32.6	34.8	4.0
40.2	28.0	3.5
62.7	17.7	2.6
67.7	13.5	1.9
72.8	7.2	1.6
80.3	10.8	1.3

EX= 5.897 MEV;J=1

THETA	SIGMA	ERROR
10.1	33.	16.
12.6	64.	18.
17.5	58.	11.
27.7	42.7	7.7
32.6	34.6	3.9
40.2	27.8	3.1
52.7	11.4	2.1
67.7	11.6	1.4
72.8	15.6	2.0
80.3	9.8	1.2
90.2	4.38	.98
100.2	5.5	2.2

EX= 5.915 MEV;J=1

THETA	SIGMA	ERROR
10.1	63.	16.
12.6	48.	17.
17.5	45.	10.
22.6	28.1	7.9
27.7	21.6	6.4
37.6	16.0	3.3
62.7	9.7	2.0
67.7	12.1	1.4
72.8	9.3	1.7
80.3	6.36	.96
100.2	6.6	1.9

EX= 5.934 MEV;J=1

THETA	SIGMA	ERROR
10.1	141.	18.
12.6	201.	26.
17.5	326.	20.
22.6	168.	14.
27.7	150.	11.
32.6	107.6	5.7
37.6	68.2	5.1
50.1	84.2	4.4
62.7	38.6	3.2
67.7	37.9	2.5
72.8	26.1	2.5
80.3	21.8	1.8

EX= 5.952 MEV;J=1

THETA	SIGMA	ERROR
10.1	43.	15.
12.6	53.	19.
17.5	83.	11.
22.6	78.	11.
27.7	73.7	8.8
32.6	33.9	3.5
37.6	44.2	4.3
40.2	54.8	3.8
50.1	48.2	3.5
62.7	33.8	3.1
67.7	30.9	2.3
80.3	16.8	1.6

EX= 5.969 MEV;J=1

THETA	SIGMA	ERROR
10.1	71.	16.
12.6	77.	20.
17.5	68.	13.
22.6	68.	11.
27.7	84.8	9.6
32.6	64.7	4.6
37.6	44.9	4.3
40.2	56.4	3.9
50.1	24.9	2.7
62.7	25.2	2.6
67.7	24.9	2.0
72.8	7.9	1.4

EX= 5.998 MEV;J=1

THETA	SIGMA	ERROR
10.1	90.	16.
12.6	131.	24.
17.5	119.	13.
22.6	139.	15.
27.7	84.8	9.6
32.6	45.5	3.9
37.6	37.4	4.6
50.1	35.2	3.1
62.7	28.1	2.7
67.7	25.3	2.1
80.3	19.4	1.7
90.2	13.8	1.7

EX= 6.010 MEV;J=1

THETA	SIGMA	ERROR
12.6	60.	19.
17.5	44.	10.
32.6	20.3	3.3
37.6	26.9	3.7
40.2	40.4	3.4
50.1	12.0	2.3
62.7	15.4	2.2
72.8	17.9	2.1
80.3	12.0	1.3

EX= 6.031 MEV;J=1

THETA	SIGMA	ERROR
10.1	31.	14.
12.6	27.	20.
17.5	40.	11.
27.7	23.5	5.0
32.6	15.6	2.9
37.6	25.3	3.9
40.2	34.5	3.3
50.1	32.3	3.1
62.7	12.3	2.1
67.7	17.3	1.7
72.8	17.7	2.1
80.3	13.4	1.7
90.2	9.3	1.3

EX= 6.041 MEV;J=1

THETA	SIGMA	ERROR
12.6	72.	19.
17.5	66.	12.
22.6	36.8	9.2
27.7	22.6	7.4
32.6	21.4	3.5
37.6	16.8	3.3
40.2	20.3	2.6
50.1	9.4	2.2
62.7	13.6	2.2
67.7	17.1	1.7
72.8	16.9	2.1
80.3	7.9	1.1
90.2	6.6	1.2

EX= 6.064 MEV;J=1

THETA	SIGMA	ERROR
37.6	6.1	2.7
40.2	10.1	2.4
62.7	7.8	1.9
67.7	12.5	1.4
72.8	6.1	1.5
80.3	6.8	1.0
90.2	6.1	1.2

EX= 6.073 MEV;J=1

THETA	SIGMA	ERROR
12.6	86.	20.
17.5	90.	11.
22.6	91.	13.
27.7	72.6	9.8
32.6	63.4	5.1
37.6	27.1	4.1
40.2	40.2	3.8
62.7	18.8	2.4
67.7	22.5	1.9
80.3	13.5	1.4

EX= 6.090 MEV;J=1

THETA	SIGMA	ERROR
17.5	10.9	7.0
32.6	17.8	3.2
40.2	20.3	2.8
50.1	10.8	3.1
62.7	11.4	2.2
67.7	12.3	1.4
72.8	14.5	1.9
80.3	3.94	.77
90.2	8.3	1.3

EX= 6.105 MEV;J=1

THETA	SIGMA	ERROR
10.1	52.	16.
12.6	98.	23.
17.5	98.	12.
22.6	78.	12.
27.7	77.9	9.4
32.6	23.9	3.4
40.2	23.3	3.2
50.1	22.7	2.7
62.7	12.8	2.3
67.7	13.3	1.5
72.8	10.0	1.8
80.3	12.6	1.4

EX= 6.146 MEV;J=1

THETA	SIGMA	ERROR
17.5	23.	10.
27.7	20.5	6.8
32.6	13.4	3.2
37.6	15.8	3.3
40.2	18.7	3.0
50.1	8.7	2.6
80.3	11.3	1.3

KEY; FOR J=1,2,OR 3, CROSS SECTION UNITS ARE MICRO-, 100 MICRO-, OR MILLI-BARNS/STERADIAN, RESPECTIVELY.

EX= 5.170 MEV/U=1

THETA	SIGMA	ERROR
10.1	28.	13.
17.5	42.	11.
22.6	29.5	8.2
27.7	49.5	8.7
32.6	28.8	4.1
37.6	21.4	3.8
40.2	27.0	3.5
62.7	14.0	2.5
67.7	9.3	1.8
72.8	12.7	1.9
80.3	11.7	1.3
100.2	12.5	2.1

EX= 6.188 MEV/U=1

THETA	SIGMA	ERROR
10.1	35.	13.
17.5	74.	12.
22.6	60.	10.
27.7	65.8	9.6
32.6	41.7	4.4
37.6	27.1	3.6
40.2	35.9	3.5
62.7	33.3	3.2
67.7	16.8	2.1
72.8	15.9	2.0
80.3	15.9	1.6
90.2	19.0	2.0
100.2	21.4	2.8

EX= 6.228 MEV/U=1

THETA	SIGMA	ERROR
27.7	17.9	7.3
32.6	6.5	2.9
37.6	5.9	2.9
40.2	8.3	2.7
62.7	10.2	2.6
67.7	8.0	1.7
72.8	12.7	2.0
80.3	10.6	1.3
90.2	6.8	1.2
100.2	10.3	1.9

EX= 6.251 MEV/U=1

THETA	SIGMA	ERROR
10.1	34.	15.
22.6	35.3	3.5
27.7	39.0	8.0
32.6	14.3	3.0
37.6	20.3	3.5
40.2	26.4	3.3
62.7	24.2	3.1
67.7	13.0	2.0
80.3	18.8	1.7
90.2	6.3	1.2

EX= 6.262 MEV/U=1

THETA	SIGMA	ERROR
10.1	21.	16.
22.6	39.6	8.7
27.7	36.9	6.9
32.6	29.0	3.9
40.2	18.5	2.9
72.8	14.3	1.9
80.3	8.2	1.1
90.2	9.0	1.4
100.2	11.0	2.6

EX= 6.274 MEV/U=1

THETA	SIGMA	ERROR
10.1	100.	18.
17.5	109.	13.
22.6	65.	10.
27.7	94.	10.
32.6	35.0	4.0
37.6	28.7	3.9
40.2	32.5	3.7
62.7	11.4	2.7
67.7	6.0	1.6
72.8	8.2	1.6
80.3	14.7	1.5
90.2	7.7	1.3

EX= 6.310 MEV/U=1

THETA	SIGMA	ERROR
10.1	35.	16.
12.6	91.	20.
22.6	70.	11.
27.7	35.8	7.3
32.6	33.5	4.3
37.6	24.9	3.6
40.2	21.1	3.4
62.7	18.9	2.9
67.7	8.3	1.7
80.3	14.5	1.5
90.2	9.5	1.1

EX= 6.332 MEV/U=1

THETA	SIGMA	ERROR
10.1	56.	17.
12.6	128.	21.
22.6	85.	12.
27.7	64.3	9.0
32.6	29.7	3.9
37.6	26.0	3.5
40.2	37.3	4.2
62.7	20.1	2.9
67.7	18.5	2.4
80.3	14.2	1.5
90.2	11.2	1.6
100.2	7.0	2.1

EX= 6.360 MEV/U=1

THETA	SIGMA	ERROR
12.6	86.	20.
17.5	74.	11.
27.7	77.9	9.7
32.6	41.9	4.5
37.6	29.5	3.7
40.2	37.0	4.0
62.7	24.5	2.9
67.7	12.1	2.0
72.8	7.7	1.5
80.3	10.5	1.3

EX= 6.381 MEV/U=1

THETA	SIGMA	ERROR
10.1	28.	12.
12.6	32.	17.
17.3	54.	11.
27.7	27.4	7.8
32.6	21.0	3.6
37.6	16.2	3.1
40.2	13.4	3.3
50.1	9.7	3.0
67.7	5.0	1.6
72.8	7.6	1.9
80.3	10.1	1.2

EX= 6.402 MEV/U=1

THETA	SIGMA	ERROR
10.1	95.	19.
12.6	131.	25.
17.5	94.	13.
22.6	50.	10.
27.7	60.6	8.9
32.6	39.7	4.6
37.6	27.3	3.7
40.2	30.0	3.8
50.1	20.5	3.3
62.8	14.5	2.6
67.7	11.1	1.9
80.3	15.1	1.6
90.2	10.5	1.5

EX= 6.449 MEV/U=1

THETA	SIGMA	ERROR
10.1	63.	16.
17.5	77.	12.
27.7	58.4	9.2
32.6	42.4	5.0
37.6	30.4	4.0
40.2	24.2	3.9
62.8	12.5	2.5
67.7	4.8	1.5
90.2	7.2	1.3
100.2	9.6	2.7

EX= 6.483 MEV/U=1

THETA	SIGMA	ERROR
10.1	42.	15.
12.6	70.	20.
17.5	71.	12.
22.6	69.	12.
32.6	32.1	4.3
37.6	23.8	3.6
40.2	13.2	3.5
67.7	5.2	2.0
80.3	5.45	.91
90.2	4.6	1.0

EX= 6.547 MEV/U=1

THETA	SIGMA	ERROR
10.1	55.	15.
12.6	43.	24.
17.5	107.	13.
27.7	59.5	7.3
32.6	34.8	4.3
37.6	29.1	4.1
50.1	15.9	2.8
67.7	13.3	2.2
72.8	10.9	1.8
80.3	11.2	1.3
90.2	9.6	1.5
100.2	8.1	2.5

EX= 6.687 MEV/U=1

THETA	SIGMA	ERROR
17.5	62.	11.
22.6	40.	12.
32.6	24.1	3.9
37.6	20.1	3.2
40.2	20.5	3.6
50.1	16.7	3.0
62.8	8.0	2.1
72.8	4.5	1.5

EX= 6.654 MEV/U=1

THETA	SIGMA	ERROR
12.6	69.	24.
17.3	58.	11.
22.6	45.	13.
27.7	32.1	6.3
37.6	41.1	4.0
40.2	38.4	3.8
50.1	15.5	2.8
62.8	9.4	2.3
67.7	12.1	2.2
80.3	18.5	1.7
90.2	11.6	1.6
100.2	6.6	2.2

EX= 6.670 MEV/U=1

THETA	SIGMA	ERROR
10.1	38.	15.
18.6	92.	18.
17.5	101.	14.
27.7	11.6	5.3
32.6	14.9	3.2
37.6	21.4	3.0
40.2	30.2	3.6
50.1	18.6	2.9
62.8	14.5	2.6
67.7	4.2	1.3
72.8	2.3	1.4
80.3	8.3	1.1
90.2	6.8	1.2
100.2	5.2	2.2

EX= 6.716 MEV/U=1

THETA	SIGMA	ERROR
12.6	46.	28.
17.5	96.	13.
22.6	88.	12.
37.6	40.5	4.5
40.2	42.2	4.3
50.1	32.6	3.3
62.8	23.4	3.0
67.7	18.6	2.6
80.3	6.7	1.7
90.2	13.3	1.7
100.2	11.4	2.1

KEY: FOR J=1,2,OR 3, CROSS SECTION UNITS ARE MICRO-, 100 MICRO-, OR MILLI-BARNS/STERADIAN, RESPECTIVELY.

EX= 6.762 MEV/J=1		
THETA	SIGMA	ERROR
10.1	19.	15.
12.6	46.	18.
17.5	39.	11.
27.7	59.0	8.2
37.6	41.3	4.1
40.2	19.9	3.2
50.1	5.0	2.5
62.8	7.8	2.6
67.7	16.3	2.5
100.2	9.2	1.8

EX= 6.788 MEV/J=1		
THETA	SIGMA	ERROR
10.1	34.	14.
17.5	17.1	7.9
27.7	35.8	7.0
32.6	20.0	4.2
37.6	31.9	4.0
40.2	15.6	2.8
67.7	7.2	1.9
80.3	17.0	1.6
90.2	9.0	1.4
100.2	6.3	2.4

EX= 6.864 MEV/J=1		
THETA	SIGMA	ERROR
10.1	109.	19.
12.6	45.	22.
22.6	45.	11.
32.6	18.7	3.6
62.8	6.0	2.2
67.7	6.3	1.9
90.2	5.3	1.1

EX= 6.912 MEV/J=1		
THETA	SIGMA	ERROR
27.7	41.1	7.2
32.6	23.6	3.9
40.2	33.7	3.8
50.1	11.4	2.7
62.8	15.7	2.7
67.7	12.3	2.2
80.3	5.6	1.4
90.2	7.7	1.3

EX= 6.939 MEV/J=1		
THETA	SIGMA	ERROR
10.1	18.	12.
17.5	38.	11.
22.6	37.4	9.1
27.7	15.8	5.7
32.6	6.9	3.2
50.1	5.6	2.4
67.7	5.0	1.5
80.3	5.0	1.5
90.2	7.2	1.3

EX= 6.953 MEV/J=1		
THETA	SIGMA	ERROR
10.1	45.	14.
27.7	44.8	8.1
32.6	18.3	3.7
50.1	6.0	2.4
62.8	5.8	2.2
80.3	3.48	.73
90.2	6.6	1.2
100.2	5.2	1.9

EX= 7.048 MEV/J=1		
THETA	SIGMA	ERROR
17.5	15.7	9.7
27.7	11.1	5.4
37.6	7.7	2.3
50.1	5.1	2.1
62.8	4.4	2.1
67.7	8.5	2.2
80.3	6.8	1.0
90.2	6.1	1.2
100.2	4.8	1.9

KEY: FOR J=1,2,OR 3, CROSS SECTION UNITS ARE MICRO-, 100 MICRO-, OR MILLI-BARNS/STERADIAN, RESPECTIVELY.

APPENDIX V

^{209}Bi Angular Distributions

APPENDIX V ^{209}Bi Angular Distributions

EX= .000 MEV U=3			EX= 1.608 MEV U=1		
THETA	SIGMA	ERROR	THETA	SIGMA	ERROR
12.1	52490.	3631.	20.1	271.	52.
16.1	15320.	977.	24.1	262.	49.
20.1	5449.	115.	26.1	313.	42.
24.1	2088.	42.	28.1	277.	41.
26.1	1289.	29.	30.1	157.	30.
28.1	844.	16.	32.2	184.	21.
30.1	551.0	9.3	36.2	118.	16.
32.1	364.2	5.1	38.2	83.8	9.5
36.2	183.2	2.2	40.2	80.2	6.5
38.2	164.7	1.3	48.2	84.6	7.6
40.2	57.80	.99	56.2	84.4	4.6
42.2	153.2	1.2	58.2	39.1	2.5
44.2	137.0	1.2	60.2	48.1	3.0
46.2	115.5	1.0	62.3	41.3	4.3
48.2	81.36	.69	64.3	33.0	5.2
50.2	52.05	.28	66.3	39.1	3.0
52.2	28.95	.14	68.3	37.1	3.6
54.2	15.96	.10	70.3	29.5	3.1
56.2	1.260	.073	72.3	27.5	2.4
58.2	3.450	.060	80.3	27.7	2.6
60.2	7.980	.090	82.3	27.1	1.8
62.2	22.78	.14	84.3	29.1	2.0
64.3	24.33	.21	86.3	30.6	2.1
66.3	22.98	.11	88.3	19.4	1.9
68.3	18.94	.13	92.3	15.1	2.1
70.3	3.610	.081	96.3	10.8	1.3
72.3	8.537	.050	100.3	10.92	.78
80.3	2.892	.031			
82.3	4.165	.024			
84.3	5.164	.025			
86.3	5.670	.031			
88.3	5.310	.033			
92.3	3.690	.041			
96.3	1.574	.015			
100.3	.724	.006			

KEY: FOR U=1,2,OR 3, CROSS SECTION UNITS ARE MICRO-, 100 MICRO-, OR MILLI-BARNS/STERADIAN, RESPECTIVELY.

Ex= .896 MEV;J=1

THETA	SIGMA	ERROR
22.6	47.	11.
27.7	25.	11.
50.4	8.5	1.7
63.0	16.3	2.7
67.7	19.7	2.9
72.6	11.3	2.0
80.2	8.2	1.7
90.1	6.8	1.5
100.2	2.38	.90

Ex= 2.492 MEV;J=1

THETA	SIGMA	ERROR
17.5	83.	11.
22.6	227.	14.
27.7	279.	19.
32.5	183.	13.
38.6	69.6	7.4
40.4	49.1	5.0
50.4	71.3	4.0
63.0	45.0	6.5
72.6	31.2	3.3
80.2	23.8	2.9
90.1	12.6	2.1
100.2	6.5	1.5

Ex= 2.564 MEV;J=1

THETA	SIGMA	ERROR
10.1	87.	23.
12.6	99.	22.
17.5	316.	18.
22.6	747.	23.
27.7	1000.	36.
32.5	734.	24.
38.6	318.	13.
40.4	198.1	8.1
50.4	388.7	7.9
67.7	106.6	6.8
72.6	107.0	6.2
80.2	88.2	5.5
90.1	54.3	4.3
100.2	31.6	3.3

Ex= 2.581 MEV;J=1

THETA	SIGMA	ERROR
10.1	63.	23.
12.6	129.	23.
17.5	263.	17.
22.6	649.	21.
27.7	907.	34.
32.5	644.	22.
38.6	184.	10.
40.4	109.6	5.9
50.4	225.5	6.6
67.7	90.8	6.3
72.6	83.6	7.1
80.2	56.2	4.4
90.1	45.8	4.0
100.2	17.0	2.4

Ex= 2.589 MEV;J=3

THETA	SIGMA	ERROR
10.1	.124	.023
12.6	.265	.026
17.5	.756	.027
22.6	1.789	.035
27.7	2.509	.056
32.5	1.657	.035
38.6	.742	.020
40.4	.583	.013
50.4	.814	.012
67.7	.270	.011
72.6	.251	.012
80.2	.235	.009
90.1	.117	.006
100.2	.057	.004

Ex= 2.617 MEV;J=1

THETA	SIGMA	ERROR
10.1	25.	16.
12.6	41.	17.
17.5	218.	16.
22.6	501.	19.
27.7	712.	30.
32.5	438.	18.
38.6	152.7	9.4
40.4	167.0	7.4
50.4	122.9	4.9
67.7	65.8	5.4
72.6	49.6	4.2
80.2	38.1	3.6
90.1	36.5	3.5
100.2	11.9	2.0

Ex= 2.740 MEV;J=2

THETA	SIGMA	ERROR
10.1	.86	.21
12.6	1.89	.25
17.5	5.39	.24
22.6	11.12	.28
27.7	14.87	.44
32.5	8.96	.26
38.6	3.88	.15
40.4	3.22	.10
50.4	4.173	.090
63.0	1.981	.098
67.7	1.601	.084
80.2	1.230	.065
90.1	.574	.044
100.2	.364	.035

Ex= 2.766 MEV;J=1

THETA	SIGMA	ERROR
22.6	58.7	7.4
27.7	46.	10.
32.5	35.0	6.3
38.6	23.0	5.2
40.4	15.3	3.0
50.4	8.4	1.7
67.7	10.5	2.1
80.2	5.8	1.4
90.1	3.1	1.0

Ex= 2.825 MEV;J=1

THETA	SIGMA	ERROR
10.1	154.	25.
12.6	99.	22.
17.5	181.	15.
22.6	250.	13.
27.7	148.	15.
32.5	47.0	7.1
38.6	64.1	7.9
40.4	63.1	5.2
50.4	31.9	2.9
80.2	18.4	2.5
90.1	11.3	2.0
100.2	6.1	1.4

Ex= 2.956 MEV;J=1

THETA	SIGMA	ERROR
12.6	47.	17.
17.5	35.4	9.2
22.6	58.0	7.3
27.7	62.	11.
32.5	37.3	6.8
38.6	28.5	6.1
50.4	18.4	2.4
67.7	6.1	1.6
72.6	5.7	1.4
80.2	5.1	1.3
90.1	4.4	1.2
100.2	3.1	1.0

Ex= 2.986 MEV;J=1

THETA	SIGMA	ERROR
10.1	66.	22.
17.5	58.	13.
22.6	61.3	7.4
27.7	61.	11.
32.5	76.1	8.6
38.6	102.2	8.9
40.4	76.2	5.5
50.4	34.7	3.0
67.7	15.8	2.6
72.6	13.1	2.2
80.2	12.6	2.1
90.1	8.9	1.7
100.2	4.8	2.4

Ex= 3.038 MEV;J=1

THETA	SIGMA	ERROR
12.6	23.	14.
22.6	24.1	5.9
27.7	24.7	7.8
32.5	42.5	7.2
38.6	35.1	5.1
40.4	27.7	3.8
50.4	15.4	2.2
72.6	3.9	1.2
90.1	4.1	1.2
100.2	3.1	2.0

Ex= 3.091 MEV;J=1

THETA	SIGMA	ERROR
10.1	26.	16.
12.6	34.	19.
22.6	44.3	7.0
27.7	59.3	9.7
32.5	41.8	6.7
38.6	30.5	6.2
40.4	30.8	4.0
50.4	16.9	2.4
63.0	7.8	2.3
72.6	8.1	1.7
80.2	9.9	1.8
90.1	6.8	1.5
100.2	5.8	1.4

Ex= 3.118 MEV;J=1

THETA	SIGMA	ERROR
18.6	21.	16.
22.6	26.1	4.9
32.5	27.6	5.8
40.4	21.4	2.5
72.6	11.7	2.0
90.1	3.4	1.1
100.2	3.1	1.0

Ex= 3.134 MEV;J=1

THETA	SIGMA	ERROR
10.1	107.	22.
12.6	173.	23.
22.6	239.	13.
27.7	258.	19.
32.5	236.	14.
38.6	213.	12.
40.4	174.7	7.7
50.4	111.0	4.9
63.0	84.1	4.5
72.6	40.4	3.8
80.2	41.5	3.8
90.1	22.2	2.8

Ex= 3.153 MEV;J=1

THETA	SIGMA	ERROR
10.1	104.	22.
12.6	121.	22.
22.6	147.	10.
27.7	152.	14.
32.5	188.	12.
38.6	210.	11.
40.4	159.2	7.2
50.4	76.7	4.0
63.0	59.7	3.7
67.7	25.9	4.6
72.6	30.1	3.3
80.2	21.6	2.7
90.1	20.8	2.7
100.2	11.9	2.0

Ex= 3.168 MEV;J=1

THETA	SIGMA	ERROR
10.1	78.	20.
12.6	90.	20.
22.6	112.2	9.4
27.7	138.	14.
32.5	154.	11.
38.6	115.2	8.6
40.4	129.8	6.7
50.4	62.2	3.7
63.0	29.8	2.8
67.7	21.0	3.9
80.2	16.3	2.4
90.1	13.3	2.1

Ex= 3.211 MEV;J=1

THETA	SIGMA	ERROR
10.1	20.	13.
12.6	40.	20.
22.6	64.6	7.9
27.7	77.	11.
32.5	72.3	8.7
38.6	83.1	7.9
40.4	68.2	5.6
50.4	27.5	2.6
63.0	20.6	2.9
67.7	14.0	2.9
80.2	12.3	2.0
90.1	11.3	2.0
100.2	5.1	1.3

KEY: FOR J=1,2,OR 3, CROSS SECTION UNITS ARE MICRO-, 100 MICRO-, OR MILLI-BARNS/STERADIAN, RESPECTIVELY.

Ex= 3.309 MEV,J=1

THETA	SIGMA	ERROR
22.6	26.7	5.7
27.7	24.7	8.2
32.5	14.9	6.2
50.4	7.8	1.6
90.1	3.4	1.1
100.2	3.1	1.0

Ex= 3.358 MEV,J=1

THETA	SIGMA	ERROR
10.1	47.	17.
12.6	36.	13.
22.6	17.6	5.4
27.7	27.2	5.8
32.5	14.2	5.5
38.6	9.5	4.6
80.2	4.8	1.3
90.1	4.1	1.2

Ex= 3.466 MEV,J=1

THETA	SIGMA	ERROR
10.1	63.	34.
12.6	71.	20.
22.6	80.2	8.7
27.7	68.	10.
32.5	50.7	8.2
38.6	68.6	7.8
40.4	60.5	5.2
50.4	27.3	2.8
63.0	20.0	2.7
67.7	22.4	3.1
90.1	6.5	1.3
100.2	4.4	1.2

Ex= 3.501 MEV,J=1

THETA	SIGMA	ERROR
12.6	28.	20.
27.7	24.7	7.2
32.5	11.9	5.4
38.6	14.0	4.8
40.4	13.4	3.3
63.0	10.0	2.1
67.7	9.2	2.0
80.2	7.8	1.6
90.1	2.39	.90
100.2	1.70	.76

Ex= 3.579 MEV,J=1

THETA	SIGMA	ERROR
12.6	39.	18.
17.5	23.3	9.1
22.6	22.8	5.3
27.7	34.6	8.2
32.5	25.4	6.0
38.6	19.5	4.9
40.4	21.1	3.8
50.4	8.0	1.8
63.0	7.8	1.8
67.7	9.6	2.1
80.2	7.5	1.6
100.2	2.38	.90

Ex= 3.597 MEV,J=1

THETA	SIGMA	ERROR
12.6	48.	17.
17.5	56.	11.
22.6	67.8	8.0
27.7	78.	12.
32.5	75.3	8.9
38.6	54.6	6.3
40.4	72.8	5.2
50.4	34.5	3.0
63.0	25.9	2.6
67.7	28.5	3.5
72.6	13.8	2.2
80.2	12.9	2.1
90.1	7.9	1.6
100.2	3.1	1.0

Ex= 3.633 MEV,J=1

THETA	SIGMA	ERROR
12.6	50.	18.
17.5	30.2	8.0
22.6	38.5	6.5
27.7	41.	10.
32.5	22.4	6.3
38.6	17.0	5.2
40.4	15.1	3.0
50.4	8.5	1.8
63.0	4.8	1.6
67.7	9.6	2.1
72.6	7.4	1.6
80.2	7.2	1.6
100.2	3.1	1.0

Ex= 3.685 MEV,J=1

THETA	SIGMA	ERROR
12.6	34.	17.
17.5	44.0	9.5
22.6	30.8	6.2
27.7	48.	11.
32.5	35.0	7.5
38.6	42.1	6.1
40.4	36.0	4.1
50.4	7.8	1.7
63.0	15.2	2.1
67.7	12.3	2.3
80.2	7.2	1.6
90.1	3.8	1.1

Ex= 3.703 MEV,J=1

THETA	SIGMA	ERROR
12.6	47.	18.
17.5	45.8	9.2
22.6	43.7	6.4
27.7	30.9	5.3
32.5	38.8	7.7
38.6	26.5	5.1
40.4	38.0	4.1
50.4	21.5	2.5
63.0	13.3	2.1
67.7	15.3	2.6
80.2	9.2	1.8
90.1	5.1	1.3

Ex= 3.765 MEV,J=1

THETA	SIGMA	ERROR
22.6	22.8	5.5
27.7	18.5	7.7
32.5	28.3	5.9
38.6	16.5	4.7
40.4	16.5	3.4
50.4	15.4	2.3
67.7	10.1	2.1
90.1	3.4	1.1
100.2	3.4	1.1

Ex= 3.803 MEV,J=1

THETA	SIGMA	ERROR
17.5	36.3	8.3
22.6	48.9	7.1
27.7	23.5	7.7
32.5	21.6	6.0
57.7	11.0	2.2
80.2	5.2	1.7
90.1	3.8	1.1
100.2	2.72	.96

Ex= 3.815 MEV,J=1

THETA	SIGMA	ERROR
10.1	54.	21.
17.5	94.	11.
22.6	88.0	8.7
27.7	75.	12.
32.5	62.6	8.4
38.6	51.1	6.8
40.4	74.8	5.5
50.4	65.0	3.8
63.0	52.8	3.7
67.7	35.1	3.9
80.2	16.3	2.4
90.1	10.2	1.9
100.2	5.8	1.4

Ex= 3.839 MEV,J=1

THETA	SIGMA	ERROR
12.6	39.	16.
17.5	15.1	5.2
27.7	13.6	7.7
32.5	12.7	4.0
40.4	10.3	2.3
63.0	7.0	1.9
67.7	7.0	1.8
90.1	3.4	1.1

Ex= 3.855 MEV,J=1

THETA	SIGMA	ERROR
10.1	25.	16.
17.5	14.7	6.5
27.7	21.0	5.1
32.5	17.2	6.0
38.6	8.0	3.2
40.4	6.3	2.6
50.4	10.8	1.4
63.0	9.1	1.3
67.7	7.0	1.8
80.2	8.5	1.7
90.1	2.05	.84
100.2	2.38	.90

Ex= 3.892 MEV,J=1

THETA	SIGMA	ERROR
10.1	65.	17.
17.5	20.7	7.4
22.6	17.0	4.6
38.6	7.0	4.6
50.4	10.8	1.9
63.0	3.7	2.1
100.2	3.4	1.1

Ex= 3.924 MEV,J=1

THETA	SIGMA	ERROR
10.1	29.	22.
12.6	40.	15.
22.6	35.9	6.0
27.7	51.9	3.0
32.5	30.6	4.8
38.6	16.5	4.5
40.4	20.3	2.4
63.0	8.2	1.9
67.7	7.9	1.9
100.2	3.4	1.1

Ex= 3.949 MEV,J=1

THETA	SIGMA	ERROR
10.1	34.	22.
22.6	30.0	5.7
27.7	35.8	9.3
32.5	34.3	7.2
40.4	11.1	2.8
50.4	16.3	2.2
63.0	11.3	2.2
67.7	7.9	1.9
72.6	8.5	1.7
80.2	7.5	1.6

Ex= 3.981 MEV,J=1

THETA	SIGMA	ERROR
10.1	283.	31.
12.6	287.	26.
17.5	637.	26.
22.6	845.	24.
27.7	355.	22.
32.5	128.	11.
38.6	177.	11.
40.4	232.3	8.9
50.4	126.6	5.2
63.0	85.2	4.6
67.7	69.4	5.5
72.6	56.0	4.5
80.2	22.5	4.7
100.2	16.3	2.4

KEY: FOR J=1,2,OR 3, CROSS SECTION UNITS ARE MICRO-, 100 MICRO-, OR MILLI-BARNS/STERADIAN, RESPECTIVELY.

EX= 4.013 MEV,J=1

THETA	SIGMA	ERROR
12.6	41.	13.
17.5	22.	13.
22.6	23.5	5.7
27.7	32.1	8.7
32.5	20.9	6.2
38.6	16.0	4.8
50.4	11.1	1.9
63.0	6.5	2.0
67.7	7.5	1.8
72.6	6.4	1.5
90.1	2.73	.97

EX= 4.047 MEV,J=1

THETA	SIGMA	ERROR
12.6	53.	20.
22.6	83.4	8.5
32.5	23.9	6.7
38.6	17.0	5.3
40.4	10.8	3.0
50.4	7.6	1.8
90.1	5.5	1.5

EX= 4.092 MEV,J=1

THETA	SIGMA	ERROR
10.1	96.	27.
12.6	102.	19.
17.5	283.	18.
22.6	463.	19.
27.7	187.	17.
32.5	79.0	9.9
38.6	108.7	8.8
40.4	113.3	6.7
50.4	86.3	4.5
63.0	56.9	3.8
67.7	41.2	4.3
72.6	25.2	3.0
90.1	22.2	2.8
100.2	7.5	1.6

EX= 4.116 MEV,J=1

THETA	SIGMA	ERROR
10.1	28.	20.
12.6	53.	16.
17.5	38.9	8.9
22.6	69.8	8.4
27.7	57.	11.
32.5	34.3	7.5
38.6	51.6	7.0
40.4	32.5	4.4
50.4	44.6	3.4
63.0	35.2	3.4
67.7	21.5	3.1
72.6	29.0	3.2
90.1	9.9	1.8

EX= 4.157 MEV,J=1

THETA	SIGMA	ERROR
10.1	147.	28.
12.6	115.	20.
17.5	350.	20.
22.6	322.	15.
27.7	234.	19.
32.5	89.	10.
38.6	129.6	9.4
40.4	118.5	6.9
50.4	50.1	3.5
63.0	45.0	3.4
67.7	32.9	3.8
72.6	29.0	3.2
80.2	19.8	2.6
90.1	17.8	2.5
100.2	10.2	3.4

EX= 4.177 MEV,J=1

THETA	SIGMA	ERROR
10.1	175.	29.
12.6	236.	26.
17.5	378.	20.
22.6	431.	18.
27.7	300.	20.
32.5	207.	14.
38.6	179.	11.
40.4	149.0	7.4
50.4	116.3	5.1
63.0	86.2	4.5
67.7	78.5	5.9
72.6	52.4	4.3
80.2	28.6	3.1
90.1	30.7	3.2
100.2	15.6	2.3

EX= 4.210 MEV,J=1

THETA	SIGMA	ERROR
10.1	149.	31.
12.6	164.	24.
17.5	285.	13.
22.6	336.	16.
27.7	216.	17.
32.5	140.	12.
38.6	136.1	9.9
40.4	137.8	7.5
50.4	75.8	4.3
63.0	66.0	4.1
67.7	49.6	4.7
72.6	43.2	3.9
80.2	32.0	3.3
90.1	23.2	2.8
100.2	14.6	2.2

EX= 4.235 MEV,J=1

THETA	SIGMA	ERROR
10.1	82.	26.
12.6	71.	21.
17.5	86.	11.
22.6	131.	11.
27.7	142.	15.
32.5	81.	10.
38.6	60.1	7.4
40.4	69.1	5.7
50.4	53.5	3.8
63.0	38.0	3.3
67.7	42.1	4.3
72.6	21.3	3.5
80.2	21.1	2.7
90.1	16.0	2.3
100.2	4.1	1.2

EX= 4.257 MEV,J=1

THETA	SIGMA	ERROR
10.1	37.	21.
12.6	70.	22.
17.5	53.5	9.5
22.6	26.1	8.0
32.5	24.6	7.9
38.6	11.5	4.6
40.4	13.1	4.2
50.4	13.0	2.4
63.0	10.7	2.4
67.7	14.0	2.5
80.2	17.0	2.4
90.1	5.1	1.3
100.2	6.8	1.5

EX= 4.286 MEV,J=1

THETA	SIGMA	ERROR
10.1	132.	27.
12.6	203.	24.
17.5	231.	16.
22.6	219.	14.
27.7	225.	19.
32.5	185.	13.
38.6	176.	11.
40.4	149.5	7.5
50.4	86.5	4.6
63.0	73.6	4.1
67.7	63.2	5.3
72.6	43.2	3.9
80.2	53.8	4.3
90.1	29.7	3.2
100.2	13.6	2.1

EX= 4.301 MEV,J=1

THETA	SIGMA	ERROR
10.1	124.	26.
12.6	164.	24.
17.5	143.	13.
22.6	148.	11.
27.7	146.	15.
32.5	127.	11.
38.6	123.1	8.9
40.4	126.2	6.7
50.4	84.1	4.4
63.0	65.2	3.9
67.7	56.6	5.0
72.6	38.3	3.7
80.2	31.3	3.3
90.1	25.3	2.9
100.2	10.2	1.9

EX= 4.326 MEV,J=1

THETA	SIGMA	ERROR
10.1	220.	28.
12.6	222.	26.
17.5	238.	17.
22.6	241.	14.
27.7	241.	19.
32.5	239.	17.
38.6	227.	12.
40.4	202.0	8.7
50.4	125.5	5.4
63.0	118.5	5.3
67.7	89.5	5.3
72.6	34.4	3.5
90.1	23.2	4.1
100.2	4.1	1.2

EX= 4.362 MEV,J=1

THETA	SIGMA	ERROR
10.1	130.	25.
12.6	191.	23.
17.5	143.	14.
22.6	166.	12.
27.7	211.	17.
32.5	184.	13.
38.6	151.	11.
40.4	116.2	7.0
50.4	61.1	4.2
63.0	81.7	4.5
67.7	61.4	5.2
72.6	39.3	3.7
90.1	24.2	2.9
100.2	10.2	1.9

EX= 4.397 MEV,J=1

THETA	SIGMA	ERROR
17.5	38.9	5.0
22.6	38.5	7.8
27.7	77.	11.
32.5	68.6	9.8
38.6	48.1	6.7
63.0	18.2	2.4
67.7	19.7	2.9
72.6	26.6	3.1
90.1	11.9	2.0
100.2	4.1	1.2

EX= 4.411 MEV,J=1

THETA	SIGMA	ERROR
10.1	104.	24.
12.6	134.	22.
17.5	222.	16.
22.6	196.	13.
27.7	158.	15.
32.5	153.	12.
38.6	122.7	9.3
40.4	121.3	8.4
50.4	115.3	5.4
63.0	73.5	4.2
67.7	86.0	6.1
72.6	46.8	4.1
90.1	23.9	2.9
100.2	9.9	1.8

EX= 4.441 MEV,J=1

THETA	SIGMA	ERROR
10.1	86.	20.
12.6	32.	19.
17.5	66.	10.
22.6	52.2	8.7
27.7	53.	11.
32.5	64.9	9.9
38.6	39.5	6.7
40.4	21.4	4.0
50.4	9.5	2.4
63.0	16.3	2.6
67.7	15.8	2.6
72.6	13.8	2.2
90.1	8.5	1.7
100.2	4.8	1.3

EX= 4.469 MEV,J=1

THETA	SIGMA	ERROR
10.1	50.	21.
12.6	68.	19.
17.5	87.	11.
22.6	55.4	7.8
27.7	72.	11.
32.5	95.	10.
38.6	94.6	8.5
40.4	66.6	5.2
50.4	49.8	3.8
63.0	37.4	3.1
67.7	33.3	3.8
72.6	25.9	3.0
90.1	13.0	2.1
100.2	9.9	1.8

EX= 4.485 MEV,J=1

THETA	SIGMA	ERROR
12.6	106.	23.
17.5	87.	11.
22.6	55.4	7.8
27.7	72.	11.
32.5	95.	10.
38.6	94.6	8.5
40.4	66.6	5.2
50.4	49.8	3.8
63.0	37.4	3.1
67.7	33.3	3.8
72.6	25.9	3.0
90.1	13.0	2.1
100.2	9.9	1.8

KEY: FOR J=1,2,OR 3, CROSS SECTION UNITS ARE MICRO-, 100 MICRO-, OR MILLI-BARNS/STERADIAN, RESPECTIVELY.

EX= 4.512 MEV,J=1

THETA	SIGMA	ERROR
12.6	65.	20.
17.5	155.	20.
22.6	66.5	8.3
27.7	94.	12.
32.5	78.	10.
38.6	55.1	7.2
40.4	45.9	4.6
50.4	44.2	3.8
63.0	39.6	3.3
67.7	21.5	3.1
72.6	18.4	2.6
90.1	21.8	2.7

EX= 4.532 MEV,J=1

THETA	SIGMA	ERROR
17.5	67.3	9.8
22.6	48.9	7.8
27.7	47.	13.
32.5	50.7	8.4
38.6	57.6	7.1
40.4	53.6	5.3
50.4	46.6	3.8
63.0	30.6	2.9
67.7	27.6	3.5
72.6	15.9	2.4
90.1	8.9	1.7

EX= 4.592 MEV,J=1

THETA	SIGMA	ERROR
17.5	38.9	8.9
22.6	59.3	8.0
27.7	40.8	9.8
32.5	25.3	6.3
38.6	16.0	6.0
40.4	12.6	4.3
50.4	7.4	2.5
63.0	4.3	2.3
67.7	15.8	2.6
72.6	13.8	2.2
80.2	7.8	1.6
90.1	4.8	1.3

EX= 4.613 MEV,J=1

THETA	SIGMA	ERROR
10.1	62.	20.
17.5	43.	26.
22.6	55.4	8.5
27.7	37.	10.
32.5	47.7	8.3
38.6	25.0	5.8
40.4	12.0	3.2
50.4	9.7	2.1
67.7	19.3	2.9
72.6	23.7	2.9
80.2	23.5	2.8
90.1	6.1	1.4
100.2	4.8	1.3

EX= 4.760 MEV,J=1

THETA	SIGMA	ERROR
10.2	437.	39.
12.6	557.	34.
17.5	282.	28.
22.6	151.	12.
27.7	167.	17.
32.5	83.	10.
38.6	84.6	8.9
50.4	72.6	4.9
63.0	62.1	4.3
67.7	65.3	5.4
72.6	46.1	4.0
80.2	37.5	3.6
90.1	17.8	2.5
100.2	9.2	1.8

EX= 4.791 MEV,J=1

THETA	SIGMA	ERROR
10.2	333.	34.
12.6	486.	33.
17.5	309.	18.
22.6	161.	12.
27.7	127.	15.
32.5	31.	11.
38.6	73.1	8.5
40.4	70.5	6.6
50.4	68.5	4.8
63.0	30.9	3.5
72.6	31.5	3.3
80.2	22.5	2.8
100.2	7.1	1.6

EX= 4.828 MEV,J=1

THETA	SIGMA	ERROR
10.2	126.	26.
12.6	128.	27.
17.5	150.	13.
27.7	64.	13.
32.5	62.6	9.3
38.6	32.5	6.0
40.4	40.2	4.7
50.4	34.0	4.0
63.0	26.9	3.1
67.7	26.3	3.4
72.6	15.6	2.3
80.2	19.1	2.5
100.2	6.5	1.5

EX= 4.853 MEV,J=1

THETA	SIGMA	ERROR
10.2	53.	19.
12.6	110.	24.
17.5	75.	10.
27.7	64.	13.
32.5	31.3	7.9
38.6	33.0	6.0
40.4	27.7	4.4
50.4	24.1	3.5
63.0	22.4	3.1
67.7	19.7	2.9
72.6	13.1	2.2
80.2	13.3	2.1
100.2	4.8	1.3

EX= 4.949 MEV,J=1

THETA	SIGMA	ERROR
12.5	49.	18.
17.5	79.	11.
27.7	68.	14.
32.5	44.7	8.2
38.6	19.0	5.4
40.4	27.4	4.1
50.4	25.2	3.3
67.7	26.3	3.4
80.2	22.1	2.7
90.1	7.2	1.6

EX= 4.965 MEV,J=1

THETA	SIGMA	ERROR
10.2	30.	21.
12.6	49.	18.
17.5	60.	11.
27.7	47.	12.
32.5	34.3	7.7
38.6	24.5	6.4
40.4	29.1	4.4
50.4	20.2	3.3
80.2	28.3	3.1
90.1	10.9	1.9
100.2	9.5	1.8

EX= 4.998 MEV,J=1

THETA	SIGMA	ERROR
12.6	89.	20.
17.5	66.	11.
32.5	37.3	8.5
38.6	21.0	6.5
50.4	19.1	3.4
63.0	23.2	3.2
67.7	27.2	3.5
72.6	16.6	2.4
90.1	10.9	1.9

EX= 5.056 MEV,J=1

THETA	SIGMA	ERROR
12.6	89.	20.
17.5	72.	11.
32.5	44.7	9.7
38.6	21.5	6.8
50.4	22.8	3.4
63.0	20.2	3.5
67.7	42.1	4.3
72.6	29.4	3.2
90.1	11.6	2.0

EX= 5.131 MEV,J=1

THETA	SIGMA	ERROR
10.2	67.	21.
12.6	65.	21.
17.5	65.	13.
27.7	53.	14.
32.5	54.	10.
38.6	51.6	8.4
40.4	45.1	5.7
50.4	45.1	4.3
63.0	20.7	3.2
80.2	15.3	2.3
100.2	8.5	1.7

EX= 5.241 MEV,J=1

THETA	SIGMA	ERROR
10.2	84.	23.
12.6	105.	23.
17.5	97.	13.
27.7	36.	15.
38.6	51.1	8.7
40.4	48.8	5.7
50.4	30.8	3.9
63.0	26.9	3.4
72.6	12.4	2.1
100.3	6.8	1.5

EX= 5.282 MEV,J=1

THETA	SIGMA	ERROR
10.2	114.	22.
12.6	152.	30.
17.5	149.	15.
27.7	133.	17.
38.6	75.6	9.6
40.4	70.8	6.4
50.4	56.8	4.3
63.0	37.8	3.9
67.7	34.2	3.9
80.2	35.1	3.5
100.3	14.6	2.2

EX= 5.312 MEV,J=1

THETA	SIGMA	ERROR
10.2	76.	23.
12.6	96.	22.
17.5	77.	12.
27.7	67.	15.
38.6	31.5	8.1
40.4	25.7	4.5
63.0	19.3	3.5
67.7	20.2	3.4
72.6	16.5	2.4
100.3	5.1	1.3

EX= 5.333 MEV,J=1

THETA	SIGMA	ERROR
10.2	18.	13.
17.5	35.	11.
27.7	22.	12.
38.6	14.0	7.1
40.4	12.3	4.4
63.0	7.8	3.4
67.7	13.2	3.6
72.6	5.3	2.5
80.2	9.5	2.6
90.1	9.6	3.3
100.3	7.5	1.6

EX= 5.360 MEV,J=1

THETA	SIGMA	ERROR
10.2	99.	21.
12.6	145.	25.
17.5	132.	16.
27.7	142.	19.
38.6	75.6	9.9
40.4	52.8	5.8
63.0	40.0	4.3
67.7	41.2	4.3
80.2	39.5	3.7
100.3	6.8	1.4

KEY: FOR J=1,2,OR 3, CROSS SECTION UNITS ARE MICRO-, 100 MICRO-, OR MILLI-BARNS/STERADIAN, RESPECTIVELY.

EX= 5.433 MEV,J=1

THETA	SIGMA	ERROR
10.2	120.	24.
12.6	130.	23.
17.5	169.	18.
27.7	86.	16.
32.5	71.	16.
38.6	78.6	9.4
40.4	63.3	5.8
50.4	56.1	4.2
63.0	53.5	4.9
67.7	45.2	4.5
72.6	46.4	4.1
80.2	33.0	3.4
90.1	25.3	2.9
100.3	5.4	1.4

EX= 5.463 MEV,J=1

THETA	SIGMA	ERROR
10.2	67.	21.
12.6	41.	18.
17.5	60.	13.
27.7	89.	17.
32.5	64.	13.
40.4	60.5	6.3
50.4	57.7	4.4
63.0	17.6	3.6
67.7	31.6	3.7
72.6	43.6	3.9
80.2	33.8	3.7

EX= 5.509 MEV,J=1

THETA	SIGMA	ERROR
10.2	183.	26.
12.6	229.	26.
17.5	193.	17.
27.7	140.	17.
32.5	125.	14.
40.4	66.7	7.2
50.4	108.2	5.9
63.0	31.5	4.3
67.7	41.7	4.3
80.2	41.9	3.8
90.1	23.2	2.8
100.3	7.1	1.6

EX= 5.569 MEV,J=1

THETA	SIGMA	ERROR
10.2	78.	22.
12.6	76.	19.
17.5	115.	14.
22.6	72.	13.
27.7	120.	19.
50.4	49.2	3.9
72.6	27.3	3.1
80.2	25.5	2.9

EX= 5.769 MEV,J=1

THETA	SIGMA	ERROR
12.6	66.	22.
17.5	72.	12.
22.6	51.	11.
27.7	80.	15.
32.5	66.	12.
50.4	37.1	4.2
63.0	9.1	3.1

EX= 5.793 MEV,J=1

THETA	SIGMA	ERROR
10.2	87.	33.
12.6	98.	26.
17.5	84.	13.
22.6	70.	11.
27.7	41.	14.
32.5	70.	12.
38.6	60.6	9.8
50.4	50.1	4.2
63.0	31.7	4.2
90.1	19.1	2.6

EX= 5.835 MEV,J=1

THETA	SIGMA	ERROR
10.2	33.	17.
22.6	58.7	9.4
27.7	52.	13.
32.5	39.8	8.8
40.4	59.3	6.4
50.4	52.2	4.5
63.0	20.4	3.3
72.6	25.7	3.2
90.1	9.6	1.8
100.3	5.1	1.3

KEY: FOR J=1,2,OR 3, CROSS SECTION UNITS ARE MICRO-, 100 MICRO-, OR MILLI-BARNS/STERADIAN, RESPECTIVELY.

REFERENCES

REFERENCES

1. J. Saudinos, G. Vallois, O. Beer, M. Gendrot, and P. Lopato, Phys. Letters 22(1966)492; J. Saudinos, G. Vallois, and O. Beer, Nucl. Sci. Appl. 3, No.2 (1967)22; G. Vallois, Centre d'Etudes Nucleaires de Saclay, Report CEA-R-3500(1968).
2. M. Lewis, F. Bertrand, and C. B. Fulmer, Phys. Rev. C7(1973)1966.
3. J. Alster, Phys. Letters 25B(1967)459; G. Bruge, J. C. Faivre, H. Faraggi, and A. Bussiere, Nucl. Phys. A146 (1970)597; R. A. Moyer, B. L. Cohen, and R. C. Diehl, Phys. Rev. C2(1970)1898; L. Cranberg, T. Oliphant, J. Levin, and C. Zafiratos, Phys. Rev. 159(1967)969; and references therein.
4. G. R. Satchler, R. H. Bassel, and R. M. Drisko, Phys. Letters, 5(1963)256.
5. M. P. Fricke and G. R. Satchler, Phys. Rev. 139(1965)567.
6. A. Scott and M. P. Fricke, Phys. Letters 20(1966)654.
7. S. A. Fulling and G. R. Satchler, Nucl. Phys. A111 (1968)81.
8. N. P. Mathur, Univ. of Delhi, Thesis (1969), unpublished.
9. O. Karban, P. D. Greaves, V. Hnizdo, J. Lowe, and G. W. Greenlees, Nucl. Phys. A147(1970)461.

10. E. Grosse, M. Dost, K. Haberkant, J. W. Hertel, H. V. Klapdor, H. J. Korner, D. Proetel, and P. von Brentano, Nucl. Phys. A174(1971)525.

11. P. Mukherjee and B. L. Cohen, Phys. Rev. 127(1962)1284; J. Bardwick and R. Tickle, Phys. Rev. 161(1967)1217.

12. G. Igo, P. D. Barnes, and E. R. Flynn, Annals of Physics 66(1971)60; G. Igo, P. D. Barnes, and E. R. Flynn, Phys. Rev. Letters 24(1970)470.

13. E. D. Earle, A. J. Ferguson, G. van Middelkoop, and G. A. Bartholomew, Phys. Lett. 32B(1970)471.

14. P. Richard, P. von Brentano, H. Weimen, W. Wharton, W. G. Weitkamp, W. W. McDonald, and D. Spalding, Phys. Rev. 183 (1969)1007.

15. C. F. Moore, J. G. Kulleck, P. von Brentano and F. Rickey, Phys. Rev. 164(1967)1559.

16. J. G. Cramer, P. von Brentano, G. W. Philips, H. Ejiri, S. M. Ferguson, and W. J. Braithwaite, Phys. Rev. Letters 21(1968)297.

17. M. Dost and W. R. Hering, Phys. Letters 26B(1968)443.

18. G. R. Satchler, Comm. Nucl. and Part. Phys. 5(1972)39.

19. H. G. Blosser, G. M. Crawley, R. de Forest, E. Kashy and B. H. Wildenthal, Nucl. Instr. and Meth. 91(1971)61.

20. W. A. Lanford, W. Benenson, G. M. Crawley, E. Kashy, I. D. Proctor, and W. F. Steele, BAPS 17(1972)895.

21. F. D. Becchetti, Jr. and G. W. Greenlees, Phys. Rev. 182 (1969)1190.

22. FORTRAN programs written by G. Hamilton, Michigan State University (unpublished) and by J. A. Rice, Michigan State University Thesis, (1973) unpublished.

23. M. B. Lewis, Nucl. Data B5, No. 3(1971)243.

24. A. Heusler and P. von Brentano, Annals of Physics 75 (1973)381; A. Heusler, private communication.

25. L. N. Blumberg, E. E. Gross, A. von der Woude, A. Zucker, and R. H. Bassel, Phys. Rev. 147(1966)812; R. C. Barrett, A. D. Hill, P. E. Hodgson, Nucl. Phys. 62(1965)133; G. W. Greenlees and G. J. Pyle, Phys. Rev. 149(1966)836; D. L. Watson, J. Lowe, J. C. Dore, R. M. Craig and D. J. Baugh, Nucl. Phys. A92(1967)193; G. R. Satchler, Nucl. Phys. A92(1967)273; G. W. Greenlees, V. Hnizdo, O. Karban, J. Lowe, and W. Makofske, Phys. Rev. C2(1970)1063.

26. F. Perey, unpublished.

27. J. Kunz, University of Colorado, unpublished.

28. C. D. Bowman, R. J. Baglan, B. L. Berman, and T. W. Philips, Phys. Rev. Letters 25(1970)1302; R. E. Toohey and H. E. Jackson, Phys. Rev. C6(1972)1440; A. Wolf, R. Moreh, A. Nof, O. Shahal, and J. Tenenbaum, Phys. Rev. C6(1972)2276; F. E. Cecil, Princeton University Thesis (1972), unpublished.

29. L. W. Fagg, W. F. Bendel, E. C. Jones, N. Ensslin, and F. E. Cecil, in Proceedings of the International Conference on Nuclear Physics, Vol. 1, ed. by J. de Boer and H. J. Mang, (North-Holland, Amsterdam, 1973) page 631.

30. R. A. Broglia, A. Molinari, and B. Sorensen, Nucl. Phys. A109(1968)353.

31. J. D. Vergados, Phys. Letters 36B(1971)12.

32. G. R. Satchler, Comm. Nuc. Part. Phys. 5(1972)145.

33. A. M. Bernstein, Advances in Nuclear Physics, Vol. 3, ed by M. Baranger and E. Vogt (Plenum Press, New York, 1969), p. 325.

34. D. Agassi and P. Schaeffer, Phys. Letters 26B(1968)703.

35. G. Astner, I. Bergstrom, J. Blomqvist, B. Fant, and K. Wikstrom, Nucl. Phys. A182(1972)219.

36. G. R. Hammerstein, R. H. Howell, and F. Petrovich, Nucl. Phys. A213(1973)45.

37. F. Petrovich, Michigan State University Thesis (unpublished); F. Petrovich, H. McManus, V. A. Madsen and J. Atkinson, Phys. Rev. Letters 22(1969)895.

38. R. M. Haybron, M. B. Johnson, and R. J. Metzger, Phys. Rev. 156(1967)1136.

39. K. H. Bray, M. Jain, K. S. Jayaraman, G. Lobianco, G. A. Moss, W.T.H. van Oers, D. O. Wells, and F. Petrovich, Nucl. Phys. A189(1972)35.

40. M. Nagoa and Y. Torizuka, Phys. Letters 37B(1971)383.

41. J. H. Heisenberg and I. Sick, Phys. Letters 32B(1970)249.

42. J. F. Ziegler and G. A. Peterson, Phys. Rev. 165(1968)1337.

43. J. Friedrick, Nucl. Phys. A191(1972)118.

44. G. R. Satchler, Phys. Letters 35B(1971)279; R. H. Howell and A. I. Galonsky, Phys. Rev. C5(1972)561; R. A. Hinrichs, D. Larson, B. M. Preedom, W. G. Love and F. Petrovich, Phys. Rev. C7(1973)1981.

45. R. Schaeffer and J. Raynal, unpublished.

46. G. Love, L. Parish, and A. Richter, Phys. Letters 31B(1970)167.

47. S. M. Austin in The Two-Body Force in Nuclei, eds. S. M. Austin and G. M. Crawley, (Plenum Press, New York, 1972).

48. G. M. Crawley, S. M. Austin, W. Benenson, V. A. Madsen, F. A. Schmittroth, and M. J. Stomp, Phys. Letters 32B (1970)92.

49. S. H. Fox and S. M. Austin, to be published; S. H. Fox, Michigan State University Thesis (unpublished).

50. P. Richard, W. Weitkamp, W. Wharton, H. Wieman, and P. von Brentano, Phys. Lett. 26B(1967)8.

51. W. True, C. Ma, and W. Pinkston, Phys. Rev. C3(1971)2421.

52. V. Gillet, A. Green, and E. Sanderson, Nucl. Phys. 88 (1966)321.

53. T.T.S. Kuo, private communication.

54. I. Hamamoto, Nucl. Phys. A155(1970)362; J. D. Vergados Phys. Letters 34B(1971)121; J. D. Vergados, Phys. Letters, 34B(1971)458 and references therein.

55. D. A. Bromley and J. Weneser, Comm. Nucl. Part. Physics 2(1968)151.

56. E. Kashy, H. G. Blosser, and D. A. Johnson in Cyclotrons--1972, eds. J. J. Burgerjon and A. Strathdee (American Institute of Physics, New York, 1972) p. 430

57. G. Francillon, Y. Terrien, and G. Vallois, Phys. Letters 33B(1970)216

58. C. Glashausser, B. G. Harvey, D. L. Hendrie, J. Mahoney, E. A. McClatchie, and J. Saudinos, Phys. Rev. Letters 21(1968)918

59. F. Petrovich, H. McManus, J. R. Borysowicz, and G. R. Hammerstein, to be published

60. W. Benenson, S. M. Austin, P. J. Locard, F. Petrovich, J. R. Borysowicz, and H. McManus, Phys. Rev. Letters 24(1970)907

61. M. R. Schmorak and R. L. Auble, Nuclear Data Sheets B5 (1971) 207

62. M. J. Martin, Nuclear Data Sheets, Nuclear Data Sheets B5(1971)287

63. S. M. Smith, P. G. Roos, C. Moazed, and A. M. Bernstein, Nucl. Phys. A173(1971)32

64. W. P. Alford and D. G. Burke, Phys. Rev. 185(1969)1560

65. W. Darcey, A. F. Jeans, and K. N. Jones, Phys. Letters 25B(1967)599

66. B. H. Wildenthal, B. M. Preedom, E. Newman, and M. R. Cates, Phys. Rev. Letters 19(1967)960; C. Ellegaard and P. Vedelsby, Phys. Letters 26B(1968)155

67. J. S. Lilley and N. Stein, Phys. Rev. Letters 19(1967) 709

68. N. Auerbach and N. Stein, Phys. Letters 27B(1968)122

69. M. B. Lewis, C. D. Goodman, and D. C. Hensley, Phys. Rev. C3(1971)2027

70. G. Vallois, J. Saudinos, O. Beer, M. Gendrot, and P. Lopato, Phys. Letters 22(1966)659

71. F. E. Bertrand and M. B. Lewis, Nucl. Phys. A168(1971) 259

72. T. B. Cleary, Yale University thesis (unpublished)

73. J. Ungrin, R. M. Diamond, P. O. Tjom, and B. Elbek, Kgl. Dan. Vidensk. Selsk. Mat.--Fys. Medd. 38,No.1 (1971)

74. R. D. Lawson and J. L. Uretsky, Phys. Rev. 108(1957) 1300; A. de-Shalit, Phys. Rev. 122(1961)1530

75. T. P. Cleary, W. D. Callender, N. Stein, C. H. King, D. A. Bromley, J. P. Coffin, and A. Gallmann, Phys. Rev. Letters 28(1972)699

76. I. Hamamoto, Nucl. Phys. A148(1970)465

77. E. Grosse, P. von Brentano, J. Solf, and C. F. Moore, Z. Physik 219(1969)75

78. J. C. Hafele and R. Woods, Phys. Letters 23(1966)579

79. J. Alster, Phys. Letters 25B(1967)459

80. E. Grosse, C. F. Moore, J. Solf, W. R. Hering, and P. von Brentano, Z. Physik 218(1969)213

81. J. W. Hertel, D. G. Fleming, J. P. Schiffer, and H. E. Gove, Phys. Rev. Letters 23(1969)488; R. A. Broglia, J. S. Lilley, R. Perazzo, and W. R. Philips, Phys. Rev. C1(1970)1508

82. C. P. Swann, BAPS 16(1971) 651

83. H. V. Klapdor, P. von Brentano, E. Grosse, and K. Haberkant, Nucl. Phys. A152(1970)263; E. Grosse, M. Dost, K. Haberkant, J. W. Hertel, H. V. Klapdor, H. J. Korner, D. Proetel, and P. von Brentano, Nucl. Phys. A174(1971)525; O. Hausser, F. C. Khanna, and D. Ward, Nucl. Phys. A194(1972)113

84. H. V. Geramb and K. Amos, Phys. Letters 32B(1970)665

85. W. G. Love and G. R. Satchler, Nucl. Phys. A101(1967) 424

86. A. Kallio and K. Kolltveit, Nucl. Phys. 53(1964)87

87. S. C. Ewald, unpublished

88. D. L. Bayer, "The Data Acquisition Task TOOTSIE", MSUCL-34(unpublished)

89. D. L. Bayer, unpublished

90. G. F. Trentleman and E. Kashy, Nucl. Instr. Meth. 82(1970)304

91. W. T. Wagner and J. E. Finck, unpublished